**School of Biomedical Sciences**

# Implications of the WNT Signalling Pathway for Adipose-derived Mesenchymal Stem Cells in a Breast Tumour Environment

**Malini Visweswaran**

**This thesis is presented for the Degree of**
**Doctor of Philosophy**
**of**
**Curtin University**

**June 2017**

**Declaration**

To the best of my knowledge and belief this thesis contains no material previously published by any other person except where due acknowledgment has been made.

This thesis contains no material which has been accepted for the award of any other degree or diploma in any university.

Signature: .....

Date: 16/06/2017

**THIS THESIS IS DEDICATED TO MY BELOVED HUSBAND**

***ANUMOD BOSE MANGAT***

# ACKNOWLEDGEMENTS

On 18 August 2011, a day after my wedding, I decided to send an email to Professor Arunasalam Dharmarajan which completely changed my life later on. After 2 years of email exchanges and persistent trying, I saw light at the end of the tunnel and ended up getting an opportunity from Prof. Dharma to pursue my PhD in his lab. This came as a rain in the desert while I was struggling with the build-up season in Northern Territory. I cannot thank Prof. Dharma enough for taking me on-board and for all the precious advice he has given, on my research throughout my PhD as well as in setting my career goals. I greatly appreciate his immense knowledge, motivation, patience, as well as his ultra-prompt responses for my queries and emails. Prof. Dharma has been instrumental in driving me and the team, even when he was going through health issues. Monday mornings won't be the same without that special email (my alarm) about the lab meeting! I am eternally grateful to have known a wonderful personality like him and to have worked under his guidance.

I would like to thank the valuable input and support of my co-supervisors Professor Philip Newsholme and Associate Professor Rodney Dilley. Prof. Philip, in spite of his busy schedule has always been of great help and support throughout, especially when reviewing my manuscripts, abstracts, and thesis in short notices. Assoc. Prof. Rodney with his extensive knowledge and experience has always been exceptional in providing insightful comments, suggestions, and materials for my research. I whole-heartedly thank both of them for their supervision and moral support.

I would like to extend my sincere thanks to Dr. Frank Arfuso, who has been absolutely incredible in providing brilliant suggestions onto the table. Dr. Frank has

been phenomenal with reviewing and proof reading my manuscripts and infinite thesis drafts. I really appreciate his prompt response and guidance in shaping my research and writing skills.

I appreciatively thank my team mates Abhijeet Deshmukh, Sebastian Pohl, and Dr. Mark Agostino for their stimulating discussions and co-operation in the lab. Their valuable inputs during our meeting sessions have been very encouraging and constructive.

I would like to take this opportunity to thank Dr. Kevin Keane for providing me with an initial induction, and assistance in getting me started in the lab. Dr. Kevin's involvement in training me on the Seahorse $XF^e96$ flux analyser has been outstanding. I really thank Dr. Kevin for all his support and time.

I would also like to take this opportunity to thank Rob Stuart, Connie Jackaman, Jeanne Le Masurier, Joanna Kelly, and all other staff and friends at the Curtin Health Innovation Research Institute (CHIRI) who assured the smooth running of the lab facilities. CHIRI and School of Biomedical Sciences has been instrumental in providing the state-of-art facilities and resources to pursue my research work. I gratefully acknowledge the Office of Research & Development-School of Biomedical Sciences scholarship for providing me the financial support during my study.

It is my pleasure to acknowledge and whole-heartedly thank all the Lab 5 members, especially Omar El Askalani, who has been a saviour whenever consumables run out or when there is an extra pair of hands needed to open a tight reagent bottle!

Aparna Warrier, I would like to thank her for all the good times we have had over the past years and for lending her shoulder at tough times. Casual chats with Aparna in

my mother-tongue have always been refreshing, making her my go-to-person for anything, anytime. I wish good luck with her thesis submission and future endeavours. I would also like to thank my other friends at CHIRI - Bhawna Gauri, Gaewyn Ellison, Ganga Senarathna, Julia Köhn, Sheena Regan, Revathy Carnagarin, and Hilai Bakhshi for their infinite backing and help throughout the study. I express my thanks to Thiru Sabapathy, Abhishek Kumar Singh, Behin Sundaraj, Adnan Mannan, Naz Hassan Huda, and Dr. Vishal Chaturvedi for their continuous support.

I would like to thank Ms. Sangeetha Kandoi for being my best friend, and teaching me the baby steps of cell culture, and implanting in me the seeds of a future researcher. I would also like to thank Sangeetha for being the link that connected me to Prof. Dharma.

At this stage, I would like to thank and remember the vital role of my teachers who opened the doors into the broad field of Science. I would like to acknowledge Ms. Sheena Devassy, Ms. Smitha Thomas, Ms. Jeyanthi, Dr. Kavitha Sankaranarayanan, and Dr. Ajitkumar for their guidance, and profound knowledge.

I would like to thank my parents for providing me with excellent education and the freedom to pursue my dreams. Apart from being a constant source of support, my Mom has been phenomenal in shaping my character and future goals. Being an Anesthesiologist, my Mom introduced me to the world of Medicine and Science, and hence I stand here today.

Ultimately, I owe a big thanks and deepest gratitude to my husband, Anumod Bose Mangat for his continuous love and support during my study. He has always been my pillar of strength, to lead me in times of adversity and confusion. Bose has been extremely supportive throughout, be it the long waits at the University car parks

during my late-night experiments, taking me out for dinner and dessert strolls to cheer me up when things does not go according to plan, looking after the household chores during my crazy Uni schedules, and what not! Kudos to You! Cannot thank you enough!

# TABLE OF CONTENTS

**Part-II Effect of ADSC-CM and sFRP4 on breast tumour cells**

**Part-III Effect of ADSC-CM and sFRP4 peptides on breast tumour cells**

**Part-II Effect of TCM and sFRP4 peptides on the transdifferentiation of ADSCs into TAFs**

# LIST OF FIGURES

# LIST OF TABLES

# LIST OF ABBREVIATIONS

µM: micromolar

2-DG: 2-Deoxy glucose

2DG6P: 2-Deoxy glucose-6-phosphate

ADSCs: Adipose-derived mesenchymal stem cells

ADSC-CM: Adipose-derived mesenchymal stem cells-derived conditioned medium

AIHW: Australian Institute of Health and Welfare

Akt: Protein kinase B

APC: Adenomatous polyposis coli

APS: Ammonium persulphate

ATP: Adenosine triphosphate

B+S: BIO+sFRP4

BCA: Bicinchoninic acid

BIO: (2'Z,3'E)-6-Bromoindirubin-3′-oxime

BM-MSCs: Bone marrow MSCs

BSA: Bovine serum albumin

C/EBPα: C/Enhancer Binding Protein α

CAFs: Carcinoma associated fibroblasts

CAM: Cell-adhesion molecules

CaMKII: Calmodulin mediated kinase II

CD: Cluster of differentiation

CRD: Cysteine-rich domain

CM: Conditioned medium

CSC: Cancer stem cell

CXCR: C-X-C chemokine receptor

DAPI: 4',6-Diamidino-2-phenylindole dihydrochloride

DCFDA: 2′,7′-Dichlorofluorescin diacetate

DCIS: Ductal carcinoma *in situ*

DEVD-R110: Asp-Glu-Val-Asp-Rhodamine 110

Dkk: Dickkopf

DMEM: Dulbecco's Modified Eagle's Medium

DMSO: Dimethyl sulphoxide

Dsh: Dishevelled

DTT: Dithiothreitol

ECL: Enhanced chemiluminescence

ECM: extracellular matrix

EGF: Epidermal growth factor

EMT: Epithelial-to-mesenchymal transition

ENA-78: Epithelial cell derived neutrophil activating peptide 78

ER: Oestrogen receptor

ErB2: Erythroblastosis oncogene B

FBS: Foetal bovine serum

FGF: Fibroblast growth factor

FSP: Fibroblast-specific protein

Frz: Frizzled

G6PDH: Glucose-6-phosphate dehydrogenase

GSK-3β: Glycogen synthase kinase-3β

GTPase: Guanosine-5'-triphosphate-ase

HCl: Hydrochloric acid

Her2: human epidermal growth factor receptor 2

HGF: Hepatocyte growth factor

HUVEC: Human umbilical vein endothelial cell

IACR: International Agency for Research on Cancer

IDH 3α: Isocitrate dehydrogenase 3α

IDP: Intrinsically disordered protein

IFN-β: Interferon-β

IL: Interleukin

JNK: Jun N-terminal kinase

Kmn: Kremen

LCIS: Lobular carcinoma *in situ*

LDS: Lithium dodecyl sulphate

LiCl: Lithium chloride

LPA: Lysophosphatidic acid

LRP: Low density lipoprotein related protein

M: Molar

MCF7: Michigan Cancer Foundation-7

MCP: Monocyte chemoattractant protein

MES: 2-(N-morpholino) ethanesulphonic acid

mM: millimolar

MSC-CM: MSC-conditioned medium

MSCs: Mesenchymal stem cells

MTT: Methylthiazolyldiphenyl-tetrazolium

NaOH: Sodium hydroxide

$NH_4Cl$: Ammonium chloride

$NH_4OH$: Ammonium hydroxide

NLD: Netrin-like domain

PBS: Phosphate buffered saline

PDGF: Platelet-derived growth factor

PD-MSCs: Placenta-derived MSCs

PEDF: Pigment epithelium-derived factor

PFA: Paraformaldehyde

pg/mL: picogram/millilitre

PKC: protein kinase C

PPARγ: peroxisome proliferator-activated receptor gamma

PR: Progesterone receptor

pRb: retinoblastoma protein

PS: Penicillin-Streptomycin

PTEN: Phosphatase and tensin homolog

RANTES: regulated on activation, normal T cell expressed and secreted

RIPA: Radioimmunoprecipitation Assay

ROS: Reactive oxygen species

RPMI: Roswell Park Memorial Institute

SDF: Stromal cell-derived factor

SDS: Sodium dodecyl sulphate

SDS-PAGE: Sodium dodecyl sulphate-polyacrylamide gel electrophoresis

sFRP: Secreted frizzled-related protein

SL-1: Stromelysin-1

TAFs: Tumour associated fibroblasts

TCF/LEF: T cell factor/Lymphoid Enhancer Factor

TCM: Tumour conditioned medium

TEMED: Tetramethylethylenediamine

TGF-β1: Transforming growth factor-beta1

TIMP: Tissue inhibitor of metalloproteinase

Tn-C: Tenascin-C

TRAIL: Tumour necrosis-related apoptosis inducing ligand

Tris: Tris(hydroxymethyl)aminomethane

Tsp-1: Thromobospondin-1

UC-MSCs: Umbilical cord tissue MSCs

VEGF: vascular endothelial growth factor

WHO: World Health Organisation

α-SMA: alpha-Smooth muscle actin

# PUBLICATIONS DURING PhD

2017 Jun Jun Olsen, Sebastian Pohl, Abhijeet Deshmukh, **Malini Visweswaran**, Natalie Ward, Frank Arfuso, Mark Agostino, Arun Dharmarajan. Role of Wnt signalling in angiogenesis. The Clinical Biochemical Reviews (Submitted).

2017 **Visweswaran, M.**, Arfuso, F., Dilley, R., Newsholme, P., Dharmarajan, A.,
The influence of breast tumour-derived factors and Wnt antagonism on the transformation of adipose-derived mesenchymal stem cells into tumour-associated fibroblasts. Experimental Cell Research (Submitted).

2017 **Visweswaran, M.**, Arfuso, F., Dilley, R., Newsholme, P., Dharmarajan, A.,
The influence of adipose tissue-derived mesenchymal stem cell environment and WNT antagonism on breast tumour cells. International Journal of Biochemistry and Cell Biology (IJBCB) (Under Review).

2015 **Visweswaran, M.**, Pohl, S., Arfuso, F., Newsholme, P., Dilley, R., Pervaiz, S., Dharamrajan, A., Multi-lineage differentiation of

mesenchymal stem cells - To Wnt, or not Wnt. Int J Biochem Cell Biol, 2015. 68: p. 139-47.

2015 **Visweswaran, M.**, Schiefer, L., Arfuso, F., Dilley, R., Newsholme, P., Dharmarajan, A., Wnt Antagonist Secreted Frizzled-Related Protein 4 Upregulates Adipogenic Differentiation in Human Adipose Tissue-Derived Mesenchymal Stem Cells. PLoS ONE, 2015. 10: p. e0118005.

2014 Schiefer, L., **Visweswaran, M.**, Perumal, V., Arfuso, F., Groth, D., Newsholme, P., Warrier, S., Dharmarajan, A., Epigenetic regulation of the secreted frizzled-related protein family in human glioblastoma multiforme. Cancer Gene Ther, 2014. 21(7): p. 297-303.

# AWARDS OBTAINED DURING PhD

2013 Received the Office of Research & Development-School of Biomedical Sciences scholarship for financial support during PhD study

2016 Received the CUPSA Thesis Completion Grant 2016 which provided additional financial support during completion of the PhD thesis

# ORAL PRESENTATIONS/POSTER PRESENTATIONS /CONFERENCES ATTENDED DURING PhD

2017 Oral Presentation on 'The reciprocal interaction between adipose tissue-derived mesenchymal stem cells and breast tumour cells mediated by Wnt antagonists' at the Australian Society for Medical Research Symposium held at Edith Cowan University, Western Australia, Australia on 7th June 2017

2017 Oral Presentation on 'The importance of Wnt signalling for adipose-derived mesenchymal stem cells ion a breast tumour environment' at the PhD completion seminar series held at the School of Biomedical Sciences, Curtin University, Western Australia, Australia on 27th April 2017

2017 Poster presentation on 'The reciprocal interaction between adipose tissue-derived mesenchymal stem cells and breast tumour cells mediated by Wnt antagonists' at the Science on the Swan Conference held at Esplanade hotel, Fremantle, Western Australia, Australia from 2nd-4th May 2017

2016 Invited talk on 'The influence of adipose tissue-derived mesenchymal stem cell environment and Wnt antagonism on breast tumour cells' and Moderator at the 2nd World Congress for Cancer and Prevention Methods held at the Furama Riverfront, Singapore from 7th – 9th November 2016

2016 Poster Presentation on ‘The influence of adipose tissue-derived mesenchymal stem cell environment and Wnt antagonism on breast tumour cells’ the International annual meeting organized by American Association for Cancer Research (AACR) held at New Orleans, Louisiana, USA from 16th-20th April, 2016

**Visweswaran, M.**, Arfuso, F., Dilley, R., Newsholme, P., Dharmarajan, A.,

The influence of adipose tissue-derived mesenchymal stem cell environment and WNT antagonism on breast tumour cells. Proceedings of the 107th Annual Meeting of the American Association for Cancer Research; 2016 Apr 16-20; New Orleans, LA. Philadelphia (PA): AACR; Cancer Res 2016;76(14 Suppl):Abstract nr 4629.

2015 Oral and Poster presentation on ‘Effect of secreted factors from adipose tissue-derived mesenchymal stem cells and Wnt antagonism on breast tumour cells’ at the Mark Liveris Student Research Seminar held at Curtin University, Western Australia, Australia on 3rd September 2015

2015 Attended the Australian Society for Medical Research WA Scientific Symposium 2015 held at Curtin University, Western Australia, Australia on 30th May 2015.

2015 Poster presentation on ‘Wnt antagonist secreted frizzled-related protein-4 upregulates adipogenic differentiation in human adipose tissue-derived mesenchymal stem cells’ at the Inaugural conference of

Science on the Swan held at Perth Convention & Exhibition Centre, Western Australia, Australia from 21st – 23rd April 2015.

2015 Co-ordinated activities at the Cancer stem cell workshop held at Curtin University, Western Australia, Australia on 24th April 2015, organized by our laboratory group

2014 Oral and Poster presentation on 'Wnt antagonist secreted frizzled-related protein-4 upregulates adipogenic differentiation in human adipose tissue-derived mesenchymal stem cells' at the Mark Liveris Student Research Seminar held at Curtin University, Western Australia, Australia on 11th November 2014

2014 Poster presentation on 'Wnt antagonist secreted frizzled-related protein 4 (sFRP4) upregulates adipogenic differentiation in human adipose tissue-derived mesenchymal stem cells' at 32nd International Wnt Meeting organized by EMBO, held at the Cable beach club resort, Broome, Western Australia, Australia from 6th-9th October 2014

2013 Attended the Mark Liveris Student Research Seminar held at Curtin University, Western Australia, Australia on 11th November 2013

2013 Attended the Eighth State Cancer Conference, Western Australia, Australia held on 24th October 2013

2013 Attended the Research Symposium organized by Centre for Cell Therapy and Regenerative Medicine (CCTRM) on 19th April 2013 at University of Western Australia, Western Australia, Australia

# THESIS LAYOUT

- This thesis comprises of 7 chapters and is divided into – Introduction, Review of Literature, Materials and Methods, 3 experimental chapters, general discussion, references, and appendices.

- The 3 experimental chapters – Chapter 4, 5, and 6 are based on each of the Aims.

    - Chapter 4 describes the 1st Aim and within this chapter, is divided into:
        - Part-I - Preliminary screening and characterisation of ADSC-CM
        - Part II – ADSC-CM combined with sFRP4
        - Part III – ADSC-CM combined with sFRP4 peptides

    - Chapter 5 describes the 2nd Aim and within this chapter is divided into:
        - Part-I – TCM combined with sFRP4
        - Part II – TCM combined with sFRP4 peptides

    - Chapter 6 describes the 3rd Aim

The general discussion chapter – Chapter 7, is further divided into discussion, conclusion, limitations, and future perspectives of this study.

# ABSTRACT

The findings reported in this thesis describe the various interactions that can occur in a breast tumour environment between the tumour cells and non-tumour cells. Adipose-derived mesenchymal stem cells (ADSCs) being the locally resident mesenchymal stem cell (MSC) population may be the initial responsive cells homing and interacting with the tumour site. Herein, in this study the effect of the paracrine factors secreted from ADSCs on breast tumour growth are described. It was observed that the ADSC conditioned medium (ADSC-CM) and ADSC extracellular matrix (ADSC-ECM) exhibited specific anti-tumour activity on the viability of breast tumour cell lines MCF7 and MDA MB 231.

Probing the inhibitory activity of ADSC-CM, it was demonstrated that the inhibitory activity of ADSC-CM originated from a non-protein component present in the <30KDa fraction of the ADSC-CM. Correlating with the decrease in viability of both tumour cell lines in response to ADSC-CM treatment, there was also a reduction in the expression of the anti-apoptotic protein Bcl-xL. Conversely, the expression of the pro-apoptotic protein Bax was also upregulated (although not statistically significant).

Examining the underlying mechanisms, it was demonstrated that ADSC-CM mediated this effect through downregulating the Wnt signalling pathway via reducing the expression of the active β-catenin in both tumour cell lines. ADSC-ECM also reduced the expression of Wnt target proteins such as cyclin D1 in MCF7

cells. However, MDA MB 231 cells did not display a significant downregulation in cyclin D1 levels in response to ADSC-CM, which could be correlated to the superior aggressive and invasive property of this cell line as compared to MCF7. Corroborating with this finding, it was also observed that ADSC-CM did not affect the migratory property of MDA MB 231, whereas it significantly reduced the migration of MCF7 cells.

Further to the effect of ADSC-CM on apoptosis-related protein levels, it was shown that ADSC-CM induces the tumour cells to enter the mitochondrial pathway of apoptosis, observed by a reduction of the transmembrane potential of the mitochondria. This is indicative of a mitochondrial membrane disruption leading to an exchange of ions with the cytosol and resulting in the reduction of mitochondrial membrane potential. It was also shown that ADSC-CM induced an increase in the caspase 3/7 activity in both tumour cell lines. MCF7 cells were associated with a pronounced increase in caspase 3/7 activity, as compared to MDA MB 231 cells. However since MCF7 is a caspase-3 deficient cell line, the observed increase could be attributed to compensatory increased activation of caspase 7 enzyme activity. In MDA MB 231 cells, the increase in caspase 3/7 activity in response to ADSC-CM was not pronounced, indicating that an alternative cell death pathway is occurring in MDA MB 231, which may not require the activation of caspases, such as the apoptosis-inducing factor (AIF)-mediated pathway reported in MDA MB 231 cells [1]. The levels of reactive oxygen species in tumour cells following ADSC-CM treatment were reduced. This could be associated with earlier reports correlating reduced ROS levels to decreased cell viability and reduced glycolytic activity.

Since Wnt signalling is one of the major pathways driving breast cancer progression, this study also examined the effect of Wnt inhibition on tumour cells and also in combination with ADSC-CM. The Wnt antagonists of interest were secreted frizzled-related protein 4 (sFRP4) and its two associated peptides SC301 and SC401, derived from its cysteine-rich domain and netrin-like domain respectively. It was observed that these Wnt antagonists affected the tumour growth resulting in reduced tumour cell viability. ADSC-CM used in combination with sFRP4 and in combination with SC301 + SC401 further reduced the cell viability of both tumour cell lines as compared to ADSC-CM alone. However, when the combination treatments (ADSC-CM with the Wnt antagonists) were performed for downstream assays, there was little or no further enhancement in their effect. There was a further downregulation in the active β-catenin expression in MCF7 cells when ADSC-CM was combined with sFRP4. In MDA MB 231 cells, there was an enhanced activation of caspase 3/7 enzymes when ADSC-CM was combined with sFRP4 and when ADSC-CM was combined with SC301. This could be because the initial increase in caspase activation due to ADSC-CM alone was not pronounced, hence there was a possibility of further increase. This was not the case in MCF7 cells, where there was an existing pronounced increase in caspase 3/7 activity due to ADSC-CM alone.

Next, this study demonstrated the change in the phenotype of ADSCs while exposed to the paracrine factors derived from the tumour cells. ADSCs were exposed to tumour conditioned medium (TCM) derived from MCF7 and MDA MB 231 cells for a short-term (4 days) and longer-term (10 days) duration. It was demonstrated that the TCM, irrespective of the cell line it was derived from, resulted in a change in the phenotype of ADSCs. An increase in their cell viability rates was observed following

treatments with TCM. Further, TCM also increased the mesenchymal marker expression in ADSCs, observed by an increase in α-SMA and vimentin expression. TCM also changed the metabolic characteristics of ADSCs, making the cells more glycolytically-driven as observed by an increase in extracellular acidification rate (ECAR) (using glycolysis stress test in a Seahorse Bioanalyser) as compared to the control ADSCs. This was also correlated to the increased glucose uptake rates observed in TCM-treated ADSCs as compared to the control ADSCs. Addition of Wnt antagonists did not revert the increased glycolytic drive observed in TCM-treated ADSCs, suggesting that Wnt antagonists were not involved with the change in metabolic phenotype of ADSCs.

Further, the effect of Wnt antagonism on the physiological function of ADSCs, i.e. adipogenic differentiation was also determined. It was observed that sFRP4 promoted the adipogenic differentiation of ADSCs, observed by an increase in lipid accumulation and adipogenesis-specific marker expression in ADSCs. This promoting effect was countered in the presence of Wnt activators such as BIO. As ADSCs are the predominant MSC population in breast, the effect of sFRP4 on the viability and differentiation potential of ADSCs is crucial before considering the use of sFRP4 as an anti-cancer agent for the treatment of breast cancer.

Overall, this thesis unravels the crosstalk occurring between ADSCs and tumour cells, reflective of an *in vivo* tumour environment. Understanding the crosstalk is also important in confirming the safety of ADSCs-based reconstructive therapies. For instance, ADSCs are being used as cellular adjuncts in autologous fat grafts for reconstructive surgeries postmastectomy in breast cancer patients. Further, this study

unravels the potential clinical application of using the paracrine factors derived from ADSCs in cell-free anti-cancer therapies as well as to use Wnt antagonists as anti-cancer agents. The previous reports on the specific tumour-homing property of ADSCs should be taken into account to exploit the possibility of using ADSCs as 'delivery vehicles' to deliver the Wnt antagonists such as sFRP4 or its peptides SC301 and SC401 specifically to the tumour site. For such applications, understanding the mechanisms of Wnt antagonism with respect to viability and differentiation potential of ADSCs is critically important.

# Chapter 1 - INTRODUCTION

Mesenchymal stem cells (MSCs) have attracted recent attention regarding their role in influencing tumour progression. MSCs are capable of influencing tumour progression by being a part of the tumour supportive stroma as well as through their paracrine interaction with the tumour cells. This study was designed to understand these various aspects of crosstalk between these non-tumorigenic MSCs and tumour cells.

Adipose-derived MSCs (ADSCs) were used as the MSC model and their interaction with breast tumour cells was studied. Considering the proximity of ADSCs to the breast tumour site, ADSCs may be the major population of cells that interact with and influence the breast tumour cells. Breast cancer is one of the most frequent cancers affecting women worldwide. In Australia, 1 in 8 women have had breast cancer by 85 years of age, indicating the high clinical significance of studying the underlying mechanisms of tumour development and progression.

ADSCs may affect tumour progression either by secreted factors or by upholding intercellular crosstalk with the tumour cells, thereby exerting a prominent influence on the tumorigenic components. Emerging evidences on the tumour-inhibitory properties of MSCs/ADSCs have brought these cells into the spotlight. Hence, it is fascinating to understand the nature of the interaction that ADSCs exert on tumour cells, in the light of devising a novel therapeutic approach against cancer. It has prompted this study to explore the influence of ADSCs and their large spectrum of secreted factors on various aspects of breast tumour cell growth. The effect of the

conditioned medium obtained during ADSC growth was examined on breast tumour cells and it was determined whether this effect was pro-tumorigenic or anti-tumorigenic.

However, the possibility of ADSCs altering their phenotype towards a tumour-supporting profile while being in a tumour environment cannot be excluded. ADSCs or MSCs in general have been shown to transform into a tumorigenic phenotype in order to facilitate progression of the disease. Therefore, in this study, the possible stimulus triggering these transformations and their regulation was investigated. Controlling this transformation may further empower efficient use of ADSCs in devising a novel therapeutic approach against cancer. ADSCs were exposed to conditioned medium derived from tumour cells simulating a tumour environment to determine whether ADSCs transform into tumour-associated fibroblasts (TAFs) under such stimuli.

Investigating both these bifurcated routes determines the implications of paracrine factors derived from ADSCs on tumour cells and vice versa and confirms the definitive role of ADSCs in regulating breast cancer - whether ADSCs secrete factors to influence tumour growth or whether they undergo spontaneous transformation in order to exert their influence on breast cancer progression.

After determining the role of ADSCs in breast tumour growth, the next approach was to check whether the above interactions or transformations could be controlled using Wnt antagonism. The influence of Wnt signalling on breast tumour cell growth and on its interaction with ADSCs were determined using the Wnt antagonist secreted frizzled-related protein 4 (sFRP4) and its peptides SC301 and SC401 to examine their role in modulating the ADSC-breast tumour cell interactions.

Additionally, the role of sFRP4 in influencing the adipogenic differentiation of ADSCs were examined. It revealed the effect of sFRP4 on ADSCs themselves, which becomes useful when devising therapeutic strategies using sFRP4 in a breast tumour environment. In such a scenario, understanding the effect of sFRP4 on the surrounding non-tumorigenic cells in the tumour microenvironment is crucial. The information obtained may help to understand the overall effect sFRP4 may exert on the tumour environment as a whole rather than just on the tumour cells.

Hence, the overall focus of the study was to elucidate the factors and the mechanisms by which ADSCs and Wnt antagonism regulate breast tumour progression, reflective of an *in vivo* condition. The various interactions that could be happening in the tumour stroma and the effect of Wnt antagonists on these various interactions were elucidated. This information may be useful in determining the action and therefore the future use of Wnt antagonists or ADSCs as therapeutic strategies for fighting cancer.

# Chapter 2 – REVIEW OF LITERATURE

## 2.1 Mesenchymal stem cells - Sources & Properties

Mesenchymal stem cells (MSCs) are multipotent progenitors capable of self-renewal and differentiation to mesenchymal cell lineages [2]. They have been isolated from various sources such as bone marrow (BM-MSCs) [3], adipose tissue [4], umbilical cord tissue (UC-MSCs) [5], periodontal ligament [6], synovial membrane [7], menstrual fluid [8], and dental pulp [9]. Bone marrow was the earliest identified source of MSCs [10], while other sources have been discovered in recent years. Although BM-MSCs have been widely studied, their use is limited by several factors, including the invasive surgery required for their collection and subsequent patient discomfort. Considering available sources of MSCs, adipose tissue presents a good reservoir of MSCs in adequate numbers that could be procured at frequent intervals, with the source being replenishable.

Adipose-derived MSCs (ADSCs) obtained from lipoaspirate were first isolated from the stromal-vascular fraction and then were confirmed to possess the characteristics of MSCs (self-renewal and multi-lineage differentiation into adipogenic, osteogenic, and chondrogenic lineages) [4, 11]. Cardiac, neurogenic, and hepatogenic differentiation of ADSCs has also been demonstrated [6, 12, 13].

In this study, the influence of ADSCs in an *in vitro* breast tumour microenvironment was examined by utilising soluble and insoluble secreted factors derived from

ADSCs. Adipose tissue being the most abundant stromal component of the breast, the role of ADSCs in breast cancer development needs to be explored [14, 15]. Given the proximity, human ADSCs may be relevant to breast cancer and can directly interact with tumour cells [16, 17]. ADSCs have been reported to interact with tumour cells either directly via cell-cell contact or in a paracrine manner, stimulating the release of various chemical messengers crucially affecting tumour growth [18-20].

## 2.2 MSC-derived factors

### 2.2.1 Conditioned Medium

In support of the concept of paracrine communication between MSCs and cancer cells, MSC-conditioned medium (MSC-CM) has been found to have diverse effects on tumorigenesis and other biological processes. For instance, secreted factors from ADSCs have been demonstrated to enhance the apoptosis and chemosensitivity of SKBR3 breast cancer cells when co-cultured with ADSCs or exposed to ADSC-conditioned medium in the presence of doxorubicin or 5-fluoruracil [21]. CM from human lung-derived MSCs has been demonstrated to exert inhibitory activity on H28, H2052, Meso4 mesothelioma cell lines by decreasing their cell viability [22]. CM from UC-MSCs and ADSCs inhibited the growth of U251 human glioma cells by inducing apoptosis [23]. Secretion of chemical messengers such as chemokines, and cytokines are often responsible for paracrine activity between these cells. It was found that UC-MSCs and BM-MSCs secreted a wide spectrum of cytokines such as

interleukin-6 (IL-6), interleukin-8 (IL-8), monocyte chemoattractant protein-1 (MCP-1), tissue inhibitor of metalloproteinase (TIMP)-2, and vascular endothelial growth factor (VEGF) [24]. The secretion of IL-6 (predominantly), along with other cytokines such as ENA-78, IL-β1, IL-8, MCP-1, RANTES, VEGF, fibroblast growth factor-4 (FGF-4), hepatocyte growth factor (HGF), TIMP-1, has also been reported [25].

### 2.2.2 MSC-Extracellular Matrix

The local microenvironment at the tumour site plays a pivotal role in shaping the overall progression of the disease. The extracellular matrix (ECM) secreted by the tumour cells and adjacent non-tumour cells is an important component of the tumour microenvironment and can regulate tumour growth. Sun et al., demonstrated that the ECM derived from UC-MSCs inhibited the proliferation of MDA MB 231 breast cancer cells by upregulating their expression of phosphatase and tensin homolog (PTEN) [26].

## 2.3 MSCs and Cancer

### 2.3.1 Tumour homing property of MSCs - Potential for clinical applications

MSCs have attracted much attention in the last decade due to their potent role in anti-cancer therapies. MSCs have been considered for these clincial applications due to their targeted tropism towards sites of injury, inflammation, and tumours [27-30], which is facilitated by the secretion of chemokines from the tumour environment [31].

The tumour-targeted tropism of MSCs has been studied in various tumour models. In an *in vivo* model of Kaposi's sarcoma, it was shown that MSCs migrate to sites of tumour growth [32]. The specific tumour-homing potential of BM-MSCs was further demonstrated in a murine model of intracranial glioma, wherein the non-MSCs caused a systemic distribution with no tumour specificity [33]. It was shown that the tumour site preferentially permitted the engraftment of MSCs [28]. The tumour-homing property of MSCs was further boosted by attaching an artificial receptor on the MSC surface that bound specifically to the tumour cell marker erb2, resulting in an improved binding of MSCs to the erb2-expressing tumour cells as compared to MSCs lacking the modification. Extrapolating these findings into developing a novel delivery strategy will aid in having increased numbers of MSCs carrying a therapeutic agent to the tumour site, and hence, improve the outcome of cell-based therapy [34]. The homing property of MSCs has been non-invasively imaged using *in vivo* bioluminescent imaging in mice injected with MSCs expressing firefly luciferase, and the MSCs were found to be present within sites of tumour

development [35]. Extensive *in vivo* migration of ADSCs towards the tumour site was seen in glioma-bearing mice [36]. Further evidence of MSCs' homing capabilities has been found in hepatocellular carcinoma when MSCs were present in higher numbers in the tumour tissue compared to the adjacent tissues [37].

In the *in vitro* environment, it has been reported that the presence of specific angiogenesis-related factors in the tumour environment can modify the *in vitro* tropism of MSCs towards U87 glioma cells [38]. Both BM-MSCs and ADSCs have been shown to migrate to glioma cells with an equal efficiency [39]. It has been shown that MSCs resident in the local breast tumour environment have a strong affinity towards the conditioned medium of the MCF7 and MDA MB 231 breast cancer cell lines [40], indicating the interaction of ADSCs with the breast tumour environment.

The highly specific nature of MSCs in migrating to the tumour site forms the basis for considering MSCs to be used as delivery vehicles harbouring chemotherapeutic agents (Figure 2.1). This would result in an efficient delivery of the therapeutic agent locally at the tumour site at the concentrations required to maximise the anti-tumour effect (Figure 2.1). At the same time, it helps to avoid the systemic distribution of the therapeutic agent. Thus, it aids to minimise any undesirable side-effects such as toxicity, and counteracts other known issues of drug delivery, such as their short-half, by ensuring a continuous supply of the drug as MSCs proliferate at the tumour site.

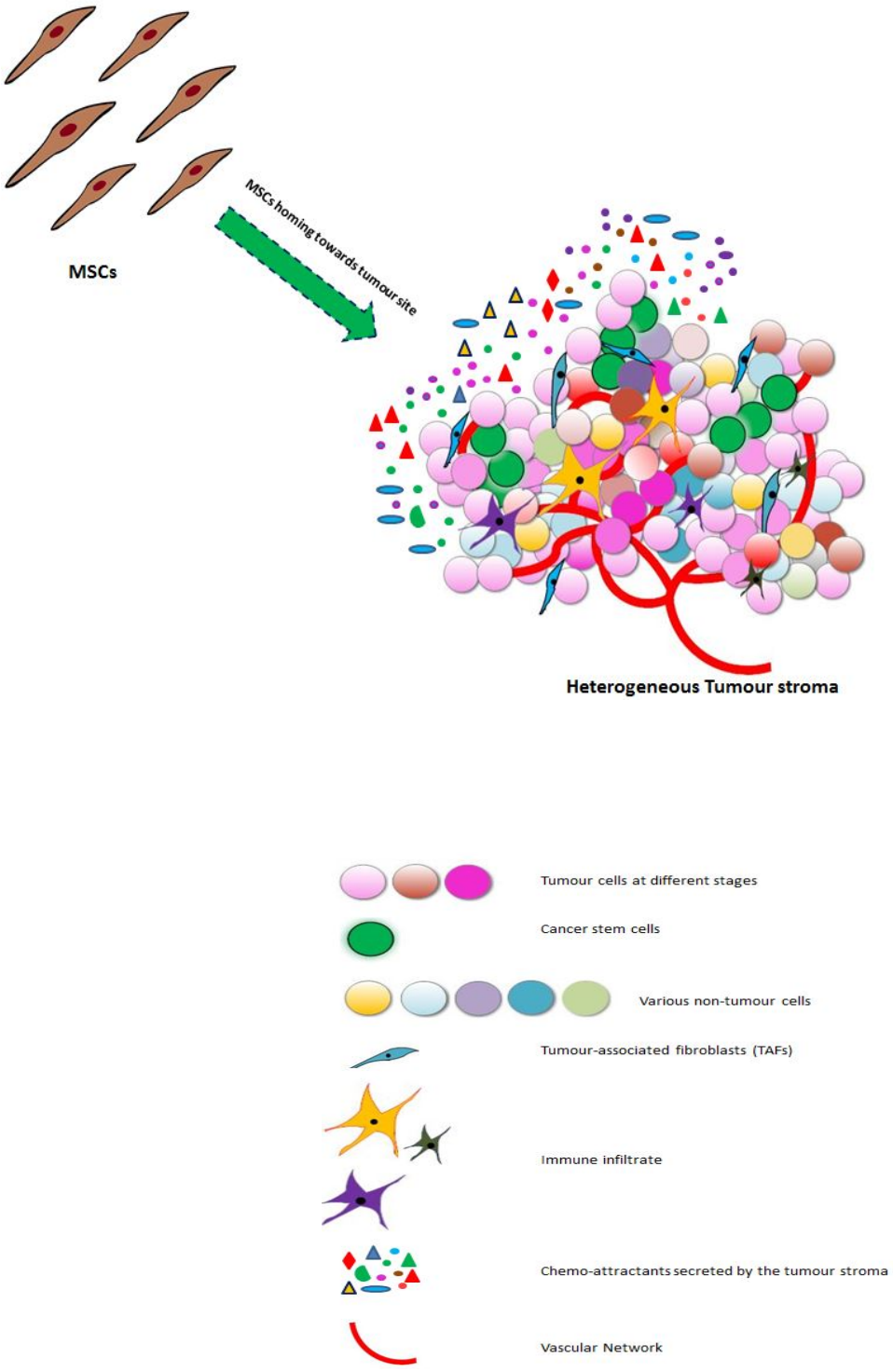


**Figure 2.1 Homing of MSCs towards tumour site**

Schematic representation of the homing potential of MSCs towards the tumour site in response to the chemotactic factors secreted in the tumour environment (Design template inspired from [41] and completely re-drawn)

### 2.3.2 Therapeutic approaches using MSCs as delivery vehicles

Due to the tumour-specific homing nature of MSCs, various studies have reported the use of MSCs as delivery vehicles to transport anti-cancer therapeutics. MSCs engineered to express Interferon-β (IFN-β) have been used as vehicles to deliver IFN-β locally at the site of the tumour [28], and to effectively reduce pulmonary metastases in mice [42]. MSCs designed to carry and release IFN-β were also found to be effective against human glioma cell lines, and were associated with an extended survival time when tested in a murine model of intracranial glioma [33]. In a canine model of melanoma, it was found that IFN-β overexpressing ADSCs, along with a low dose of cisplatin, resulted in high rates of tumour cell apoptosis [43]. Another study used MSCs to deliver the anti-angiogenic factor pigment epithelial derived factor (PEDF), which resulted in increased apoptosis in a murine model of intracranial glioma, with extended survival of the mice [38]. Placental-derived MSCs (PD-MSCs) modified to express PEDF, inhibited angiogenesis and increased the rates of apoptosis when injected into a mouse model of melanoma [44]. Another study demonstrated an anti-tumour effect when genetically modified MSCs were used to increase thymidine kinase expression [45]. Other sources of MSCs such as human foetal MSCs have been used as carriers for gene delivery [46]. MSCs modified to express tumour necrosis-related apoptosis inducing ligand (TRAIL) have been shown to have anti-cancer effects on several tumours including cervical cancer [47]. Similarly, TRAIL-ADSCs have been shown to induce cell death in multiple myeloma cells, which was accompanied by caspase-8 activation [48]. TRAIL-induced ADSCs have also been shown to produce short-term and long-term tumour inhibitory effects in brainstem gliomas, causing a reduction in tumour volume and

prolonging the survival duration respectively [49]. Also, MSCs engineered to express Il-12 showed tumour-suppressing activity in a mouse melanoma model and prevented the development of lung metastases [50]. The above anti-tumour effects contributed by engineered MSCs are listed in Table 2.1.

**Table 2.1 Various anti-tumour effects generated by engineered MSCs**

| **Chemical messengers generated by engineered MSCs** | **Tumour type** | **Effect on tumour** | **References** |
|---|---|---|---|
| IFN-β | Melanoma & Breast cancer | Reduced pulmonary metastases in mice | [42] |
| IFN-β | Intracranial glioma | Extended survival time of mice | [33] |
| IFN-β | Canine melanoma | Enhanced tumour cell apoptosis in combination with cisplatin | [43] |
| PEDF | Intracranial glioma | Enhanced tumour apoptosis and extended survival time of mice | [38] |
| PEDF | Melanoma | Increased apoptosis and inhibited angiogenesis in mice | [44] |

| | | | |
|---|---|---|---|
| Thymidine kinase | Prostate cancer | Inhibited growth of subcutaneous PC3 prostate cancer xenografts in nude mice | [45] |
| TRAIL | Cervical cancer | Apoptosis of tumour cells | [47] |
| TRAIL | Multiple myeloma | Increased tumour cell apoptosis | [48] |
| TRAIL | Brain stem gliomas | Reduction in tumour volume and increased survival time | [49] |
| IL-12 | Melanoma | Reduced lung metastases | [50] |

### 2.3.3 Importance of MSC-Tumour Crosstalk in the Tumour Microenvironment

Before considering MSCs for clinical applications in delivering anti-cancer therapeutics, it is important to gather a detailed understanding of their influence on the respective cancer cells while in their naïve state. The interaction of MSCs with tumour cells will also add an insight into the cellular crosstalk occurring during physiological conditions. Hence, studying the influence generated by MSCs on tumour cells is of utmost importance to unravel the molecular mechanisms occurring in a tumour microenvironment.

The tumour environment has a complex heterogeneous milieu where the tumour growth is not completely controlled by the tumour cells alone, but in fact various

other non-tumour cells play a vital role. The non-tumour cells consist of MSCs, tumour-associated fibroblasts (TAFs), macrophages, endothelial cells, pericytes, dendritic cells, and lymphocytes [51, 52]. Amongst these, MSCs form a major population influencing tumour growth, and the crosstalk between MSCs and the tumour environment has received a lot of clinical attention. The complex relationship between ADSCs and breast tumour cells has been well documented [53]. The ways in which MSCs impact the various hallmarks of tumour growth could be by cell-cell communication, paracrine signalling by secretion of specific moieties, conversion into TAFs, and influencing the angiogenic potential of the tumour cells [16, 54, 55]. Contradictory reports on the tumour supportive and tumour inhibitory roles of MSCs on cancer cells have been documented previously, and will now be discussed.

Understanding the interaction between ADSCs and breast cancer cells also have relevance in terms of their regenerative aspect. To overcome the drawbacks of conventional fat grafting, ADSCs have been used as cellular adjuncts, which improved the retention and the outcome of autologous fat grafting and cell-assisted lipotransfer [56-59]. However, the possibility of ADSCs influencing the growth of the residual tumour cells and hence the overall clinical outcome should not be neglected before warranting its use in therapeutic approaches.

### 2.3.4 Effects on tumour cells – Anti-tumour effect

As previously reported, MSCs exhibited anti-tumorigenic properties by inhibiting protein kinase B [60] activation through cell-cell communication [32]. It was found that glioma cells co-injected with MSCs resulted in a less vascular and smaller

tumour in an *in vivo* model, while conditioned medium from the MSC-glioma culture decreased the angiogenic potential of endothelial cells by downregulating the platelet-derived growth factor (PDGF)/PDGF-receptor network [19]. It was found that microvesicles secreted from BM-MSCs were capable of inhibiting the growth of various tumour cell lines such as the hepatoma cell line Hep G2, Kaposi's sarcoma, and ovarian cancer cell line Skov-3. Further, MSC-derived microvesicles also inhibited tumour growth when these tumour cell lines were injected into severe combined immunodeficiency mice [61]. MSCs were shown to improve the chemosensitivity and apoptosis rates of SKBR3 breast cancer cells when exposed to ADSCs or their conditioned medium [62]. ADSCs, when cultured at a high density, expressed IFN-β, and thereby exhibited an inhibitory effect on MCF7 breast cancer cells [63]. Further, when MDA MB 231 breast cancer cells and BM-MSCs were co-cultured, BM-MSCs inhibited the growth of MDA MB 231 cells [64]. MSCs have been found to inhibit tumour proliferation by inducing apoptosis in a breast cancer model [65]. The growth inhibition of MSCs on non-solid tumours such as leukaemia has also been reported [66]. Moreover, the effect of MSCs on tumour cells can be very much context-dependent within the tissue environment. One study showed that co-culture of ADSCs with MCF7 breast cancer cells upregulated the tumour cell growth while the conditioned medium obtained from ADSCs inhibited the growth of MCF7 cells [67]. ADSC-CM has been shown to improve the therapeutic efficacy of anti-cancer chemotherapeutic drugs. For instance, a study demonstrated that human foetal MSCs possessed high levels of insulin growth factor binding proteins, which sequestered insulin-like growth factors and therefore inhibited the proliferation of hepatocellular carcinoma cells and improved the therapeutic efficiency of the chemotherapeutic drugs sorafenib and sunitinib [18].

A study on murine cancer cell lines such as the hepatoma H22, Lymphoma YAC-1 and EL-4, and the rat insulinoma INS-1 cell line, using mouse BM-MSCs, was found to generate anti-tumour effects both *in vitro* and *in vivo* [68]. Pre-activation of MSCs with tumour necrosis factor-α enhanced the anti-tumour property of MSCs by reducing the metastasis of breast cancer MDA MB 231 cells to the lungs of mice [69]. Another means of cell-cell communication by which MSCs could affect tumour growth is via extracellular vesicles. It has been shown that microvesicles generated by human Wharton's jelly MSCs were inhibitory to bladder carcinoma cells both *in vitro* and *in vivo* [70].

With regards to Wnt signalling, it was found that actively proliferating breast cancer cells had a downregulated expression of the Wnt antagonist Dickkopf-1 (Dkk-1), resulting in an active Wnt signalling pathway [71]. Additionally, the role of Dkk-1 in breast cancer was further confirmed when Dkk-1 secreted by MSCs derived from the dermis tissue of a dead human foetus inhibited the growth of the breast cancer cell line MCF7 by antagonising the Wnt signalling pathway [72]. Additionally, the same MSCs were used for co-culture and for harvesting conditioned medium to study their effect on two hepatoma cells lines H7402 and HepG2, and found it to be inhibitory to tumour cell growth [73]. In a previous study from the same group, it was found that the conditioned medium from human foetus-derived MSCs inhibited the proliferation of MCF7 breast cancer cells [74]. A further study demonstrated that the secretion of Dkk-1 by ADSCs was responsible for their tumour-inhibiting property on K562 myelogenous leukaemia cells, and that neutralising or silencing Dkk-1 resulted in attenuation of this anti-tumour effect [75].

It has been suggested that the effects contributed by MSCs could be arising from the secreted factors present in the MSC conditioned medium, and this could alleviate the need for devising cell-based therapies involving the administration of cells [76].

### 2.3.5 Effect on tumour cells – Pro-tumour effect

There are a number of contrasting reports on the effects of MSCs on tumour growth, with evidence supporting a role of MSCs in tumour proliferation. One study reported that BM-MSCs upregulated the proliferation rates in 4T1 mouse breast cancer cells upon co-culture with mouse BM-MSCs or exposure to mouse BM-MSC-derived conditioned medium [77]. In the same study, it was demonstrated that human umbilical vein endothelial cells (HUVEC) developed more branched endothelial networks when exposed to conditioned medium derived from coculture of the DU-145 prostate cell line and BM-MSCs [77]. Similar promoting effects have been reported in the interaction of ADSCs with H460 or U87MG tumour cells under *in vitro* and *in vivo* conditions [78]. ADSCs have also been shown to promote growth of prostate cancer [79]. MSCs have been reported to promote the growth and metastasis of colon cancers [80], promote angiogenesis rates [81], and facilitate the development of colorectal tumours in mice [82]. One study showed the increased metastatic capacity in colon cancer cells due to ADSCs mediated through upregulated Wnt signalling [83]. It has been found that BM-MSCs contributed to tumour microenvironments [84] and promoted tumour cell proliferation through direct cell-cell interactions, and molecules such as PTK787/ZK 222584 reduced the promoting effect of MSCs [85]. Amongst the other cells present in a breast tumour

environment, stromal fibroblasts promoted tumour growth and angiogenesis through the secretion of stromal cell derived factor (SDF)-1/CXCL12 [86]. One study stated that breast tumour cells stimulated the production of SDF-1 from ADSCs, which in turn stimulated the C-X-C chemokine receptor type 4 (CXCR4) in the tumour cells to enhance their migration and invasion potential [17]. Angiogenic-promoting effects were also contributed by the conditioned medium of multipotent stromal cells, which resulted in decreased apoptosis, improved angiogenesis and survival by activating the PI3K-Akt signalling pathway [87]. Omental ADSCs promoted vascularisation in endometrial tumours [88], and enhanced growth and invasion of ovarian cancer cells [89]. It was found that MSCs induced epithelial-to-mesenchymal transition (EMT) in the breast tumour environment [90]. MSCs within the tumour environment were demonstrated to promote metastasis in breast cancer [91]. Another study revealed the supportive effect of BM-MSCs on breast cancer stem cells (CSCs), wherein MSCs augmented the breast CSC population by generating a cytokine network involving IL6 and CXCL7 [81]. A study demonstrating the role of secreted factors of MSCs on breast tumour development showed that exosomes (40-100nm vesicles) secreted in the MSC-conditioned medium promoted the migration of MCF7 breast cancer cells and resulted in activation of the Wnt signalling pathway [92].

Until now, the interaction of MSCs and tumour cells has resulted in contrasting reports, which may be attributed to the various sources of MSCs, differences in the tumour cell types, method of administration/treatment, and tumour micorenvironment, which determine the myriad chemical cues in the tumour stroma. Hence, the use of MSCs/ADSCs or their paracrine factors needs to be carfully studied while devising cell-based and cell-free therapeutic approaches respectively and the anti-tumour activities of ADSCs/ADSC-CM needs to be confirmed.

Otherwise, the alternative option could be to use ADSCs as delivery vehicles to carry and deliver anti-tumorigenic drugs to the tumour site. For this purpose, the effect of such anti-tumorigenic molecules on the viability and differentiation potential of ADSCs needs to be understood and the chances of ADSCs undergoing spontaneous oncogenic transformation needs to be alleviated.

## 2.4 Cancer

Cancer can be defined as a multi-step molecular disease, primarily characterised by the uncontrolled growth of cells out of a normal tissue, forming a neoplasm or tumour that later achieves a malignant status [93-95]. In brief, malignancy is the ability of such cells to perform limitless proliferation and invade other tissues to spread their abnormal growth. Cancer results when normal cells escape the reigns of tightly regulated growth mechanisms, leading to the accumulation of several genetic abnormalities and epigenetic dysregulations that may have developed due to various reasons. The whole process of developing cancerous tissues from normal tissues is termed carcinogenesis.

Cancer can be broadly classified into 5 major types depending on its cell of origin (Figure 2.2).

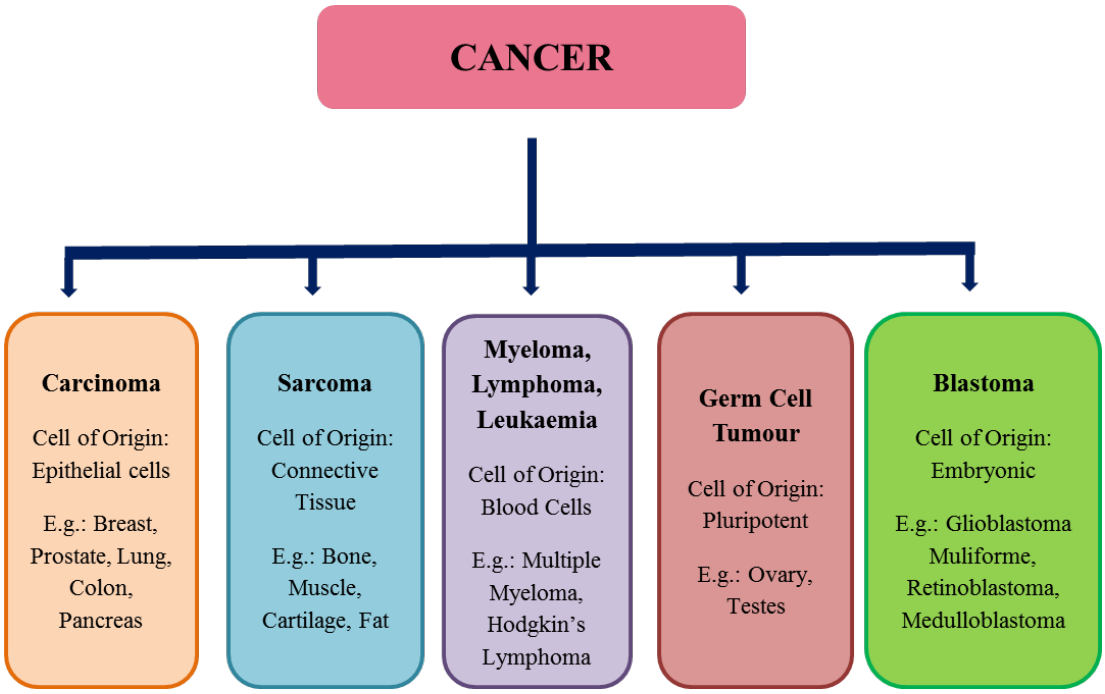


**Figure 2.2 Classification of types of cancer**

Cancers classified broadly into 5 major types based on their cell of origin – Carcinoma [96-99], Sarcoma [100, 101], Haematological malignancies [102-105], germ cell tumour [106-108], and blastoma [109-113].

### 2.4.1 Hallmarks of Cancer

The 10 hallmarks of cancer reported in previous studies are summarised in Figure 2.3 and the key attributes are described below.

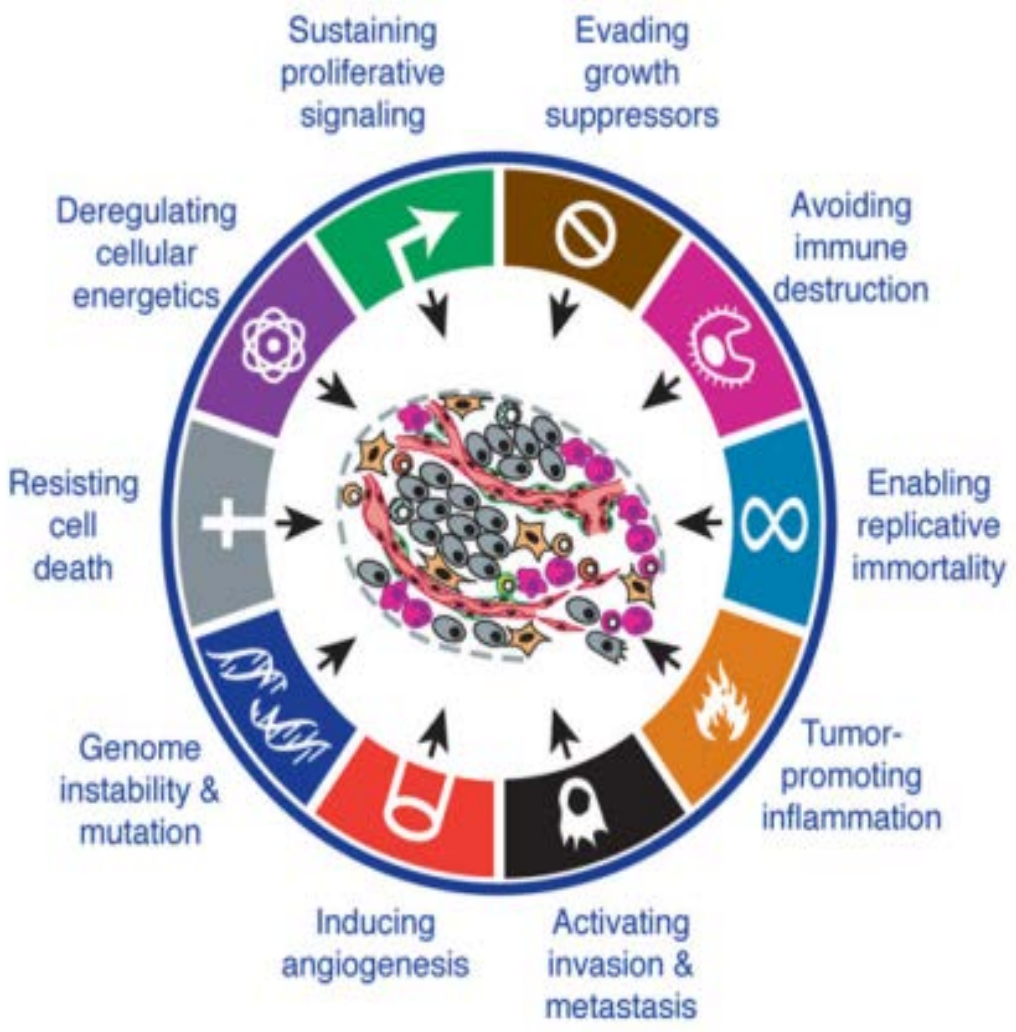


**Figure 2.3 Hallmarks of cancer**

Key characteristics associated with cancer cells are described within the hallmarks of cancer [114].

#### 2.4.1.1 Sustaining proliferative signalling

Tumour cells are independent of proliferative signals from the tissue microenvironment, which are normally required by non-tumour cells to grow and expand. Tumour cells develop the potential to secrete their own set of growth factors. Such independency from external growth signals results in the escape of tumour cells from normal homeostatic mechanisms, resulting in aberrant cell proliferation [115].

#### 2.4.1.2 Evading growth suppressors

The anti-growth mechanisms that maintain homeostasis in a normal tissue are evaded in the case of cancerous tissue. The retinoblastoma protein (pRb) pathway plays a major role in generating anti-growth signals in normal tissues, which works by altering the functionality of the E2F transcription factors, resulting in the inhibition of genes required for cell cycle progression from G1 to S phase [116]. In the case of a cancer cell, the pRb pathway is inhibited, resulting in an active E2F transcription factor that does not block their cell cycle progression [114].

#### 2.4.1.3 Evading immune destruction

Avoiding immune surveillance has been recognised as one of the emerging hallmarks of cancer [114]. Both innate and adaptive arms of the immune system have been shown to play a role in tumour eradication. This is substantiated by the fact that the

incidence rates of cancer have been demonstrated to be higher in immunocompromised individuals [117]. Also, it was observed in animal models that deficiency of immune system components or combined immunodeficienies in T cells and Natural killer cells led to an increased incidence of carcinogen-induced tumours [118, 119]. Cancer cells have been shown to perform this by secreting transforming growth factor-β (TGF-β) or other immune-suppressive factors thereby inactivating the immune components [120, 121].

#### 2.4.1.4 Enabling replicative immortality

The most characteristic feature of tumour cells is their ability to continue limitless proliferation at non-physiologic rates. The presence of consistently active growth-promoting oncogenes and the above factors – self-sufficiency in growth signals, disrupted tumour suppressor genes, altered interaction with the ECM, evasion of anti-growth signals, and evasion of apoptosis, all contribute to developing the boundless proliferation rates of cancer cells [115].

#### 2.4.1.5 Tumour-promoting inflammation

Tumour-associated inflammation has been recognised as another hallmark of cancer [114]. Tumours have been identified to be heavily infiltrated by cells of the immune systems reflecting the conditions seen during inflammation in non-neoplastic tissues [31]. Tumour-associated inflammation enhances tumour progression by various

means, such as providing growth factors, proangiogenic molecules, and ECM-modifying enzymes, thereby assisting in tumour invasion and metastasis [122-124].

#### 2.4.1.6 Activating invasion and metastasis

Cancer cells have the innate capability to invade the surrounding tissues, migrate to distant sites, and establish new colonies at the secondary tumour site, which is a process termed metastasis. Metastasis requires the tumour cells to intravasate and enter the circulation to reach the new site, and then exit by extravasation. The systemic spread of cancer cells from the primary tumour site is the major reason underlying deaths from cancer [125]. The mechanisms behind the heightened invasive potential of cancer can be varied. One of them is the loss of E-cadherin expression from the surface of epithelial cancer cells. E-cadherin is a cell-cell adhesion molecule connecting two epithelial cells and is required to keep cell behaviour in check. In the tumour environment, E-cadherin expression is lost, allowing the cells to migrate freely, thus aiding in the acquisition of invasive and metastatic capabilities [115, 126]. This process of changing the phenotype and adhesion molecule expression patterns on the cell surface is termed epithelial-to-mesenchymal transition (EMT). For instance, in breast cancer, the epithelial breast cancer cells change their morphology into a more mesenchymal phenotype, acquiring a spindle shape and developing extensive intercellular communications by forming gap junctions. These alterations allow the cancer cells to become more invasive and motile, and encourage metastasis.

Additionally, other cell adhesion molecules (CAMs) such as N-CAM weaken the cells' adhesive property in many tumours [127, 128]. The increased invasiveness can also be attributed to the presence of active proteases such as matrix metalloproteases on the cancer cell surface, helping them to push their way through the stroma in order to invade new areas [129, 130].

#### 2.4.1.7 Inducing angiogenesis

Tumour cells have the capability to induce and sustain the formation of new blood vessels from progenitor cells such as stem cells or endothelial precursor cells, so as to ensure a constant supply of nutrients and oxygen to the tumour site. This process is termed vasculogenesis or neovascularisation. Tumour cells can also induce angiogenesis, which is the sprouting of new branches of capillaries from the pre-existing endothelial cells (Patan et al., 2004). Angiogenesis is highly relevant during the metastasis of tumours to distant sites in the body. Angiogenesis accompanied with lymphangiogenesis, which is the formation of new lymphatic vessels, assists in the sustained supply of oxygen and nutrients to the secondary tumour site and the removal of waste products [131]. Such broadening of the blood capillary network aids in maintenance of the tumour bulk. Tumours achieve this by upregulating pro-angiogenic molecules such as VEGF and FGF2 and/or downregulating the expression of anti-angiogenic molecules such as thrombospondin-1 or IFN-β [115, 132-134]. The triggering of the angiogenic switch is an integral part of tumour development [115, 135].

One of the pioneering studies in this area indicated that when anti-angiogenic molecules were introduced into tumour-bearing mice, they caused a reduction of

tumour growth [132]. Anti-angiogenic therapy has been suggested for cancer treatment, which is generally administered at comparitively lower doses and more frequent intervals than conventional chemotherapy. It has been characterised by low or no toxicity and acts by killing the endothelial cells in capillaries surrounding the tumour sites [136].

#### 2.4.1.8 Genome instability and mutation

Carcinogenesis is a slow, multi-step, cellular transformation wherein genetic mutations are accumulated over time. One of the reasons could be attributed to defects in their cell cycle regulators [137], DNA repair, and cellular checkpoint mechanisms. The genetic alterations stem from abnormalities in balancing the expression of oncogenic and tumour suppressor genes. The activity of 2 checkpoint kinases, Chk1 and Chk2, which are normally active only during DNA damage, gets distorted during carcinogenesis [138]. The mutations in *Chk2* were first observed in Li Fraumeni syndrome [139]. Reports suggest that alterations in *Chk2* were found in families predisposed to breast cancer and colon cancer [140]. Defects in *Chk1* have been identified in only a few cancers [141-143].

#### 2.4.1.9 Resisting cell death

Apoptosis is defined as programmed cell death and is characterised by a specific, step-wise process beginning with breakdown of cytoplasmic and nuclear contents, extrusion of the cytoplasm, degradation and fragmentation of the chromosomes and nucleus [144]. Apoptosis has been characterised by distinct morphological features progressing through two stages, starting with the formation of apoptotic bodies that are eventually phagocytosed and degraded [145]. The formation of apoptotic bodies has been characterised by cell shrinkage, activation of endonucleases, cytoplasmic condensation, and nuclear fragmentation, ultimately activating the cysteine proteases (called procaspases) to generate an active caspase casacade that results in cell death [146, 147]. The mitochondria and the members of the Bcl-2 protein family tightly regulate these processes [148]. While cell death can alternatively occur via necrosis, apoptosis is a more energy-dependent and tightly regulated process affecting individual cells or cell clusters [149]. In instances where there is decreased availability of intracellular ATP or caspases, the cell death mechanism switches from an energy-dependent apoptosis into an energy-independent necrosis [149-151]. p53 is a tumour suppressor gene that controls non-physiological proliferation rates associated with DNA damage by upregulating the pro-apoptotic gene Bax, followed by the Bax-mediated release of cytochrome C from mitochondria, leading to the step-wise execution of later apoptotic events. In a cancer cell, *p53* remains inactivated, thus evading the above cell death inducing events [115].

#### 2.4.1.10 Deregualting cellular energetics

Deregulation of cellular energetics has been proposed as a major hallmark of cancer development [114]. Cancer cells metabolically adapt themselves and the cellular energetics is re-routed in order to provide for higher demand by the cancer cells to sustain their growth, proliferation, and biosynthesis of macromolecules. These metabolic changes include rapid glucose transport, reduced mitochondrial oxidative phosphorylation, along with increased aerobic glycolytic rate which is termed as the Warburg effect. Thus there exists a 'glycolytic switch' in the cancer cells to provide for their increasing metabolic needs [93, 152].

### 2.4.2 Stemness – Presence of Cancer stem cells

The maintenance of the tumour bulk in a cancerous tissue is facilitated by the presence of a cancer cell having a stem cell-like property, generally referred to as cancer stem cells (CSCs) or cancer stem-like cells. These CSCs play an important role in tumour maintenance and spread, as well as tumour recurrence. In a tumour environment, a CSC stems from either dedifferentiation of the differentiated tumour cells back into the stem cell state, transdifferentiation of normal cells to attain the CSC phenotype, or a differentiation of resident stem cells into the tumorigenic stem cell [153].

A CSC is known to possess the following properties [153]:

- Expresses cancer stem cell-specific surface markers

- Develops sphere-like structures upon *in vitro* culture
- Clonogenic potential
- Capable of initiating the recurrence of the tumour
- Resistance to conventional anti-cancer therapies such as chemotherapy or radiation

### 2.4.3 Supporting Tumour Stroma

Previously published evidence indicates that, during a cancerous condition, the microenvironment surrounding the cancerous tissue becomes significantly altered and plays a pivotal role in the maintenance and progression of the disease [31]. Tumour cells are capable of altering their integrin-mediated adhesion to the ECM by modifying the type of integrins expressed on the cell surface, which can bind to specific molecules in the ECM [154, 155]. These integrin receptors transmit growth promoting signals from the tumour microenvironment to promote tumour growth [115].

It was also demonstrated that the specific alignment of collagen could be used as a prognostic biomarker for breast cancer [156]. Additionally, alteration in collagen metabolism has been reported in many cancers [157]. Later, it was demonstrated that a higher interstitial pressure results in dampening the delivery of chemotherapeutic agents to the target site in pancreatic cancer [158]. The growth-promoting effects of desmoplasia, which is characterised by a dense fibrous ECM around the tumour site, was reported in breast tumour where it enhanced integrin-mediated

mechanotransduction, leading to an increase in phosphoinositide 3-kinase (PI3K) signalling [159].

The tumour microenvironment is composed of various cell types such as TAFs, (which are also referred to as carcinoma-associated fibroblasts (CAFs)), endothelial cells, fibroblasts, pericytes, and leukocytes, together with the ECM. Amongst these, the TAFs form a major population of the stromal component in breast and pancreatic carcinomas [160, 161] and are considered to be a factory of several pro-metastatic factors [162], that have been shown to promote tumour growth [163]. TAFs are a rich source of growth factors and mitogens such as HGF, epidermal growth factor (EGF), and FGF, which are capable of stimulating tumour cell proliferation [164]. TAFs also secrete survival cues such as insulin-like growth factor-1 and -2 [165, 166], and generate pro-angiogenic factors such as VEGF, FGF2, and SDF-1α, which stimulate angiogenesis in the tumour environment [86, 161, 162, 167, 168]. It has been found that TAFs play a role in altering the ECM composition in the tumour tissue, facilitating the generation of elongated collagen fibres and leading to a poor prognosis [169].

## 2.5 Human Breast

The research focus for this study is on breast cancer, and hence it is important to describe the basic biology and function of the human breast. Human breasts, otherwise known as the mammary glands, have a complex anatomy and are composed of predominantly the mammary glandular tissue, adipose tissue, and loose

connective tissue known as ‘Cooper's ligaments’ [170] (Figure 2.4). The breast is primarily a hormonally regulated lactating organ, and the physiological function of the breast tissue is to synthesise, secrete, and eject milk. The glandular tissue consists of numerous lactiferous ducts and lobes [171], where each lobe consists of many lobules with alveoli at one end [172]. Numerous (15-20) lactiferous ducts converge to form the nipple. The breast sits on the pectoralis major muscle, and the blood supply to the breast is supplied by the axillary, internal thoracic, and intercostal arteries [171].

### 2.5.1 Development of the Breast

Breast tissue development starts off with the formation of the mammary crest and mammary buds during embryonic development and later undergoes limited growth and maturation during infancy [170]. Upon reaching puberty and post-puberty, drastic changes take place within the mammary gland that are triggered by the ovulation and menstruation cycles, thereby facilitating enhanced breast development. This stage witnesses the elongation and branching of the existing ducts and formation of epithelial cell clusters at the end of each duct, which are called lobules [173, 174]. There is also an enhanced deposition of adipose tissue observed during this stage [175]. Further, the complete remodelling and full development of the breast are controlled by hormonal changes that take place during pregnancy and lactation, when it fully matures to be a functional lactating organ. At this stage, the epithelial cells in the ducts proliferate and differentiate into milk-secreting cells [176]. Involution of the fully developed breast occurs during post-lactation and later

at menopause [170]. Cessation of lactation is accompanied by regression and apoptosis of the epithelial cells and return of the breast to the non-lactating state [170]. The post-lactation involution may happen several times during the reproductive life of a woman after each pregnancy, but the final involution of the glandular tissue occurs during the menopausal period, when the glandular tissue is replaced by dense adipose tissue [177].

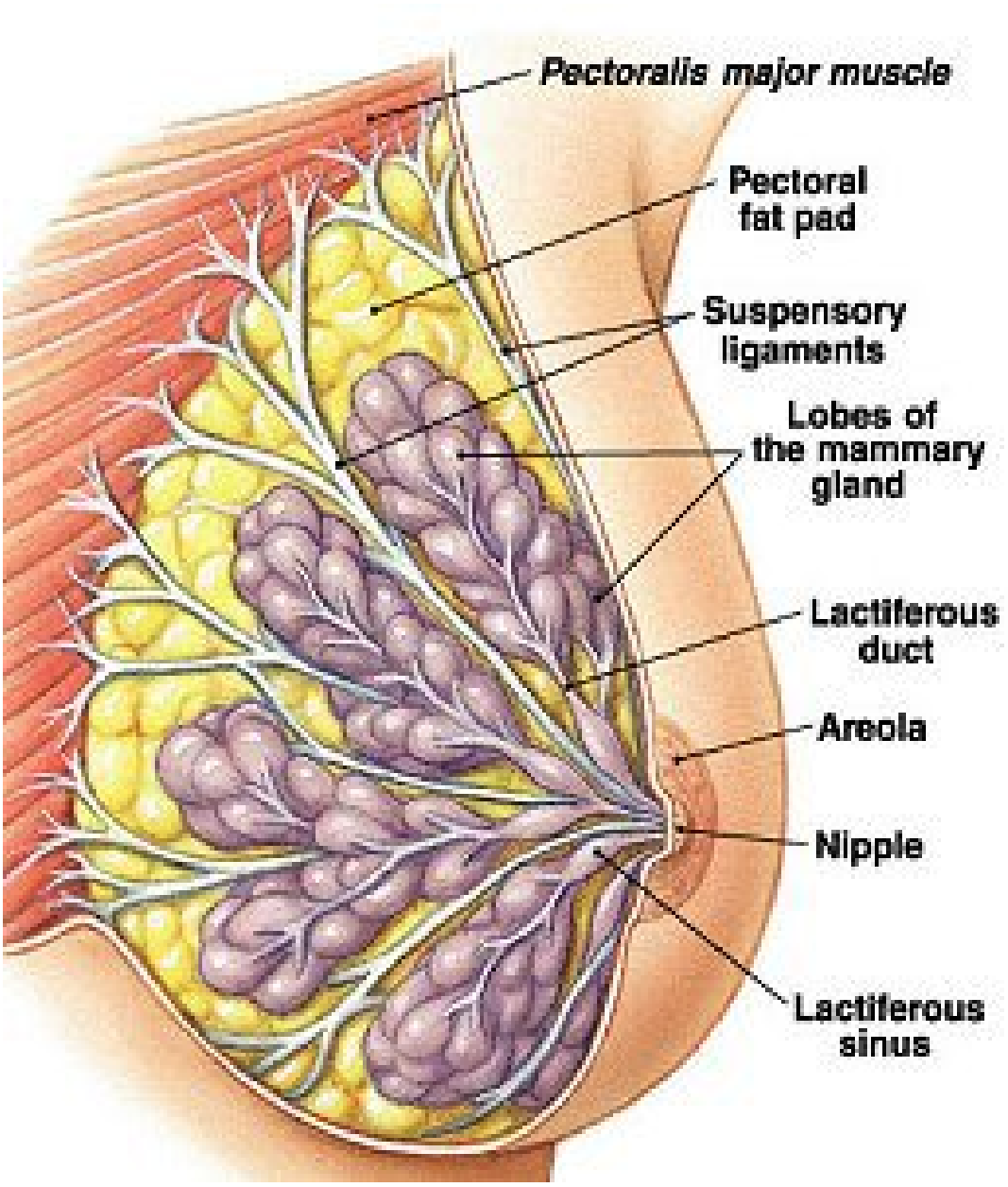

**Figure 2.4 Anatomy of the human breast organ**

**(Adapted from www.delrio.dcccd.edu)**

Different parts of the human breast are shown. The breast is mainly composed of glandular tissue comprising several groups of lobules resulting in lobes, amongst which the lactiferous ducts run. The breast tissue is physically supported by the pectoralis major muscle.

## 2.5.2 Breast Cancer

Breast cancer is the type of cancer originating in the mammary gland, mostly from the ducts and lobules. Breast cancer is a complex heterogeneous disease with various immunohistological and molecular sub-types present. Such heterogeneity results in varied clinical prognoses, therapeutic responses, and survival outcome. Hence, the treatment option vary with the specific sub-type presented. This, combined with its increased rates of occurrence and metastatic potential, makes it a major global health concern.

### 2.5.2.1 Incidence Statistics of Breast Cancer in Australia

The rates shown below are sourced from the Australian Institute of Health and Welfare (AIHW, 2014), Cancer Council Australia and World Health Organisation (WHO)-International Agency for Research on Cancer (IARC) GLOBOCAN 2012.

- Prevalence worldwide: Breast cancer is the second most commonly diagnosed cancer and the most frequent cancer in women [178]
- Prevalence in Australia: Breast cancer is the third most commonly diagnosed cancer and the most frequent cancer affecting every 1 in 8 Australian women
- Frequency of occurrence: In Australia, by the year 2020, the numbers are expected to rise to 17,210 women (47 women/day) from a current figure of 15,600 (42 women/day). It is generally uncommon in men, with only 145 men diagnosed in 2015 in Australia
- Mortality rates: Breast cancer is currently the second leading cancer-causing death in Australian women, preceded by only lung cancer (Cancer Council Australia website)

The greatest incidence rates of breast cancer are in countries such as Australia, North America, parts of South America, and Europe, and the lowest incidence rates occur in parts of Asia and Africa (Figure 2.5).

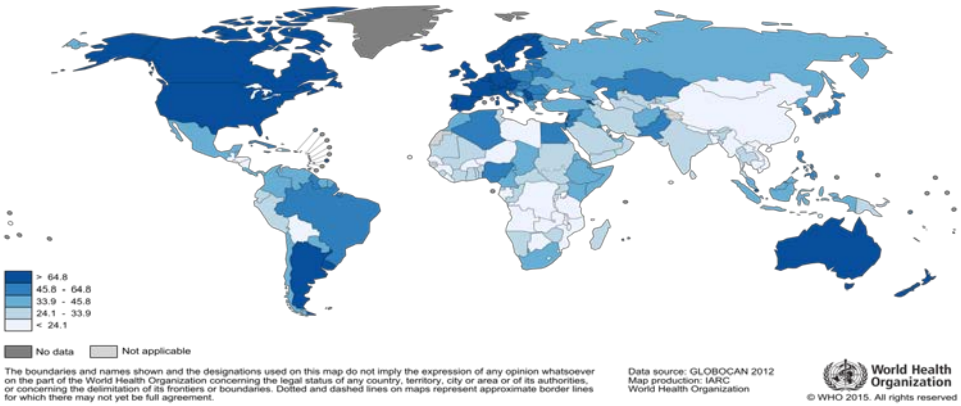


**Figure 2.5 Estimated incidence of breast cancer worldwide**

The estimated global incidence of breast cancer incidence in 2012 reported by WHO-IACR GLOBOCAN 2012.

## 2.5.3 Classification of Breast Cancer

Breast cancer can be classified based on various parameters (Figure 2.6) and has been reported in many previous studies [179-181]:

### 2.5.3.1 Invasiveness

Breast cancer can be broadly divided into invasive and non-invasive cancers. Among the latter, it can be further sub-classified into two types:

**i) Ductal carcinoma *in situ* (DCIS)**

Ductal carcinomas *in situ* are locally developed tumours confined within the ducts and have not invaded the surrounding tissue. It is the 'pre-invasive' stage of the carcinoma. DCIS has further been divided into 3 grades – low, intermediate, and high-grade DCIS.

**ii) Lobular carcinoma *in situ* (LCIS)**

Lobular carcinomas *in situ* are locally developed tumours confined within the breast lobules at the termini of the lactiferous ducts. LCIS is relatively less prevalent and mostly remains undetectable by mammogram.

Amongst the invasive carcinomas, they are further subdivided into groups based on their histopathological characteristics.

### 2.5.3.2 Histological subtypes of Invasive Breast Cancer

**i) Invasive ductal carcinoma**

Invasive carcinomas are aggressive tumours that grow out of the ducts or lobules and invade the surrounding breast tissue and regional lymph nodes, and then spread to distant organs during metastasis. 70-80% of breast cancers fall into this category.

**ii) Invasive lobular carcinoma**

Invasive lobular carcinomas are the second most commonly diagnosed breast cancer type, ranging in frequency from 5-10%.

Apart from these, the other invasive types of breast cancer include mucinous, papillary, medullary, micropapillary, and tubular.

**2.5.3.3.Molecular subtypes of breast cancer**

The molecular subtypes of breast cancer have been reported in many previous. Below is the classification of breast cancer based on its molecular subtypes. They are broadly classified into oestrogen receptor positive (ER+) and oestrogen receptor negative (ER-) [32], depending upon their oestrogen hormone dependency.

Further subtyping is done based on the presence of other hormone receptors, such as progesterone receptor (PR) [182], and genes such as human epidermal growth factor 2 (Her2)/ErB2.

**i) ER+ Breast Cancer**

- ER+ Luminal-like
    - Luminal A

- Luminal B

The ER+ luminal subtype is further sub-divided into Luminal A and Luminal B, with differences in their gene expression patterns. The luminal A subtype belongs to a low histological grade tumour and is found to possess a higher level of ER-activated genes, and lower levels of proliferation-associated genes.

On the other hand, luminal B tumours belong to a higher histological grade and have higher proliferation levels, lower levels of the hormone receptors, and hence have a poorer prognosis .

**ii) ER- Breast Cancer**

- Basal-like (ER-, PR-, HER2-)/Triple negative
- Her2+ (ER rarely positive, PR-, HER2+)
- Normal breast-like (ER-, HER2-, PR unknown)
- Claudin-low (ER-, PR-, Her2-)

**iii) Basal-like/Triple Negative**

The basal-like subtypes are high histological grade tumours [183] lacking receptors for oestrogen, progesterone, and *Her2*. They are reported to originate from the basal cells of the breast, and they consistently express high levels of proliferation-related genes and other genes present in the normal breast basal epithelial cells, adipose tissue, or myoepithelial cells. A few examples of the genes include P cadherins, caveolins 1 and 2, and basal cytokeratins [184]. These cancer cells lack the

expression of ER, PR, and *Her2*, and hence become difficult to treat with specific-targeting drugs [185].

### iv) Her2+/ErB2+

The Her2+ subtype possesses cells that have a high expression of *Her2* or *ErB2*, which are involved in regulating various activities of the cells such as their proliferation and differentiation. They also lack the expression of the oestrogen and progesterone receptors on their surface.

### v) Claudin-low

These cancers do not express any of the hormone receptors, and belong to the triple-negative breast cancer category. The cells have high rates of EMT and high expression of stem cell-related genes, and a lower expression of cell adhesion-related genes [186].

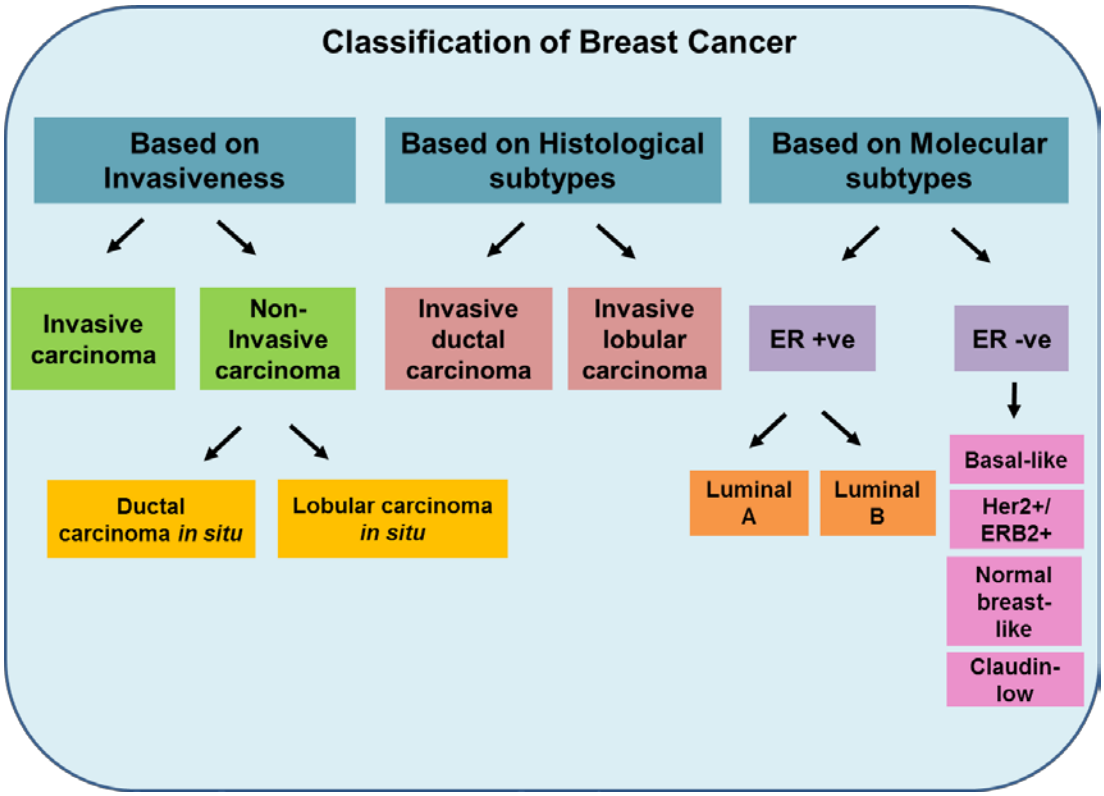


**Figure 2.6 Classification of breast cancer**

Breast cancer can be classified based on three criteria: its invasiveness, histopathological subtypes, and molecular subtypes. The major types within each of these criteria have been described.

## 2.6 Adipose Tissue and ADSCs in the Breast Tumour Microenvironment

This study focuses on the interaction between ADSCs and breast cancer cells in an *in vitro* environment, which is most likely to reflect the signalling processes occuring in an *in vivo* environment. Compared to normal breast tissues, breast cancer tissues are generally found to have higher expression of aromatase enzyme, which is a key enzyme of oestrogen biosynthesis [187]. The major site of oestrogen synthesis within the breast is the adipose tissue, due to its high levels of aromatase expression. As adipose tissue forms a predominant component of the breast, the level of oestrogen within the breast adipose tissue is 10 times greater than in blood [188]. It has been shown that mature adipocytes in adipose tissue have the capability to convert androgen to oestrogen by using their aromatase enzymes [189]. This can become a major risk factor during the development of an ER+ tumour because there is a constant, local supply for the hormone. Several studies have indicated the role of upregulated estrogen biosynthesis by adipose tissue present in the tumour environment in contributing to ER+ breast cancer development [190]. Adipose tissue has been shown to influence breast tissue development in both a paracrine and endocrine fashion [191-193]. Understanding the biology of adipose tissue, which forms the bulk of the human breast, and therefore, studying ADSCs, which are the major stem cell population within adipose tissue, and their interaction with breast cancer cells becomes clinically imperative.

## 2.7 Wnt signalling pathway

Wnt signalling molecules are secreted glycoproteins consisting of 350-400 amino acids, of which 23-24 are highly conserved cysteine residues [194]. Human Wnts (Molecular weight: 39KDa-46KDa) are the integral components of the canonical and the non-canonical Wnt signalling pathways that play a pivotal role in cell proliferation, differentiation, polarity, and migration [194].

### 2.7.1 Canonical Wnt Signalling Pathway

The canonical Wnt signalling pathway is β-catenin mediated, where the Wnt ligand binding forms a ternary complex with the Frizzled (Frz) receptor and the low density lipoprotein related protein 5/6 (LRP5/6) co-receptor to initiate the activated state. This triggers Dishevelled (Dsh) to phosphorylate and inhibit glycogen synthase kinase-3β (GSK-3β) activity. Axin, adenomatous polyposis coli (APC), and GSK-3β are the components of the destruction complex. Hence, inhibition of GSK3β activity inactivates the destruction complex, stabilises β-catenin, and consequently β-catenin gets unbound from the destruction complex. Thus, unphosphorylated β-catenin accumulates in the cytoplasm and translocates to the nucleus where it replaces the co-repressors from the transcriptional factor complex composed of T cell factor/Lymphoid Enhancer factor (TCF/LEF), and triggers the transcription of Wnt target genes (Figure 2.7). In the absence of Wnt during the inactive state of the pathway, β-catenin remains bound to the destruction complex and is phosphorylated

by the active GSK-3β, which subsequently results in the proteasomal degradation of β-catenin [195]. Hence, the downstream processes involving the translocation of β-catenin into the nucleus and the subsequent activation of Wnt target genes remains turned off.

### 2.7.2 Non-canonical Wnt Signalling Pathway

The non-canonical Wnt pathways are β-catenin independent, and one of them- the Wnt/$Ca^{2+}$ pathway (which is involved in cell migration), regulates the activation of calmodulin mediated kinase II (CaMKII) and protein kinase C (PKC), and the release of intracellular calcium (Figure 2.8) [195]. A second non-canonical pathway controls cell polarity and cytoskeletal organization by activating Rho-GTPases and Jun N-terminal kinases (JNKs) (Figure 2.9) [195].

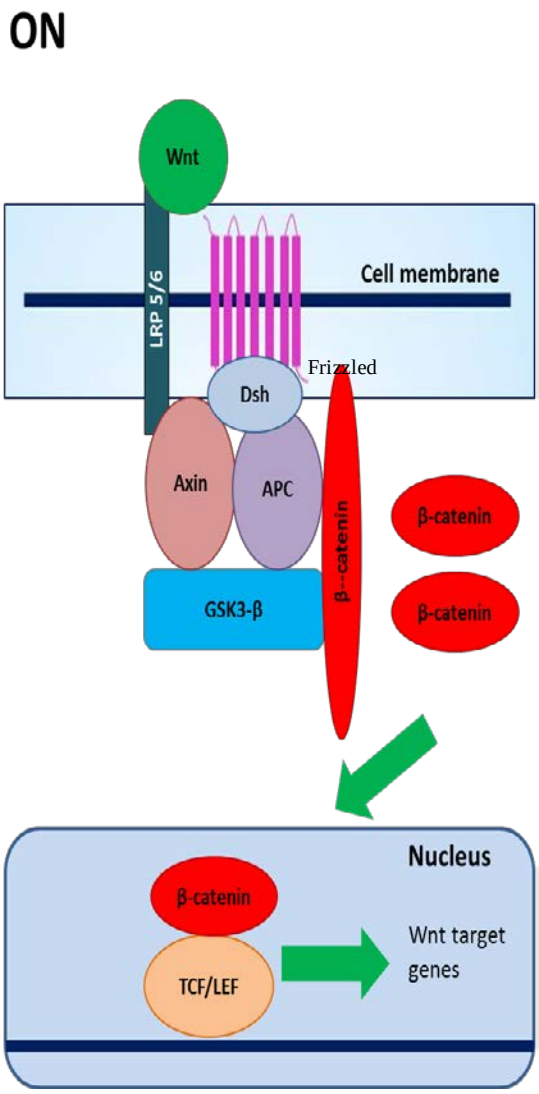


**Figure 2.7 Canonical Wnt signalling pathway in the ON/activated state**

The binding of a Wnt ligand to the Frz receptor and the LRP5 co-receptor recruits Dishevlled (Dsh) to the cell membrane. This results in the inactivation of the destruction complex composed of Axin, APC, and GSK3β, thereby allowing the β-catenin to remain unphosphorylated and unbound from the destruction complex. The unphosphorylated β-catenin translocates to the nucleus and triggers the transcription of Wnt target genes.

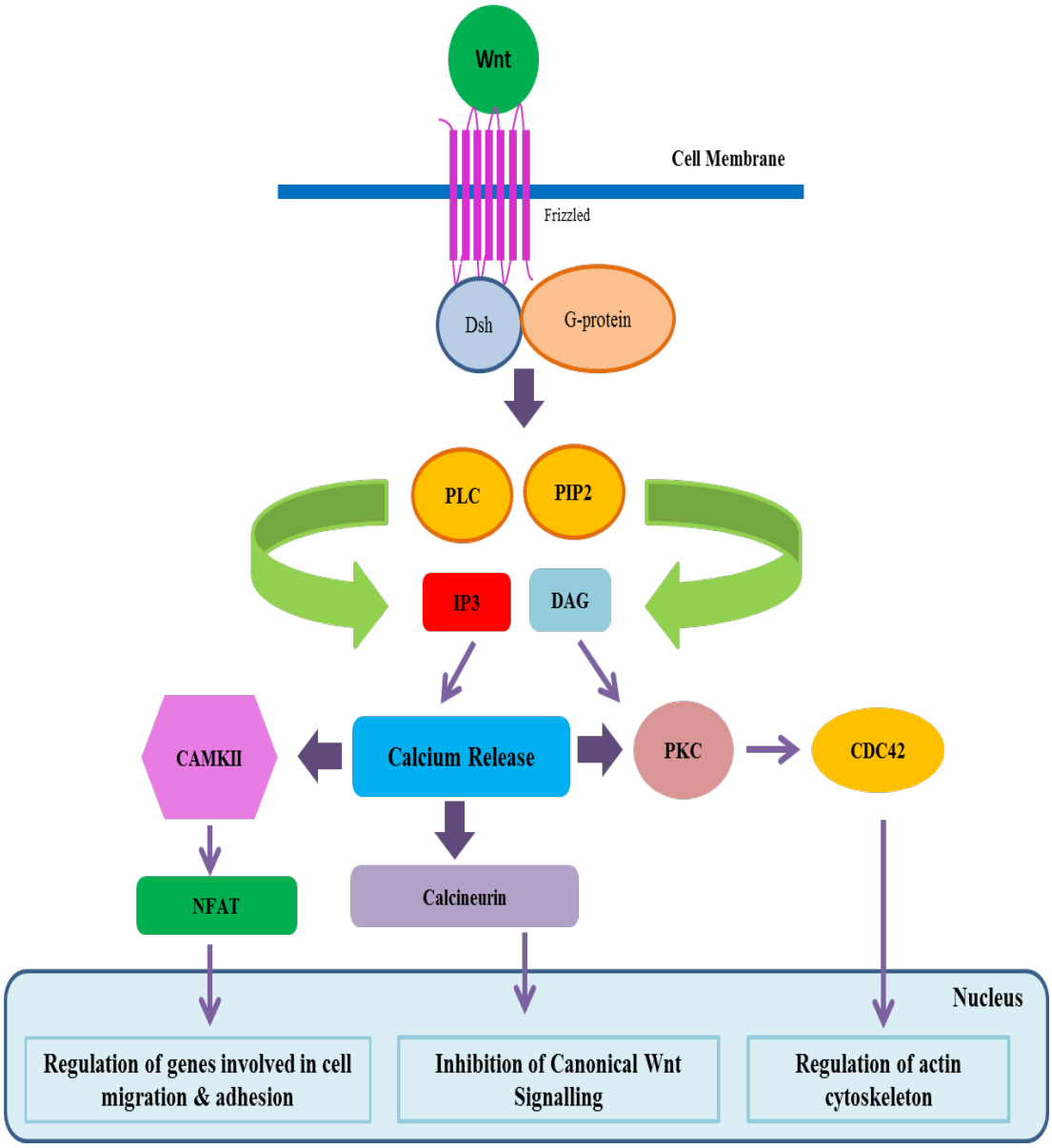


**Figure 2.8 Wnt/$Ca^{2+}$ Non-canonical Wnt signalling pathway**

The non-canonical Wnt/$Ca^{2+}$ pathway is β-catenin independent. The binding of Wnt to the receptor complex activates Dsh and continues to signal through the nuclear factor of activated T-cells intracellular cascade.

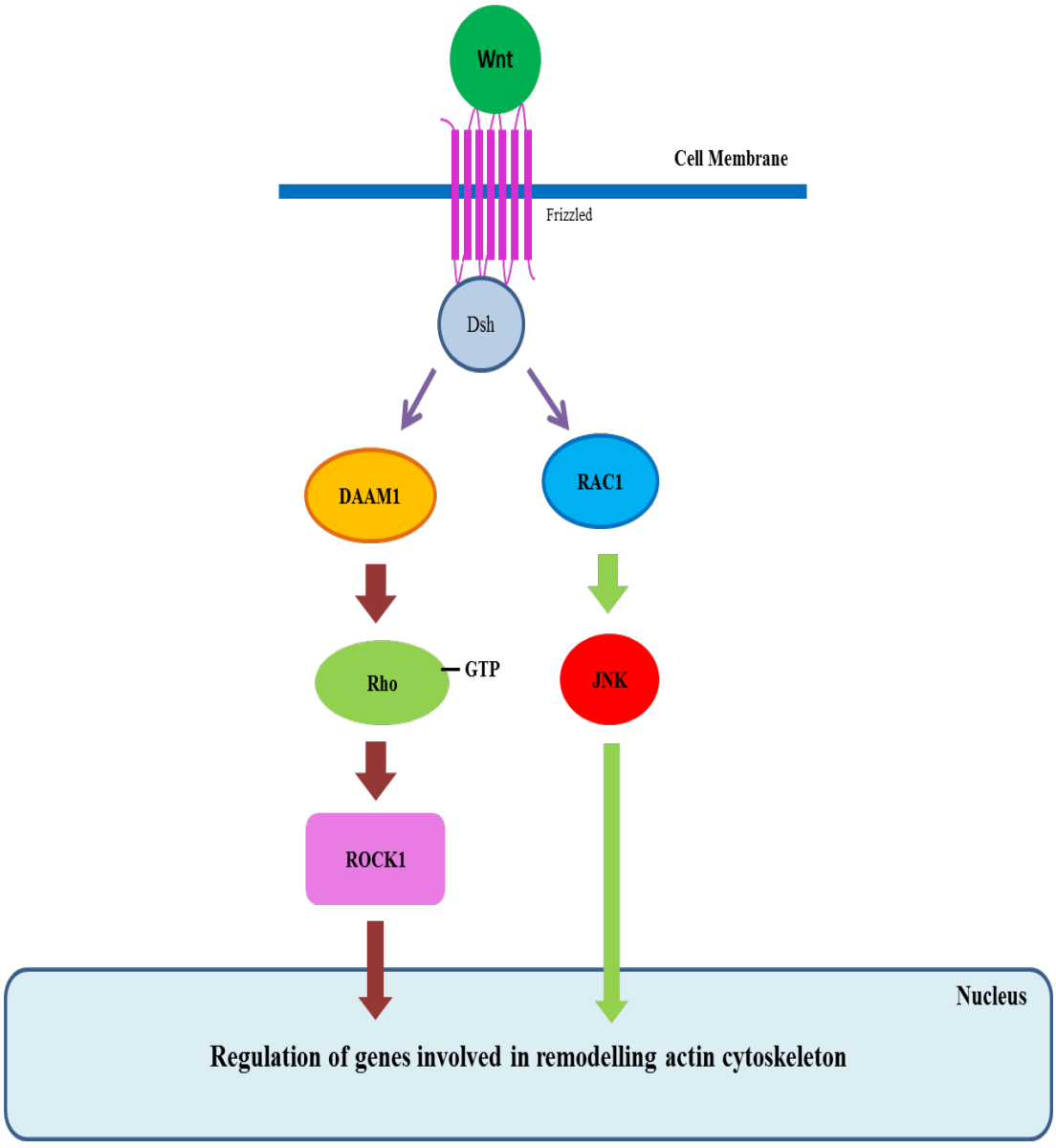


**Figure 2.9 Wnt-planar cell polarity (PCP) Non-canonical Wnt signalling pathway**

The Wnt-PCP non-canonical pathway is also β-catenin independent. After a Wnt ligand binds to the receptor complex, it triggers Dsh and then continues onto the c-jun N-terminal kinase (JNK) cascades.

## 2.8 Antagonists of the Wnt signalling pathway

The major antagonists or inhibitors of the Wnt signalling pathway belong to the family of secreted Frizzled-related proteins (sFRPs). Other Wnt antagonists such as the Dkk family includes 4 members (Dkk 1-4) with two specific cysteine-rich domains (Cys-1 and Cys-2), and they inhibit canonical Wnt signalling by binding to the LRP5/6 co-receptor [196]. Dkks also interact with the co-receptor Kremen (Kmn)-1 and Kmn-2 to form a ternary complex of Dkk1-LRP5/6-Kmn, thereby interrupting Wnt signalling [197]. Other naturally-occuring Wnt antagonists are Wnt-inhibitory factor 1 and Cerberus [198]. In addition to the naturally occurring Wnt antagonists, there are pharmacologically derived antagonists such as XAV939 [147] and iCRT3 [148]. As sFRPs are the major focus of this study, the sections below will describe the biology and functionality of sFRPs and then sFRP4 in detail.

### 2.8.1 Secreted Frizzled-related proteins

sFRPs are the first identified secreted antagonists of the canonical and non-canonical Wnt signalling pathways and**,** in humans**,** they are 5 in number (sFRP1-5) [182, 198-200]. The expression of sFRPs has been found in several human tissues such as breast, ovary, prostate, heart, and skin. Other than functioning as Wnt antagonists, sFRPs have been reported to be increased during apoptosis in various tissues such as mammary gland, ovarian corpus luteum, and ventral prostate [201-203].

### 2.8.2 Structure of sFRPs

By inactivating Wnt, sFRPs prevent the accumulation of active unphosphorylated β-catenin in the cytoplasm and reduce Wnt regulated mechanisms such as cellular proliferation [198]. The Frz receptors possess an extracellular cysteine-rich domain (CRD) composed of 120 amino acids at the N-terminal region [204], which shares structural homology to the CRD in the N-terminal region of sFRPs [205] (Figure 2.10).

The sFRPs were initially termed as FRZB-like proteins due to their 30-50% structural similarity [199, 206, 207]. FrzB-1 (which was later renamed sFRP3) was the founding member of the sFRP family of extracellular Wnt antagonists, initially identified in the cartilage of Drosophila [208]. FrzB-1 was later shown to bind to both Wnt 8 and Wnt 1, where it inhibited Wnt 8 activity in Xenopus [209, 210]. Although sFRPs share similar CRDs with the Frz receptors, they lack the transmembrane domains that are present in Frz receptors. Hence, sFRPs exist in the secreted form in the cell's exterior and are not bound to the cell surface (Figure 2.10).

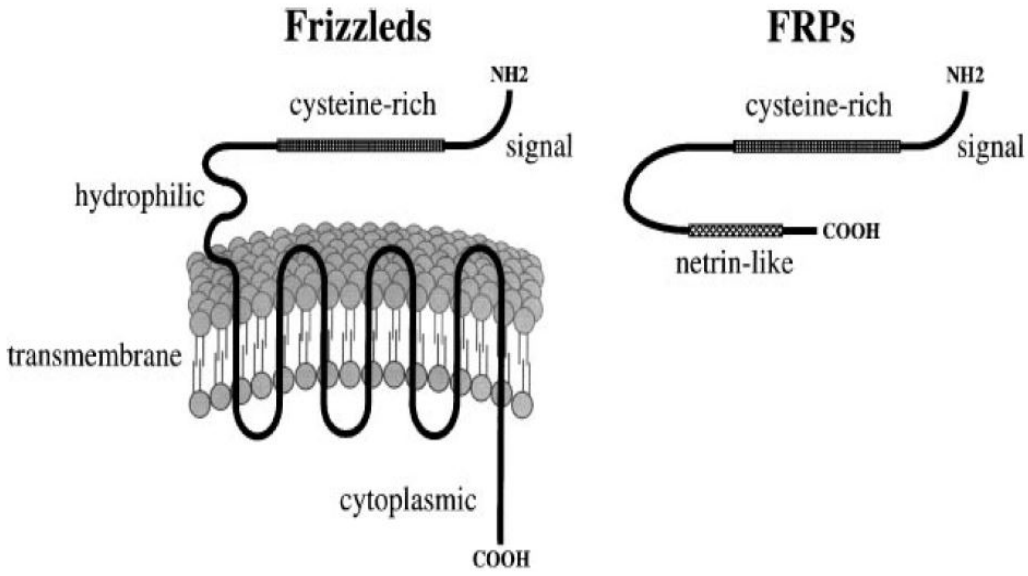


**Figure 2.10 Structural similarity between Frz receptor and sFRPs**

Frz receptors (on left) and sFRPs (on right) possess morphological homology on the CRD at their N-terminal region, but sFRPs lack the transmembrane domains and hence exist as free secreted proteins (as adapted from [204]).

### 2.8.2 Structural Homology between the sFRP isoforms

There exists a homology between the various sFRPs isoforms, where sFRP1, 2, and 5 form a subgroup and sFRP3 and 4 form a different subgroup (Figure 2.11). The level of amino acid identity between the different sFRPs is maximal between sFRP1 and 5, having 50% identity, while sFRP2, 3, and 4 display 37%, 19%, and 17% respectively [199, 211].

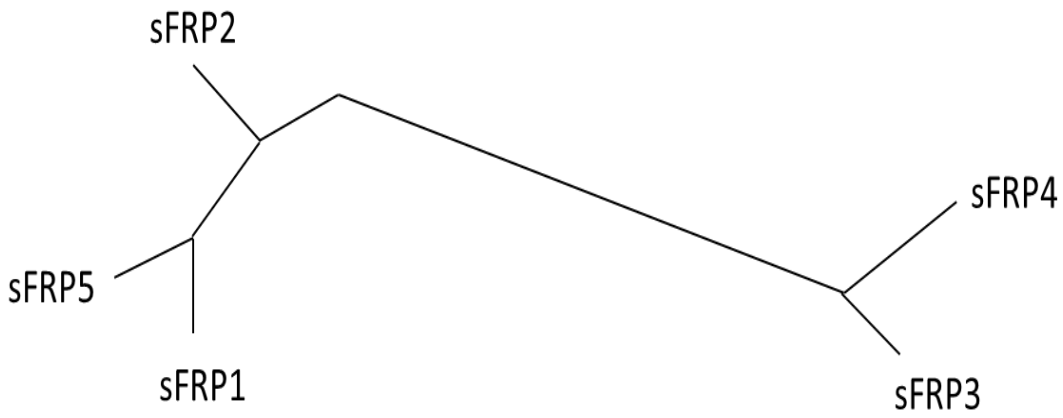


**Figure 2.11 Phylogenetic analyses of the members of the human sFRP family of Wnt antagonists**

sFRP1, sFRP2, and sFRP5 share the highest level of homology while sFRP3 and sFRP4 have the least homology and form a different sub-group (adapted & re-drawn from [199]).

### 2.8.3 Mechanism of Wnt Antagonism by sFRPs

sFRPs anatgonise Wnt signalling either by interfering with the Wnt-Frz interaction via directly binding to the Wnt or by binding to the Frz receptor, thereby forming a non-functional complex. While the latter mechanism (sFRP-Frz binding) is facilitated by the CRD of the sFRPs [182]**,** the former mechanism (sFRP-Wnt binding) can occur either via the CRD [212] or NLD in the C-terminal region of sFRPs [213].

When sFRPs interfere with the Wnt-Frz interaction, this allows the destruction complex composed of Axin, APC, and GSK3β to stay active. The active GSK3β phosphorylates β-catenin and this leads to the proteosomal degradation of the β-catenin. Thus, the Wnt target genes remain untranscribed and turned off (Figure 2.12). sFRPs have been found to downregulate β-catenin expression [198, 207, 214, 215]. Further, the biphasic regulation potential of sFRPs was elucidated wherein the Wnt protein binding to the CRD of sFRPs inhibits β-catenin stabilization, while the Wnt binding to the NLD at the C-terminal domain of sFRPs allows the CRD at the N-terminal of sFRPs to be free to interact with Frz and, hence, facilitate Wnt signalling [213].

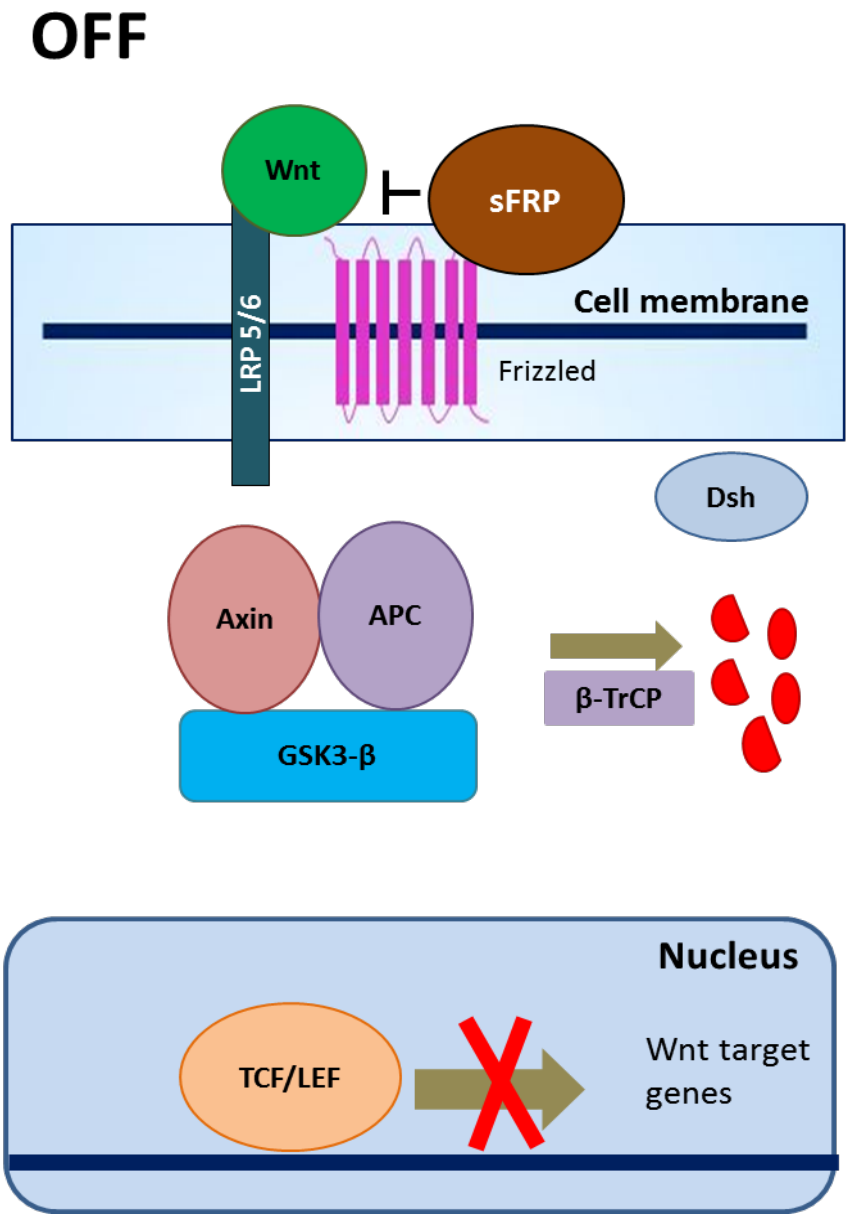


**Figure 2.12 Canonical Wnt signalling pathway in the OFF/Inhibited state**

SFRPs interfere with the Wnt-Frz binding and hence block the downstream events. The active destruction complex phosphorylates β-catenin and degrades it, leaving the Wnt target genes untranscribed.

## 2.8.5 Secreted Frizzled-related protein 4 (sFRP4)

This study focusses particularly on sFRP4, and hence, this section will describe the biology and functionality of sFRP4. Prof. Dharmarajan's laboratory was the first to isolate sFRP4 from the rat cDNA library [201]. The gene encoding for sFRP4 in humans is located on chromosome 7p14.1 [216].

### 2.8.6 sFRP4 peptides

This study also focusses on the shorter peptide fractions derived from the sFRP4 whole protein. The whole protein sequence consists of 2 domains that are 110 amino acids each, which are the cysteine-rich domain (CRD) at the N-terminal region and the netrin-like domain (NLD) at the C-terminal region. This laboratory has previoulsy demonstrated that the CRD inhibited angiogenesis while the NLD promoted apoptosis of HUVECs [217]. From each domain, a library of peptides was synthesised and their efficacy was tested in order to identify the most active peptide fragment. The most active peptide in terms of their anti-tumorigenic properties was chosen from each domain, termed as 'SC301' and 'SC401' derived from the CRD and NLD respectively. SC301 and SC401 are 15 and 20 amino acids in length respectively (Figure 2.13). The actual sequence of these peptides could not be revealed due to regulations concerning its intellectual property rights, which is presently being handled by the Curtin Commercialisation Board.

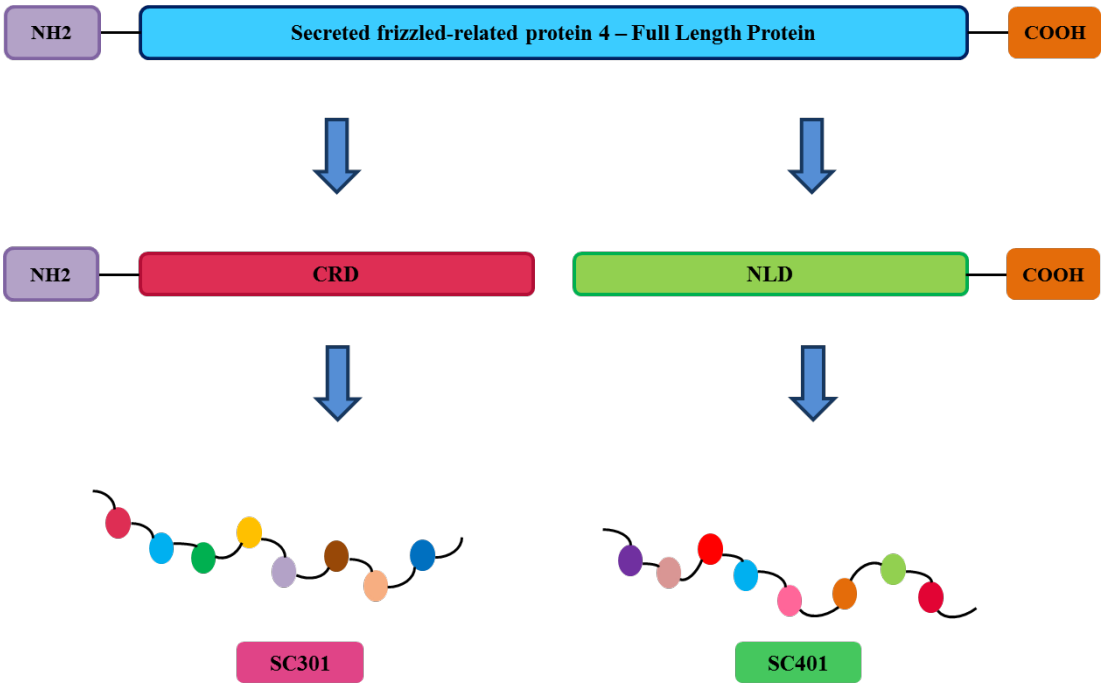


**Figure 2.13 Schematic representation of the origin of peptides from sFRP4 protein**

The full length sFRP4 protein is composed of 2 domains – CRD at the amino terminal and NLD at the carboxy terminal region. Peptide fragments SC301 and SC401 have been derived from the CRD and NLD domains respectively.

Apart from elucidating the inhibitory role of sFRP4 in β-catenin stabilisation and the PKB/Akt pathway, its role in apoptosis, mammary differentiation, and epidermal differentiation has also been demonstrated [201, 202, 218, 219].

### 2.8.7 Key biological functions of sFRP4

#### i) Wnt antagonsim:

SFRP4 has been reported to inhibit both the canonical and the non-canonical Wnt signalling pathways [198, 215]. sFRP4 has also been reported to downregulate the expression of β-catenin [203, 207, 215].

#### ii) Pro-apoptotic:

In animal studies, sFRP4 expression has been found to be correlated with apoptosis in various tissues such as mammary gland, ovary, prostate, and uterus [201-203, 218, 220, 221]. Similar observations have been reported in human tissues such as skin, mammary gland, cartilage, and myocardial cells [218, 219, 222-225].

#### iii) Anti-angiogenic:

Previous research in this laboratory demonstrated, for the first time, that sFRP4 exhibited anti-angiogenic properties in *in vivo* systems by reducing vascularity, and also in *in vitro* settings by inhibiting endothelial cell migration and sprouting [215].

## 2.9 Wnt Signalling and Wnt Antagonists in Cancer

Abberant activation of Wnt signalling leads to an upregulation in the levels of β-catenin [226], which has been found to lead to cancer [227]. The reason underlying this abberant activation of Wnt signalling could arise from gene mutations or overexpression of Wnts [228-231]. Wnt signalling is one of the key signalling pathways involved in the self-renewal of stem cells and in the development of cancer originating from various cell types [232]. It could also be due to lack of expression of the Wnt antagonists as tumours have been generally found to reduce the expression of sFRPs, as they are pro-apoptotic in nature [198]. However, the restoration of sFRP expression decreases the tumorigenic potential and increases apoptosis in many cancers, as discussed in the following paragraphs.

Wnt antagonists such as sFRPs and Dkks have been considered to be downregulated in different cancers such as breast, cervix, mesothelium, and stomach [71, 233-238]. It has been reported that Dkk1 is epigenetically silenced in colorectal cancer [233]. Silencing of Dkk3 by tumour-specific promotor methylation was present in 78% of breast tumour samples, and it was demonstrated that ectopic expression of Dkk3 decreased the migration and downregulated the expression of stem cell markers in breast cancer [239].

Studies showed that sFRP gene promotors were methylated in mesothelioma tissue [236]. Similar epigenetic inactivation of sFRP genes was seen in gastric cancer [234, 238], colorectal cancer [240], and glioblastoma multiforme [241], which in turn

allows aberrant activation of the Wnt signalling pathway [240]. SFRP1 was also shown to be downregulated in colorectal cancer [242, 243].

Contrastingly, a few studies have reported an increase in sFRP expression in cancers of glioma, breast, colon, and prostate [216, 244-248]. The reason postulated for this phenomenon was blamed on an ineffective homeostatic mechanism attempting to stop the tumour growth [249].

### 2.9.1 sFRP4 and Cancer – Anti-tumorigenic activity of sFRP4

SFRP4 has been described to have potent anti-tumorigenic properties in various types of cancers. This section discusses the role of sFRP4 in cancer types apart from breast cancer.

SFRP4 expression has been reported to be lost in several cancers [236, 237, 250-253]. For instance, the expression of sFRP4 deteriorates progressively as ovarian cancer progresses [254]. It was also reported that loss of sFRP4 expression led to the development of an aggressive phenotype in ovarian cancer cells [255]. Additionally, it was reported that exogenously introduced sFRP4 improved the sensitivity of chemoresistant ovarian cancer cells and hence reduced its aggressiveness [256]. Furthermore, treatment with recombinant sFRP4 downregulated EMT and cell migration in ovarian cancer cells by regulating the Wnt signalling pathway [255].

SFRP4 was also observed to be epigenetically silenced in mesothelioma cells, and the re-expression of sFRP4 induced apoptosis in mesothelioma cells [229, 236]. Forced expression of sFRP4 also decreased proliferation in prostate cancer cells [257]. In endometrial cancer, it has been reported that sFRP4 inhibited proliferation of endometrial cancer cells via regulation of Wnt7a, and hence, the loss of expression of sFRP4 led to the onset of endometrial cancer by removing its inhibition of Wnt signalling [250]. In cervix cancer, it was reported that sFRP expression is lowered in human cervical cancer tissues, and when these cancer cells were transfected with sFRP, the rates of apoptosis increased [235, 237].

The main characteritics of sFRP4 identified so far are described in Figure 2.14.

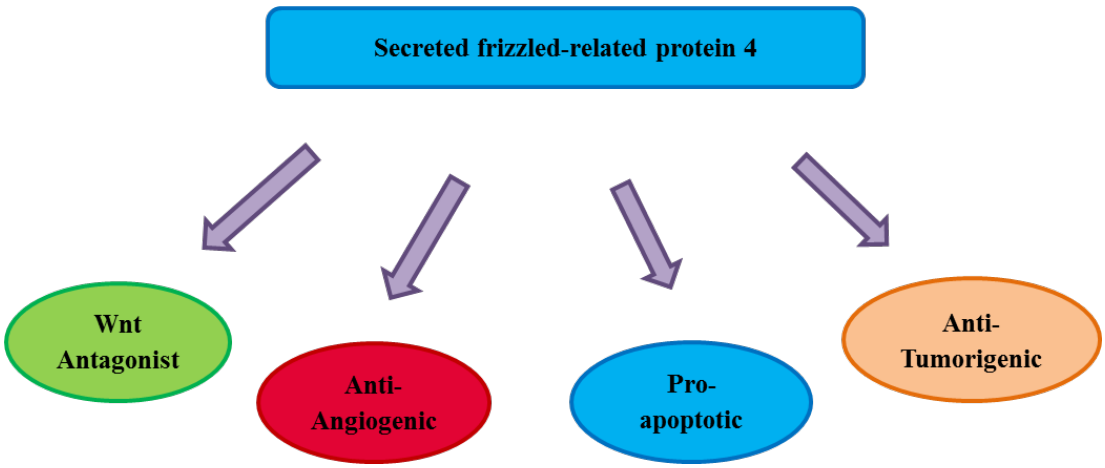


**Figure 2.14 Characteristics of sFRP4**

The above figure shows the main attributes of sFRP4 that account for its therapeutic potential in cancer.

### 2.9.2 Wnt Signalling and Wnt antagonists in Breast Cancer

Amongst the various signalling pathways that have been reported to influence breast cancer are Wnt/β-catenin, nuclear factor-γb, Hedgehog, Notch, and signal transducer and activator of transcription 3 [258, 259], the Wnt signalling pathway is a key player. In breast cancer, upregulated β-catenin expression is considered to be a poor prognostic marker [260], and it has been shown that activation of Wnt signalling has resulted in increased invasive potential of MCF-7 breast cancer cells [261]. It was found that high β-catenin activity induced Cyclin D1 expression and correlated with progression of breast cancer [260].

An activated state of Wnt signalling has been reported in actively proliferating MCF7 breast cancer cells. Moreover, a downregulated expression of Dkk1 was observed in those cells [71]. Further, Dkk1 secreted from MSCs played a role in inhibiting the growth of MCF7 breast cancer cells [72]. Also, the conditioned medium originating from MSCs was demonstrated to inhibit the growth of MCF7 cells [72].

In invasive breast cancers, results have suggested low expression of *sFRP1* [262]. Of particular interest to this study is the role of Wnt signalling and its antagonist sFRP4 on breast cancer. Research from this laboratory has previously demonstrated that sFRP4 is a potent inhibitor of oestradiol-induced growth in the oestradiol-responsive breast tumour cell line MCF7 [263]. In addition to its antagonism of Wnt signalling and its pro-apoptotic nature, the anti-angiogenic property exhibited by sFRP4 makes it a potential tumour suppressor that could be worth considering in order to reduce tumour cell invasiveness or aggressiveness.

## 2.10 Differentiation of MSCs into Tumour-associated fibroblasts (TAFs) in the presence of a tumorigenic environment

### 2.10.1 Tumour stroma

The tumour stroma comprises a heterogeneous mixture of tumour cells and various types of non-tumour cells such as mesenchymal stem cells, macrophages, endothelial cells, epithelial cells, and fibroblasts [30, 41, 264]. Apart from tissue-resident MSC population, recruited MSCs have also been shown to be a part of the tumour microenvironment in earlier studies [265, 266]. Being in such an interactive milieu with the tumour cells, the non-tumorigenic components also co-evolve to acquire a tumorigenic phenotype, eventually contributing to tumour growth [267]. Below is a schematic representation of a heterogeneous tumour stroma composed of multiple cell types (Figure 2.15).

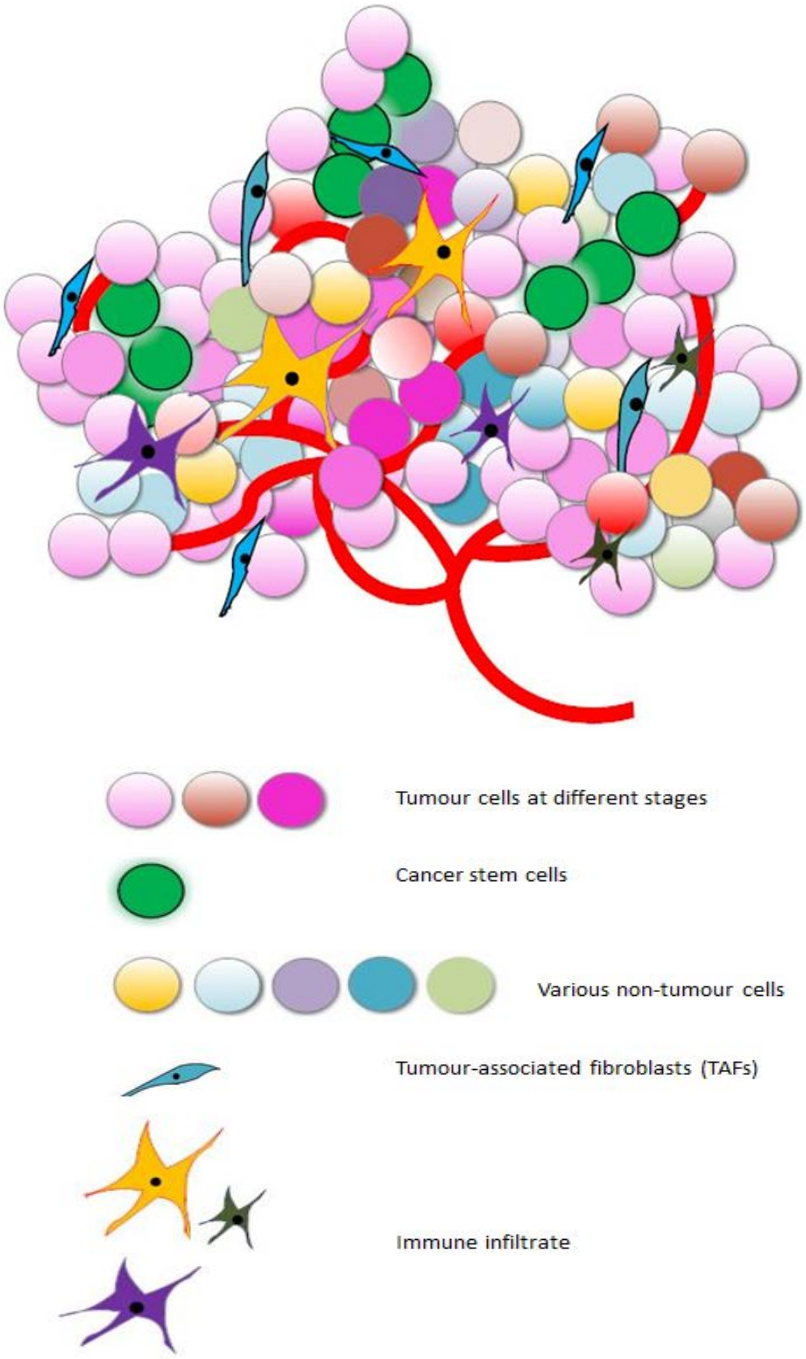


**Figure 2.15 Diverse cell types present within a heterogeneous tumour stroma**

Schematic representation of the different cell types that are present within a tumour environment influencing the progression of the disease (design template inspired and re-drawn from [267]).

### 2.10.2 Significance of TAFs in Tumour Progression

The interplay between the tumour stromal components is reciprocally regulated, although the mechanism is not fully understood. Amongst the various components of the tumour environment, the TAFs form a major population of the stromal component, as seen in breast and pancreatic carcinomas [160, 161]. TAFs, also known as carcinoma-associated fibroblasts (CAFs) or myofibroblasts, were shown to contribute functionally and structurally towards tumour progression by the secretion of various paracrine and autocrine regulators within the tumour microenvironment. TAFs have been considered to be a promising target against which novel anti-cancer therapies could be directed [268].

The tumour promoting property of TAFs has been demonstrated in several studies. In one of them, PDGF-CC recruits TAFs to the tumour stroma and thereby promotes tumour growth [163]. There is limited evidence toward the role of TAFs in ECM remodelling. One recent study demonstrated that TAFs contribute to collagen elongation within the tumour stroma of head and neck squamous cell carcinoma, oesophageal adenocarcinoma, and colorectal adenocarcinoma, thereby enhancing tumour invasion and progression, leading to a poor prognosis [169].

### 2.10.3 Characterisation of TAFs

TAFs express distinct tumour-supportive characteristics that brand them different from normal fibroblasts. To name a few, TAFs are a rich source of : 1) Fibroblast specific protein (FSP) and fibroblast activated protein (FAP); 2) Tumour aggressive

markers - tenascin-C (Tn-C), thrombospondin-1 (Tsp-1), and stromelysin (SL-1) [269]; 3) Myofibroblast and neovascularising factors – α-smooth muscle actin (α-SMA), vimentin, [16, 269], desmin, and VEGF [269]; and 4) Tumorigenic growth factors – TGFβ, basic FGF, HGF, EGF, and interleukin-6 [164, 269]. Additionally, TAFs differentiated from ADSCs demonstrated increased expression of SDF-1 and CCL5 [16]. TAFs generate pro-angiogenic factors such as VEGF, FGF2, and SDF-1α, stimulating neovascularisation and angiogenesis in the tumour environment [86, 161, 162, 167, 168], and secrete survival cues such as insulin-like growth factor-1 and -2 [165, 166].

### 2.10.4 Origin of TAFs

TAFs can originate from a variety of resident cells or circulating cells in and around the tumour stroma, such as mesenchymal stem cells, resting fibroblasts, endothelial cells, pericytes, and epithelial cells [270-272]. Evidence indicates that the tumour environment can play a role in even transforming mature adipocytes to a less adipogenic profile while developing a more modified phenotype, termed a cancer-associated adipocyte, which has more cancer-promoting attributes [54, 273]. Within the tumour stroma, the origin of TAFs can be attributed to various sources [163]. Amongst them, MSCs are a major population capable of conversion into TAFs, especially considering the proximity and the complex relationship that exits between ADSCs and breast tumour cells within the breast tumour microenvironment.

Emerging evidence suggests that MSCs can contribute to the tumour stroma by differentiating into TAFs/CAFs/myofibroblasts [269, 274]. These are the subset of cells within the tumour stroma that contribute to tumour progression and invasiveness by supporting rapid tumour growth and metastasis [16]. In spite of the immunophenotypic and trilineage differentiation similarities, there are significant differences that exist between the TAFs (which are also termed as 'specialised MSCs') and the naïve MSCs in terms of their chemokine and growth factor secretions, with TAFs being a richer source [271]. TAFs have a heightened secretion of various cytokines such as VEGF, TGFβ1, Il-1, Il-10, and tumour necrosis factor-α when compared to MSCs, and the TAFs possess a higher proliferation rate compared to MSCs [271].

Delineation of the differences between the naïve MSCs and the tumour-derived MSCs 'educated' by the tumour environment has been demonstrated. The tumour-derived-MSCs can then contribute to tumour progression by stimulating various mechanisms such as EMT, tumour cell proliferation, and angiogenesis [275]. This study highlights the potential of MSCs to be transformed to attain a tumour-supporting phenotype, which needs to be curbed before considering MSC-based anti-cancer treatment strategies.

### 2.10.5 Factors stimulating conversion into TAFs/CAFs

The conditioned medium derived from tumour cells aided in the *in vitro* conditioning of MSCs to convert to TAFs, and enhanced the expression of TAF markers in MSCs [16, 269, 274]. Two of these studies showed that a long-term *in vitro* treatment in the presence of tumour cell conditioned medium (TCM) for 16-30 days was required for the MSCs to acquire a TAF/myofibroblastic phenotype [269, 274]. A third study showed that ADSCs differentiated into TAFs upon treatment with conditioned medium from breast tumour cells such as MCF7 and MDA MB 231 [16]. ADSCs have been reported to differentiate into TAFs under the influence of A549 lung cancer cells, CM from SKOV-3, OVCAR-3 ovarian cancer cells upregulating the periostin expression involved in cell adhesion and proliferation [276, 277]. A549-CM also transformed ADSCs into TAFs with upregulation of α-SMA, VEGF, SDF-1 [278].

Exosomes derived from the breast cancer cell lines MCF-7 and MDA MB231 have stimulated the differentiation of ADSCs into TAFs, as characterised by the presence of α-SMA [279]. Exosomes from the ovarian cancer cell lines Skov-3 and OVCAR-3 induced ADSCs to convert to the TAF phenotype, expressing TAF-markers such as α-SMA, SDF-1, and TGFβ-1 [280].

However, it needs to be noted that MSCs do not undergo spontaneous *in vitro* transformation under normal culure conditions [281]. Therefore, in view of MSCs' *in vivo* tumour tropism to solid tumour sites and their potential differentiation into TAFs, it indicates that MSCs could be considered as an origin for TAFs.

### 2.10.6 Pathways involved in the conversion of MSCs into TAFs

The activation of multiple signalling pathways has been associated with the transformation of MSCs into TAFs. It was identified that the TGFβ1 present in the conditioned medium of breast tumour cells stimulated the conversion of ADSCs into TAFs via activation of the Smad pathway. The conversion was inhibited when a neutralising antibody to TGFβ1 was used or when the TGFβ1 receptor kinase was inhibited by SB431542 [16]. The ovarian cancer Skov-3 cell line-derived exosomes induced TAF conversion in ADSCs by the activation of a Smad-dependent pathway, as detected by the phosphorylation of Smad-2 [280]. Smad pathway activation was also reported in ADSCs treated with exosomes derived from MCF-7 and MDA MB231 breast cancer cell lines [279]. OVCAR-3 ovarian cancer cell line-derived exosomes induced TAF conversion in ADSCs by the activation of a Smad-independent pathway, as detected by the phosphorylation of Akt [280] Lysophosphatidic acid has been demonstrated to induce differentiation of ADSCs into myofibroblast-like cells through the TGF-β-Smad pathway [282]. Similarly, LPA has also been demonstrated to induce differentiation into a TAF phenotype in peritumoural fibroblasts [283]. The role of LPA was further confirmed in in vivo conditions where A549 cells co-transplanted with ADSCs increased the tumour volume and weight, whereas no increase was observed when A549 cells co-transplanted with ADSCs where LPA receptors were silenced [278].

TGFβ secreted by cancer cells attracts the fibroblasts in the tumour stroma towards them [284], and when the fibroblasts attain proximity to the cancer cells, the TGFβ converts the fibroblasts into myofibroblasts [285]. It was reported that conditioned

medium from oesophageal squamous cell carcinoma cell lines transdifferentiated stromal fibroblasts into myofibroblasts through activation by TGF-β treatment, which was in turn inhibited when treated with a TGF-β inhibitor (Noma et al., 2008). Other than the conversion of fibroblasts into myofibroblasts, TGFβ contributes to tumour progression by stimulating angiogenesis and promoting tumour cell escape from immunosurveillance [286]. Although PDGF is not directly involved with this transdifferentiation, it contributes to it by stimulating TGFβ release by macrophages in order to recruit fibroblasts to the area [285]. Inhibition of TGFβ signalling by the pseudoreceptor bone morphogenetic protein and activin membrane-bound inhibitor homologue results in suppression of the transformation of MSCs into TAFs [287].

These studies indicate that multiple intracellular signalling pathways may be activated, such as the Wnt signalling pathway, during this transformation [279, 280]; further highlighting the importance of Wnt signalling in cancer. Moreover, canonical Wnt antagonism is suggested to inhibit MSC to TAF differentiation in carcinomas, but this had the opposite effect in sarcoma (malignant fibrous histiocytoma), where recombinant Dkk-1 promoted the transformation of MSCs [288]. Several studies have indicated the tight interrelation between TGFβ and Wnt signalling pathways. It was demonstrated that TGFβ upregulated the accumulation of β-catenin and LEF1 in prostate cancer cells and keratinocytes [289], induced quick transclocation of β-catenin into the nucleus in BM-MSCs [290], and upregulated β-catenin induced transcription in human dermal fibroblasts [291]. Another study demonstrated the anti-fibrotic effect of the Wnt antagonist Dkk1, thereby rescuing the TGFβ-induced fibrosis [292]. They also showed that TGFβ activated the canonical Wnt pathway, and found downregulated Dkk1 expression levels in fibrotic tissues [292]. Pro-angiogenic molecules secreted by the TAFs have been suggested to be a possible

therapeutic target [271]. Hence, Wnt antagonists such as sFRP4, which has been shown to be both anti-angiogenic and pro-apoptotic [201, 215], could be a potential candidate to reduce the aggressiveness of TAFs.

### 2.10.7 Metabolic reprogramming in TAFs

The role of metabolism and activation/inhibition of various pathways in cancer cells have attracted a lot of clinical attention, making specific regulatory enzymes or transporters targets in anti-cancer approaches. Normal cells metabolise glucose to pyruvate through the pathway of glycolysis followed by the entry of pyruvate into the tricarboxylic acid (TCA) cycle in the mitochondria, leading to maximal adenosine triphosphate (ATP) production by oxidative phosphorylation and minimal lactate production under normoxic conditions [293]. Alternatively, under anaerobic conditions, the pyruvate is largely converted into lactate in normal cells, a process termed anaerobic glycolysis [293] (Figure 2.16).

However, in cancer cells, even in the presence of abundant oxygen, aerobic glycolysis takes place where glucose gets predominately converted into lactate, and is considered as their major source of energy production [293] (Figure 2.16). Additionally, the tumour niche is composed of rapidly proliferating cells that are also under hypoxic conditions, which further increases their dependence on glycolysis to meet their energy demands. This metabolic switch observed in cancer cells towards glycolysis in aerobic conditions was discovered by Otto Warburg and is named the Warburg effect [93]. In fact, the tumour cells switch to a less efficient pathway in terms of energy production, as oxidative phosphorylation generates 36 ATPs as

compared to only 2 ATPs per molecule of glucose during its conversion into lactate. However, it is compensated by an increased glucose uptake and a high rate of glycolysis triggered by a continuous supply of nutrients such as glucose. One of the reasons for this metabolic shift in cancer cells is because aerobic glycolysis converts glucose to lactate 10-100 times quicker than the oxidation of glucose using oxidative phosphorylation [294], thereby facilitating the cancer cells to continue their rapid rate of proliferation. Thus, cancer cells are characterised by a higher rate of glucose uptake and a larger production of lactate to meet their metabolic demands. Overall, cancer cells shift their metabolic profile to meet their needs for increased proliferation and synthesis of biomass including nucleotides, amino acids, and lipids, rather than just increased ATP production [293].

However, cancer cells are a heterogeneous mixture of cells exhibiting cells in various bio-energetic states, and it is becomingly increasingly clear that there are cancer cells within the tumour niche that rely on oxidative phosphorylation to assist their increased energy needs [295-298]. The diversity in their metabolic phenotypes is constantly evolving to adapt to the changing microenvironment, which benefits them with an advantage to thrive in an unfavourable environment [299]. Most often, the ability of cancer cells to perform oxidative phosphorylation is overpowered by a highly active glycolytic function, and the capacity to produce ATP via oxidative phosphorylation is kept as a reserve mechanism to be used if required or to compensate for a reduced ATP generation [299].

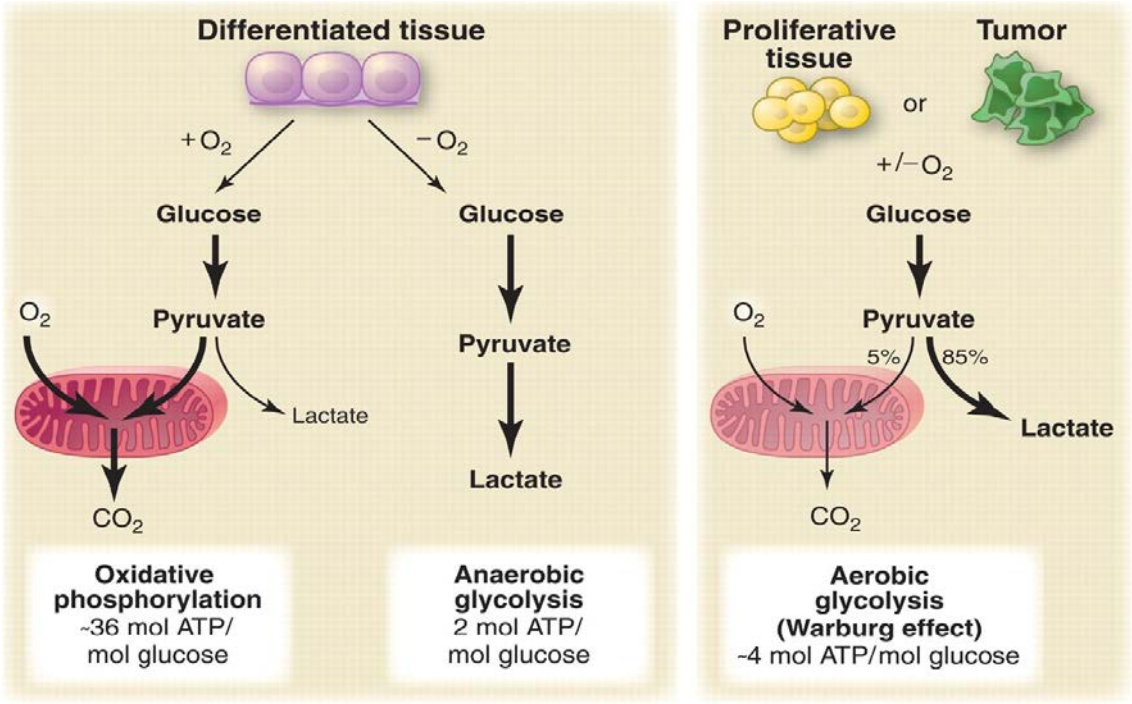


**Figure 2.16: Schematic representation of the metabolic pathway in normal cells and tumour cells [293].** In normal cells, glucose gets converted into pyruvate, which then enters oxidative phosphorylation and results in maximal production of ATP. During anaerobic conditions in normal cells, anaerobic glycolysis occurs where the pyruvate gets converted into lactate, resulting in the minimal production of ATP. In cancer cells, even in the presence of oxygen, the glucose gets converted into lactate (the process of aerobic glycolysis), which results in a less efficient mechanism of energy production.

Although the various metabolic phenotypes of cancer cells have been demonstrated, there is less information in the literature regarding the metabolic state of TAFs present in the tumour stroma. It has been reported that the functional activation of fibroblasts and their subsequent transformation into TAFs is accompanied by metabolic reprogramming, resulting in the induction of aerobic glycolysis and thereby increasing the generation of L-lactate, pyruvate, and ketone bodies in the tumour environment, which are later utilised by the cancer cells [300]. Upregulation

of the glycolytic pathway in TAFs through an increased expression of phosphoglycerate kinase-1, which is a component of the glycolytic pathway, results in enhanced proliferation of TAFs and promotion of tumour growth *in vivo* [301]. It was reported that when normal fibroblasts are treated with TGFβ1 or PDGF to convert them into TAFs, there occurs a switch from oxidative phosphorylation to aerobic glycolysis [302]. The metabolic reprogramming in TAFs is characterised by the downregulation of isocitrate dehydrogenase 3α (IDH 3α). Hence, an overexpression of IDH 3α has been demonstrated to prevent this transformation [302]. The downregulation of IDH 3α observed during the transformation has been demonstrated to result in a series of events leading to the stabilisation of hypoxia inducible factor-1α, which then upregulates the level of glycolysis and glycolytic enzymes [302].

The metabolic intermediates such as pyruvate and lactate secreted by TAFs through aerobic glycolysis serve as onco-metabolites in the tumour microenvironment, creating a dynamic metabolic crosstalk with the tumour cells. The adjacent tumour cells then take up these metabolites and re-enter the TCA cycle, followed by oxidative phosphorylation promoting a highly efficient energy production to fulfil their energy needs. This process of metabolic coupling between adjacent cell types in a tumour microenvironment is called the 'reverse Warburg effect'. It involves cancer cells inducing a metabolic shift in the neighbouring cells towards aerobic glycolysis in order to continue the supply of energy-rich metabolites for the cancer cells [299, 303, 304]. Hence, it is understood that TAFs are a key component of the tumour stroma by acting as a metabolic 'fuel' source and creating an energy-rich microenvironment favouring tumour progression. Hence, targeting the metabolic state of the tumour environment as a whole, by uncoupling the metabolic crosstalk

between TAFs and tumour cells, will help to cut off the energy supply fuelling tumour growth. Therefore, it will be a novel therapeutic approach in anti-cancer therapies by targeting the root of the disease.

The above evidences show the metabolic switch occurring during the formation of TAFs from their various precursor fibroblast cells. However, an understanding of the metabolic switch happening during the transformation of ADSCs into TAFs is limited. Therefore, this study investigated the shift in the metabolic pattern exhibited during the transformation of ADSCs into TAFs over short-term and long-term treatment durations. Further, the alteration of the metabolic state of TAFs following treatments with Wnt antagonists was also examined.

## 2.11 Differentiation of ADSCs into adipocytes in a normal non-tumorigenic state and role of Wnt signalling in adipogenesis

Obesity and overweight are emerging as foremost health concerns on a global scale [305]. They can significantly impact the quality of life [306] and are also associated with many related health concerns such as type II diabetes mellitus, hypertension, and elevated cancer risk [307, 308]. Many signalling pathways tightly regulate the process of adipogenic differentiation. Amongst them, the Wnt signalling pathway plays an important role in its regulation [309].

### 2.11.1 Role of activated Wnt signalling on adipogenesis

An activated canonical Wnt signalling pathway contributes to a downregulated adipogenic fate, as shown by various Wnt agonists such as Wnt10b, and inhibitors of GSK-3β such as lithium chloride (LiCl) [310] and CHIR 99021 [311], on 3T3 pre-adipocytes. On the other hand, the non-canonical Wnt ligands Wnt4 and Wnt5a have been demonstrated to promote adipogenesis on 3T3 cells mediated via the Wnt/$Ca^{2+}$ non-canonical pathway. One possible mechanism underlying this is the antagonising effect of Wnt5a on the canonical Wnt signalling pathway, and hence upregulating adipogenesis [312].

MSCs are a good source of adipogenic precursor cells, and the role of the Wnt agonist 6-bromo-indirubin-3'-oxime (a GSK-3β inhibitor) on adipogenic differentiation of MSCs has been demonstrated [313, 314]. In MSCs, the expression of the two Wnt antagonists sFRP4 and Dkk1 were shown to be upregulated during the process of adipogenic differentiation, as compared to their undifferentiated stem cell state [315].

### 2.11.2 Role of Wnt antagonists on adipogenesis

ADSCs are an apt source of MSCs to study adipogenesis because ADSCs possess a strong adipogenic differentiation capability, which is their prime physiological purpose. A study showed that when the expression of the Wnt antagonists sFRP4 and Dkk1 were silenced in ADSCs, it resulted in an activated Wnt signalling and the

downregulation of adipogenic differentiation, which was demonstrated by decreased lipid accumulation and adipogenesis-specific marker expression [315]. A short 48 hour treatment using the Wnt antagonists sFRP1 and sFRP4 upregulated adiponectin secretion in human MSCs [316]. Overall, it indicates that an inactivated state of Wnt signalling is highly relevant to shift MSCs towards the adipogenic fate.

This tightly balanced link between Wnt signalling and adipogenesis could be considered when developing novel therapeutic strategies to target obesity and diabetes. The importance of Wnt signalling-mediated regulation of adipogenesis and related metabolic disorders has been demonstrated in a few clinical studies. One study showed that the levels of the Wnt antagonist sFRP4 were directly proportional to weakened glucose and triglyceride metabolism [317]. Another study reported that sFRP4 could be used as a biomarker for predicting the development of type II diabetes mellitus [318].

Given the importance of Wnt antagonists in adipogenesis, the role of recombinant sFRP4 on the adipogenic differentiation fate of ADSCs was investigated. It becomes highly relevant as ADSCs are a major population of adipogenic precursors within the breast. The major part of this study teases out the cellular crosstalk between ADSCs and breast tumour cells in the light of the Wnt antagonist sFRP4 to examine whether a combination of sFRP4 and ADSCs could be used to combat the tumorigenic environment in the breast. At the same time, it becomes important to know and understand the effect of sFRP4 on non-tumour cells such as ADSCs in a normal non-tumorigenic environment, in order to consider using these sFRP4 and ADSCs for therapeutic approaches.

# Chapter 3 - MATERIALS AND METHODS

The detailed list of reagents/chemicals (including company and catalogue number) used for this study is provided in Appendix-II

## 3.1 Cell Culture

Human adipose tissue-derived mesenchymal stem cells (ADSCs) purchased from Lonza Australia and the two breast cancer cell lines – MCF-7 and MDA MB-231 used for the study were purchased from American Type Culture Collection.

### 3.1.1 ADSCs

The cell lines comprising a homogenous population of MSCs derived from human adipose tissue were purchased from Lonza, Australia. The flow cytometric characterisation of the ADSC surface markers was performed previously by the supplier. It was characterised for presence of CD44, CD90, and CD105 expression, and absence of CD34 and CD45 expression. The cells were cultured in Low glucose-Dulbecco's modified Eagle's medium (DMEM) or Roswell Park Memorial Institute (RPMI)-1640 containing 10% foetal bovine serum (FBS) and 1% Penicillin-Streptomycin (PS) antibiotics. The FBS was heat-inactivated by placing inside a

water bath at 56$^{o}$C for 30 minutes and then allowed to cool before aliquotting into 50mL tubes and stored at -20$^{o}$C for future use.

### 3.1.2 MCF-7 cells

The MCF-7 cells are a malignant adenocarcinoma breast cancer cell line, first isolated from the pleural effusions of a 69-year old Caucasian woman [319]. The cells are luminal epithelial in nature, possess cytoplasmic oestrogen receptors and hence can process oestradiol, making it an oestrogen receptor positive (ER+) cell line (https://www.atcc.org/Products/All/HTB-22.aspx, http://www.mcf7.com/). The cells were grown in RPMI-1640 containing 10% foetal bovine serum and 1% PS antibiotics.

### 3.1.3 MDA MB-231 cells

The MDA MB-231 cells are a malignant adenocarcinoma breast cancer cell line first isolated from pleural effusions of a 51-year old Caucasian woman (https://www.atcc.org/Products/All/HTB-26.aspx). The cells are classified under the triple negative breast cancer (TNBC) category, which possess no oestrogen, progesterone, and human epidermal growth factor (Her2/neu) receptors. The cells were grown in RPMI-1640 containing 10% foetal bovine serum and 1% PS antibiotics.

## 3.14 Isolation of CSCs and their characterisation

MCF7 CSCs and MDA MB 231 CSCs were isolated from their respective adherent tumour cell populations based on their sphere-forming capabilities. Briefly, the tumour cells were seeded into a 6 well plate having an ultra-low adherence tissue culture surface. CSC-specific serum-free medium containing a 1:1 ratio of RPMI medium and high-glucose DMEM-F12 medium, supplemented with 20ng/mL EGF, 20ng/mL bFGF, and 1X B27 supplement was used. The cells were allowed to grow for 3 days after which the subsequent experiments for characterisation of CSCs and CCK-8 cell viability assay was performed.

In order to characterise the CSCs, the expression of breast CSC marker CD44 was performed. The CD44 expression was examined through immunoblotting (protocol described in section 3.5), confocal microscopy (protocol described in section 3.6), and flow cytometry. For flow cytometric characterisation, CSCs were stained with both CD44 and CD 24 antibody (double staining) and the CD44+/CD24+ populations were determined.

### 3.1.4 Trypsinisation of cells

All the above cell lines were trypsinised by adding 0.5mL 1X TrypLE Express/25 $cm^2$ of tissue culture surface and the tissue culture flask/plate was placed inside the incubator at 37$^oC$ for 2-3 minutes. Once the cells had dislodged from the tissue culture, which was observed under an inverted microscope (Nikon TS-100), the concentration of TrypLE in the tissue culture flask/plate was diluted using PBS or medium at a rate of 9mL/mL of TrypLE express used. After collecting the dislodged cells into a fresh 15mL or 50mL tube, the cells were centrifuged at 2000 rpm for 5 minutes to obtain the cell pellet. The supernatant was discarded and the cell pellet was resuspended in 1mL of culture medium and mixed gently for cell counting.

### 3.1.5 Cell counting using a haemocytometer

The cell pellet resuspended in 1mL of the culture medium was mixed well before collecting an aliquot for cell counting. 10µL of the cell suspension was mixed with 10µL of 0.4% trypan blue dye and 80µL PBS. From this, 10µL was loaded onto a haemocytometer/Neubauer chamber and the number of cells in the four large corner squares were counted and averaged. The average cell number obtained is at $10^4$ units and was multiplied by the dilution factor (10). The resulting cell number was converted to $10^6$ and the appropriate number of cells was seeded/plated for further experiments.

### 3.1.6 Cryopreservation of cells

For cryopreservation, the cells were routinely trypsinised, and centrifuged and the cell pellet was resuspended in 1mL of normal culture medium for counting purposes. Following cell counting, 900µL of cell suspension in normal growth medium (containing 10% FBS) were transferred to a cryovial (atleast 1 x $10^6$ cells/cryovial) and placed on ice. 100µL of sterile filtered molecular biology-grade dimethyl sulphoxide (DMSO) was added to the chilled cryovial.

The cryovial was transferred to -80$^o$C after placing inside the Mr. Frosty. Before placing the cryovial, the Mr. Frosty was stored at room temperature and isopropanol was added up to the indicated levels in the Mr.Frosty. Mr. Frosty a allows controlled rate of cooling of the cryovials while stored at -20$^o$C at 1$^o$C/minute. On the next day, the cryovial was transferred from the Mr. Frosty into the liquid nitrogen vessel for long-term storage.

### 3.1.7 Recombinant sFRP4 Protein and peptides

Recombinant sFRP4 was exogenously added to the cells at a dose of 250pg/mL, which was previously validated by our laboratory [215, 320, 321], and the treatment durations are as indicated for each experiment.

The sFRP4 peptides were termed ‘SC301’ and ‘SC401’ derived from the - CRD and NLD respectively. From each domain, a library of peptides was initially synthesised and the most active peptide in terms of its anti-tumorigenic properties was chosen

from each domain. SC301 and SC401 are 15 and 20 amino acids in length respectively. Prof. Dharmarajan's laboratory have demonstrated their potency in various tumours originating from breast, ovary, prostate, glioblastoma, and head and neck. The findings have been unpublished due to regulations concerning their intellectual property rights.

## 3.2 Assessment of Cell viability

The rates of cell viability for various experiments were measured using the 3-(4,5-Dimethyl-2-thiazolyl)-2,5-diphenyl-2H-tetrazolium bromide or methylthiazolyldiphenyl-tetrazolium bromide (MTT) assay, where the tetrazolium salts present in the reagent are reduced to formazan crystals (water-insoluble) by the cellular NADPH-dependent oxidoreductases. Hence the amount of formazan that is dissolved in DMSO (Reagentplus®) is measured by its absorbance and indicates the viability of the cells.

### 3.2.1 Optimisation of Seeding Density

In order to optimise the seeding density for the cell viability assay for ADSCs, the cells were seeded at different cell densities in 96 well plates and the MTT assay was performed after 24, 48, and 72 hours. For the tumour cells, the seeding density was previously standardised in this laboratory [256]. The optimal seeding densities used are listed in Table 3.1.

**Table 3.1 Seeding density for cell lines**

| **Cell lines** | **Seeding density/mL** |
|---|---|
| ADSCs | 25,000 cells/mL |
| MCF-7 (adherent) | 50,000 cells/mL |
| MDA MB-231 (adherent) | 50,000 cells/mL |
| MCF-7 (CSCs) | 50,000 cells/mL |
| MDA MB-231 (CSCs) | 50,000 cells/mL |

## 3.2.2 Optimisation of MTT incubation time

For optimising the duration of incubation after addition of MTT for ADSCs, the cells were seeded at the optimised seeding density as above and incubated at 37$^{o}$C for 1hour, 2hour, 3hour, and 4hour time-points. The optimal incubation time was determined to be 4 hours. For the tumour cells, the incubation time was previously standardised [322, 323].

### 3.2.3 MTT protocol performed on ADSCs, MCF-7, and MDA MB 231 cells

For ADSCs and tumour cells, the cells were seeded at the optimum seeding density in a 96-well plate and allowed to adhere overnight to the tissue culture surface. On the next day, the growth medium was aspirated and respective treatments were performed on the cells. The wells contained 100µL of culture medium – either non-conditioned medium or conditioned medium as per the experiment. The treatments with sFRP4, SC301, SC401, SC301+SC401 were performed so that the treatment wells contained these Wnt antagonists at 250pg/mL concentration.

MTT was prepared as 5mg/mL concentration in PBS followed by sterile filtration and was stored at $4^{o}$C (tube wrapped in aluminium foil as MTT is light-sensitive) for future use. Following the treatment on the cells, 10µL of MTT (5mg/mL) was added (in dark conditions) to 100µL of culture medium/well. The plate was wrapped in aluminium foil and incubated for 4 hours at $37^{o}$C. The resulting formazan crystals were dissolved in 100µL DMSO. The absorbance read at 555nm using a plate reader (Enspire multimode, Perkin Elmer) corresponded to cell viability.

### 3.2.4 CCK8 Cell Viability Assay for CSCs

For measuring the proliferation of CSCs, the tumour cells were seeded for CSC isolation in an ultra-low adherence 96 well plate. On Day 3, once the CSCs had formed their spheroid bodies the respective treatments were performed. After the

treatment, 10µL of CCK8 reagent (specific for suspension cells) were added to the medium for a further incubation of 4 hours at 37$^{o}$C. The absorbance read at 405nm using a plate reader (Enspire multimode, Perkin Elmer) corresponded to cell viability. The CCK8 reagent uses the water-soluble tetrazolium salt (WST-8) and hence is suitable for measuring cell proliferation in suspension cells such as CSCs.

## 3.3 Assessment of Reactive oxygen species by DCFDA Assay

MCF7 and MDA MB 231 tumour cells were plated in black 96 well plates in phenol red-free RPMI containing 10% FBS and 1% PS. The cells were allowed to adhere overnight. The next day 10µL of 100µM 2′,7′-Dichlorofluorescin diacetate (DCFDA) was added to all wells for 15 minutes pre-incubation. After 15 minutes, 80µL medium was taken out and treatments were added. 100µL phenol red-free conditioned medium or phenol red-free non-conditioned medium were used. 250pg/mL sFRP4, SC301, SC401, or SC301+SC401 were added to the wells. The plate was incubated and the reactive oxygen species (ROS) generated following the treatments were measured real-time immediately up to 4 hours at various time-points using a plate reader (Enspire multimode, Perkin Elmer) at excitation/emission settings of 482/535nm.

## 3.4 Assessment of Apoptosis

### 3.4.1 JC-1 Assay

A JC1 assay was performed to detect early events of apoptosis occurring after treatment with ADSC-CM on the MCF7 and MDA MB 231 breast cancer cells. Briefly, after 72hours treatment of tumour cells with ADSC-CM in the presence and absence of Wnt antagonists in a black 96 well plate, the medium was replaced with fresh medium and the JC1 dye was added at 10µL/100µL of medium in a 96 well plate. The cells were incubated for 30 minutes at 37$^{o}$C. After the incubation period, the plate was centrifuged to remove the supernatant and then subjected to two washes with assay buffer (200µL assay buffer/well) to remove any excess unbound dye. Immediately after the washes, the fluorescence emitted was measured using a plate reader (Enspire multimode, Perkin Elmer). The JC1 assay measures the level of mitochondrial depolarisation occurring during apoptosis, and the cells were studied to detect a shift in the dye fluorescence from red to green. Healthy cells with high mitochondrial potential contained aggregations of JC1 dye complexes within their healthy mitochondria, detected by red fluorescence with excitation/emission wavelengths of 535nm/595nm. At the same time, the unhealthy apoptotic cells with a low mitochondrial potential contained the dye in its monomeric form, detected by green fluorescence with excitation/emission wavelengths of 535nm/595nm. A low red:green ratio is indicative of mitochondrial depolarisation, and hence, their entry into apoptosis.

### 3.4.2 Caspase 3/7 Assay

ADSC-CM was harvested for treatment in the presence of Wnt antagonists on the two tumour cell lines, and after the 72 hour treatment duration, the cells were harvested and cell lysates were prepared using lysis buffer that was included in the caspase 3/7 kit. The cell lysate was then used to perform the caspase 3/7 assay as per the manufacturer's instructions. Briefly, the cells were harvested after desired treatments and 50µL of 1X cell lysis buffer (prepared as indicated in Table 3.2) was added to the cell pellet and incubated on ice for 30 minutes. The cell lysate was then centrifuged at 5000rpm for 5 minutes, and 50µL of the supernatant was transferred to a black 96 well plate. As a negative control, 50µL of the 1X lysis buffer was added to the 96 well plate. 50µL of the 2X substrate working solution was added to all the wells containing samples or negative control. The plate was then wrapped in aluminium foil and then incubated at room temperature for 30 minutes. R110 was used a reference standard and dilutions were prepared (as listed in Table 3.3) and 100µL of each dilution was added to wells prior to measuring the fluorescence. After 30 minutes of incubation, the levels of caspase3/7 were measured with a plate reader (Enspire multimode, Perkin Elmer) using excitation/emission at 496/520nm.

**Table 3.2 Reagent preparation for caspase 3/7 assay**

| **Item** | **Preparation** |
|---|---|
| 5mM Z-DEVD-R110 | 264µL of DMSO added directly into the vial of Z-DEVD-R110 |
| 1M DTT | 650µL $dH_2O$ added directly to the vial of DTT |
| 5mM R110 Reference standard | 273µL DMSO added directly to vial containing 0.5mg R110 |
| 1X Cell Lysis Buffer | 50µL of 20X cell lysis buffer + 950µL $dH_2O$ |
| 2X Reaction Buffer | 400µL of the 5X reaction buffer + 10µL 1M DTT + 590µL dH2O |
| 2X Substrate working solution | 10µL of 5mM Z-DEVD-R110 substrate + 990µL of 2X reaction buffer |
| 1X Reaction Buffer | 100µL of 5X Reaction buffer + 400µL $dH_2O$ |

### 3.4.2.2 Dilutions of R110 prepared as standards

Along with the samples, R110 standards were also prepared for measuring their fluorescence. R110 standards were prepared as shown in Table 3.3 and 100µL of each of them was added to each well of the 96-well black microplate. The fluorescence of R110 standards were read along with the samples as a positive control.

**Table 3.3 Preparation of R110 standard dilutions**

| **Concentrations** | **Preparation** |
|---|---|
| 25µM | 25µL of 100µM R110 + 75µL of 1X Reaction Buffer |
| 20µM | 20µL of 100µM R110 + 80µL of 1X Reaction Buffer |
| 15µM | 15µL of 100µM R110 + 85µL of 1X Reaction Buffer |
| 10µM | 10µL of 100µM R110 + 90µL of 1X Reaction Buffer |
| 5µM | 5µL of 100µM R110 + 95µL of 1X Reaction Buffer |
| 0µM | 0µL of 100µM R110 + 100µL of 1X Reaction Buffer |

## 3.5 Assessment of protein expression by Western blotting

### 3.5.1 Preparation of whole cell lysate

The whole-cell lysates cells were obtained using a 1X RIPA lysis buffer (prepared as in Table 3.4). Briefly, the growth medium was aspirated and the cells were washed twice with 1x PBS. The cells were scraped off the tissue culture surface (either a 6-well plate or a 24-well plate using a 23mm sterile cell scraper into PBS and centrifuged to obtain a cell pellet at 14000g for 10 minutes. The resulting cell pellet was resuspended with 1X lysis buffer (1X LB) containing 1X RIPA buffer, 1X protease-phosphatase inhibitor cocktail and 1mM phenyl methane sulfonyl fluoride (PMSF). Alternatively, 1X LB was added directly to the cells in the culture dish after medium aspiration and PBS washes. 100µL and 25µL of 1X LB (containing 1X proteinase phosphatase inhibitor cocktail and 1M PMSF) were added to each well of a 6-well plate and 24-well plate respectively.

**Table 3.4 Composition of 1X lysis buffer**

| **Components** | **Volume for 100µL** |
|---|---|
| 1X RIPA buffer | 98.9µL |
| 100X Proteinase Phosphatase Inhibitor Cocktail | 1µL |
| 1M PMSF | 0.1µL |

### 3.5.2 Quantification of the protein lysate using BCA Assay

The total protein content of the whole cell lysate was quantified using a colorimetric detection and quantitation method using the bicinchoninic acid (BCA) assay. Briefly, serial dilutions of protein standards ranging from 25µg/mL to 2mg/mL were prepared using bovine serum albumin stock (2mg/mL) and milliQ water (prepared as in Table 3.5). 10uL of the standards were pipetted into Eppendorf tubes or 96 well plates. The cell lysate samples were diluted 1:4 with milliQ water. 10µL of the protein standards and diluted cell lysate samples were transferred into Eppendorf tubes or 96 well plates. The BCA working reagent was prepared fresh by mixing 50 parts of Reagent A with 1 part of Reagent B and mixed well. 200µL of this working reagent was added to the protein standards and samples, mixed well, and allowed to incubate for 30 minutes at 37$^{o}$C. After the incubation, the absorbance of the standards and samples was measured using a Nanodrop reader (Thermo Scientific Nd-1000) if performed in Eppendorf tubes, or a plate reader (Enspire multimode, Perkin Elmer) if the assay was performed in 96 well plates. Once a valid standard curve was obtained, the concentrations of total protein content of the cell lysates were calculated.

**Table 3.5 Preparation of BSA standards for BCA assay**

| **Standards** | **Volume of BSA (µL)** | **Volume of MilliQ water (µL)** | **Concentration (mg/mL)** |
|---|---|---|---|
| A | 300 | 0 | 0.025 |
| B | 375 | 125 | 0.125 |
| C | 325 | 325 | 0.250 |
| D | 175 of vial B dilution | 175 | 0.500 |
| E | 325 of vial C dilution | 325 | 0.750 |
| F | 325 of vial E dilution | 325 | 1 |
| G | 325 of vial F dilution | 325 | 1.5 |
| H | 100 of vial G dilution | 400 | 2 |
| I | 0 | 400 | 0 = Blank |

### 3.5.3 SDS-PAGE Electrophoresis

**Using hand-cast gels:** The SDS-PAGE gels required for performing electrophoresis were hand-cast using 10% resolving gels and 4% stacking gels. The gels were prepared using the following components listed in Table 3.6, and 3.7 respectively.

The resolving gel was layered with isopropanol to form a uniform gel surface and was allowed to polymerise and solidify for an hour. After 1 hour the isopropanol was poured off and excess isopropanol was dried using a filter paper. The stacking gel was poured on top of the resolving gel and a 10-well comb was placed. The gel was allowed to polymerise and solidify for 30 minutes. Ammonium persulphate (APS) was prepared fresh before use. Both APS and tetramethylethylenediamine (TEMED) were added just prior to pouring the gel in the cassette.

After 30 minutes of pouring the stacking gel, the gel cassettes were placed in a Biorad Tetra cell Tank containing 1X Tris-SDS-glycine running buffer. 100mL of the 10X running buffer was diluted 10 times with 900mL of $dH_2O$ to prepare 1X running buffer.

**Table 3.6 Composition of resolving gel (10%)**

| **Item** | **Volume required for 10mL** |
|---|---|
| 30% Acrylamide/Bisacrylamide | 3.3 mL |
| Resolving gel buffer (1.5M TrisHCl) pH: 8.8 | 2.5 mL |
| 10% SDS | 0.1 mL |
| 10% APS | 50 µL |
| TEMED | 5µL |
| $dH_2O$ | 4.1 mL |

**Table 3.7 Composition of stacking gel (4%)**

| **Item** | **Volume required for 10mL** |
|---|---|
| 30% Acrylamide/Bisacrylamide | 1.3 mL |
| Stacking gel buffer (0.5M Tris-HcL) pH: 6.8 | 2.5 mL |
| 10% SDS | 0.1 mL |
| 10% APS | 50 µL |
| TEMED | 10 µL |
| $dH_2O$ | 6.1 mL |

**Table 3.8 Composition of 10X running buffer**

| **Item** | **Amount required for making 1L** |
|---|---|
| Tris Base | 30.3g |
| Glycine | 144.0g |
| SDS | 10gm |

The samples for loading were prepared as in Table 3.9. An appropriate volume of cell lysate corresponding to 10-20µg was taken in a fresh Eppendorf tube and the volume was made up to 15µL with milliQ water. Sample buffer was prepared by mixing 4X Laemmeli buffer with β-mercaptoethanol at a 1:10 ratio. 5µL of the prepared sample buffer was added to 15µL of cell lysate-water mixture, so that the sample buffer reached the final concentration of 1X. The sample tubes were given a short spin to mix well and placed for heat denaturation in a 95$^{o}$C dry bath for 5 minutes. Immediately after denaturation, the sample tubes were placed on ice and loaded onto the SDS-PAGE gel. A pre-stained ladder was also loaded in one of the lanes. The electrophoretic run was performed at 200V for 40 minutes or until the dye front reached the bottom of the gel.

**Table 3.9 Sample preparation for gel electrophoresis for pre-cast gels**

| **Components** | **Volume** |
|---|---|
| Whole cell lysate | Volume corresponding to 10-20µg |
| MilliQ water | Dilute the cell lysate up to 15µL |
| 4X Laemmeli Sample Buffer mixed with β-mercaptoethanol (1:10) | 5µL |

**Using pre-cast gels:** Alternatively, for performing electrophoresis 4-12% pre-cast Bis-Tris SDS-PAGE gels were also used. The 1X running buffer was prepared from a stock of 20X 2-(N-morpholino)ethanesulfonic acid (MES) running buffer by diluting with MilliQ water. 10-20µg of cell lysates were prepared for loading (prepared as in Table 3.10) by mixing with lithium dodecyl sulphate (LDS) and reducing agent, and were heated at 95$^{o}$C for 5 minutes in a dry bath. Following heating, the samples were placed on ice until loading. 40µL of the samples were loaded per well and the run was performed at 165V for 30 minutes.

**Table 3.10 Sample preparation for gel electrophoresis for pre-cast gels**

| **Components** | **Volume** |
|---|---|
| Whole cell lysate | Volume corresponding to 10-20µg |
| MilliQ water | Dilute the cell lysate up to 31.2µL |
| LDS | 12µL |
| Reducing agent | 4.8µL |

## 3.5.4 Immunoblotting

Following electrophoresis, the protein bands in the gel were wet-transferred onto a nitrocellulose membrane using a Biorad transfer apparatus. The nitrocellulose membrane was pre-wetted in milliQ water for atleast 10 minutes prior to the transfer. Briefly, the gel was placed on the nitrocellulose membrane and sandwiched between tissue paper stacks and fibre pads on both sides. The gel-membrane assembly was placed within the transfer apparatus containing 1X transfer buffer (prepared as in Table 3.11). The transfer was performed from the gel onto the membrane at 100V for 1 hour at room temperature with an ice-cold gel pack immersed within the 1X transfer buffer in the tank.

**Table 3.11 Composition of 10X transfer buffer**

| Item | Amount required for making 1L |
|---|---|
| Tris Base | 30.3g |
| Glycine | 144.0g |

The 10X transfer buffer was diluted 10 times with water to prepare the 1X transfer buffer, and methanol was added to the 1X transfer buffer just before use (100mL of 10X transfer buffer + 100 mL of methanol were added to 800 mL of $dH_2O$). Alternatively, the protein bands were electro-transferred onto the nitrocellulose membrane using iBlot transfer stacks and device (Thermo Fischer Scientifc).

After the transfer, blocking of the membrane was performed for 1 hour or overnight at $4^oC$ using a 5% non-fat dry milk solution prepared in 1X PBST. 5 x 4 minutes washes were performed with 1X PBST. Incubation of the blot with anti-human rabbit primary antibodies specific for target proteins was carried out overnight at $4^oC$ on a shaker. The blots were also probed with an antibody against β-actin as the house-keeping control. All the primary antibodies were prepared in 5% bovine serum albumin (BSA) solution in 1X PBST. The blots were then washed with 1X PBST for 5 x 4 minutes washes. This was followed by anti-rabbit HRP-conjugated secondary antibody incubation for 1 hour at room temperature. The secondary antibody was prepared in a 5% non-fat dry milk solution in 1X PBST. The blots were washed in 1X PBST after the secondary antibody incubation and chemiluminescence detection was performed. The reagent 1 and 2 of the Amersham ECL Western blotting

detection kit were aliquoted in a tube wrapped with aluminium foil (as reagents are light-sensitive) and thawed to room temperature. Equal volumes of Reagent 1 and 2 were mixed well and added on the surface of the blot to form a thin film and incubated in dark conditions for 30-60 seconds. Densitometry of the detected bands was used to quantify the protein expression using Image Lab software (Biorad), and the resulting band intensities were normalised to β-actin.

### 3.5.5 Quantification of bands of Immunoblotting

The bands detected by chemiluminescence were analysed by densitometric calculations using the BioRad software Image Lab. The lanes and bands were detected using the software followed by its relative quantitative measurement. Bands of the control sample were considered as reference bands against which all other bands were comparatively quantitated. This fold change (Band intensity of treatment band/Band intensity of reference band) of the target protein was provided by the software. Similarly, samples were analysed for their house-keeping protein (β-actin). The ratio of target protein expression/house-keeping protein expression was considered as the sample's relative protein expression.

## 3.6 Assessment of protein expression by Immunofluorescence

The cells were seeded in 96 well plates and allowed to attach. Specific treatments were performed following which the growth medium was aspirated. The cells were gently washed with PBS and fixed with 4% paraformaldehyde (PFA) for 20 minutes

at room temperature. Following fixation, the cells were rinsed twice with PBS and an additional permeabilisation step was performed for 2-5 minutes using 0.3% saponin in PBS. Following permeabilisation, the cells were rinsed with PBS and blocked using blocking buffer for 1 hour at room temperature. The blocking buffer contained 0.5% BSA, 0.3% saponin, and 1% normal goat serum (Table 3.12). The cells were then rinsed with 3 washes of PBS, after which the primary antibody incubation (at 1:200 concentration in blocking buffer) was performed overnight at $4^{o}$C.

On the next day, primary antibody solution was removed and followed by 3 PBS washes. The secondary antibody incubation was performed using a FITC–tagged secondary antibody (at 1:200 concentration prepared in blocking buffer) for 1 hour at room temperature. Following 3 PBS washes, the cells were incubated with DAPI (4',6-Diamidino-2-phenylindole dihydrochloride) nuclear stain for 5 minutes, rinsed, and observed under an inverted confocal fluorescent microscope (Nikon).

**Table 3.12 Composition of blocking buffer in 1X PBS**

| **Components** | **Concentration** |
|---|---|
| BSA | 0.5% |
| Saponin | 0.3% |
| Normal goat serum | 1% |

### 3.6.1 Quantification of Immunofluorescence intensities

Micrographs of the control and treatment wells were captured at random locations using a Nikon confocal microscope. The images were captured using a 10X objective

with its normal field of view. Additionally, using the same objective, a broader field of view was also captured at the same location in order to capture multiple images to be subsequently stitched together by the Nikon NIS Elements software. The images were captured and exported to TIFF format using Nikon NIS-elements software, the fluorescence intensities of the whole micrographs were analysed using Image J software. The intensities were measured using a minimum of 5 images per treatment group followed by calculating their average fluorescence intensity. The fluorescence intensity of the untreated control was considered as a reference and the fluorescence intensities of other treatment groups were compared against the control intensity.

## 3.7 Assessment of migration potential of tumour cells

### 3.7.1 Scratch Wound Assay

Tumour cells (MCF7 or MDA MB 231) were plated onto Ibidi chambers (Ibidi) at a density of 40,000 cells/70µL/chamber and allowed to adhere overnight. Once the cells attained around 90% confluence, the cell culture insert within the dish was removed, exposing the gap between the two chambers. Alternatively, tumour cells were grown to 90% confluence after which a scratch was made using a 200µL sterile tip. The cells were rinsed with PBS to remove any debris and replaced with ADSC-CM treatments. The width of the gap before and after the treatment was measured to calculate the distance migrated using Image J software.

### 3.7.2 Quantification of the distance migrated in the scratch-wound assay

The micrographs of the scratch were captured at T0 and T24 time-points of the treatment duration. The width of the scratch was measured using Image J software (National Institute of Health) by drawing a line across the scratch width and measuring its length using the software. The distance migrated was then calculated by subtracting the width of the scratch after 24 hours (T24) from width of scratch at 0 hour (T0).

## 3.8 Harvest of CM from ADSCs (ADSC-CM)

For conditioned medium harvest, ADSCs were cultured in RPMI (the ADSC medium here was matched with that of tumour cell medium (RPMI) to avoid any variation) containing 10% foetal bovine serum and 1% PS. On attaining around 80-85% confluence, the ADSC medium was replaced with serum-free RPMI and conditioning was performed for 3, 12, 24, and 48 hours. The harvested conditioned medium was spun at 2000g for 10 minutes and the supernatant was filtered using 0.22µm syringe filters. These conditioned medium was harvested and added fresh onto the tumour cells, and the respective assays were carried out. The general aspects of tumour cells measured were: proliferation, migration, apoptosis, ROS, gene expression, and protein expression.

### 3.8.1 Molecular weight cut-off for ADSC-CM

The ADSC-CM was filtered using molecular weight cut-off (MWCO) filters of size 30KDa. The purpose behind using the 30KDa MWCO filters was to identify whether the sFRP4 containing fraction of ADSCs was responsible for any of the ADSC-CM's inhibitory effects. Upon filtration, the ADSC-CM was separated into 2 fractions- the >30KDa fraction was present in the retentate on top of the filter while the <30KDa fraction was eluted through the filter and present in the bottom. The <30KDa fraction and >30KDa fraction were collected from the flow-through and run on an SDS-PAGE to confirm the molecular weights. Further, the <30KDa fraction was used for cell viability studies to determine its growth inhibitory capability.

### 3.8.2 Denaturation of ADSC-CM

To determine the biochemical property of the component/s present within the ADSC-CM contributing to its anti-tumour effect, the denaturation of the ADSC-CM was performed. This elucidated whether the growth inhibitory property of the ADSC-CM was due to a protein or a non-protein component present in the medium. Denaturation was performed by boiling the medium at $95^{o}C$ for 5 minutes so as to inactivate the biological function of the protein components. The denatured ADSC-CM was then cooled to room temperature before adding to the tumour cells to test for any growth inhibitory property.

## 3.9 Treatment with ADSC-derived Extracellular Matrix (ECM)

### 3.9.1 Preparation of ADSC-derived ECM

The ADSCs were seeded at confluent densities in a 96 well plate (10,000-15,000 cells/well) and were allowed to grow and secrete ECM for up to 3 days. On Day 3, the ADSCs were decellularised in order to obtain the ADSC-derived ECM. For decellularisation, the ADSCs were treated with 20mM ammonium hydroxide and 0.5% Triton-X 100 reagent for 2-3 minutes and thereafter rinsed thrice with ice-cold PBS to remove any cell debris. Decellularisation was confirmed by performing DAPI staining and the plates were examined using an inverted fluorescent microscope (Nikon).

### 3.9.2 Treatment of tumour cell lines with ADSC-derived ECM

After decellularisation of ADSCs, the tumour cell lines were seeded (at 5000 cell/well) onto the ADSC-secreted ECM in a 96 well plate and allowed to grow on this matrix. As a control, tumour cell lines were grown on a normal tissue culture-treated surface. Treatments were performed in the presence and absence of 250pg/mL sFRP4, SC301, SC401, and SC301+SC401. An MTT cell viability assay was performed on the tumour cell lines at the 24, 48, and 72 hour time-points.

## 3.10 Harvest of Tumour Conditioned Medium

For tumour conditioned medium (TCM) harvest, MCF7 and MDA MB 231 cells were cultured up to around 90% confluence in T175 or T75 flasks in RPMI medium containing 10% FBS and 1% PS. For conditioning, the medium was changed to serum-free RPMI containing 1% PS, and the conditioning was performed for 24 hours. 25mL of fresh serum-free RPMI containing 1% PS was added to a T175 flask, and 10mL of the same was added to a T75 flask for conditioning. After 24 hours, the TCM was harvested and spun down at 2000g for 10 minutes, and filtered through 0.22µm syringe filters to perform treatments on ADSCs.

### 3.10.1 Treatment of ADSCs with TCM derived from MCF7 and MDA MB 231 cells (MCF7-TCM or MDA MB 231 TCM)

To assess the transforming potential of ADSCs into TAFs, ADSCs were cultured for a period of 4-10 days in the presence of 24 hour TCM harvested from the two tumour cell lines. As positive control for myofibroblast transformation, ADSCs were treated for 10 days with different doses of TGF-β at 0.2ng/mL, 2ng/mL, 5ng/mL, and 10ng/mL, and LPA at 5µM and 10µM to induce differentiation towards a TAF phenotype. The change in the morphology of the ADSCs upon exposure to TGFβ and LPA was observed using an inverted microscope (Nikon TS-100). Further, in order to confirm that the TGF-β-induced differentiation could be rescued, a pharmacological inhibitor of TGF-β receptor signalling - SB431542 was used at

10μM for 4 days. To understand the role of Wnt signalling in the transformation of ADSCs, 250pg/mL of sFRP4, SC301, SC401, and SC301+SC401 were supplemented to the TCM derived from MCF7 and MDA MB 231 cells on the ADSCs.

The treated ADSCs were analysed for their cell viability using an MTT cell viability assay after 4-day and 10-day treatments. For the MTT cell viability assay, ADSCs were seeded at 2500 cells/well in a 96 well plate. ADSCs were seeded at 3000 cells/$cm^2$ in 96 well plates and 6 well plates in RPMI containing 10% FBS and 1% PS for performing immunofluorescence and immunoblotting respectively for TAF-associated markers. ADSCs were seeded at 1000 cells/well of a white 96-well plate for performing the glucose uptake assay. ADSCs were seeded at 3000 cells/well of a specific 96 well plate designed for Seahorse flux analysis to perform the glycolysis stress test. After the cells had attached, the medium was replaced by MCF7-TCM and MDA MB 231-TCM and supplemented with 250pg/mL sFRP4, SC301, SC401, and SC301+SC401. Non-differentiated ADSCs growing in non-conditioned serum-free RPMI were used as a control. After the indicated treatment durations (4 days or 10 days), the medium was removed and rinsed once with PBS, and then the samples were processed for immunofluorescence, Western blotting, and Seahorse flux analysis.

ADSCs were seeded at 1000 cells/well of a white 96-well plate for performing the glucose uptake assay. After the cells have attached, the medium was replaced with MCF7 TCM and MDA MB 231 TCM in in the presence and absence of sFRP4, SC301, SC401, and SC301+SC401. Non-differentiated ADSCs growing in non-conditioned serum-free RPMI were used as a control. On Day 10, the medium was

removed and rinsed once with PBS, and then the samples were processed for immunofluorescence and Western blotting.

## 3.11 Assessment of Metabolic Reprogramming by Seahorse Flux Analysis

Potential alterations in metabolic flux following the transformation ADSCs into TAFs was assessed using Seahorse XFe96 flux analyser (Agilent Technologies) and a standard glycolysis stress test, which allows the determination of glycolytic rate, glycolytic capacity, and glycolytic reserve (Table 3.15). A change in the metabolic phenotype of ADSCs switching from oxidative phosphorylation to glycolysis was assessed after treating the ADSCs with TCM from MCF7 and MDA MB 231 tumour cell lines.

ADSCs were seeded at 3000 cells/well in a 96 well plate specifically designed for Seahorse analysis in RPMI medium containing 10% FBS and 1% PS. After ADSCs attached to the plate surface, the medium was replaced with MCF7-TCM and MDA MB 231-TCM in treatment groups. ADSCs grown in serum-free RPMI were used as a control. sFRP4, SC301, SC401, and SC301+SC401 at 250pg/mL were added to the TCM-containing wells and wells containing non-conditioned control medium. The treatments were performed for 4 days and 10 days.

On the day before the assay, the Seahorse cartridge containing the sensor probes was immersed in 200µL calibration solution in a utility plate and incubated in a non-$CO_2$ incubator at 37$^{o}$C for hydration. The hydration was performed for 24 hours prior to

starting the assay. Glucose-free DMEM was prepared for the assay using DMEM powder dissolved and made up to 1L using sterile autoclaved milliQ water. 2mM glutamine, 1mM sodium pyruvate, and phenol red were added to the medium (Table 3.13) and the pH was adjusted to 7.35 ± 0.05 using freshly prepared 1M NaOH. The medium was then filtered using a 0.2µm bottle-top sterile filter unit via a vacuum filtration method and was stored at 4$^{o}$C for future use.

**Table 3.13: Composition of glucose-free medium for Seahorse assay**

| **Component** | **Amount** |
|---|---|
| DMEM (Glucose-free) powder | 1 full bottle for preparing 1L medium |
| Glutamine | 2Mm |
| Sodium pyruvate | 1mM |
| Phenol red | 3mL |
| Sterile autoclaved milliQ water | 1L |

On the day of the assay, the medium in the wells was gently removed and 4 medium changes were performed manually using glucose-free medium. After performing the medium changes on the plate, the final medium volume per well was 175µL and was incubated at 37$^{o}$C in the non-$CO_2$ incubator for at least 1 hour. The assay was performed through injection of 3 metabolic compounds in the designated ports of the cartridge – glucose, oligomycin, and 2-deoxyglucose (2-DG) (Table 3.14). All injection volumes were maintained at equal volumes of 25µL.

- Injection of glucose through port A facilitates exposure to a saturating concentration of 25mM glucose. For this, 2mL of 45% glucose + 23mL glucose-free DMEM was mixed resulting in 200mM glucose, pH was adjusted

to 7.35±0.05 at 37$^{o}$C, followed by sterile filtration. From this, 25µL was added into the cartridge port to result in a final concentration of 25mM glucose inside the well.

- The second injection through port B facilitates the exposure to 1µM oligomycin, which inhibits ATP synthase in the oxidative phosphorylation. For this, 5mM stock solutions were prepared in DMSO, and from this 9µM working stocks were prepared in glucose-free DMEM. From this, 25µL was injected through the cartridge port, resulting in a final concentration of 1µM oligomycin inside the well.
- The third injection through port C facilitates the exposure to 100mM 2-deoxy glucose (2-DG), which acts as an analogue of glucose by converting itself into 2-DG-phosphate and blocks glycolysis. For this, 1M of 2-DG was prepared in glucose-free DMEM, pH was adjusted to 7.35±0.05 at 37$^{o}$C using 1M NaOH, followed by sterile filtration. From 1M 2-DG, 25µL was added through cartridge port, resulting in a final concentration of 100mM 2-DG inside the well.
- The fourth injection through port D was 25µL of glucose-free DMEM medium. This was performed for maintaining equal injection volumes in all the ports.

The assay was designed using Wave software, and prior to running the assay, the cartridge was calibrated in the Seahorse analyser. The cartridge was placed on the utility plate and equilibrated while on the utility plate. Following completion of calibration and equilibration, the cell culture plate was inserted into the machine.

**Table 3.14: Injection pattern into the cartridge ports**

| **Injection port** | **Metabolite injected** | **Conc. used for injection** | **Vol. used for injection** | **Vol. in well during injection** | **Dil Factor in well** | **Final conc. in well** |
|---|---|---|---|---|---|---|
| A | Glucose | 200mM | 25µL | 175µL | 8X | 25mM |
| B | Oligomycin | 9µM | 25µL | 200µL | 9X | 1µM |
| C | 2-DG | 1M | 25µL | 225µL | 10X | 100mM |
| D | Glucose-free DMEM | NA | 25µL | 250µL | NA | NA |

The metabolic parameters measured were:

**Table 3.15: Metabolic parameters measured using glycolysis stress test with Seahorse XF$^{e}$96 flux analyser**

| **Metabolic parameter** | **Significance** | **Equation** |
|---|---|---|
| Glycolytic rate | Provides the rate of glycolysis (conversion of glucose to pyruvate) under basal conditions. It is obtained by measuring ECAR after addition of saturating concentration of glucose. | Maximum ECAR measurement before oligomycin injection – Last rate measurement before glucose injection |
| Glycolytic capacity | Provides the maximum glycolytic capacity by measuring ECAR following addition of oligomycin (an ATP synthase inhibitor), which shifts the energy production to glycolysis. | Maximum ECAR measurement after oligomycin injection – Last measurement before glucose injection |
| Glycolytic reserve | Measures the difference between the maximum glycolytic capacity and glycolytic rate at basal conditions. It indicates the ability of the cell to respond during lack of energy production through oxidative phosphorylation. | Glycolytic capacity – Glycolytic rate |
| Non-glycolytic acidification | Measures the ECAR after addition of 2-DG, Indicates ECAR caused by cell processes other than glycolysis. | Minimum ECAR measurement after addition of 2-DG |

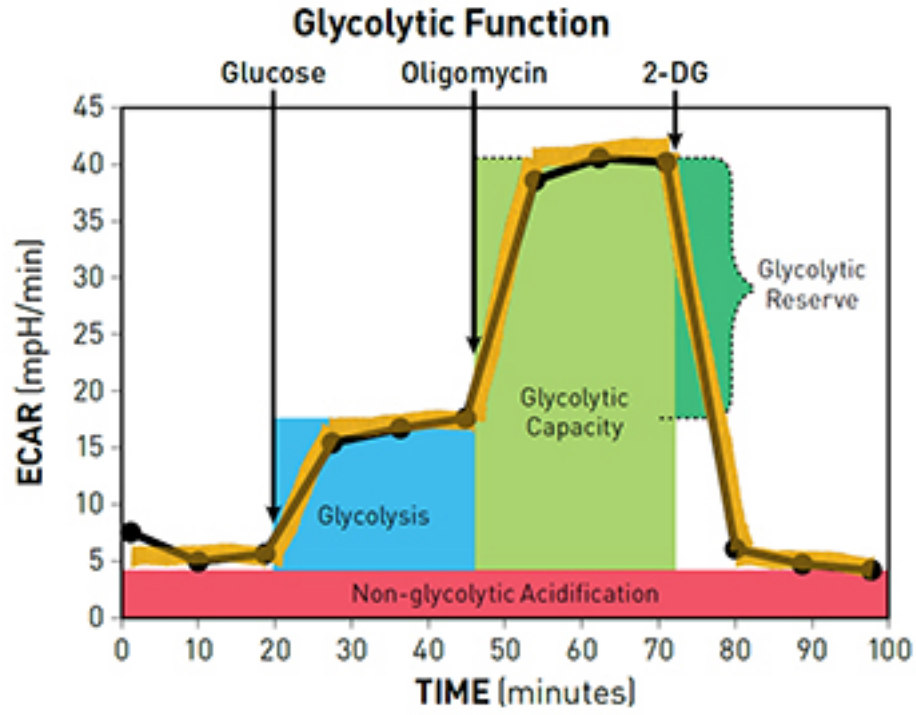


**Figure 3.1: Glycolysis stress test profile of the key parameters of glycolytic function.**

Sequential injection of metabolites - glucose, oligomycin, and 2-DG which allows the measurement of glycolytic rate, glycolytic capacity, glycolytic reserve, and non-glycolytic acidification by measuring the ECAR (Figure sourced from the Glycolysis stress test user guide, Agilent Technologies).

## 3.11 Assessment of rate of glucose uptake using glucose uptake assay

Glucose uptake by the ADSCs was measured using the luminescence-based glucose uptake glo-assay kit. ADSCs were seeded at 1000 cells/well in a white 96 well plate and allowed to attach to the tissue culture surface. After that, cells were exposed to

MCF7-TCM and MDA MB 231-TCM ± sFRP4, SC301, SC401, and SC301+SC401 for 4 days. After 4 days of treatment, the medium was removed slowly and the cells were washed gently with 100µL PBS twice to remove any residual glucose. After the PBS wash, 50µL of 2-DG was added at 1mM and incubated for 10 minutes at 37$^{o}$C. 1mM 2-DG was freshly prepared in PBS from the 100mM 2-DG stock provided in the kit. 2-DG is a glucose analogue that is transported across the cell membrane (similar to glucose) and is phosphorylated into 2-DG-6-phosphate (2-DG6P). Once the 2DG6P accumulated inside the cell, the reaction was stopped after 10 minutes of incubation by adding 25µL stop buffer, which lyses the cells and stops the reaction. 25µL of neutralisation buffer was added to neutralise the acid and this was followed by the addition of 100µL of 2DG-6-phosphate (2DG6P) detection reagent. The detection reagent consists of glucose-6-phosphate dehydrogenase (G6PDH), $NaDP^{+}$, reductase, ultra-glo recombinant luciferase, and proluciferin substrate (Table 3.15), and was prepared at least 1 hour before addition to allow it to equilibrate to room temperature. Following addition of the detection reagent, the cells were incubated at room temperature for 30 minutes up to 6 hours, and the luminescence was recorded using a plate reader (Enspire multimode, Perkin Elmer). The luminescence corresponds to the concentration of 2DG6P, which correlates to the amount of glucose taken up by the cells.

**Table 3.16: Composition of Detection Reagent**

| Component | Per Reaction |
|---|---|
| Luciferase reagent | 100µL |
| NADP+ | 1µL |
| G6PDH | 2.5µL |
| Reductase | 0.5µL |
| Reductase substrate | 0.0625µL |

## 3.12 Characterization of ADSCs by adherence, surface markers, and tri-lineage differentiation

The plastic adherence property of ADSCs was observed by culturing in low glucose DMEM containing 10% FBS and 1% PS antibiotics at 37$^{o}$C in the presence of 5% $CO_2$. The surface markers had been previously analysed by flow cytometric characterization by Lonza when the cell line was purchased. Further, for characterising the multipotent property of ADSCs, tri-lineage differentiation was performed into adipogenic, osteogenic, and chondrogenic lineages. Briefly, the cells were seeded at the appropriate seeding densities, grown to 90% confluence in growth medium, and then replaced by the respective differentiation medium (Invitrogen) for specific durations. Undifferentiated ADSCs maintained in basal growth medium served as control.

At the end of the differentiation period, lineage-specific staining was performed to visualise the differentiation and observed using bright field microscopy with an inverted Nikon microscope. Briefly, cells were fixed with 4% PFA for 30 minutes,

and rinsed with PBS. Following fixation, lineage-specific staining methods such as Oil Red O, alizarin red/von Kossa, and alcian blue were used for detecting adipogenic, osteogenic, and chondrogenic lineages respectively.

## 3.13 Treatment doses for Wnt activators and Wnt antagonists for differentiation studies

The following regulators of the Wnt signalling pathway were used: Wnt activators (i) LiCl, and (ii) BIO, and the Wnt antagonist sFRP4. The doses of these molecules required for the differentiation assay were standardised using an MTT assay. The surface-adherent ADSCs were treated for 48 hours with different doses of LiCl (ranging from 1mM-20mM), BIO (ranging from 0.5µM-10µM), and sFRP4 (ranging from 100pg/mL to 1µg/mL). Following the treatment, the MTT assay was performed as described above (section 2.2.3).

### 3.13.1 Adipogenic differentiation

For adipogenic differentiation, ADSCs at passage 4 were seeded at 10,000 cells/$cm^2$, and allowed to grow to 90% confluence. On Day 5 post-seeding, the adipogenic induction was initiated by replacing basal growth medium with adipogenic differentiation medium in treatment wells, while control ADSCs were maintained in their growth medium. The adipogenic medium was individually supplemented with appropriate doses of the Wnt regulators LiCl, BIO, and sFRP4 (as standardised by the MTT assay) during the period of differentiation. Later, a combination treatment

containing both BIO and sFRP4 was also performed to observe the interaction between the Wnt activator and antagonist on adipogenesis. The medium was replenished every 3-4 days. Morphological observations for accumulation of lipid droplets in all treatment conditions were recorded and photographed at regular intervals throughout the adipogenic differentiation period using an inverted Nikon microscope. On Day 7 post-induction, cells were analysed for lipid accumulation by Oil red O staining and were harvested to detect the protein expression of adipogenic markers. 24 well-plates were used for histochemical staining while 6 well-plates were used for protein extraction.

### 3.13.2 Oil Red O staining and quantification

A working solution of Oil Red O stain was prepared by adding 30mL stock solution (0.5% Oil Red O in 100% isopropanol) with 20mL distilled water. On day 7, the cells were fixed with 4% PFA for 30 minutes, rinsed with PBS, and stained with the Oil Red O working solution for 30 minutes. Cells were rinsed with PBS, observed for the stained intracellular lipid droplets, and photographed using a bright field inverted Nikon microscope and Nikon software. Quantification of the stained area was performed by eluting the stain off the plate by incubation with 100% isopropanol for 1 hour, followed by measuring the absorbance of the elutes at 510nm using an EnSpire multimode plate reader (Perkin Elmer).

## 3.14 Osteogenic differentiation

ADSCs were seeded at 5000 cells/$cm^2$ in 6 well plates and grown for 4 days in normal ADSC growth medium. After 4 days, the medium was replaced by osteogenic differentiation medium and the differentiation was continued for 28 days with regular medium changes every 3-4 days.

### 3.14.1 Von-Kossa Staining

After 28 days, the medium was aspirated and rinsed with PBS before fixing it with 4% PFA for 30 minutes. Cells were rinsed with PBS. Cells were incubated with 1% silver nitrate solution under ultraviolet light for 20 minutes. Cells were rinsed with PBS and counterstained with 5% sodium thiosulphate for 5 minutes to remove any residual unbound silver. Following this, the cells were rinsed with PBS and observed under a Nikon inverted microscope to capture micrographs.

### 3.14.2 Alizarin Red S Staining

After differentiation into osteogenic lineage for 28 days, the cells were rinsed and fixed using 4% PFA for 30 minutes. Followed by a rinse with PBS, it was stained with 2% alizarin red S solution (pH: 4.2) for 2-3 minutes. Then cells were rinsed thrice in PBS and viewed under a Nikon inverted microscope to capture micrographs.

## 3.15 Chondrogenic differentiation

ADSCs were seeded at high cell densities of in 6 well plate using a micromass culture technique where the cells are seeded at high cell densities to form a small droplet on the culture surface. The cells were seeded at 0.16 x $10^6$ cells/mL cell density and a 5µL droplets of the cell solution was placed in the centre of the well in a 6 well plate. The cells were cultured in normal ADSC growth medium for 2 hours at 37$^o$C followed by shifting their medium to chondrogenic differentiation medium, and the differentiation was continued for 21 days with regular medium changes every 3-4 days.

### 3.15.1 Alcian Blue Staining

The medium was removed after 21 days of chondrogenic differentiation followed by rinsing with PBS. The cells were then fixed with 4% PFA for 30 minutes. Then cells were rinsed with PBS and stained with 1% alcian blue solution for 30 minutes. The

cells were then rinsed with 0.1N HCl thrice for 30 minutes and viewed under a Nikon inverted microscope to capture micrographs.

## 3.16 Data analysis

The experiments were performed in multiple replicates and the mean values ± SEM were calculated. Statistical significance was calculated using a Student's t-test to compare between the values of the treatment conditions against untreated controls (indicated by *), and if required in between two treatment groups (indicated by #). A p value of $<0.05$ was considered statistically significant and any treatments which generated non-significant results were left unindicated in the figures.

# AIMS

**1. To determine the effect of ADSC-secreted factors on the breast tumour cell lines MCF7 and MDA MB 231 with regard to Wnt antagonism (Described in Chapter 4)**

1a. To determine the effect of ADSC-conditioned medium (ADSC-CM) and to characterise the components within ADSC-CM contributing to its influence on tumour cell lines

1b. To determine the effect of ADSC-CM in combination with the Wnt antagonist sFRP4 on the breast tumour cell lines

1c. To determine the effect of ADSC-CM in combination with the sFRP4 peptides on breast tumour cell lines

**2. To determine the effect of breast tumour-derived factors from MCF7 and MDA MB 231 cell lines on the transformation of ADSCs into tumour associated fibroblasts with regard to Wnt antagonism (Described in Chapter 5)**

2a. To determine the effect of tumour-conditioned medium (TCM) in combination with the Wnt antagonist sFRP4 on the transformation of ADSCs into TAFs

2b. To determine the effect of TCM in combination with the sFRP4 peptides on the transformation of ADSCs into TAFs

**3. To determine the role of the Wnt antagonist sFRP4 on the adipogenic differentiation of ADSCs (Described in Chapter 6)**

# Chapter 6 - Effect of sFRP4 on the adipogenic differentiation of ADSCs

This part of the study has been published and is included in the appendix-III

**Visweswaran, M**, Schiefer, L, Arfuso, F, Dilley, R, Newsholme, P, Dharmarajan, A. Wnt antagonist secreted frizzled-related protein 4 upregulates adipogenic differentiation in human adipose tissue-derived mesenchymal stem cells. PLoS One, 2015;10[406]:e0118005.

## 6.1 Introduction

In the previous chapters the role of using Wnt antagonists as potent anti-cancer agents for the treatment of breast cancer were discussed, since they are capable of targeting the tumour cells as well as regulating the reciprocal interactions present in the tumour environment. The paracrine interaction between ADSCs and breast tumour cells, with regard to Wnt antagonism further potentiating the anti-tumour activity of the above interaction were examined. Further, the outcome of Wnt antagonists on regulating the tumour environment by decreasing the rate of differentiation of ADSCs into TAFs. To summarise, our entire study so far has elucidated the role of Wnt antagonism on:

1) Breast tumour cells,

2) Potentiating the anti-tumour activity of ADSC-derived factors, and

3) Blocking a tumour-supportive environment by inhibiting the differentiation of ADSCs into TAFs

Next, the effect of Wnt antagonism on ADSCs themselves and on their primary physiological function, which is adipogenic differentiation was investigated. As mentioned earlier, ADSCs are an important aspect of the breast tumour environment as ADSCs are present within the breast adipose tissue. Hence, investigating the effect of Wnt antagonists on ADSCs themselves becomes clinically imperative. Together with the earlier chapters, it will generate a comprehensive study on the effect of using sFRP4 as an anti-cancer agent for breast cancer.

ADSCs are attractive candidates in studying mechanisms involved in adipose biology, taking into account their strong adipogenic differentiation capability when compared to MSCs derived from other sources such as bone marrow [5-8]. ADSCs also have osteogenic and chondrogenic differentiation capability, fulfilling their MSC characteristics [5,6]. While adipogenic differentiation has been shown to be regulated by different signalling pathways, the Wnt signalling pathway is considered a key player regulating adipogenesis [9-12]. This pathway is controlled at various phases by an array of Wnt activating and inhibiting molecules. So far there are no studies examining the impact of continuous supplementation of exogenous sFRP4 on adipogenic differentiation. Hence, in this chapter, the effects of Wnt antagonism using sFRP4 with regard to changes in cell morphology, lipid droplet accumulation, and adipogenesis-specific protein expression in ADSCs were examined. On the other hand, although the role of Wnt activators in determining the fate of adipocyte precursors in murine models has been demonstrated [9], there are only few reports about the role of the Wnt antagonists in determining ADSC differentiation. An inhibitory effect on adipocyte lipid accumulation has been shown by Wnt activating

molecules such as Wnt 10b, glycogen synthase kinase 3β inhibitors such as lithium chloride (LiCl) [9], and 6-bromo indirubin 3'oxime (BIO) [15]. Additional to the effect of sFRP4, in this chapter the inhibitory effect of the above pharmacological Wnt activators, such as LiCl and BIO, on the levels of adipogenesis-specific proteins in ADSCs will be also described.

## 6.2 Methodology

ADSCs were cultured to 90% confluence in low-glucose DMEM containing 10% FBS and 1% PS antibiotics (section 3.1.1) and shifted to adipogenic differentiation medium in the presence and absence of specific treatments with Wnt regulators for indicated durations. A dose response was performed for the Wnt regulators to determine their effects on the cell viability of ADSCs using MTT assay (section 3.2.3) and a minimally lethal dose of Wnt regulators were chosen for experiments. Morphological changes were monitored throughout differentiation process and following a 7-day differentiation, Oil red O staining was performed for detecting lipid accumulation (section 3.13.2), and protein isolation was performed for Western blotting (section 3.5).

## 6.3 Results

### 6.3.1 ADSC characterization and tri-lineage differentiation

To confirm the multi-potent nature of the ADSCs, their differentiation into adipogenic (7 days), osteogenic (28 days), and chondrogenic (21 days) lineages was examined. The results of the lineage-specific staining at the end of the indicated differentiation period showed the presence of lipid droplets, calcium mineralisation and proteoglycan deposition in the adipogenic, osteogenic, and chondrogenic differentiation respectively confirming the tri-lineage differentiation capacity of ADSCs (Figure 6.1).

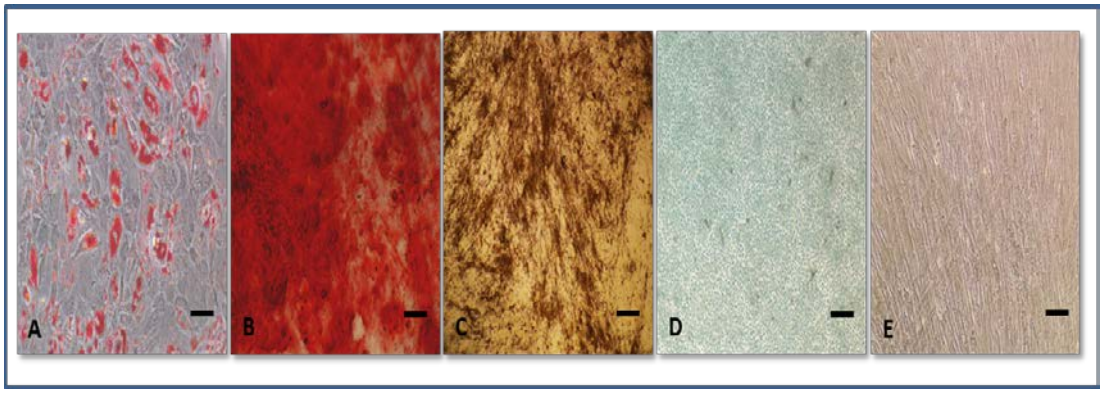


**Figure 6.1 Trilineage differentiation of ADSCs visualised by staining techniques**

ADSCs were subjected to adipogenic, osteogenic, and chondrogenic differentiation following which they were stained and observed microscopically (A) Intracellular lipid globules of adipogenically differentiated ADSCs stained positively by Oil Red O (B) Calcium deposition of osteogenically differentiated ADSCs stained positively by Alizarin Red, (C) Mineralization of osteogenically differentiated ADSCs stained positively by Von Kossa, (D) Glycosaminoglycan deposition of chondrogenically differentiated ADSCs stained positively by Alcian blue, and (E) Fibroblast morphology of undifferentiated ADSCs. Scale bar = 10µM.

### 6.3.2 Standardization of treatment doses for the Wnt activators and Wnt antagonist

ADSCs were treated for 48 hours with various doses of the Wnt regulators – LiCl, BIO, and sFRP4, and the resulting cell viability was analysed using an MTT assay. The cell viability of ADSCs was inhibited in a dose-dependent manner (Figure 6.2A and 6.2B). As a result, the doses of these Wnt regulators selected for subsequent experiments were 10mM (LiCl), 0.5µM (BIO), 100pg/mL (sFRP4) and 1ng/mL (sFRP4), in accordance with the minimum lethality caused by the dose.

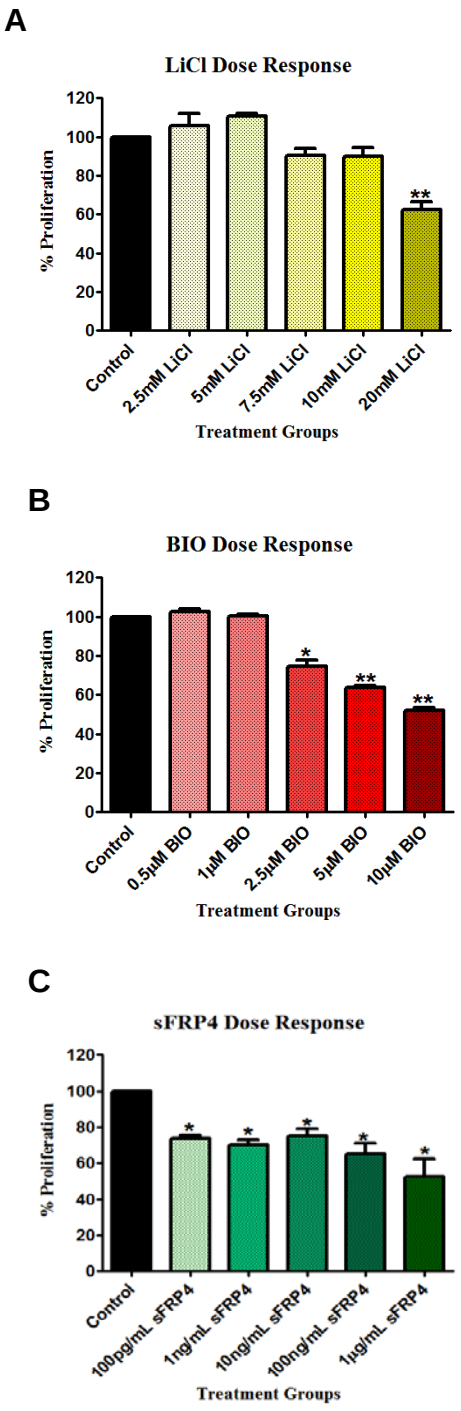


**Figure 6.2 Dose response of ADSCs with Wnt regulators**

ADSCs grown in their normal growth medium were treated with various doses of specific Wnt regulators for 48 hour followed by measurement of proliferation using MTT assay. Treatment in the presence of Wnt activators (A) LiCl, (B) BIO, and Wnt antagonist (C) sFRP4 (* $p<0.05$ and ** $p<0.001$).

### 6.3.3 Adipogenic differentiation of ADSCs in the presence of Wnt regulators

Adipogenic differentiation was induced on the ADSCs at 90% confluence and continued for 7 days. The adipogenic media were supplemented with the selected doses of LiCl (10mM), BIO (0.5µM), and sFRP4 (100pg/mL and 1ng/mL). The untreated adipogenic media served as controls for the adipogenesis. Also, undifferentiated ADSCs cultured in the basal ADSC growth medium served as the non-induced control. The cells were regularly observed for morphology changes and lipid droplet formation.

Irrespective of the treatment conditions, the transformation of morphology from a spindle-like shape into a rounded shape was initiated by Day 1 (Figure 3A). In all the treatment conditions, the lipid droplets started appearing at Day 4, but by Day 7 there was a further increase seen in lipid droplet content of the sFRP4 (1ng/mL)-treated compared to the adipogenic control groups (Figure 6.3B). In the treatment groups containing the LiCl and BIO, adipogenesis remained low with lesser lipid droplet content (Figure 6.3B). Non-induced ADSCs retained their fibroblastic morphology with no lipid accumulation.

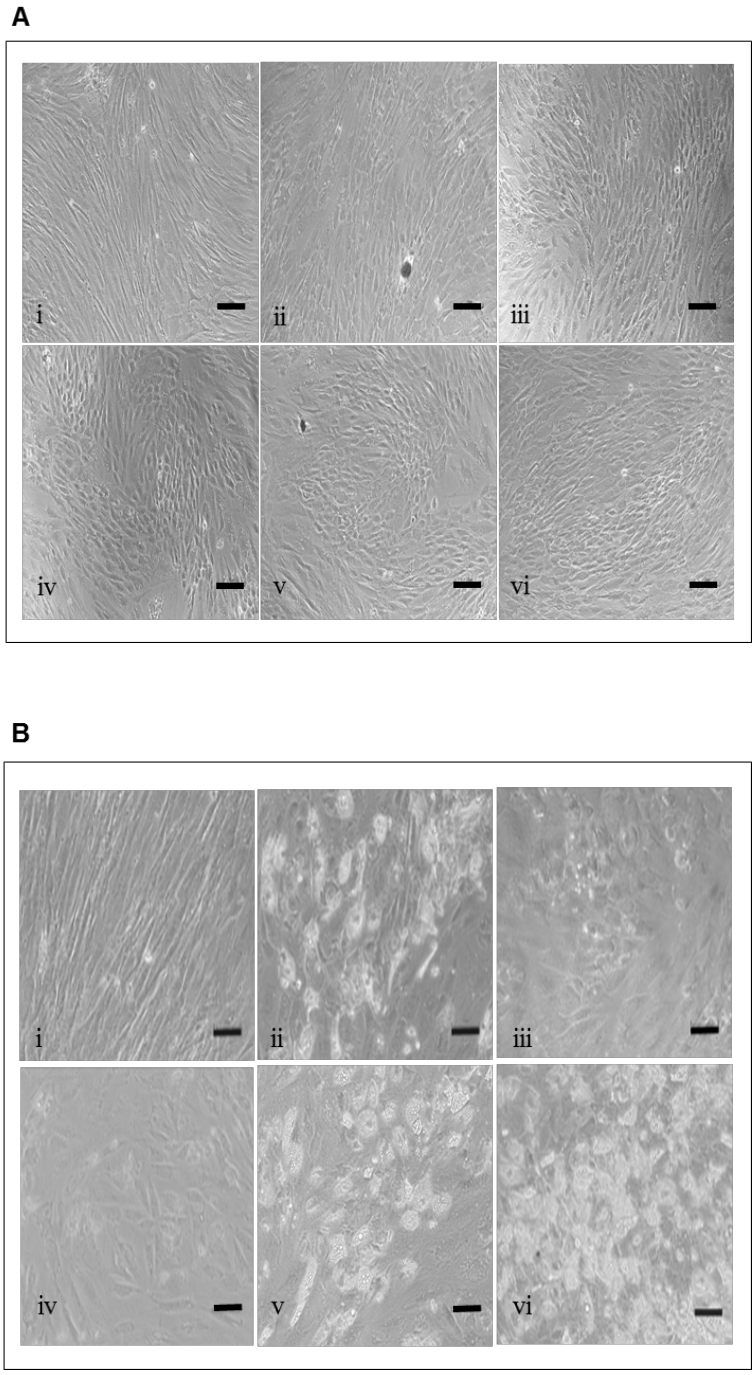


**Figure 6.3 Morphology of ADSCs during adipogenic differentiation**

ADSCs were adipogenically differentiated at 90% confluence and morphology was observed at (A) Day 1 and (B) Day 7. Treatment conditions were (i) non-induced control medium, (ii) adipogenic control, (iii) 10mM LiCl, (iv) 0.5µM BIO, (v) 100pg/mL sFRP4, and (vi) 1ng/mL sFRP4 in both (A) and (B). Scale bar = 10µM.

### 6.3.4 Oil Red O staining and quantification of the degree of adipogenesis

Oil Red O staining was performed on Day 7 of adipogenic differentiation, and the stained (red) intracellular lipid droplets were visualised using bright field microscopy. The least lipid droplet accumulation was observed in the groups with LiCl, and BIO and the highest observed in sFRP4 1ng/mL group (Figure 6.4A) in comparison to the untreated adipogenic controls.

To further quantify the total stained area in each treatment condition, Oil red O was eluted from the stained wells using 100% isopropanol for 1 hour and absorbance measured at 510nm using plate reader (Enspire multimode, Perkin Elmer). While the Wnt activators LiCl and BIO caused a 2.7-fold and 12-fold decrease in the lipid droplet content, sFRP4 at 1ng/mL produced a 1.5-fold increase in lipid accumulation (Figure 6.4B) in comparison to the untreated adipogenic controls.

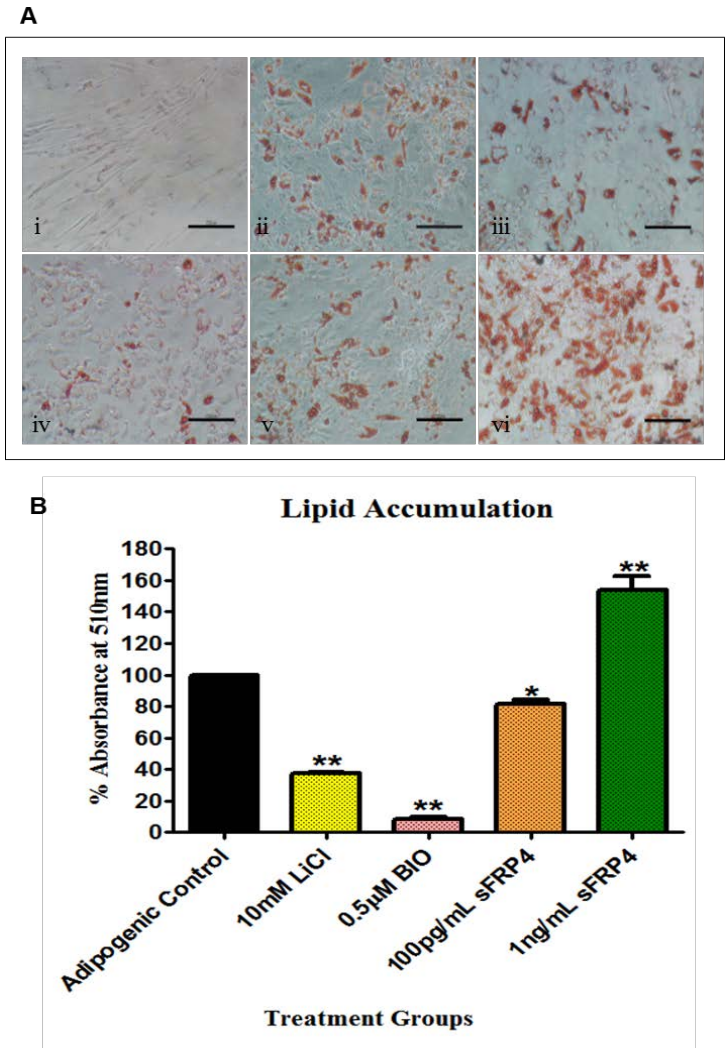


**Figure 6.4 Oil red O staining and quantification**

ADSCs were adipogenically differentiated at 90% confluence and stained with Oil red O staining for lipid accumulation. (A) Microscopic observations of the stained lipid droplets. Treatment conditions were (i) non-induced control, (ii) adipogenic control, (iii) 10mM LiCl, (iv) 0.5µM BIO, (v) 100pg/mL sFRP4, and (vi) 1ng/mL sFRP4. Scale bar = 250µM (B) Quantification of the stained lipid droplets were performed using the eluted Oil red O stain via measuring absorbance at 510nm. The readings were normalised to background values of non-induced control ADSCs. The values of all treatment conditions were compared to the adipogenic control group (* $p<0.05$ and ** $p<0.001$).

### 6.3.5 Effect of the Wnt regulators on adipogenic marker protein expression of differentiated ADSCs

To study the effect of the Wnt regulators on adipogenesis in ADSCs at the protein level, immunoblotting was performed using antibodies against the key adipogenic marker proteins PPARγ, CCAAT enhancer binding protein (C/EBPα), and acetyl CoA carboxylase. sFRP4 at 1ng/mL concentration significantly upregulated the expression of PPARγ by 1.2-fold, C/EBPα by 1.23-fold, and acetyl CoA carboxylase by 1.3-fold respectively (Figure 6.5A, 6.5B, 6.5C). The expression of PPARγ, C/EBPα, and acetyl CoA carboxylase was decreased significantly with LiCl (by 1.6, 2.6, 1.9-fold respectively) and BIO (by 7, 17, 5.6-fold respectively) treatments (Figure 6.5, 6.6, 6.7).

The increase in expression of the three key adipogenic marker proteins by sFRP4 (at 1ng/mL) indicated the promoting effect of Wnt antagonism on adipogenesis. On the contrary, the downregulation of adipogenic marker proteins observed in the LiCl- and BIO-treated ADSCs confirmed the inhibitory action of Wnt signalling activation on adipogenesis (Figure 6.5, 6.6, 6.7).

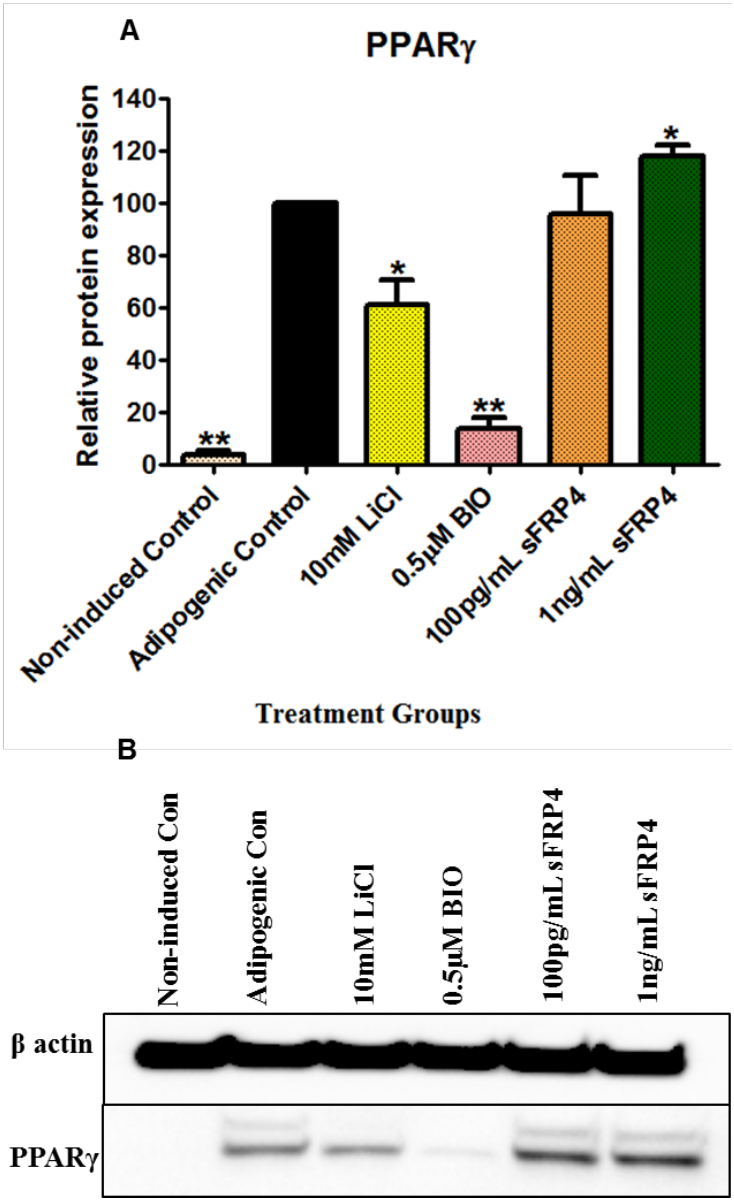


**Figure 6.5 Protein expression of PPARγ**

(A) Protein expression of adipogenic specific marker PPARγ was determined by immunoblotting. (B) Representative blot image of PPARγ. All values were compared to the adipogenic medium control (*$p<0.05$ and ** $p<0.001$).

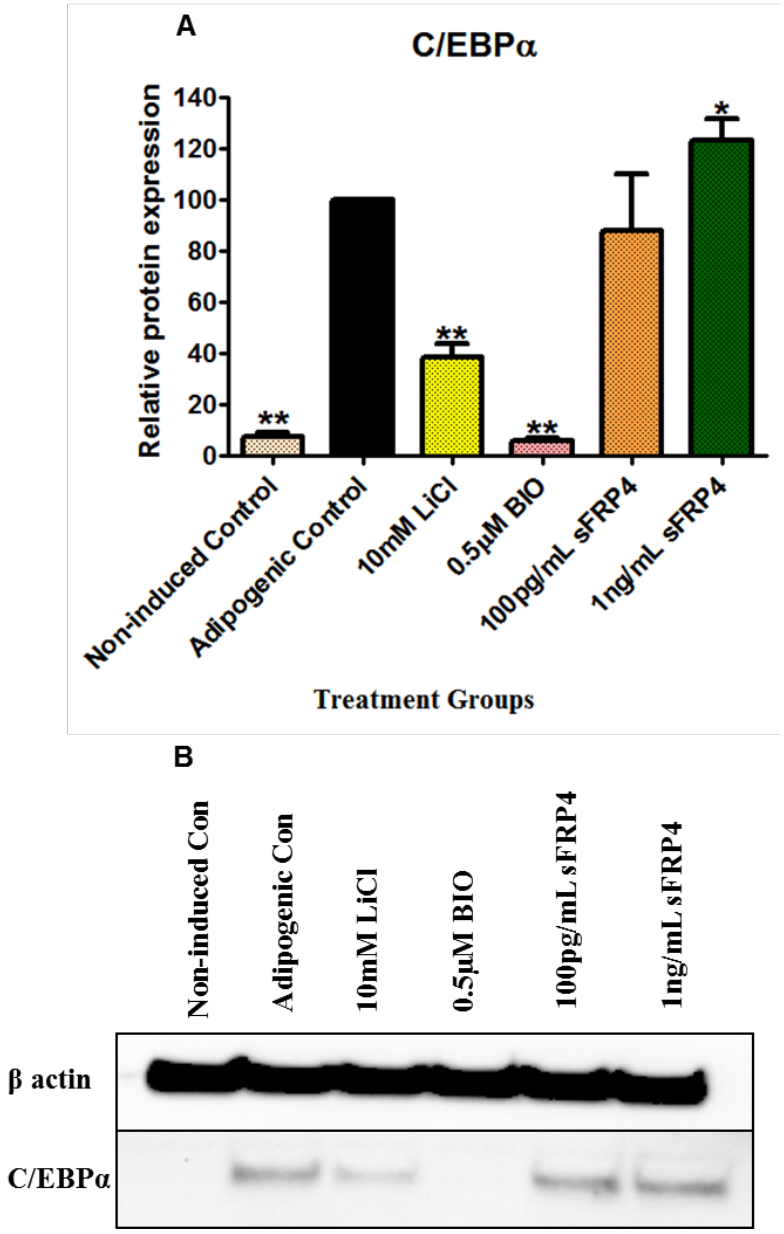


**Figure 6.6 Protein expression of C/EBPα**

(A) Protein expression of adipogenic specific marker C/EBPα was determined by immunoblotting. (B) Representative blot image of C/EBPα. All values were compared to the adipogenic medium control (*p<0.05 and ** p<0.001).

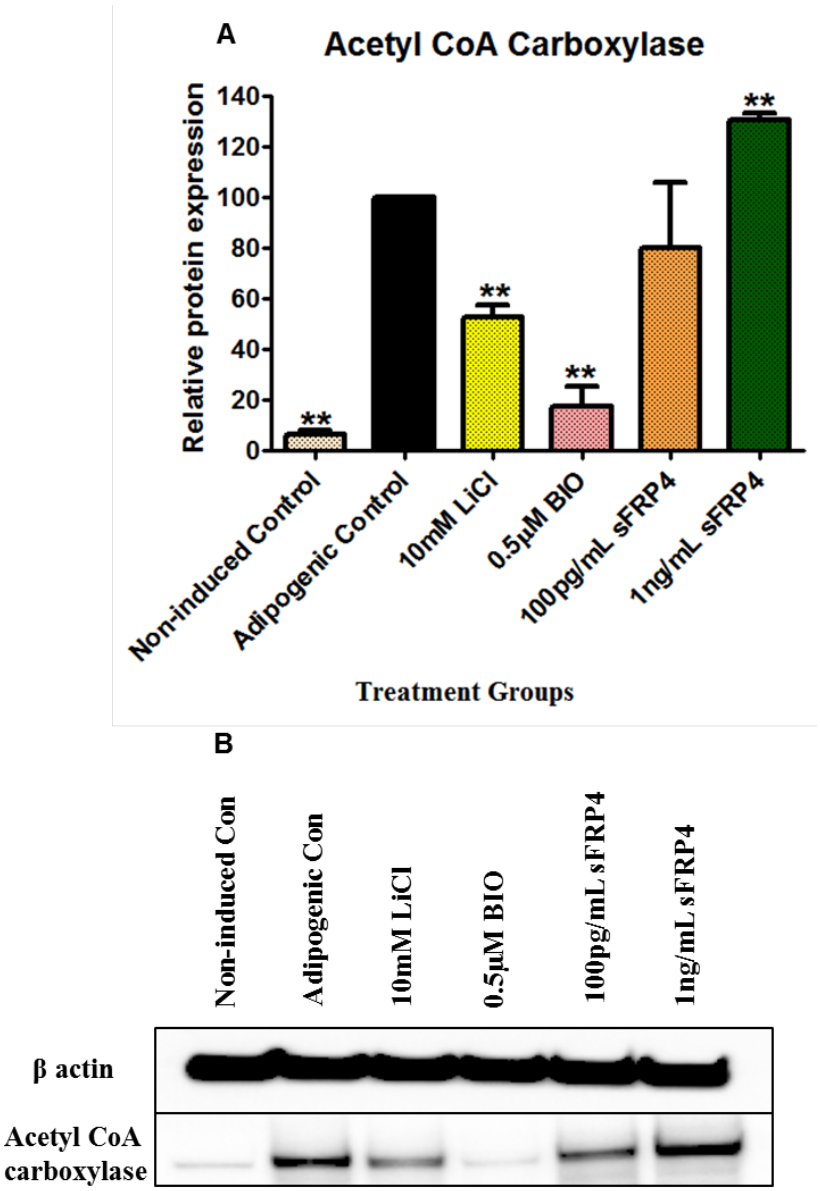


**Figure 6.7 Protein expression of acetyl CoA carboxylase**

(A) Protein expression of adipogenic specific marker acetyl CoA carboxylase was determined by immunoblotting. (B) Representative blot image of acetyl CoA carboxylase. All values were compared to the adipogenic medium control (*$p<0.05$ and ** $p<0.001$).

### 6.3.6 Effect of combination treatment (BIO+sFRP4) on adipogenic differentiation

To study the simultaneous effect of the Wnt activator and antagonist on adipogenic differentiation, the degree of lipid accumulation in the presence of both BIO at 0.5µM and sFRP4 at 1ng/mL (BIO+sFRP4) was observed. The morphology of the cells changed from the spindle-like shape to a rounded shape on Day 1 of differentiation in both BIO-only and BIO+sFRP4 treatment groups. However, on Day 7 the lipid accumulation remained unchanged in the BIO+sFRP4 treatment group when compared to the BIO-only group (Figure 6.8A). This was confirmed by Oil red O staining and its quantification (Figure 6.8B and 6.8C), which showed no significant difference in lipid accumulation between BIO-only and BIO+sFRP4 treatment groups. This indicated the strong inhibitory action of BIO on adipogenesis, which was not reversed by the adipogenic-promoting effect of sFRP4.

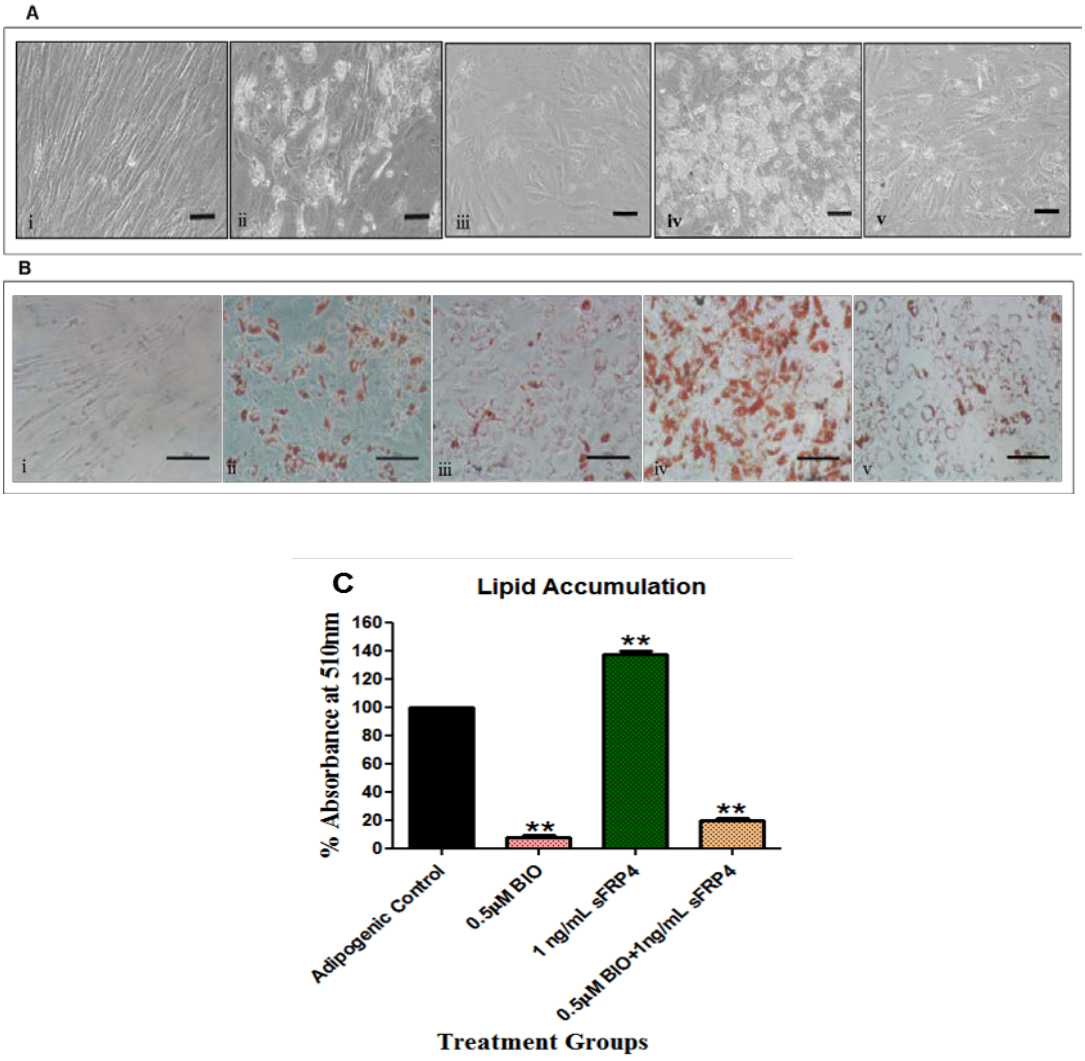


**Figure 6.8 Combinatorial effect of BIO+sFRP4 on adipogenic differentiation**

ADSCs were adipogenically differentiated at 90% confluence and their morphology was observed (A) Before and (B) after Oil red O staining. Treatment conditions were (i) non-induced control media, (ii) adipogenic control, (iii) 0.5µM BIO, (iv) 1ng/mL sFRP4, and (v) 0.5µM BIO + 1ng/mL sFRP4 in both (A) and (B). Scale bar = 10µM in (A) and 250µM in (B). (C) Quantification of the stained lipid droplets were performed using the eluted Oil red O stain via measuring absorbance at 510nm. The readings were normalised to background values of non-induced control ADSCs. The values of all treatment conditions were compared to the adipogenic control group (** $p<0.001$).

## 6.4 Discussion

From the previous chapters, the anti-tumour effects of sFRP4 in breast cancer by imposing its inhibitory activity on breast cancer cells themselves as well as on the entire tumour environment by affecting the crosstalk between breast tumour cells and ADSCs were exemplified. This has prompted us to examine the effect of sFRP4 on ADSCs themselves, which are an integral component of the breast tumour environment. It is crucial to understand the effect of sFRP4 on the ADSCs during normal conditions and also on their standard physiological functions, such as adipogenic differentiation, before presenting sFRP4 at the forefront of anti-breast cancer therapies. Unravelling the effect sFRP4 may have on the ADSCs is also important in order to exploit the improved inhibition on tumour viability contributed by the combination of ADSCs and sFRP4.

To add to its clinical importance, this study may have implications on the obese and overweight conditions that are becomingly increasingly prevalent worldwide, posing major health and economic challenges [305]. Apart from significantly affecting quality of life [306], obesity has several significant co-morbidities associated with it [307, 308]. Hence, understanding the molecular mechanisms contributing to the obese condition, such as increased proliferation of existing pre-adipocytes or increased differentiation from their precursor ADSCs, becomes significant in order to develop novel therapeutic controls for obesity.

ADSCs, being adipose tissue-derived, possess adipogenesis as their prime physiological purpose [407], and possess higher adipogenic differentiation potential [408, 409]. ADSCs could also be the predominantly recruited population during

adipocyte hyperplasia, taking into account their *in vivo* abundance compared to other MSC sources [4, 410]. Hence ADSCs were suitable candidates for studying the underlying mechanisms of adipogenesis in relation to obesity.

Among the several pathways that regulate adipogenesis, the canonical Wnt signalling pathway is thought to be a key player, but this complex area has not been fully investigated. The association between the Wnt signalling pathway and adipogenesis was investigated by using the Wnt antagonist sFRP4 and Wnt activators LiCl and BIO. The role of the Wnt signalling pathway as an adipogenic switch has been well established [9], with considerable evidence now indicating the crucial role of Wnt activation in blocking adipogenesis. The inhibitory effect of canonical Wnt ligands such as Wnt-1 and Wnt 10b has been demonstrated on 3T3-L1 preadipocytes [310], and an activated Wnt pathway has been shown to block adipogenic differentiation of pericytes [411]. Few studies have shown the impact of the GSK3β inhibitors on adipogenesis [310, 314, 412]. sFRP4 had been found to be highly expressed during adipogenic differentiation [315], making it likely that sFRP4 could be playing a positive role in this process. In this study, the direct effect of recombinant sFRP4 on the adipogenic differentiation of ADSCs was investigated. A previous study showed an increase in adiponectin secretion after a short 48-hour treatment with recombinant sFRP4 [316]. Hence, the effect of the continuous supplementation of recombinant sFRP4 throughout the differentiation period on adipogenesis was examined. Therefore, the sFRP4 treatment as performed for 7 days to detect its effect on lipid droplet accumulation and adipogenic proteins. A continuous supplementation of the Wnt activators LiCl and BIO during adipogenic induction was performed. The continuous sFRP4 treatment at 1ng/mL increased the lipid droplet accumulation in spite of the effect of sFRP4 in reducing cell viability. The observed decrease in lipid

accumulation at 100pg/mL sFRP4 could be attributed to its effect on cell viability. It was also found that a higher dose of sFRP4 (1ng/mL) was required for upregulating the expression of adipogenesis-specific proteins PPARγ, C/EBPα, and acetyl CoA carboxylase. PPARγ and C/EBPα are the two key transcription factors responsible for the development of a mature adipocyte [413], while acetyl CoA carboxylase is the key enzyme involved in fatty acid biosynthesis. The suppressive effect exerted by the Wnt signalling pathway on these adipogenic regulators [310] was overcome with sFRP4 treatment in these experiments.

In this study, the treatments with LiCl and BIO were also performed so that the down-regulating effect of these molecules on adipogenesis could be used as a control against the inducing effect of sFRP4. A significant decrease in the expression of PPARγ, C/EBPα, and acetyl CoA carboxylase proteins in BIO-treated ADSCs was observed. While the effect of LiCl on PPARγ and C/EBPα was evident in previous studies [21], this data demonstrated for the first time its down-regulating effect on the protein levels of acetyl CoA carboxylase in ADSCs. The identical levels of lipid accumulation between the BIO-only treatment and the BIO+sFRP4 combination treatment indicated the strong adipogenic inhibition rendered by activation of Wnt signalling via BIO, and also could have been because the effect of BIO is at the intracellular level as compared to the extracellular action of sFRP4. Hence, this confirms the necessity of accomplishing Wnt inhibition, which could be carefully considered while engineering adipose grafts for patients undergoing reconstructive surgeries and soft tissue augmentation.

This study is important in the context of developing better control measures over the obesity and related metabolic diseases such as Type 2 diabetes, wherein sFRP4 levels are shown to be elevated [318]. These findings provide a detailed account of the

interplay between the activation and antagonism of the canonical Wnt signalling pathway linked with human adipogenesis and facilitate a better understanding of adipose tissue biology. Correlating with the earlier chapters, this study provides a complete story regarding the utilisation of sFRP4 as an anti-cancer agent for a breast cancer, as well as the inevitable effect it may render on the ADSCs themselves, which are a predominant MSC population in the breast, in facilitating their normal adipogenic differentiation.

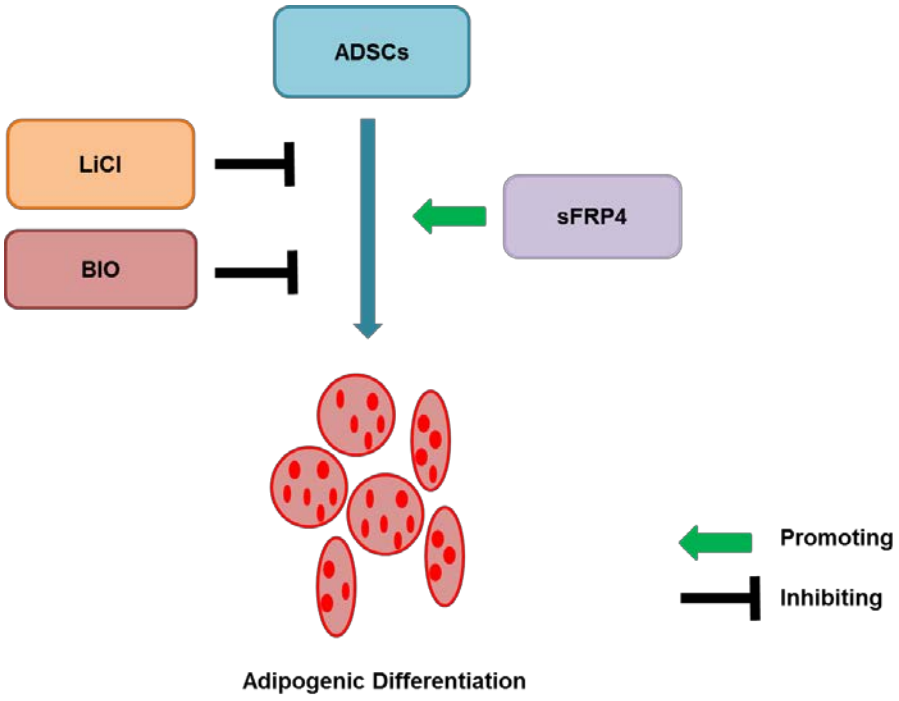


**Figure 6.9 Schematic representation of findings from Chapter 6**

Wnt regulators influence the adipogenic differentiation of ADSCs. Wnt activators, LiCl, and BIO (GSK3-β inhibitors) inhibit adipogenic differentiation, while Wnt antagonist sFRP4 upregulate the adipogenic differentiation in ADSCs.

# Chapter 7 - GENERAL DISCUSSION

## 7.1 DISCUSSION

The findings from this study unravelled potential effects of ADSCs in an *in vitro* breast tumour model. ADSCs are present within breast adipose tissue and hence the results from this study may be reflective of the cellular and paracrine interactions occurring within the breast tumour stroma. In this study interactions between ADSCs and breast tumour cells have been explored at various levels. One of them was by studying the signalling crosstalk between the 2 cell types via examining the paracrine signalling. For this purpose, the secreted factors derived from ADSCs were used to examine their effects on breast tumour cells, by using the soluble secreted factors in the ADSC-CM and the insoluble secreted factors in the ADSC-ECM.

After initial screening of ADSC-CM harvested from various time-points of conditioning, the ADSC-CM harvested at 48 hour of conditioning possessed inhibitory activity on the viability of both the tumour cell lines. The anti-tumour activity of ADSC-CM was found to be the most effective after 72 hour of treatment on tumour cells. In order to determine the specificity in its inhibitory action, ADSC-CM following harvesting was also treated on ADSCs themselves (as a control cell line). It was observed that ADSC-CM did not inhibit cell viability of ADSCs. Hence the inhibitory activity was specifically anti-tumourigenic and was not as a result of depletion of any medium components during the conditioning process. The specificity of the effect was also supported by ADSC-CM inhibiting the migratory potential of MCF7 cells but not MDA MB 231 cells. This could be associated with the higher aggressive and invasive property of the basal type MDA MB 231 cell line,

increased production of IL-8 chemokine which is known to induce migration [358-361] in comparison to the luminal type MCF7 cell line.

The characterisation of ADSC-CM by molecular weight cut off fractionation and heat denaturation revealed that the inhibitory property was retained within a non-protein component present in the <30KDa fraction of the ADSC-CM. This suggests that the anti-tumour activity observed could be due to a secreted biomolecule belonging to the class of lipids, nucleic acids, or proteins named IDPs, which possess no secondary structure and hence does not get denatured by heat.

Extending the anti-tumour activity on tumour cell viability to other aspects of tumour growth, several assays were performed such as migration assay, JC1 assay to measure the mitochondrial membrane potential, caspase 3/7 activity, and protein expressions for Wnt target and apoptosis-related proteins. ADSC-CM induced both the tumour cell lines to enter the intrinsic apoptotic pathway causing mitochondrial membrane depolarisation. This is indicative of a disruption in the mitochondrial membrane and opening of the mitochondrial permeability transition pore leading to an influx of ions resulting in a decreased transmembrane potential as observed.

Following their effect on mitochondrial membrane depolarisation, the caspase 3/7 activity was examined. It was found that ADSC-CM induced a pronounced increase in caspase 3/7 activity in MCF7 cells as compared to the 5-10% increase in MDA MB 231 cells. It needs to be noted here MCF7 are devoid of caspase 3 enzyme due to a deletion mutation in the Casp-3 gene [375], hence the observed increase in the caspase activity could be from compensatory increase in the activity of caspase 7 enzyme. In MDA MB 231 cells, the observed decrease in mitochondrial membrane potential is indicative of damaged mitochondrial membrane suggesting that the cells

are targeted for cell death through the mitochondrial (intrinsic) pathway. However, the observed increase in their effector caspase activity was only mild, indicating that there could be an alternative cell death pathway occurring, which is still mitochondria-regulated but is independent of caspase activity or which does not mandatorily require caspase activation. Cell death pathways mediated through apoptosis-inducing factor (AIF) has been demonstrated to facilitate this mitochondria-regulated cell death in MDA MB 231 cells without the absolute necessity of having the caspases activated [1]. Also, in MDA MB 231 cells, the fold change in the expression of pro-apoptotic Bax protein caused due to ADSC-CM treatment was less as compared to MCF7 cells, suggesting that an alternative pathway could be occurring in MDA MB 231 cells.

Additionally, ADSC-CM reduced the generation of reactive oxygen species in both tumour cell lines. The protein expression of active β-catenin and Bcl-xL proteins were reduced with ADSC-CM treatment in both tumour cell lines, with an increase in Bax expression (Bax, statistically not significant). ADSC-CM also reduced cyclin D1 expression in MCF7 cells but not in MDA MB 231 cells, with a decreasing trend observed in the latter. The unchanged levels of cyclin D1 in MDA MB 231 cells could be due to the cell's being highly aggressive and proliferative, and in turn could be correlated to their unchanged migration rates after ADSC-CM treatment, as cyclin D1 and migration rates have been reported to be directly proportional [414].

Next, the combination of ADSC-CM with Wnt antagonists was performed. There was an enhanced reduction in tumour cell viability when ADSC-CM was combined with sFRP4 and also ADSC-CM with SC301+SC401. However, in the various subsequent assays displaying the mitochondrial membrane depolarisation, caspase 3/7 activity, ROS generation, there was no enhanced effects when ADSC-CM was

combined with sFRP4/SC301/SC401/SC301+SC401, except for the caspase activity in MDA MB 231 cells. In MDA MB 231 cells, the combination of ADSC-CM with sFRP4 and ADSC-CM with SC301 resulted in a further increase in caspase 3/7 activity. This could be because the initial increase in caspase 3/7 activity was mild and hence there was a possibility that it could be further upregulated to some extent with the combination with the mentioned Wnt antagonists.

The results indicate that ADSC-CM and Wnt antagonists mediate their effect through Wnt signalling pathway by reducing active β-catenin expression in tumour cell lines. A further reduction in the Wnt signalling pathway was only observed when ADSC-CM was combined with sFRP4 in MCF7 cells. Therefore, it suggests that Wnt signalling is one of the signalling pathways commonly targeted by both ADSC-CM and Wnt antagonists. Hence it is possible that a saturating effect has occurred by attacking on the same site and hence was no additive effect was observed when ADSC-CM was combined with sFRP4/peptides in the downstream assays. Or it could be because the effects exerted by ADSC-CM and Wnt antagonists are facilitated through distinct targets from different signalling pathways in the tumour cells.

Apart from ADSC-CM, the ADSC-ECM was also observed to possess inhibitory activity on tumour cell viability of both tumour cell lines after various treatment durations. The inhibitory response of MDA MB 231 cells increased with treatment duration, with these cells displaying only 7% inhibition after 48 hours of treatment, followed by 28% inhibition after 72 hour treatment. On the other hand, MCF7 cells showed a 30% inhibition from 48 hour treatment onwards. This suggests that MDA MB 231 cells required longer exposure to the ADSC-ECM as compared to MCF7

cells to generate the maximum inhibitory response, which could be associated to the comparatively highly invasive potential of MDA MB 231 cells.

On the other hand, ADSCs could impart a pro-tumorigenic effect by converting themselves into tumour-associated fibroblasts in the presence of a tumour environment. ADSCs have been shown to increase their viability rates in the presence of TCM. While both the control non-conditioned medium and the TCM are serum-free in nature, the heightened cell viability in TCM-treated ADSCs is related to the specific tumour-derived factors present in the TCM. Treatment with sFRP4/SC301/SC401/SC301+SC401 partly reversed this protective/promoting effect of TCM by lowering the cell viability. While the viability was not fully lowered similar to the control levels, it was significantly lowered as compared to the TCM-treated ADSCs. This suggests one potential mechanism by which Wnt antagonists could be used to target transformation of ADSCs into TAFs in a tumour environment.

Next, it was observed that the marker expression of TAF-associated markers was upregulated in the presence of TCM derived from both the tumour cell lines. The Wnt antagonists sFRP4/SC301/SC401/SC301+SC401 could downregulate the increase in MCF7 TCM-induced marker expression for α-SMA and vimentin. With MDA MB 231 TCM, supplementation of sFRP4/SC301/SC401/SC301+SC401 were successful in downregulating the expression of vimentin, while only SC401/SC301+SC401 downregulated the expression of α-SMA. This suggests that Wnt antagonists partly controlled the TCM-induced transformation of ADSCs into a tumorigenic profile by reducing the hyper-proliferative state of ADSCs as well as reducing the markers of the transition, alpha smooth muscle actin and vimentin.

A change in the metabolic phenotype of the ADSCs was also observed when treated with TCM for 10 days, with TCM-treated ADSCs being more glycolytically driven than the control ADSCs. It was also observed that the control ADSCs took longer time to respond to a glycogenic stimulation with a saturating concentration of glucose and oligomycin. It was only after the mitochondrial respiration was shut down completely with oligomycin, the control ADSCs exhibited a delayed response by increasing their ECAR. On the other hand, the TCM-treated ADSCs exhibited an increase in ECAR immediately after addition of glucose, suggesting that the TCM protected or preserved the metabolic activity in these cells, orienting it to a more glycolytically-responsive and driven phenotype.

Results so far suggest that ADSCs exert a dual effect like a double-edged sword. While the secreted factors from ADSCs - ADSC-CM and ADSC-ECM could be considered as a possible therapeutic option against cancer, ADSCs themselves could co-evolve along with tumour cells to transform into a tumour-promoting profile. These activities could be carefully controlled by Wnt antagonists, where it enhanced the anti-tumour potential (further reduction in tumour cell viability), as well as reduced the pro-tumorigenic transformation of ADSCs.

Furthermore, the effect of the Wnt antagonism on the prime physiological function of ADSCs has also been investigated. Adipogenic differentiation is one of the major differentiation pathways to which ADSCs differentiate. The adipogenic differentiation medium was supplemented with Wnt antagonist sFRP4 to examine the role of Wnt antagonism on the cell fate determination. This is important when therapies using Wnt antagonists are to be considered, especially in a breast cancer setting where ADSCs are the tissue-resident stem cell population within the breast adipose tissue. Hence the probable effect of sFRP4 on the stem cell fate is important

to be understood. It was observed that sFRP4 promoted the adipogenic differentiation of ADSCs by observing an increase in lipid accumulation and adipogenesis-specific marker profile. The increased lipid accumulation was countered by the addition of BIO which is a Wnt activator by inhibiting GSK-3β activity. This could be due to the location of activity of sFRP4 and BIO, sFRP4 acts at the receptor level by binding to the Frizzled receptor or Wnt ligand whereas BIO inhibits the activity of the downstream GSK-3β in the cytoplasm. The knowledge of the type of effect sFRP4 poses on the ADSCs, in terms of regulating their viability and differentiation becomes clinically important to develop novel anti-cancer therapies. For instance, ADSCs are potent carrier of anti-cancer drugs and can act as vehicles to deliver the activity of sFRP4 as an anti-tumourigenic drug to the tumour site.

Hence this study begins to provide a comprehensive understanding on the various effects ADSCs and Wnt antagonism can instil in a breast tumour environment. The reciprocal interaction existing between ADSCs and breast tumour cells were examined, wherein it was found that the paracrine factors from ADSCs exhibit an anti-tumour activity and conversely the paracrine factors from tumour cells transform ADSCs into a more pro-tumorigenic phenotype to support tumour development. Additionally, the effective role of Wnt antagonism in modulating these interactions were examined. Wnt antagonism resulted in an enhancement of anti-tumour viability when combined with ADSC-CM but did not appear to have an enhanced effect on the underlying events. Wnt antagonists played a beneficial role from a therapeutic perspective by partly downregulating the oncogenic transformation of ADSCs. Further, the role of Wnt antagonism in promoting the physiological function of ADSCs, adipogenic differentiation was also demonstrated.

## 7.2 CONCLUSION

The main outcomes arising from this thesis studies relates to the implications of the presence of ADSCs and Wnt signalling antagonists in a breast tumour environment. Apart from understanding the communications occurring in a tumour stroma, the interaction between ADSCs and breast cancer cells are relevant from a regenerative point of view as well. ADSCs are being considered as cellular adjuncts in breast reconstructive surgeries post mastectomy surgery in breast cancer patients. Hence, the possible influences the ADSCs can have on the residual tumour cells should not be neglected.

Below are the key points summarised from this study.

A first outcome demonstrates an anti-tumour activity of the paracrine factors secreted from ADSCs via ADSC-CM and ADSC-ECM. The advantage of requiring only the paracrine factors alleviates the need to deliver the ADSCs themselves in the therapeutic approach. The ADSC secretome may offer benefits in terms of being a good candidate for cell-free therapies, which may be safer and beneficial compared to cell-based approaches. A second outcome highlights the advantage of using Wnt antagonists in combination with ADSC-CM for devising anti-cancer strategies as Wnt antagonists enhanced the inhibitory response of tumour cells in terms of further decreasing their viability.

A third outcome also highlights the importance of tumour stroma in the co-evolution of non-tumour cells. It was observed that paracrine factors originating from tumour cells transformed the ADSC phenotype into a tumour-supportive nature. Additionally, the Wnt antagonists downregulated the transformation of ADSCs into

TAFs, which alleviated the co-evolution of a non-tumour cell type into a tumorigenic phenotype. Such processes are vital for the tumour development, which was partially blocked by the Wnt antagonists.

A fourth outcome demonstrates the potential effect the sFRP4 will exert on ADSCs in terms of their viability and differentiation potential. Taking into account the possibility of using sFRP4 as an anti-tumorigenic agent in a breast tumour site, which will contain predominant population of ADSCs, it is important to understand the effect of Wnt antagonism on the normal cell fate determination of ADSCs. A promoting effect of sFRP4 was observed on the adipogenic differentiation of ADSCs. The role of sFRP4 on the differentiation processes of ADSCs (tumorigenic/normal adipogenic) could be put into use while devising anti-cancer approaches which utilise ADSCs as 'delivery vehicles' exploiting their specific tumour-homing property in order to deliver Wnt antagonists such as sFRP4 that are anti-tumorigenic in nature.

Overall, these studies describe the various roles ADSCs may play in a breast tumour environment. The secreted factors from ADSCs inhibit breast tumour cell growth aspects, whereas the tumour-derived secreted factors transform ADSCs into TAFs. Additionally, it highlights the role of Wnt antagonists sFRP4 and its peptides to further influence the activity of ADSC-derived soluble secreted factors, to downregulate the transformation of ADSCs into TAFs, and in upregulating the adipogenic differentiation of ADSCs.

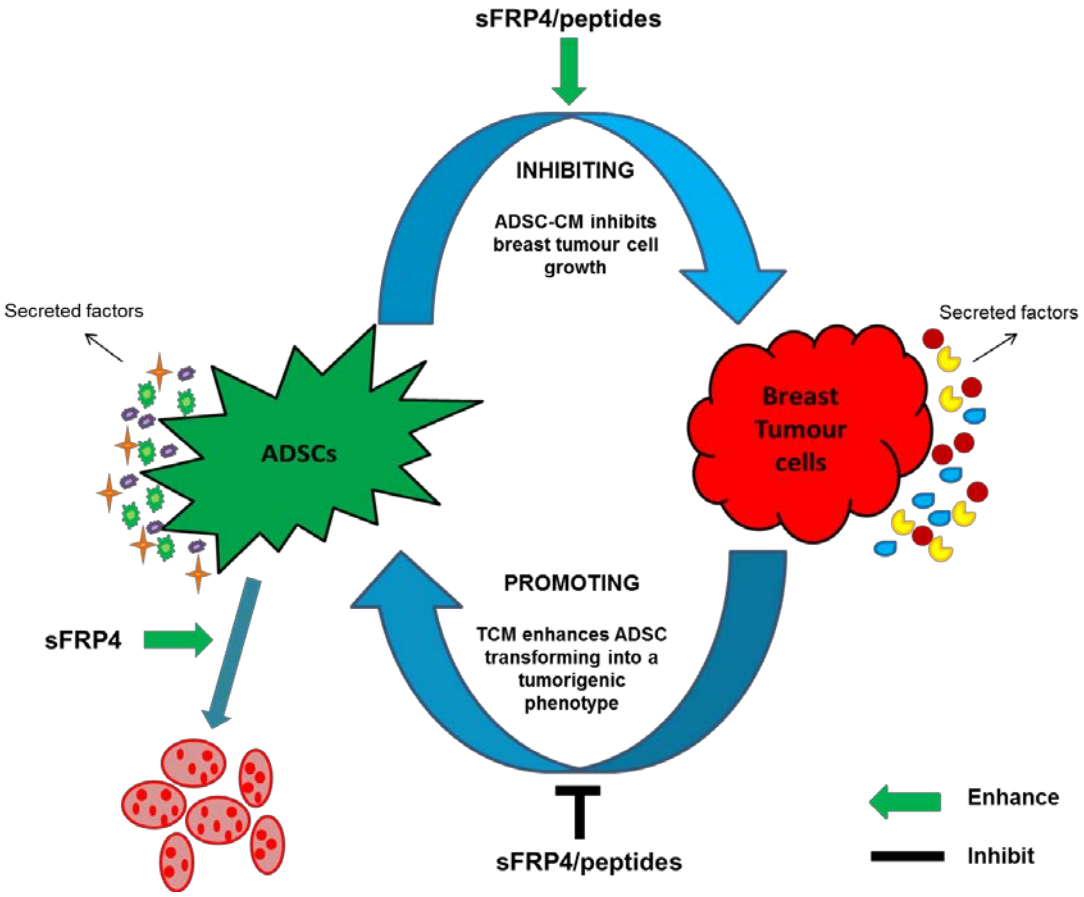


**Figure 7.1 Schematic represntation of findings from this thesis**

Secreted factors in ADSC-CM inhibit various aspects of breast tumour cell growth, with sFRP4/peptides showing an enhanced effect on reducing tumour cell viability. On the other hand, TCM from MCF7 and MDA MB 231 cells promote the tumorigenic potential of ADSCs, transforming ADSCs into a tumorigenic phenotype or TAFs. sFRP4/peptides exert an inhibiting effect on the TCM-induced transformation of ADSCs. Further, sFRP4 was also shown to upregulate the adipogenic differentiation of ADSCs.

## 7.3 LIMITATIONS

The harvest of ADSC-CM for the experiments and the numerous treatment groups described in chapter 4 was extremely time-consuming, as ADSCs were slow-growers and required several days during each experiment to attain around 80% confluence to be ready for CM harvest. It was followed by 2 days (48 hour) of medium conditioning and 3 days (72 hour) of treatment on tumour cells. An attempt was made initially for harvesting ADSC-CM and storing it at -80$^{o}$C for future use. However, the freeze-thawed ADSC-CM exhibited deleterious effects on tumour cells during treatment, observed by a total change in the tumour cell morphology upon ADSC-CM treatment and the tumour cells looked very unhealthy under the microscope. Hence, ADSC-CM was always freshly harvested for the experiments and hence for each experiment, there was a waiting period for the ADSCs to grow and attain confluence, after which the CM harvest and experiments were performed.

Also, working with secreted factors (ADSC-CM, TCM, ADSC-ECM) posed the risk of having batch-to-batch variations during each harvest of secreted factors. We attempted to minimise the effect of such batch-to-batch variations on our results by maintaining uniform cell culture and harvesting conditions, shifting to serum-free medium for conditioning at around the same ADSC confluence, limiting the variation of medium composition by always purchasing medium from the same company, and performing multiple repeats of the assays.

The transfection of ADSCs with sFRP4 was also attempted in order to harvest ADSC-CM from these sFRP4-overexpressing ADSCs and to compare its anti-tumour effects to the CM harvested from normal ADSCs. This was designed taking into account the capability of ADSCs/MSCs to carry ‘drug cargo’ and to act as ‘delivery

vehicles' specifically to the tumour site. Many studies have generated MSCs overexpressing specific proteins/enzymes. However, after many unsuccessful attempts to transfect ADSCs using lipofectamine-2000/-3000 (Figure S5), the decision to move forward was made following which the CM harvested from normal non-transfected ADSCs was supplemented exogenously with recombinant sFRP4 protein.

Exosome isolation was performed to examine another means of communication between the ADSCs and tumour cells. However, low yields of exosomes (Figure S6) despite performing the isolation from an almost confluent T75 flask of ADSCs, indicated the need to upscale the ADSC culture area such as to use a T175 flask and isolating exosomes from a larger amount of CM. This was considered to be practically non-feasible, as ADSCs were slow-growing and would require an inordinate amount of time required to generate such large batches of ADSCs for the range of optimisation assays and subsequent experiments.

## 7.4 FUTURE PERSPECTIVES

- Further to the current results, the cell-to-cell interaction between ADSCs and breast cancer cells through direct co-culture could be performed to understand whether the cell-cell contact exerts a similar anti-tumour effect on the breast cancer cells.
- The cellular crosstalk using exosomes was initiated in this study, which unfortunately could not be continued. As this is one of the key means of cell-to-cell communication, this could be continued once the exosome isolation

techniques have been up scaled. In addition, methods for scaling-up production of cells and CM could be performed for future studies.

- Also, an invasion assay using the transwell chamber system could also be done as a further validation to the migration assay performed in the present study.
- In the present study, the ROS generation was measured using only the DCFDA assay. More specific assays for ROS and antioxidant measurement could be performed.
- The difference in the caspase 3/7 activity between MCF7 and MDA MB 231 cells could be further confirmed by detecting the procaspase and cleaved caspase protein expressions. This could be used to confirm the absence of caspase-3 enzyme in MCF7 cells, which might further validate the pronounced increase in caspase 3/7 activity in these cells to caspase-7.
- The role of other non-tumour cells such as macrophages, endothelial cells, etc in the tumour stroma could also be studied in terms of their transformation into a tumorigenic phenotype and the role of Wnt antagonists in those interactions.
- The effect of CM derived from CSCs could be used to study their role in transformation of ADSCs into TAFs. This could not performed in the current study, as large batches of fresh CSC-CM was required for treating the ADSCs and was also limited by the availability of ADSCs (which are slow growing compared to the tumour cell cultures) to perform all these experiments/treatment groups. Hence, this would be one of the experiments to be considered for future studies. CSCs possessing higher tumorigenic

potential compared to the non-CSC tumour cell population might possess a stronger effect on the ADSC transformation.

- Overall, the current study described the *in vitro* results which give an indication about the *in vivo* scenario. However, the *in vivo* conditions can be more complex and need to be further investigated. Taking a future perspective of this research, it would include the use of animal models wherein MCF7 and MDA MB 231 breast cancer cells would be injected into the mouse in order to facilitate tumour development. This would be followed by intra-tumoural injections of ADSC-CM (treatment group) or control medium (control group) for various durations and the tumour size was monitored and measured. A previous study performed similar experiments in C57BL/6 mice wherein ADSC-CM was injected into the tumour developed from B16 melanoma cells [415].

# Chapter 8 – BIBLIOGRAPHY


1. Kim, E.A., et al., *Dioscin induces caspase-independent apoptosis through activation of apoptosis-inducing factor in breast cancer cells.* Apoptosis, 2014. 19(7): p. 1165-75.
2. Pittenger, M.F., et al., *Multilineage potential of adult human mesenchymal stem cells.* Science, 1999. 284(5411): p. 143-147.
3. Bianco, P., et al., *Bone Marrow Stromal Stem Cells: Nature, Biology, and Potential Applications.* STEM CELLS, 2001. 19(3): p. 180-192.
4. Zuk, P.A., et al., *Multilineage cells from human adipose tissue: implications for cell-based therapies.* Tissue Eng, 2001. 7(2): p. 211-28.
5. Weiss, M. and D. Troyer, *Stem cells in the umbilical cord.* Stem Cell Reviews, 2006. 2(2): p. 155-162.
6. Seo, B.M., et al., *Investigation of multipotent postnatal stem cells from human periodontal ligament.* Lancet, 2004. 364(9429): p. 149-55.
7. Harvanova, D., *Isolation and characterisation of synovial mesenchymal stem cells.* Folia Biologica (Praha), 2011. 57: p. 119-124.
8. Patel, A.N., et al., *Multipotent menstrual blood stromal stem cells: isolation, characterization, and differentiation.* Cell Transplant, 2008. 17(3): p. 303-11.
9. Agha-Hosseini, F., et al., *In vitro isolation of stem cells derived from human dental pulp.* Clinical Transplantation, 2010. 24(2): p. E23-E28.
10. Friedenstein, A.J., R.K. Chailakhjan, and K.S. Lalykina, *THE DEVELOPMENT OF FIBROBLAST COLONIES IN MONOLAYER*

*CULTURES OF GUINEA-PIG BONE MARROW AND SPLEEN CELLS.* Cell Proliferation, 1970. 3(4): p. 393-403.

11. Zuk, P.A., et al., *Human adipose tissue is a source of multipotent stem cells.* Mol Biol Cell, 2002. 13(12): p. 4279-95.
12. Choi, Y.S., et al., *Differentiation of human adipose-derived stem cells into beating cardiomyocytes.* Journal of Cellular and Molecular Medicine, 2010. 14(4): p. 878-889.
13. Safford, K.M., et al., *Neurogenic differentiation of murine and human adipose-derived stromal cells.* Biochem Biophys Res Commun, 2002. 294(2): p. 371-9.
14. Zhao, M., et al., *Mesenchymal stem cells in mammary adipose tissue stimulate progression of breast cancer resembling the basal-type.* Cancer Biology & Therapy, 2012. 13(9): p. 782-792.
15. Zhao, M., et al., *Multipotent adipose stromal cells and breast cancer development: think globally, act locally.* Molecular Carcinogenesis, 2010. 49(11): p. 923-927.
16. Jotzu, C., et al., *Adipose tissue derived stem cells differentiate into carcinoma-associated fibroblast-like cells under the influence of tumor derived factors.* Cell Oncol, 2011. 34(1): p. 55-67.
17. Muehlberg, F.L., et al., *Tissue-resident stem cells promote breast cancer growth and metastasis.* Carcinogenesis, 2009. 30(4): p. 589-97.
18. Yulyana, Y., et al., *Paracrine Factors of Human Fetal MSCs Inhibit Liver Cancer Growth Through Reduced Activation of IGF-1R/PI3K/Akt Signaling.* Molecular Therapy, 2015. 23(4): p. 746-756.

19. Ho, I.A., et al., *Human bone marrow-derived mesenchymal stem cells suppress human glioma growth through inhibition of angiogenesis.* STEM CELLS, 2013. 31(1): p. 146-55.

20. Kucerova, L., et al., *Altered features and increased chemosensitivity of human breast cancer cells mediated by adipose tissue-derived mesenchymal stromal cells.* BMC Cancer, 2013. 13(1): p. 1-13.

21. Kucerova, L., et al., *Altered features and increased chemosensitivity of human breast cancer cells mediated by adipose tissue-derived mesenchymal stromal cells.* BMC Cancer, 2013. 13(1): p. 535.

22. Cortes-Dericks, L., et al., *Human lung-derived mesenchymal stem cell-conditioned medium exerts in vitro antitumor effects in malignant pleural mesothelioma cell lines.* Stem Cell Research & Therapy, 2016. 7: p. 25.

23. Yang, C., et al., *Conditioned Media from Human Adipose Tissue-Derived Mesenchymal Stem Cells and Umbilical Cord-Derived Mesenchymal Stem Cells Efficiently Induced the Apoptosis and Differentiation in Human Glioma Cell Lines In Vitro.* BioMed Research International, 2014. 2014: p. 109389.

24. Park, C.W., et al., *Cytokine Secretion Profiling of Human Mesenchymal Stem Cells by Antibody Array.* International Journal of Stem Cells, 2009. 2(1): p. 59-68.

25. Walter, M., et al., *Interleukin 6 Secreted from Adipose Stromal Cells Promotes Migration and Invasion of Breast Cancer Cells.* Oncogene, 2009. 28(30): p. 2745-2755.

26. Sun, B., et al., *Human umbilical cord blood mesenchymal stem cell-derived extracellular matrix prohibits metastatic cancer cell MDA-MB-231 proliferation.* Cancer Letters, 2010. 296(2): p. 178-185.

27. Maxson, S., et al., *Concise review: role of mesenchymal stem cells in wound repair.* Stem Cells Transl Med, 2012. 1(2): p. 142-9.

28. Studeny, M., et al., *Bone marrow-derived mesenchymal stem cells as vehicles for interferon-beta delivery into tumors.* Cancer Res, 2002. 62(13): p. 3603-8.

29. Yagi, H. and Y. Kitagawa, *The role of mesenchymal stem cells in cancer development.* Frontiers in Genetics, 2013. 4: p. 261.

30. Cuiffo, B.G. and A.E. Karnoub, *Mesenchymal stem cells in tumor development: Emerging roles and concepts.* Cell Adhesion & Migration, 2012. 6(3): p. 220-230.

31. Dvorak, H., *Tumors: wounds that do not heal.* N Eng J Med, 1986. 26: p. 1650 - 1659.

32. Khakoo, A., et al., *Human mesenchymal stem cells exert potent antitumorigenic effects in a model of Kaposi's sarcoma.* J Exp Med, 2006. 5: p. 1235 - 1247.

33. Nakamizo, A., et al., *Human bone marrow-derived mesenchymal stem cells in the treatment of gliomas.* Cancer Res, 2005. 65(8): p. 3307-18.

34. Komarova, S., et al., *Targeting of mesenchymal stem cells to ovarian tumors via an artificial receptor.* J Ovarian Res, 2010. 3(12): p. 1757-2215.

35. Kidd, S., et al., *Direct evidence of mesenchymal stem cell tropism for tumor and wounding microenvironments using in vivo bioluminescent imaging.* STEM CELLS, 2009. 27(10): p. 2614-23.

36. Lamfers, M., et al., *Homing properties of adipose-derived stem cells to intracerebral glioma and the effects of adenovirus infection.* Cancer Lett, 2009. 274(1): p. 78-87.

37. Hernanda, P.Y., et al., *Tumor promotion through the mesenchymal stem cell compartment in human hepatocellular carcinoma.* Carcinogenesis, 2013. 34(10): p. 2330-40.

38. Wang, Q., et al., *Mesenchymal stem cells over-expressing PEDF decreased the angiogenesis of gliomas.* Biosci Rep, 2012. 24: p. 24.

39. Pendleton, C., et al., *Mesenchymal Stem Cells Derived from Adipose Tissue vs Bone Marrow: <italic>In Vitro</italic> Comparison of Their Tropism towards Gliomas.* PLoS ONE, 2013. 8(3): p. e58198.

40. Senst, C., et al., *Prospective dual role of mesenchymal stem cells in breast tumor microenvironment.* Breast Cancer Res Treat, 2013. 137(1): p. 69-79.

41. Junttila, M.R. and F.J. de Sauvage, *Influence of tumour micro-environment heterogeneity on therapeutic response.* Nature, 2013. 501(7467): p. 346-354.

42. Studeny, M., et al., *Mesenchymal Stem Cells: Potential Precursors for Tumor Stroma and Targeted-Delivery Vehicles for Anticancer Agents.* Journal of the National Cancer Institute, 2004. 96(21): p. 1593-1603.

43. Ahn, J.o., et al., *Anti-Tumor Effect of Adipose Tissue Derived-Mesenchymal Stem Cells Expressing Interferon-? and Treatment with Cisplatin in a Xenograft Mouse Model for Canine Melanoma.* PLoS ONE, 2013. 8(9): p. e74897.

44. Chen, Q., et al., *Antitumor activity of placenta-derived mesenchymal stem cells producing pigment epithelium-derived factor in a mouse melanoma model.* Oncol Lett, 2012. 4(3): p. 413-418.

45. Song, C., et al., *Thymidine kinase gene modified bone marrow mesenchymal stem cells as vehicles for antitumor therapy.* Hum Gene Ther, 2011. 22(4): p. 439-49.

46. Chan, J., et al., *Human fetal mesenchymal stem cells as vehicles for gene delivery.* Stem Cells, 2005. 23(1): p. 93-102.

47. Grisendi, G., et al., *Adipose-derived mesenchymal stem cells as stable source of tumor necrosis factor-related apoptosis-inducing ligand delivery for cancer therapy.* Cancer Res, 2010. 70(9): p. 3718-29.

48. Ciavarella, S., et al., *In vitro anti-myeloma activity of TRAIL-expressing adipose-derived mesenchymal stem cells.* Br J Haematol, 2012. 157(5): p. 586-98.

49. Choi, S.A., et al., *Therapeutic efficacy and safety of TRAIL-producing human adipose tissue-derived mesenchymal stem cells against experimental brainstem glioma.* Neuro Oncol, 2011. 13(1): p. 61-9.

50. Elzaouk, L., K. Moelling, and J. Pavlovic, *Anti-tumor activity of mesenchymal stem cells producing IL-12 in a mouse melanoma model.* Exp Dermatol, 2006. 15(11): p. 865-74.

51. Balkwill, F.R., M. Capasso, and T. Hagemann, *The tumor microenvironment at a glance.* J Cell Sci, 2012. 125(Pt 23): p. 5591-6.

52. Pattabiraman, D.R. and R.A. Weinberg, *Tackling the cancer stem cells [mdash] what challenges do they pose?* Nat Rev Drug Discov, 2014. 13(7): p. 497-512.

53. Bielli, A., et al., *Adult adipose-derived stem cells and breast cancer: a controversial relationship.* SpringerPlus, 2014. 3(1): p. 1-10.

54. Chandler, E.M., et al., *Implanted adipose progenitor cells as physicochemical regulators of breast cancer.* Proceedings of the National Academy of Sciences of the United States of America, 2012. 109(25): p. 9786-9791.

55. Pinilla, S., et al., *Tissue resident stem cells produce CCL5 under the influence of cancer cells and thereby promote breast cancer cell invasion.* Cancer Lett, 2009. 284(1): p. 80-5.

56. Koellensperger, E., et al., *The impact of human adipose tissue-derived stem cells on breast cancer cells: implications for cell-assisted lipotransfers in breast reconstruction.* Stem Cell Research & Therapy, 2017. 8(1): p. 121.

57. Domenis, R., et al., *Adipose tissue derived stem cells: in vitro and in vivo analysis of a standard and three commercially available cell-assisted lipotransfer techniques.* Stem Cell Res Ther, 2015. 6: p. 2.

58. Mailey, B., et al., *A comparison of cell-enriched fat transfer to conventional fat grafting after aesthetic procedures using a patient satisfaction survey.* Ann Plast Surg, 2013. 70(4): p. 410-5.

59. Sterodimas, A., et al., *Autologous fat transplantation versus adipose-derived stem cell-enriched lipografts: a study.* Aesthet Surg J, 2011. 31(6): p. 682-93.

60. Cabioglu, N., et al., *Chemokine receptor CXCR4 expression in breast cancer as a potential predictive marker of isolated tumor cells in bone marrow.* Clin Exp Metastasis, 2005. 22(1): p. 39-46.

61. Bruno, S., et al., *Microvesicles derived from human bone marrow mesenchymal stem cells inhibit tumor growth.* Stem Cells Dev, 2013. 22(5): p. 758-71.

62. Kucerova, L., et al., *Altered features and increased chemosensitivity of human breast cancer cells mediated by adipose tissue-derived mesenchymal stromal cells.* BMC Cancer, 2013. 13: p. 535.

63. Ryu, H., et al., *Adipose tissue-derived mesenchymal stem cells cultured at high density express IFN-beta and suppress the growth of MCF-7 human breast cancer cells.* Cancer Lett, 2014. 352(2): p. 220-7.

64. Zhou, Y., et al., *Effect of truncated neurokinin-1 receptor expression changes on the interaction between human breast cancer and bone marrow-derived mesenchymal stem cells.* Genes Cells, 2014. 19(9): p. 676-91.

65. Sun, B., et al., *Therapeutic potential of mesenchymal stromal cells in a mouse breast cancer metastasis model.* Cytotherapy, 2009. 11(3): p. 289-98, 1 p following 298.

66. Ramasamy, R., et al., *Mesenchymal stem cells inhibit proliferation and apoptosis of tumor cells: impact on in vivo tumor growth.* Leukemia, 2007. 21(2): p. 304-10.

67. Trivanovic, D., et al., *Characteristics of human adipose mesenchymal stem cells isolated from healthy and cancer affected people and their interactions with human breast cancer cell line MCF-7 in vitro.* Cell Biol Int, 2014. 38(2): p. 254-65.

68. Lu, Y.R., et al., *The growth inhibitory effect of mesenchymal stem cells on tumor cells in vitro and in vivo.* Cancer Biol Ther, 2008. 7(2): p. 245-51.

69. Lee, R.H., et al., *Preactivation of human MSCs with TNF-alpha enhances tumor-suppressive activity.* Cell Stem Cell, 2012. 11(6): p. 825-35.

70. Wu, S., et al., *Microvesicles derived from human umbilical cord Wharton's jelly mesenchymal stem cells attenuate bladder tumor cell growth in vitro and in vivo.* PLoS One, 2013. 8(4): p. e61366.

71. Zhou, X.L., et al., *Downregulation of Dickkopf-1 is responsible for high proliferation of breast cancer cells via losing control of Wnt/beta-catenin signaling.* Acta Pharmacol Sin, 2010. 31(2): p. 202-10.

72. Qiao, L., et al., *Dkk-1 secreted by mesenchymal stem cells inhibits growth of breast cancer cells via depression of Wnt signalling.* Cancer Letters, 2008. 269(1): p. 67-77.

73. Qiao, L., et al., *Suppression of tumorigenesis by human mesenchymal stem cells in a hepatoma model.* Cell Res, 2008. 18(4): p. 500-7.

74. Qiao, L., et al., *NF-[kappa]B downregulation may be involved the depression of tumor cell proliferation mediated by human mesenchymal stem cells.* Acta Pharmacol Sin, 2008. 29(3): p. 333-340.

75. Zhu, Y., et al., *Human mesenchymal stem cells inhibit cancer cell proliferation by secreting DKK-1.* Leukemia, 2009. 23(5): p. 925-33.

76. Madrigal, M., K.S. Rao, and N.H. Riordan, *A review of therapeutic effects of mesenchymal stem cell secretions and induction of secretory modification by different culture methods.* Journal of Translational Medicine, 2014. 12(1): p. 1-14.

77. Zhang, B., et al., *Mesenchymal stem cell secretes immunologically active exosomes.* Stem Cells Dev, 2013. 24: p. 24.

78. Yu, J.M., et al., *Mesenchymal stem cells derived from human adipose tissues favor tumor cell growth in vivo.* Stem Cells Dev, 2008. 17(3): p. 463-73.

79. Prantl, L., et al., *Adipose Tissue Derived Stem Cells Promote Prostate Tumor Growth.* The Prostate, 2010. 70(15): p. 1709-1715.

80. Shinagawa, K., et al., *Mesenchymal stem cells enhance growth and metastasis of colon cancer.* Int J Cancer, 2010. 127(10): p. 2323-33.

81. Liu, S., et al., *Breast cancer stem cells are regulated by mesenchymal stem cells through cytokine networks.* Cancer Res, 2011. 71(2): p. 614-24.

82. Tsai, K., et al., *Mesenchymal stem cells promote formation of colorectal tumors in mice.* Gastroenterology, 2011. 3: p. 1046 - 1056.

83. Chen, D., et al., *Paracrine factors from adipose-mesenchymal stem cells enhance metastatic capacity through Wnt signaling pathway in a colon cancer cell co-culture model.* Cancer Cell International, 2015. 15(1): p. 42.

84. Roorda, B., et al., *Bone marrow-derived cells and tumor growth: contribution of bone marrow-derived cells to tumor micro-environments with special focus on mesenchymal stem cells.* Crit Rev Oncol Hematol, 2009. 3: p. 187 - 98.

85. Roorda, B.D., et al., *Mesenchymal stem cells contribute to tumor cell proliferation by direct cell-cell contact interactions.* Cancer Invest, 2010. 28(5): p. 526-34.

86. Orimo, A., et al., *Stromal fibroblasts present in invasive human breast carcinomas promote tumor growth and angiogenesis through elevated SDF-1/CXCL12 secretion.* Cell, 2005. 121(3): p. 335-48.

87. Hung, S.C., et al., *Angiogenic effects of human multipotent stromal cell conditioned medium activate the PI3K-Akt pathway in hypoxic endothelial cells to inhibit apoptosis, increase survival, and stimulate angiogenesis.* Stem Cells, 2007. 25(9): p. 2363-70.

88. Klopp, A., et al., *Omental adipose tissue-derived stromal cells promote vascularization and growth of endometrial tumors.* Clin Cancer Res, 2012. 3: p. 771 - 782.

89. Chu, Y., et al., *Adipose-derived mesenchymal stem cells promote cell proliferation and invasion of epithelial ovarian cancer.* Experimental Cell Research, 2015. 337(1): p. 16-27.

90. Martin, F.T., et al., *Potential role of mesenchymal stem cells (MSCs) in the breast tumour microenvironment: stimulation of epithelial to mesenchymal transition (EMT).* Breast Cancer Res Treat, 2010. 124(2): p. 317-26.

91. Karnoub, A., et al., *Mesenchymal stem cells within tumour stroma promote breast cancer metastasis.* Nature, 2007. 7162: p. 557 - 563.

92. Lin, R., S. Wang, and R.C. Zhao, *Exosomes from human adipose-derived mesenchymal stem cells promote migration through Wnt signaling pathway in a breast cancer cell model.* Molecular and Cellular Biochemistry, 2013. 383(1): p. 13-20.

93. Warburg, O., *On the origin of cancer cells.* Science, 1956. 123(3191): p. 309-14.

94. Barrett, J.C., *Mechanisms of multistep carcinogenesis and carcinogen risk assessment.* Environmental Health Perspectives, 1993. 100: p. 9-20.

95. Schedin, P. and A. Elias, *Multistep tumorigenesis and the microenvironment.* Breast Cancer Research, 2004. 6(2): p. 93-101.

96. Veronesi, U., et al., *Breast cancer.* The Lancet. 365(9472): p. 1727-1741.

97. Ridge, C.A., A.M. McErlean, and M.S. Ginsberg, *Epidemiology of Lung Cancer.* Seminars in Interventional Radiology, 2013. 30(2): p. 93-98.

98. Fleming, M., et al., *Colorectal carcinoma: Pathologic aspects.* Journal of Gastrointestinal Oncology, 2012. 3(3): p. 153-173.

99. Taylor, R.A., et al., *Human epithelial basal cells are cells of origin of prostate cancer, independent of CD133 status.* Stem Cells, 2012. 30(6): p. 1087-96.

100. Gorlick, R. and C. Khanna, *Osteosarcoma.* J Bone Miner Res, 2010. 25(4): p. 683-91.

101. Leddy, L.R. and R.E. Holmes, *Chondrosarcoma of bone.* Cancer Treat Res, 2014. 162: p. 117-30.

102. Deschler, B. and M. Lübbert, *Acute myeloid leukemia: Epidemiology and etiology.* Cancer, 2006. 107(9): p. 2099-2107.

103. Roman, E. and A.G. Smith, *Epidemiology of lymphomas.* Histopathology, 2011. 58(1): p. 4-14.

104. Rodriguez-Abreu, D., A. Bordoni, and E. Zucca, *Epidemiology of hematological malignancies.* Ann Oncol, 2007. 18 Suppl 1: p. i3-i8.

105. Seifert, M., et al., *Cellular origin and pathophysiology of chronic lymphocytic leukemia.* The Journal of Experimental Medicine, 2012. 209(12): p. 2183-2198.

106. Talerman, A., *Germ cell tumours.* Ann Pathol, 1985. 5(3): p. 145-57.

107. Ulbright, T.M., *Germ cell tumors of the gonads: a selective review emphasizing problems in differential diagnosis, newly appreciated, and controversial issues.* Mod Pathol, 2005. 18 Suppl 2: p. S61-79.

108. Nogales, F.F., I. Dulcey, and O. Preda, *Germ cell tumors of the ovary: an update.* Arch Pathol Lab Med, 2014. 138(3): p. 351-62.

109. Alcantara Llaguno, S.R. and L.F. Parada, *Cell of origin of glioma: biological and clinical implications.* British Journal of Cancer, 2016. 115(12): p. 1445-1450.

110. Zong, H., R.G.W. Verhaak, and P. Canoll, *The cellular origin for malignant glioma and prospects for clinical advancements.* Expert Review of Molecular Diagnostics, 2012. 12(4): p. 383-394.

111. Valtz, N.L., et al., *An embryonic origin for medulloblastoma.* New Biol, 1991. 3(4): p. 364-71.

112. Dyer, M.A. and R. Bremner, *The search for the retinoblastoma cell of origin.* Nat Rev Cancer, 2005. 5(2): p. 91-101.

113. Bremner, R. and J. Sage, *The origin of human retinoblastoma.* Nature, 2014. 514(7522): p. 312-313.

114. Hanahan, D. and Robert A. Weinberg, *Hallmarks of Cancer: The Next Generation.* Cell, 2011. 144(5): p. 646-674.

115. Hanahan, D. and R.A. Weinberg, *The Hallmarks of Cancer.* Cell, 2000. 100(1): p. 57-70.

116. Weinberg, R.A., *The retinoblastoma protein and cell cycle control.* Cell, 1995. 81(3): p. 323-330.

117. Vajdic, C.M. and M.T. van Leeuwen, *Cancer incidence and risk factors after solid organ transplantation.* Int J Cancer, 2009. 125(8): p. 1747-54.

118. Teng, M.W., et al., *Immune-mediated dormancy: an equilibrium with cancer.* J Leukoc Biol, 2008. 84(4): p. 988-93.

119. Kim, R., M. Emi, and K. Tanabe, *Cancer immunoediting from immune surveillance to immune escape.* Immunology, 2007. 121(1): p. 1-14.

120. Yang, L., Y. Pang, and H.L. Moses, *TGF-beta and immune cells: an important regulatory axis in the tumor microenvironment and progression.* Trends Immunol, 2010. 31(6): p. 220-7.

121. Shields, J.D., et al., *Induction of lymphoidlike stroma and immune escape by tumors that express the chemokine CCL21.* Science, 2010. 328(5979): p. 749-52.

122. DeNardo, D.G., P. Andreu, and L.M. Coussens, *Interactions between lymphocytes and myeloid cells regulate pro- versus anti-tumor immunity.* Cancer Metastasis Rev, 2010. 29(2): p. 309-16.

123. Grivennikov, S.I., F.R. Greten, and M. Karin, *Immunity, inflammation, and cancer.* Cell, 2010. 140(6): p. 883-99.

124. Qian, B.Z. and J.W. Pollard, *Macrophage diversity enhances tumor progression and metastasis.* Cell, 2010. 141(1): p. 39-51.

125. Sporn, M.B., *The war on cancer.* Lancet, 1996. 347(9012): p. 1377-81.

126. Christofori, G. and H. Semb, *The role of the cell-adhesion molecule E-cadherin as a tumour-suppressor gene.* Trends Biochem Sci, 1999. 24(2): p. 73-6.

127. Kaiser, U., B. Auerbach, and M. Oldenburg, *The neural cell adhesion molecule NCAM in multiple myeloma.* Leuk Lymphoma, 1996. 20(5-6): p. 389-95.

128. Johnson, J.P., *Cell adhesion molecules of the immunoglobulin supergene family and their role in malignant transformation and progression to metastatic disease.* Cancer Metastasis Rev, 1991. 10(1): p. 11-22.

129. Coussens, L.M., et al., *Inflammatory mast cells up-regulate angiogenesis during squamous epithelial carcinogenesis.* Genes Dev, 1999. 13(11): p. 1382-97.

130. Stetler-Stevenson, W.G., *Matrix metalloproteinases in angiogenesis: a moving target for therapeutic intervention.* J Clin Invest, 1999. 103(9): p. 1237-41.

131. Folkman, J., *Tumor angiogenesis: therapeutic implications.* N Engl J Med, 1971. 285(21): p. 1182-6.

132. Hanahan, D. and J. Folkman, *Patterns and Emerging Mechanisms of the Angiogenic Switch during Tumorigenesis.* Cell, 1996. 86(3): p. 353-364.

133. Folkman, J. and Y. Shing, *Angiogenesis.* J Biol Chem, 1992. 267(16): p. 10931-4.

134. Volpert, O.V., K.M. Dameron, and N. Bouck, *Sequential development of an angiogenic phenotype by human fibroblasts progressing to tumorigenicity*. Oncogene, 1997. 14(12): p. 1495-502.

135. Bergers, G. and L.E. Benjamin, *Tumorigenesis and the angiogenic switch.* Nat Rev Cancer, 2003. 3(6): p. 401-10.

136. Ribatti, D., *The chick embryo chorioallantoic membrane in the study of tumor angiogenesis.* Rom J Morphol Embryol, 2008. 49(2): p. 131-5.

137. Kamb, A., *Cell-cycle regulators and cancer.* Trends Genet, 1995. 11(4): p. 136-40.

138. Bartek, J. and J. Lukas, *Chk1 and Chk2 kinases in checkpoint control and cancer.* Cancer Cell, 2003. 3(5): p. 421-9.

139. Bell, D.W., et al., *Heterozygous germ line hCHK2 mutations in Li-Fraumeni syndrome.* Science, 1999. 286(5449): p. 2528-31.

140. Schutte, M., et al., *Variants in CHEK2 Other than 1100delC Do Not Make a Major Contribution to Breast Cancer Susceptibility.* The American Journal of Human Genetics, 2003. 72(4): p. 1023-1028.

141. Bertoni, F., et al., *CHK1 frameshift mutations in genetically unstable colorectal and endometrial cancers.* Genes Chromosomes Cancer, 1999. 26(2): p. 176-80.

142. Menoyo, A., et al., *Somatic mutations in the DNA damage-response genes ATR and CHK1 in sporadic stomach tumors with microsatellite instability.* Cancer Res, 2001. 61(21): p. 7727-30.

143. Vassileva, V., et al., *Genes involved in DNA repair are mutational targets in endometrial cancers with microsatellite instability.* Cancer Res, 2002. 62(14): p. 4095-9.

144. Wyllie, A.H., J.F. Kerr, and A.R. Currie, *Cell death: the significance of apoptosis.* Int Rev Cytol, 1980. 68: p. 251-306.

145. Kerr, J.F.R., A.H. Wyllie, and A.R. Currie, *Apoptosis: A basic biological phenomenon with wide-ranging implications in tissue kinetics.* British Journal of Cancer, 1972. 26(4): p. 239-257.

146. Birkey Reffey, S., et al., *X-linked inhibitor of apoptosis protein functions as a cofactor in transforming growth factor-beta signaling.* J Biol Chem, 2001. 276(28): p. 26542-9.

147. Maguire, T., et al., *The inhibitors of apoptosis of Epiphyas postvittana nucleopolyhedrovirus.* J Gen Virol, 2000. 81(Pt 11): p. 2803-11.

148. Saraste, A. and K. Pulkki, *Morphologic and biochemical hallmarks of apoptosis.* Cardiovasc Res, 2000. 45(3): p. 528-37.

149. Elmore, S., *Apoptosis: A Review of Programmed Cell Death.* Toxicologic pathology, 2007. 35(4): p. 495-516.

150. Denecker, G., et al., *Death receptor-induced apoptotic and necrotic cell death: differential role of caspases and mitochondria.* Cell Death Differ, 2001. 8(8): p. 829-40.

151. Leist, M., et al., *Intracellular adenosine triphosphate (ATP) concentration: a switch in the decision between apoptosis and necrosis.* J Exp Med, 1997. 185(8): p. 1481-6.

152. Cantor, J.R. and D.M. Sabatini, *Cancer Cell Metabolism: One Hallmark, Many Faces.* Cancer discovery, 2012. 2(10): p. 881-898.

153. Donnenberg, A.D., et al., *The Cancer Stem Cell: Cell Type or Cell State?* Cytometry. Part A : the journal of the International Society for Analytical Cytology, 2013. 83(1): p. 5-7.

154. Giancotti, F.G. and E. Ruoslahti, *Integrin signaling.* Science, 1999. 285(5430): p. 1028-1032.

155. Lukashev, M.E. and Z. Werb, *ECM signalling: orchestrating cell behaviour and misbehaviour.* Trends Cell Biol, 1998. 8(11): p. 437-41.

156. Conklin, M.W., et al., *Aligned collagen is a prognostic signature for survival in human breast carcinoma.* Am J Pathol, 2011. 178(3): p. 1221-32.

157. Jodele, S., et al., *Modifying the soil to affect the seed: role of stromal-derived matrix metalloproteinases in cancer progression.* Cancer Metastasis Rev, 2006. 25(1): p. 35-43.

158. Provenzano, P.P. and S.R. Hingorani, *Hyaluronan, fluid pressure, and stromal resistance in pancreas cancer.* British Journal of Cancer, 2013. 108(1): p. 1-8.

159. Levental, K.R., et al., *Matrix Crosslinking Forces Tumor Progression by Enhancing Integrin signaling.* Cell, 2009. 139(5): p. 891-906.

160. Kalluri, R. and M. Zeisberg, *Fibroblasts in cancer.* Nat Rev Cancer, 2006. 6(5): p. 392-401.

161. Ostman, A. and M. Augsten, *Cancer-associated fibroblasts and tumor growth--bystanders turning into key players.* Curr Opin Genet Dev, 2009. 19(1): p. 67-73.

162. Pietras, K., et al., *Functions of paracrine PDGF signaling in the proangiogenic tumor stroma revealed by pharmacological targeting.* PLoS Med, 2008. 5(1): p. e19.

163. Anderberg, C. and K. Pietras, *On the origin of cancer-associated fibroblasts.* Cell Cycle, 2009. 8(10): p. 1461-2.

164. Bhowmick, N.A., E.G. Neilson, and H.L. Moses, *Stromal fibroblasts in cancer initiation and progression.* Nature, 2004. 432(7015): p. 332-7.

165. LeBedis, C., et al., *Peripheral lymph node stromal cells can promote growth and tumorigenicity of breast carcinoma cells through the release of IGF-I and EGF.* International Journal of Cancer, 2002. 100(1): p. 2-8.

166. Strnad, H., et al., *Head and neck squamous cancer stromal fibroblasts produce growth factors influencing phenotype of normal human keratinocytes.* Histochem Cell Biol, 2010. 133(2): p. 201-11.

167. Amano, K., et al., *Enhancement of ischemia-induced angiogenesis by eNOS overexpression.* Hypertension, 2003. 41(1): p. 156-62.

168. Ikeda, O., et al., *Evaluation of tumor angiogenesis using dynamic enhanced magnetic resonance imaging: comparison of plasma vascular endothelial growth factor, hemodynamic, and pharmacokinetic parameters.* Acta Radiol, 2004. 45(4): p. 446-52.

169. Hanley, C.J., et al., *A subset of myofibroblastic cancer-associated fibroblasts regulate collagen fiber elongation, which is prognostic in multiple cancers*. 2015. 2015.

170. Hassiotou, F. and D. Geddes, *Anatomy of the human mammary gland: Current status of knowledge.* Clinical Anatomy, 2013. 26(1): p. 29-48.

171. Ellis, M.J. and C.M. Perou, *The genomic landscape of breast cancer as a therapeutic roadmap.* Cancer Discov, 2013. 3(1): p. 27-34.

172. Ramsay, D.T., et al., *Anatomy of the lactating human breast redefined with ultrasound imaging.* Journal of Anatomy, 2005. 206(6): p. 525-534.

173. Russo, J., R. Rivera, and I.H. Russo, *Influence of age and parity on the development of the human breast.* Breast Cancer Res Treat, 1992. 23(3): p. 211-8.

174. Russo, J. and I.H. Russo, *Toward a physiological approach to breast cancer prevention.* Cancer Epidemiol Biomarkers Prev, 1994. 3(4): p. 353-64.

175. Birkenfeld, A. and N.G. Kase, *Functional anatomy and physiology of the female breast.* Obstet Gynecol Clin North Am, 1994. 21(3): p. 433-44.

176. Russo, J. and I.H. Russo, *Development of the human breast.* Maturitas, 2004. 49(1): p. 2-15.

177. Milanese, T.R., et al., *Age-related lobular involution and risk of breast cancer.* J Natl Cancer Inst, 2006. 98(22): p. 1600-7.

178. Kamangar, F., G.M. Dores, and W.F. Anderson, *Patterns of cancer incidence, mortality, and prevalence across five continents: defining priorities to reduce cancer disparities in different geographic regions of the world.* J Clin Oncol, 2006. 24(14): p. 2137-50.

179. Dai, X., et al., *Breast cancer intrinsic subtype classification, clinical use and future trends.* American Journal of Cancer Research, 2015. 5(10): p. 2929-2943.

180. Malhotra, G.K., et al., *Histological, molecular and functional subtypes of breast cancers.* Cancer Biology & Therapy, 2010. 10(10): p. 955-960.

181. Yanagawa, M., et al., *Luminal A and luminal B (HER2 negative) subtypes of breast cancer consist of a mixture of tumors with different genotype.* BMC Research Notes, 2012. 5: p. 376-376.

182. Bafico, A., et al., *Interaction of Frizzled Related Protein (FRP) with Wnt Ligands and the Frizzled Receptor Suggests Alternative Mechanisms for FRP Inhibition of Wnt Signaling.* Journal of Biological Chemistry, 1999. 274(23): p. 16180-16187.

183. Badve, S., et al., *Basal-like and triple-negative breast cancers: a critical review with an emphasis on the implications for pathologists and oncologists.* Mod Pathol, 2011. 24(2): p. 157-167.

184. Elsheikh, S.E., et al., *Caveolin 1 and Caveolin 2 are associated with breast cancer basal-like and triple-negative immunophenotype.* British Journal of Cancer, 2008. 99(2): p. 327-334.

185. Bertucci, F., P. Finetti, and D. Birnbaum, *Basal Breast Cancer: A Complex and Deadly Molecular Subtype.* Current Molecular Medicine, 2012. 12(1): p. 96-110.

186. !!! INVALID CITATION !!! [67].

187. Chen, S., et al., *Breast tumor aromatase: functional role and transcriptional regulation.* Endocrine-Related Cancer, 1999. 6(2): p. 149-56.

188. Sasaki, Y., et al., *Immunolocalization of estrogen-producing and metabolizing enzymes in benign breast disease: comparison with normal breast and breast carcinoma.* Cancer Sci, 2010. 101(10): p. 2286-92.

189. Miller, L.R., et al., *INFLUENCE OF RADICAL PROSTATECTOMY ON SERUM HORMONE LEVELS.* The Journal of Urology, 1998. 160(2): p. 449-453.

190. Bulun, S.E., et al., *Regulation of Aromatase Expression in Estrogen-Responsive Breast and Uterine Disease: From Bench to Treatment.* Pharmacological Reviews, 2005. 57(3): p. 359-383.

191. Mohamed-Ali, V., J.H. Pinkney, and S.W. Coppack, *Adipose tissue as an endocrine and paracrine organ.* Int J Obes Relat Metab Disord, 1998. 22(12): p. 1145-58.

192. Park, J., D.M. Euhus, and P.E. Scherer, *Paracrine and Endocrine Effects of Adipose Tissue on Cancer Development and Progression.* Endocrine Reviews, 2011. 32(4): p. 550-570.

193. Vona-Davis, L. and D.P. Rose, *Adipokines as endocrine, paracrine, and autocrine factors in breast cancer risk and progression.* Endocr Relat Cancer, 2007. 14(2): p. 189-206.

194. Miller, J.R., *The Wnts.* Genome Biol, 2002. 3(1): p. 28.

195. Komiya, Y. and R. Habas, *Wnt signal transduction pathways.* Organogenesis, 2008. 4(2): p. 68-75.

196. Hall, C.L., et al., *p21CIP-1/WAF-1 induction is required to inhibit prostate cancer growth elicited by deficient expression of the Wnt inhibitor Dickkopf-1.* Cancer Res, 2010. 70(23): p. 9916-26.

197. Mao, B., et al., *Kremen proteins are Dickkopf receptors that regulate Wnt/beta-catenin signalling.* Nature, 2002. 417(6889): p. 664-7.

198. Kawano, Y. and R. Kypta, *Secreted antagonists of the Wnt signalling pathway.* Journal of Cell Science, 2003. 116(13): p. 2627-2634.

199. Jones, S.E. and C. Jomary, *Secreted Frizzled-related proteins: searching for relationships and patterns.* Bioessays, 2002. 24(9): p. 811-20.

200. Boudin, E., et al., *The role of extracellular modulators of canonical Wnt signaling in bone metabolism and diseases.* Seminars in Arthritis and Rheumatism, 2013(0).

201. Wolf, V., et al., *DDC-4, an apoptosis-associated gene, is a secreted frizzled relative.* FEBS Letters, 1997. 417(3): p. 385-389.

202. Lacher, M.D., et al., *Role of DDC-4//sFRP-4, a secreted Frizzled-related protein, at the onset of apoptosis in mammary involution.* Cell Death Differ, 2003. 10(5): p. 528-538.

203. Drake, J.M., R.R. Friis, and A.M. Dharmarajan, *The role of sFRP4, a secreted frizzled-related protein, in ovulation.* Apoptosis, 2003. 8(4): p. 389-97.

204. Wodarz, A. and R. Nusse, *MECHANISMS OF WNT SIGNALING IN DEVELOPMENT.* Annual Review of Cell and Developmental Biology, 1998. 14(1): p. 59-88.

205. !!! INVALID CITATION !!! [117, 118].

206. Rattner, A., et al., *A family of secreted proteins contains homology to the cysteine-rich ligand-binding domain of frizzled receptors.* Proc Natl Acad Sci U S A, 1997. 94(7): p. 2859-63.

207. Melkonyan, H.S., et al., *SARPs: a family of secreted apoptosis-related proteins.* Proc Natl Acad Sci U S A, 1997. 94(25): p. 13636-41.

208. Hoang, B., et al., *Primary structure and tissue distribution of FRZB, a novel protein related to Drosophila frizzled, suggest a role in skeletal morphogenesis.* Journal of Biological Chemistry, 1996. 271(42): p. 26131-26137.

209. Wang, S., et al., *Frzb, a Secreted Protein Expressed in the Spemann Organizer, Binds and Inhibits Wnt-8.* Cell, 1997. 88(6): p. 757-766.

210. Leyns, L., et al., *Frzb-1 Is a Secreted Antagonist of Wnt Signaling Expressed in the Spemann Organizer.* Cell, 1997. 88(6): p. 747-756.

211. Bovolenta, P., et al., *Beyond Wnt inhibition: new functions of secreted Frizzled-related proteins in development and disease.* J Cell Sci, 2008. 121(Pt 6): p. 737-46.

212. Lin, K., et al., *The cysteine-rich frizzled domain of Frzb-1 is required and sufficient for modulation of Wnt signaling.* Proceedings of the National Academy of Sciences, 1997. 94(21): p. 11196-11200.

213. Uren, A., et al., *Secreted frizzled-related protein-1 binds directly to Wingless and is a biphasic modulator of Wnt signaling.* J Biol Chem, 2000. 275(6): p. 4374-82.

214. Zhou, Z., et al., *Up-regulation of human secreted frizzled homolog in apoptosis and its down-regulation in breast tumors.* International Journal of Cancer, 1998. 78(1): p. 95-99.

215. Muley, A., et al., *Secreted frizzled-related protein 4: an angiogenesis inhibitor.* Am J Pathol, 2010. 176(3): p. 1505-16.

216. Abu-Jawdeh, G., et al., *Differential expression of frpHE: a novel human stromal protein of the secreted frizzled gene family, during the endometrial cycle and malignancy.* Lab Invest, 1999. 79(4): p. 439-47.

217. Longman, D., et al., *The role of the cysteine-rich domain and netrin-like domain of secreted frizzled-related protein 4 in angiogenesis inhibition in vitro.* Oncol Res, 2012. 20(1): p. 1-6.

218. Constantinou, T., *SFRP-4 abrogates Wnt-3a-induced β-catenin and Akt/PKB signalling and reverses a Wnt-3a-imposed inhibition of in vitro mammary differentiation.* Journal of Molecular Signaling, 2008. 3: p. 10.

219. Maganga, R., *Secreted frizzled related protein (sFRP4) promotes epidermal differentiation and apoptosis.* Biochemical and Biophysical Research Communications, 2008. 377: p. 606-611.

220. Guo, X., et al., *Stromal fibroblasts activated by tumor cells promote angiogenesis in mouse gastric cancer.* J Biol Chem, 2008. 28: p. 19864 - 19871.

221. Hsieh, J.C., et al., *A new secreted protein that binds to Wnt proteins and inhibits their activities.* Nature, 1999. 398(6726): p. 431-6.

222. Berndt, T., et al., *Secreted frizzled-related protein 4 is a potent tumor-derived phosphaturic agent.* J Clin Invest, 2003. 112(5): p. 785-94.

223. James, I.E., et al., *FrzB-2: a human secreted frizzled-related protein with a potential role in chondrocyte apoptosis.* Osteoarthritis and Cartilage, 2000. 8(6): p. 452-463.

224. Schumann, H., et al., *Expression of secreted frizzled related proteins 3 and 4 in human ventricular myocardium correlates with apoptosis related gene expression.* Cardiovascular Research, 2000. 45(3): p. 720-728.

225. White, L., et al., *Expression of secreted frizzled-related protein 4 in the primate placenta.* Reproductive BioMedicine Online, 2009. 18(1): p. 104-110.

226. Eastman, Q. and R. Grosschedl, *Regulation of LEF-1/TCF transcription factors by Wnt and other signals.* Curr Opin Cell Biol, 1999. 11(2): p. 233-40.

227. Moon, R.T., et al., *WNT and beta-catenin signalling: diseases and therapies.* Nat Rev Genet, 2004. 5(9): p. 691-701.

228. Giles, R.H., J.H. van Es, and H. Clevers, *Caught up in a Wnt storm: Wnt signaling in cancer.* Biochimica et Biophysica Acta (BBA) - Reviews on Cancer, 2003. 1653(1): p. 1-24.

229. He, B., et al., *Blockade of Wnt-1 signaling induces apoptosis in human colorectal cancer cells containing downstream mutations.* Oncogene, 2005. 24(18): p. 3054-8.

230. Lustig, B. and J. Behrens, *The Wnt signaling pathway and its role in tumor development.* J Cancer Res Clin Oncol, 2003. 129(4): p. 199-221.

231. Polakis, P., *Wnt signaling and cancer.* Genes Dev, 2000. 14(15): p. 1837-51.

232. Reya, T. and H. Clevers, *Wnt signalling in stem cells and cancer.* Nature, 2005. 434(7035): p. 843-850.

233. Aguilera, O., et al., *Epigenetic inactivation of the Wnt antagonist DICKKOPF-1 (DKK-1) gene in human colorectal cancer.* Oncogene, 2006. 25(29): p. 4116-21.

234. Nojima, M., et al., *Frequent epigenetic inactivation of SFRP genes and constitutive activation of Wnt signaling in gastric cancer.* Oncogene, 2007. 26(32): p. 4699-713.

235. Ko, J., et al., *Human Secreted Frizzled-Related Protein Is Down-regulated and Induces Apoptosis in Human Cervical Cancer.* Experimental Cell Research, 2002. 280(2): p. 280-287.

236. Lee, A.Y., et al., *Expression of the secreted frizzled-related protein gene family is downregulated in human mesothelioma.* Oncogene, 2004. 23(39): p. 6672-6676.

237. Wong, S.C.C., et al., *Expression of frizzled-related protein and Wnt-signalling molecules in invasive human breast tumours.* The Journal of Pathology, 2002. 196(2): p. 145-153.

238. Cheng, Y.Y., et al., *Frequent epigenetic inactivation of secreted frizzled-related protein 2 (SFRP2) by promoter methylation in human gastric cancer.* Br J Cancer, 2007. 97(7): p. 895-901.

239. Xiang, T., et al., *Epigenetic silencing of the WNT antagonist Dickkopf 3 disrupts normal Wnt/β-catenin signalling and apoptosis regulation in breast cancer cells.* Journal of Cellular and Molecular Medicine, 2013. 17(10): p. 1236-1246.

240. Suzuki, H., et al., *Epigenetic inactivation of SFRP genes allows constitutive WNT signaling in colorectal cancer.* Nat Genet, 2004. 36(4): p. 417-22.

241. Schiefer, L., et al., *Epigenetic regulation of the secreted frizzled-related protein family in human glioblastoma multiforme.* Cancer Gene Ther, 2014. 21(7): p. 297-303.

242. Caldwell, G.M., et al., *The Wnt antagonist sFRP1 in colorectal tumorigenesis.* Cancer Res, 2004. 64(3): p. 883-8.

243. Caldwell, G.M., et al., *The Wnt antagonist sFRP1 is downregulated in premalignant large bowel adenomas.* British Journal of Cancer, 2006. 94(6): p. 922-927.

244. Feng Han, Q., et al., *Expression of sFRP-4 and beta-catenin in human colorectal carcinoma.* Cancer Lett, 2006. 231(1): p. 129-37.

245. Hrzenjak, A., et al., *Inverse correlation of secreted frizzled-related protein 4 and β-catenin expression in endometrial stromal sarcomas.* The Journal of Pathology, 2004. 204(1): p. 19-27.

246. Huang, S., et al., *Coexpression of SFRP1 and WIF1 as a Prognostic Predictor of Favorable Outcomes in Patients with Colorectal Carcinoma*. BioMed Research International, 2014. 2014: p. 8.

247. Roth, W., et al., *Secreted Frizzled-related proteins inhibit motility and promote growth of human malignant glioma cells.* Oncogene, 2000. 19(37): p. 4210-20.

248. Wissmann, C., et al., *WIF1, a component of the Wnt pathway, is down-regulated in prostate, breast, lung, and bladder cancer.* J Pathol, 2003. 201(2): p. 204-12.

249. Drake, J., et al., *Expression of secreted frizzled-related protein 4 (SFRP4) in primary serous ovarian tumours.* Eur J Gynaecol Oncol, 2009. 30(2): p. 133-41.

250. Carmon, K.S. and D.S. Loose, *Secreted frizzled-related protein 4 regulates two Wnt7a signaling pathways and inhibits proliferation in endometrial cancer cells.* Mol Cancer Res, 2008. 6(6): p. 1017-28.

251. Furlong, M.T. and P.J. Morin, *Rare activation of the TCF/beta-catenin pathway in ovarian cancer.* Gynecol Oncol, 2000. 77(1): p. 97-104.

252. Qi, J., et al., *Hypermethylation and expression regulation of secreted frizzled-related protein genes in colorectal tumor.* World Journal of Gastroenterology : WJG, 2006. 12(44): p. 7113-7117.

253. Zou, H., et al., *Aberrant methylation of secreted frizzled-related protein genes in esophageal adenocarcinoma and Barrett's esophagus.* International Journal of Cancer, 2005. 116(4): p. 584-591.

254. Ford, C.E., et al., *The Wnt gatekeeper SFRP4 modulates EMT, cell migration and downstream Wnt signalling in serous ovarian cancer cells.* PLoS One, 2013. 8(1): p. e54362.

255. Jacob, F., et al., *Loss of Secreted Frizzled-Related Protein 4 Correlates with an Aggressive Phenotype and Predicts Poor Outcome in Ovarian Cancer Patients.* Plos one, 2012. 7(2): p. e31885.

256. Saran, U., et al., *Secreted frizzled-related protein 4 expression is positively associated with responsiveness to Cisplatin of ovarian cancer cell lines in vitro and with lower tumour grade in mucinous ovarian cancers.* BMC Cell Biology, 2012. 13(1): p. 25.

257. Horvath, L.G., et al., *Membranous expression of secreted frizzled-related protein 4 predicts for good prognosis in localized prostate cancer and inhibits PC3 cellular proliferation in vitro.* Clin Cancer Res, 2004. 10(2): p. 615-25.

258. Nwabo Kamdje, A.H., et al., *Signaling pathways in breast cancer: therapeutic targeting of the microenvironment.* Cell Signal, 2014. 26(12): p. 2843-56.

259. Pires, B.R., et al., *Targeting Cellular Signaling Pathways in Breast Cancer Stem Cells and its Implication for Cancer Treatment.* Anticancer Res, 2016. 36(11): p. 5681-5691.

260. Lin, S.Y., et al., *Beta-catenin, a novel prognostic marker for breast cancer: its roles in cyclin D1 expression and cancer progression.* Proc Natl Acad Sci U S A, 2000. 97(8): p. 4262-6.

261. Lin, R., S. Wang, and R.C. Zhao, *Exosomes from human adipose-derived mesenchymal stem cells promote migration through Wnt signaling pathway in a breast cancer cell model.* Mol Cell Biochem, 2013. 383(1-2): p. 13-20.

262. Ugolini, F., et al., *WNT pathway and mammary carcinogenesis: loss of expression of candidate tumor suppressor gene SFRP1 in most invasive carcinomas except of the medullary type.* Oncogene, 2001. 20(41): p. 5810-7.

263. McLaren, S.A., et al., *The Role of Secreted Frizzled Related Protein 4 (sFRP-4) in Regulating Oestradiol-Induced Growth of the MCF-7 Breast Cancer Cell Line.* Journal of Analytical Oncology, 2014. 3: p. 1-10.

264. Ridge, S.M., F.J. Sullivan, and S.A. Glynn, *Mesenchymal stem cells: key players in cancer progression.* Molecular Cancer, 2017. 16(1): p. 31.

265. Wels, J., et al., *Migratory neighbors and distant invaders: tumor-associated niche cells.* Genes Dev, 2008. 22(5): p. 559-74.

266. Dwyer, R.M., et al., *Monocyte chemotactic protein-1 secreted by primary breast tumors stimulates migration of mesenchymal stem cells.* Clin Cancer Res, 2007. 13.

267. Junttila, M.R. and F.J. de Sauvage, *Influence of tumour micro-environment heterogeneity on therapeutic response.* Nature, 2013. 501(7467): p. 346-54.

268. Togo, S., et al., *Carcinoma-Associated Fibroblasts Are a Promising Therapeutic Target.* Cancers, 2013. 5(1): p. 149-169.

269. Spaeth, E.L., et al., *Mesenchymal stem cell transition to tumor-associated fibroblasts contributes to fibrovascular network expansion and tumor progression.* Plos one, 2009. 4(4): p. 7.

270. Augsten, M., *Cancer-Associated Fibroblasts as Another Polarized Cell Type of the Tumor Microenvironment.* Frontiers in Oncology, 2014. 4: p. 62.

271. Paunescu, V., et al., *Tumour-associated fibroblasts and mesenchymal stem cells: more similarities than differences.* J Cell Mol Med, 2011. 15(3): p. 635-46.

272. Grisendi, G., et al., *Understanding tumor-stroma interplays for targeted therapies by armed mesenchymal stromal progenitors: the Mesenkillers.* Am J Cancer Res, 2011. 1(6): p. 787-805.

273. Dirat, B., et al., *Cancer-associated adipocytes exhibit an activated phenotype and contribute to breast cancer invasion.* Cancer Res, 2011. 71(7): p. 2455-65.

274. Mishra, P., et al., *Carcinoma-associated fibroblast-like differentiation of human mesenchymal stem cells.* Cancer Res, 2008. 11: p. 4331 - 4339.

275. Sun, Z., S. Wang, and R.C. Zhao, *The roles of mesenchymal stem cells in tumor inflammatory microenvironment.* Journal of Hematology & Oncology, 2014. 7: p. 14-14.

276. Heo, S.C., et al., *Periostin mediates human adipose tissue-derived mesenchymal stem cell-stimulated tumor growth in a xenograft lung adenocarcinoma model.* Biochimica et Biophysica Acta (BBA) - Molecular Cell Research, 2011. 1813(12): p. 2061-2070.

277. Choi, K.U., et al., *Lysophosphatidic acid-induced expression of periostin in stromal cells: Prognoistic relevance of periostin expression in epithelial ovarian cancer.* Int J Cancer, 2011. 128(2): p. 332-42.

278. Jeon, E.S., et al., *Mesenchymal stem cells stimulate angiogenesis in a murine xenograft model of A549 human adenocarcinoma through an LPA1 receptor-dependent mechanism.* Biochim Biophys Acta, 2010. 1801(11): p. 1205-13.

279. Cho, J.A., et al., *Exosomes from breast cancer cells can convert adipose tissue-derived mesenchymal stem cells into myofibroblast-like cells.* Int J Oncol, 2012. 40(1): p. 130-8.

280. Cho, J.A., et al., *Exosomes from ovarian cancer cells induce adipose tissue-derived mesenchymal stem cells to acquire the physical and functional characteristics of tumor-supporting myofibroblasts.* Gynecol Oncol, 2011. 123(2): p. 379-86.

281. Torsvik, A. and R. Bjerkvig, *Mesenchymal stem cell signaling in cancer progression.* Cancer Treat Rev, 2013. 39(2): p. 180-8.

282. Jeon, E.S., et al., *Cancer-derived lysophosphatidic acid stimulates differentiation of human mesenchymal stem cells to myofibroblast-like cells.* Stem Cells, 2008. 26(3): p. 789-97.

283. Mazzocca, A., et al., *Tumor-secreted lysophostatidic acid accelerates hepatocellular carcinoma progression by promoting differentiation of peritumoral fibroblasts in myofibroblasts.* Hepatology, 2011. 54(3): p. 920-30.

284. Postlethwaite, A.E., et al., *Stimulation of the chemotactic migration of human fibroblasts by transforming growth factor beta.* J Exp Med, 1987. 165(1): p. 251-6.

285. Ronnov-Jessen, L. and O.W. Petersen, *Induction of alpha-smooth muscle actin by transforming growth factor-beta 1 in quiescent human breast gland fibroblasts. Implications for myofibroblast generation in breast neoplasia.* Lab Invest, 1993. 68(6): p. 696-707.

286. De Wever, O. and M. Mareel, *Role of tissue stroma in cancer cell invasion.* J Pathol, 2003. 200(4): p. 429-47.

287. Shangguan, L., et al., *Inhibition of TGF-beta/Smad signaling by BAMBI blocks differentiation of human mesenchymal stem cells to carcinoma-associated fibroblasts and abolishes their protumor effects.* Stem Cells, 2012. 30(12): p. 2810-9.

288. Matushansky, I., et al., *Derivation of sarcomas from mesenchymal stem cells via inactivation of the Wnt pathway.* J Clin Invest, 2007. 117(11): p. 3248-57.

289. Edlund, S., et al., *Transforming growth factor-beta1 (TGF-beta)-induced apoptosis of prostate cancer cells involves Smad7-dependent activation of p38 by TGF-beta-activated kinase 1 and mitogen-activated protein kinase kinase 3.* Mol Biol Cell, 2003. 14(2): p. 529-44.

290. Jian, H., et al., *Smad3-dependent nuclear translocation of β-catenin is required for TGF-β1-induced proliferation of bone marrow-derived adult human mesenchymal stem cells.* Genes & Development, 2006. 20(6): p. 666-674.

291. Sato, M., *Upregulation of the Wnt/beta-catenin pathway induced by transforming growth factor-beta in hypertrophic scars and keloids.* Acta Derm Venereol, 2006. 86(4): p. 300-7.

292. Akhmetshina, A., et al., *Activation of canonical Wnt signalling is required for TGF-β-mediated fibrosis.* Nature Communications, 2012. 3: p. 735.

293. Vander Heiden, M.G., L.C. Cantley, and C.B. Thompson, *Understanding the Warburg Effect: The Metabolic Requirements of Cell Proliferation.* Science (New York, N.Y.), 2009. 324(5930): p. 1029-1033.

294. Liberti, M.V. and J.W. Locasale, *The Warburg Effect: How Does it Benefit Cancer Cells?* Trends Biochem Sci, 2016. 41(3): p. 211-8.

295. Sotgia, F., et al., *Understanding the Warburg effect and the prognostic value of stromal caveolin-1 as a marker of a lethal tumor microenvironment.* Breast Cancer Research : BCR, 2011. 13(4): p. 213-213.

296. Guppy, M., et al., *Contribution by different fuels and metabolic pathways to the total ATP turnover of proliferating MCF-7 breast cancer cells.* Biochem J, 2002. 364(Pt 1): p. 309-15.

297. Kallinowski, F., et al., *Tumor blood flow: the principal modulator of oxidative and glycolytic metabolism, and of the metabolic micromilieu of human tumor xenografts in vivo.* Int J Cancer, 1989. 44(2): p. 266-72.

298. Zu, X.L. and M. Guppy, *Cancer metabolism: facts, fantasy, and fiction.* Biochem Biophys Res Commun, 2004. 313(3): p. 459-65.

299. Zheng, J.I.E., *Energy metabolism of cancer: Glycolysis versus oxidative phosphorylation (Review).* Oncology Letters, 2012. 4(6): p. 1151-1157.

300. Guido, C., et al., *Metabolic reprogramming of cancer-associated fibroblasts by TGF-beta drives tumor growth: connecting TGF-beta signaling with "Warburg-like" cancer metabolism and L-lactate production.* Cell Cycle, 2012. 11(16): p. 3019-35.

301. Wang, J., et al., *Characterization of phosphoglycerate kinase-1 expression of stromal cells derived from tumor microenvironment in prostate cancer progression.* Cancer Res, 2010. 70(2): p. 471-80.

302. Zhang, D., et al., *Metabolic reprogramming of cancer-associated fibroblasts by IDH3alpha downregulation.* Cell Rep, 2015. 10(8): p. 1335-48.

303. Pavlides, S., et al., *The reverse Warburg effect: Aerobic glycolysis in cancer associated fibroblasts and the tumor stroma.* Cell Cycle, 2009. 8(23): p. 3984-4001.

304. Gonzalez, C.D., et al., *Autophagy, Warburg, and Warburg Reverse Effects in Human Cancer.* BioMed Research International, 2014. 2014: p. 10.

305. Fock, K.M. and J. Khoo, *Diet and exercise in management of obesity and overweight.* Journal of Gastroenterology and Hepatology, 2013. 28: p. 59-63.

306. Mitchell, R.J., et al., *Associations between obesity and overweight and fall risk, health status and quality of life in older people.* Aust N Z J Public Health, 2014. 38(1): p. 13-8.

307. Bray, G.A., *Medical consequences of obesity.* J Clin Endocrinol Metab, 2004. 89(6): p. 2583-9.

308. Ghoorah, K., et al., *Obesity and cardiovascular outcomes: a review.* Eur Heart J Acute Cardiovasc Care, 2014.

309. Christodoulides, C., et al., *Adipogenesis and WNT signalling.* Trends in Endocrinology & Metabolism, 2009. 20(1): p. 16-24.

310. Ross, S.E., et al., *Inhibition of Adipogenesis by Wnt Signaling.* Science, 2000. 289(5481): p. 950-953.

311. Bennett, C.N., et al., *Regulation of Wnt Signaling during Adipogenesis.* Journal of Biological Chemistry, 2002. 277(34): p. 30998-31004.

312. Nishizuka, M., et al., *Wnt4 and Wnt5a promote adipocyte differentiation.* FEBS Letters, 2008. 582(21–22): p. 3201-3205.

313. Iorio, M.V., et al., *MicroRNA gene expression deregulation in human breast cancer.* Cancer Res, 2005. 65(16): p. 7065-70.

314. Zaragosi, L.E., et al., *Effects of GSK3 inhibitors on in vitro expansion and differentiation of human adipose-derived stem cells into adipocytes.* BMC Cell Biol, 2008. 9(11): p. 1471-2121.

315. Park, J.R., Jung, Y.-S. Lee, K.-S. Kang, *The roles of Wnt antagonists Dkk1 and sFRP4 during adipogenesis of human adipose tissue-derived mesenchymal stem cells.* 2008.

316. Ehrlund, A., et al., *Characterization of the Wnt inhibitors secreted frizzled-related proteins (SFRPs) in human adipose tissue.* J Clin Endocrinol Metab, 2013. 98(3): p. 2012-3416.

317. Hoffmann, M.M., et al., *Association of secreted frizzled-related protein 4 (SFRP4) with type 2 diabetes in patients with stable coronary artery disease.* Cardiovasc Diabetol, 2014. 13: p. 155.

318. Mahdi, T., et al., *Secreted frizzled-related protein 4 reduces insulin secretion and is overexpressed in type 2 diabetes.* Cell Metab, 2012. 16(5): p. 625-33.

319. Comsa, S., A.M. Cimpean, and M. Raica, *The Story of MCF-7 Breast Cancer Cell Line: 40 years of Experience in Research.* Anticancer Res, 2015. 35(6): p. 3147-54.

320. Warrier, S., et al., *Wnt antagonist, secreted frizzled-related protein 4 (sFRP4), increases chemotherapeutic response of glioma stem-like cells.* Oncol Res, 2013. 21(2): p. 93-102.

321. Perumal, V., et al., *Therapeutic approach to target mesothelioma cancer cells using the Wnt antagonist, secreted frizzled-related protein 4: Metabolic state of cancer cells.* Exp Cell Res, 2016. 341(2): p. 218-24.

322. Balijepalli, M.K., S. Tandra, and M.R. Pichika, *Antiproliferative activity and induction of apoptosis in estrogen receptor-positive and negative human breast carcinoma cell lines by Gmelina asiatica roots.* Pharmacognosy Research, 2010. 2(2): p. 113-119.

323. Tate, C.R., et al., *Targeting triple-negative breast cancer cells with the histone deacetylase inhibitor panobinostat.* Breast Cancer Research, 2012. 14(3): p. R79.

324. Quail, D.F. and J.A. Joyce, *Microenvironmental regulation of tumor progression and metastasis.* Nat Med, 2013. 19(11): p. 1423-37.

325. Dasari, V.R., et al., *Upregulation of PTEN in Glioma Cells by Cord Blood Mesenchymal Stem Cells Inhibits Migration via Downregulation of the PI3K/Akt Pathway.* PLOS ONE, 2010. 5(4): p. e10350.

326. Kidd, S., et al., *Mesenchymal stromal cells alone or expressing interferon-beta suppress pancreatic tumors in vivo, an effect countered by anti-inflammatory treatment.* Cytotherapy, 2010. 12(5): p. 615-25.

327. Takahara, K., et al., *Adipose-derived stromal cells inhibit prostate cancer cell proliferation inducing apoptosis.* Biochem Biophys Res Commun, 2014. 446(4): p. 1102-7.

328. Ohlsson, L.B., et al., *Mesenchymal progenitor cell-mediated inhibition of tumor growth in vivo and in vitro in gelatin matrix.* Exp Mol Pathol, 2003. 75(3): p. 248-55.

329. Secchiero, P., et al., *Human Bone Marrow Mesenchymal Stem Cells Display Anti-Cancer Activity in SCID Mice Bearing Disseminated Non-Hodgkin's Lymphoma Xenografts.* PLOS ONE, 2010. 5(6): p. e11140.

330. Madrigal, M., K.S. Rao, and N.H. Riordan, *A review of therapeutic effects of mesenchymal stem cell secretions and induction of secretory modification by different culture methods.* Journal of Translational Medicine, 2014. 12(1): p. 260.

331. Li, L., et al., *Human mesenchymal stem cells play a dual role on tumor cell growth in vitro and in vivo.* Journal of Cellular Physiology, 2011. 226(7): p. 1860-1867.

332. Cho, J.A., et al., *Hyperthermia-treated mesenchymal stem cells exert antitumor effects on human carcinoma cell line.* Cancer, 2009. 115(2): p. 311-23.

333. Widowati, W., et al., *Conditioned medium from normoxia (WJMSCs-norCM) and hypoxia-treated WJMSCs (WJMSCs-hypoCM) in inhibiting cancer cell proliferation.* Biomarkers and Genomic Medicine, 2015. 7(1): p. 8-17.

334. Jang, G.-B., et al., *Blockade of Wnt/β-catenin signaling suppresses breast cancer metastasis by inhibiting CSC-like phenotype.* Scientific Reports, 2015. 5: p. 12465.

335. King, T.D., M.J. Suto, and Y. Li, *The Wnt/beta-catenin signaling pathway: a potential therapeutic target in the treatment of triple negative breast cancer.* J Cell Biochem, 2012. 113(1): p. 13-8.

336. Schlosshauer, P.W., et al., *APC truncation and increased beta-catenin levels in a human breast cancer cell line.* Carcinogenesis, 2000. 21(7): p. 1453-6.

337. Lacroix-Triki, M., et al., *beta-catenin/Wnt signalling pathway in fibromatosis, metaplastic carcinomas and phyllodes tumours of the breast.* Mod Pathol, 2010. 23(11): p. 1438-48.

338. Lopez-Knowles, E., et al., *Cytoplasmic localization of beta-catenin is a marker of poor outcome in breast cancer patients.* Cancer Epidemiol Biomarkers Prev, 2010. 19(1): p. 301-9.

339. Xu, J., et al., *β-Catenin Is Required for the Tumorigenic Behavior of Triple-Negative Breast Cancer Cells.* PLOS ONE, 2015. 10(2): p. e0117097.

340. Khramtsov, A.I., et al., *Wnt/β-Catenin Pathway Activation Is Enriched in Basal-Like Breast Cancers and Predicts Poor Outcome.* The American Journal of Pathology, 2010. 176(6): p. 2911-2920.

341. Suzuki, H., et al., *Frequent epigenetic inactivation of Wnt antagonist genes in breast cancer.* Br J Cancer, 2008. 98(6): p. 1147-56.

342. Ugolini, F., et al., *Differential expression assay of chromosome arm 8p genes identifies Frizzled-related (FRP1/FRZB) and Fibroblast Growth Factor Receptor 1 (FGFR1) as candidate breast cancer genes.* Oncogene, 1999. 18(10): p. 1903-10.

343. Veeck, J., et al., *Aberrant methylation of the Wnt antagonist SFRP1 in breast cancer is associated with unfavourable prognosis*. Oncogene, 2006. 25(24): p. 3479-88.

344. Veeck, J., et al., *Wnt signalling in human breast cancer: expression of the putative Wnt inhibitor Dickkopf-3 (DKK3) is frequently suppressed by promoter hypermethylation in mammary tumours.* Breast Cancer Res, 2008. 10(5): p. R82.

345. Klopocki, E., et al., *Loss of SFRP1 is associated with breast cancer progression and poor prognosis in early stage tumors.* Int J Oncol, 2004. 25(3): p. 641-9.

346. Bernemann, C., et al., *Influence of secreted frizzled receptor protein 1 (SFRP1) on neoadjuvant chemotherapy in triple negative breast cancer does not rely on WNT signaling.* Mol Cancer, 2014. 13: p. 174.

347. Matsuda, Y., et al., *WNT signaling enhances breast cancer cell motility and blockade of the WNT pathway by sFRP1 suppresses MDA-MB-231 xenograft growth.* Breast Cancer Res, 2009. 11(3): p. R32.

348. Schlange, T., et al., *Autocrine WNT signaling contributes to breast cancer cell proliferation via the canonical WNT pathway and EGFR transactivation.* Breast Cancer Res, 2007. 9(5): p. R63.

349. Lamb, R., et al., *Wnt Pathway Activity in Breast Cancer Sub-Types and Stem-Like Cells.* PLOS ONE, 2013. 8(7): p. e67811.

350. McLaren, S., et al., *The role of secreted frizzled related protein 4 (sFRP-4) in regulating oestradiol-induced growth of the MCF-7 breast cancer cell line.* J Anal Oncol, 2014. 3(1): p. 1-10.

351. Wang, J. and J. Yi, *Cancer cell killing via ROS: to increase or decrease, that is the question.* Cancer Biol Ther, 2008. 7(12): p. 1875-84.

352. Muehlberg, F.L., et al., *Tissue-resident stem cells promote breast cancer growth and metastasis.* Carcinogenesis, 2009. 30.

353. Hanson, S.E., J. Kim, and P. Hematti, *Comparative analysis of adipose-derived mesenchymal stem cells isolated from abdominal and breast tissue.* Aesthet Surg J, 2013. 33(6): p. 888-98.

354. Kim, J., et al., *Comparison of Breast and Abdominal Adipose Tissue Mesenchymal Stromal/Stem Cells in Support of Proliferation of Breast Cancer Cells.* Cancer investigation, 2013. 31(8): p. 550-554.

355. Cousin, B., et al., *Adult Stromal Cells Derived from Human Adipose Tissue Provoke Pancreatic Cancer Cell Death both In Vitro and In Vivo.* PLoS ONE, 2009. 4(7): p. e6278.

356. Yu, X., et al., *Human Adipose Derived Stem Cells Induced Cell Apoptosis and S Phase Arrest in Bladder Tumor.* Stem Cells International, 2015. 2015: p. 12.

357. Dirndorfer, D., et al., *The α-Helical Structure of Prodomains Promotes Translocation of Intrinsically Disordered Neuropeptide Hormones into the Endoplasmic Reticulum.* The Journal of Biological Chemistry, 2013. 288(20): p. 13961-13973.

358. Hunakova, L., et al., *Modulation of markers associated with aggressive phenotype in MDA-MB-231 breast carcinoma cells by sulforaphane.* Neoplasma, 2009. 56(6): p. 548-56.

359. Nagaraja, G.M., et al., *Gene expression signatures and biomarkers of noninvasive and invasive breast cancer cells: comprehensive profiles by representational difference analysis, microarrays and proteomics.* Oncogene, 2006. 25(16): p. 2328-38.

360. Gordon, L.A., et al., *Breast cell invasive potential relates to the myoepithelial phenotype.* Int J Cancer, 2003. 106(1): p. 8-16.

361. Voss, M.J., et al., *Luminal and basal-like breast cancer cells show increased migration induced by hypoxia, mediated by an autocrine mechanism.* BMC Cancer, 2011. 11(1): p. 158.

362. He, B., et al., *Secreted frizzled-related protein 4 is silenced by hypermethylation and induces apoptosis in beta-catenin-deficient human mesothelioma cells.* Cancer Res, 2005. 65(3): p. 743-8.

363. Lee, A.Y., et al., *Expression of the secreted frizzled-related protein gene family is downregulated in human mesothelioma.* Oncogene, 2004. 23(39): p. 6672-6.

364. Horvath, L.G., et al., *Secreted frizzled-related protein 4 inhibits proliferation and metastatic potential in prostate cancer.* Prostate, 2007. 67(10): p. 1081-90.

365. Schumacker, P.T., *Reactive oxygen species in cancer cells: live by the sword, die by the sword.* Cancer Cell, 2006. 10(3): p. 175-6.

366. Simon, H.-U., A. Haj-Yehia, and F. Levi-Schaffer, *Role of reactive oxygen species (ROS) in apoptosis induction.* Apoptosis, 2000. 5(5): p. 415-418.

367. Mates, J.M. and F.M. Sanchez-Jimenez, *Role of reactive oxygen species in apoptosis: implications for cancer therapy.* Int J Biochem Cell Biol, 2000. 32(2): p. 157-70.

368. Fleury, C., B. Mignotte, and J.-L. Vayssière, *Mitochondrial reactive oxygen species in cell death signaling.* Biochimie, 2002. 84(2–3): p. 131-141.

369. Brodska, B. and A. Holoubek, *Generation of reactive oxygen species during apoptosis induced by DNA-damaging agents and/or histone deacetylase inhibitors.* Oxid Med Cell Longev, 2011. 2011: p. 253529.

370. Chen, Q., et al., *Production of reactive oxygen species by mitochondria: central role of complex III.* J Biol Chem, 2003. 278(38): p. 36027-31.

371. Aronis, A., et al., *Potentiation of Fas-mediated apoptosis by attenuated production of mitochondria-derived reactive oxygen species.* Cell Death Differ, 0000. 10(3): p. 335-344.

372. Shi, D.-y., et al., *The role of cellular oxidative stress in regulating glycolysis energy metabolism in hepatoma cells.* Molecular Cancer, 2009. 8: p. 32-32.

373. McIlwain, D.R., T. Berger, and T.W. Mak, *Caspase Functions in Cell Death and Disease.* Cold Spring Harbor Perspectives in Biology, 2013. 5(4).

374. Jänicke, R.U., et al., *Caspase-3 Is Required for DNA Fragmentation and Morphological Changes Associated with Apoptosis.* Journal of Biological Chemistry, 1998. 273(16): p. 9357-9360.

375. Liang, Y., C. Yan, and N.F. Schor, *Apoptosis in the absence of caspase 3.* Oncogene, 2001. 20(45): p. 6570-8.

376. Musgrove, E.A., et al., *Cyclin D as a therapeutic target in cancer.* Nat Rev Cancer, 2011. 11(8): p. 558-572.

377. Sun, B., et al., *Human umbilical cord blood mesenchymal stem cell-derived extracellular matrix prohibits metastatic cancer cell MDA-MB-231 proliferation.* Cancer Lett, 2010. 296(2): p. 178-85.

378. Kidd, S., et al., *Origins of the tumor microenvironment: quantitative assessment of adipose-derived and bone marrow-derived stroma.* PLoS One, 2012. 7.

379. Shimoda, M., K.T. Mellody, and A. Orimo, *Carcinoma-associated fibroblasts are a rate-limiting determinant for tumour progression.* Seminars in Cell & Developmental Biology, 2010. 21(1): p. 19-25.

380. Raffaghello, L., et al., *Cancer associated fibroblasts in hematological malignancies.* Oncotarget, 2015. 6(5): p. 2589-603.

381. Quante, M., et al., *Bone marrow-derived myofibroblasts contribute to the mesenchymal stem cell niche and promote tumor growth.* Cancer Cell, 2011. 2: p. 257 - 272.

382. Polanska, U.M. and A. Orimo, *Carcinoma-associated fibroblasts: non-neoplastic tumour-promoting mesenchymal cells.* J Cell Physiol, 2013. 228(8): p. 1651-7.

383. Gottschling, S., et al., *Mesenchymal stem cells in non-small cell lung cancer–different from others? Insights from comparative molecular and functional analyses.* Lung Cancer, 2013. 80.

384. Ding, G., et al., *Comparison of the characteristics of mesenchymal stem cells obtained from prostate tumors and from bone marrow cultured in conditioned medium.* Exp Ther Med, 2012. 4.

385. Xu, X., et al., *Isolation and comparison of mesenchymal stem-like cells from human gastric cancer and adjacent non-cancerous tissues.* J Cancer Res Clin Oncol, 2011. 137.

386. Mercier, I., et al., *Human breast cancer-associated fibroblasts (CAFs) show caveolin-1 downregulation and RB tumor suppressor functional inactivation: Implications for the response to hormonal therapy.* Cancer Biol Ther, 2008. 7(8): p. 1212-25.

387. Rozenchan, P.B., et al., *Reciprocal changes in gene expression profiles of cocultured breast epithelial cells and primary fibroblasts.* Int J Cancer, 2009. 125(12): p. 2767-77.

388. Hawsawi, N.M., et al., *Breast carcinoma-associated fibroblasts and their counterparts display neoplastic-specific changes.* Cancer Res, 2008. 68(8): p. 2717-25.

389. Kalluri, R., *The biology and function of fibroblasts in cancer.* Nat Rev Cancer, 2016. 16(9): p. 582-98.

390. Sugimoto, H., et al., *Identification of fibroblast heterogeneity in the tumor microenvironment.* Cancer Biol Ther, 2006. 5(12): p. 1640-6.

391. Orimo, A., et al., *Stromal fibroblasts present in invasive human breast carcinomas promote tumor growth and angiogenesis through elevated SDF-1/CXCL12 secretion.* Cell, 2005. 3: p. 335 - 348.

392. Rosenthal, E., et al., *Elevated expression of TGF-beta1 in head and neck cancer-associated fibroblasts.* Mol Carcinog, 2004. 40(2): p. 116-21.

393. Cho, J.A., et al., *Exosomes from breast cancer cells can convert adipose tissue-derived mesenchymal stem cells into myofibroblast-like cells.* Int J Oncol, 2012. 40.

394. Cho, J.A., et al., *Exosomes from ovarian cancer cells induce adipose tissue-derived mesenchymal stem cells to acquire the physical and functional characteristics of tumor-supporting myofibroblasts.* Gynecol Oncol, 2011. 123.

395. Paunescu, V., et al., *Tumour-associated fibroblasts and mesenchymal stem cells: more similarities than differences.* J Cell Mol Med, 2011. 15.

396. Jian, H., et al., *Smad3-dependent nuclear translocation of beta-catenin is required for TGF-beta1-induced proliferation of bone marrow-derived adult human mesenchymal stem cells.* Genes Dev, 2006. 20(6): p. 666-74.

397. Luo, H., et al., *Cancer-associated fibroblasts: a multifaceted driver of breast cancer progression.* Cancer Lett, 2015. 361(2): p. 155-63.

398. Hanley, C.J., et al., *A subset of myofibroblastic cancer-associated fibroblasts regulate collagen fiber elongation, which is prognostic in multiple cancers.* Oncotarget, 2016. 7(5): p. 6159-6174.

399. Tyan, S.W., et al., *Breast cancer cells induce cancer-associated fibroblasts to secrete hepatocyte growth factor to enhance breast tumorigenesis.* PLoS One, 2011. 6(1): p. e15313.

400. Lebret, S.C., et al., *Induction of epithelial to mesenchymal transition in PMC42-LA human breast carcinoma cells by carcinoma-associated fibroblast secreted factors.* Breast Cancer Res, 2007. 9(1): p. R19.

401. Subramaniam, K.S., et al., *Cancer-associated fibroblasts promote proliferation of endometrial cancer cells.* PLoS One, 2013. 8(7): p. e68923.

402. Noma, K., et al., *The essential role of fibroblasts in esophageal squamous cell carcinoma-induced angiogenesis.* Gastroenterology, 2008. 134(7): p. 1981-93.

403. Kellermann, M.G., et al., *Mutual paracrine effects of oral squamous cell carcinoma cells and normal oral fibroblasts: induction of fibroblast to myofibroblast transdifferentiation and modulation of tumor cell proliferation.* Oral Oncol, 2008. 44(5): p. 509-17.

404. Bhuvanalakshmi, G., et al., *Secreted frizzled-related protein 4 inhibits glioma stem-like cells by reversing epithelial to mesenchymal transition, inducing apoptosis and decreasing cancer stem cell properties.* PLoS One, 2015. 10(6): p. e0127517.

405. Martinez-Outschoorn, U.E., F. Sotgia, and M.P. Lisanti, *Power surge: supporting cells "fuel" cancer cell mitochondria.* Cell Metab, 2012. 15(1): p. 4-5.

406. Kato, M., et al., *Cbfa1-independent decrease in osteoblast proliferation, osteopenia, and persistent embryonic eye vascularization in mice deficient in Lrp5, a Wnt coreceptor.* J Cell Biol, 2002. 157(2): p. 303-14.

407. Yu, G., et al., *Adipogenic Differentiation of Adipose-Derived Stem Cells*, in *Adipose-Derived Stem Cells*, J.M. Gimble and B.A. Bunnell, Editors. 2011, Humana Press. p. 193-200.

408. Chi, Y., et al., *[Adipogenic Potentials of Mesenchymal Stem Cells from Human Bone Marrow, Umbilical Cord and Adipose Tissue are Different]*. Zhongguo Shi Yan Xue Ye Xue Za Zhi, 2014. 22(3): p. 588-94.

409. Ragni, E., et al., *Adipogenic potential in human mesenchymal stem cells strictly depends on adult or foetal tissue harvest.* The International Journal of Biochemistry & Cell Biology, 2013. 45(11): p. 2456-2466.

410. Kern, S., et al., *Comparative analysis of mesenchymal stem cells from bone marrow, umbilical cord blood, or adipose tissue.* STEM CELLS, 2006. 24(5): p. 1294-301.

411. Kirton, J.P., et al., *Wnt/beta-catenin signaling stimulates chondrogenic and inhibits adipogenic differentiation of pericytes: potential relevance to vascular disease?* Circ Res, 2007. 101(6): p. 581-9.

412. Lee, S., et al., *Anti-obesity effects of 3-hydroxychromone derivative, a novel small-molecule inhibitor of glycogen synthase kinase-3.* Biochem Pharmacol, 2013. 85(7): p. 965-76.

413. Okamura, M., et al., *COUP-TFII acts downstream of Wnt/beta-catenin signal to silence PPARgamma gene expression and repress adipogenesis.* Proc Natl Acad Sci U S A, 2009. 106(14): p. 5819-24.

414. Li, Z., et al., *Cyclin D1 functions in cell migration.* Cell Cycle, 2006. 5(21): p. 2440-2.

415. Lee, J.-H., et al., *Effect of adipose-derived stem cell-conditioned medium on the proliferation and migration of B16 melanoma cells.* Oncology Letters, 2015. 10(2): p. 730-736.

Every reasonable effort has been made to acknowledge the owners of copyright material. I would be pleased to hear from any copyright owner who has been omitted or incorrectly acknowledged.

# Chapter 9 - APPENDICES

# APPENDIX – I

## SUPPLEMENTARY RESULTS

### Characterisation of ADSC-CM

ADSC-CM harvested at various time-points of conditioning – 3hr, 12hr, 24hr, and 48 hour were run using SDS-PAGE for determining the molecular weights of proteins present within the ADSC-CM. ADSC-CM expressed proteins corresponding to the 50KDa size range, irrespective of the time-point (3hr, 12hr, 24hr, and 48hr) at which the ADSC-CM was harvested (Figure S1A).

In order to confirm the molecular weight filtration using the 30KDa moelcular weight cut-off filter (MWCO), the whole ADSC-CM (harvested at 48 hour of conditioning), its <30KDa filtrate, and its >30KDa retentate were run using SDS-PAGE. The <30KDa filtrate showed absence of bands in the size range of 50KDa, confirming successful MWCO filtration (Figure S1B). Also, the >30KDa retentate showed presence of strong bands at the 50KDa range and above as well (Figure S2B). The 30KDa MWCO filter also helped to categorise the ADSC-CM in terms of the presence of the secreted protein sFRP4. sFRP4 is a 50KDa protein and is expressed by ADSCs. The 30KDa fractionation yielded fractions with and without the sFRP4 (50KDa) proteins. As a positive control, recombinant sFRP4 protein was

also loaded onto the SDS-PAGE gel (Figure S1). The anti-tumour activity was determined to originate from a molecular weight fraction lower than 30KDa, thereby indicating that it is contributed from a non-sFRP4 conatining molecular fraction of the ADSC-CM.

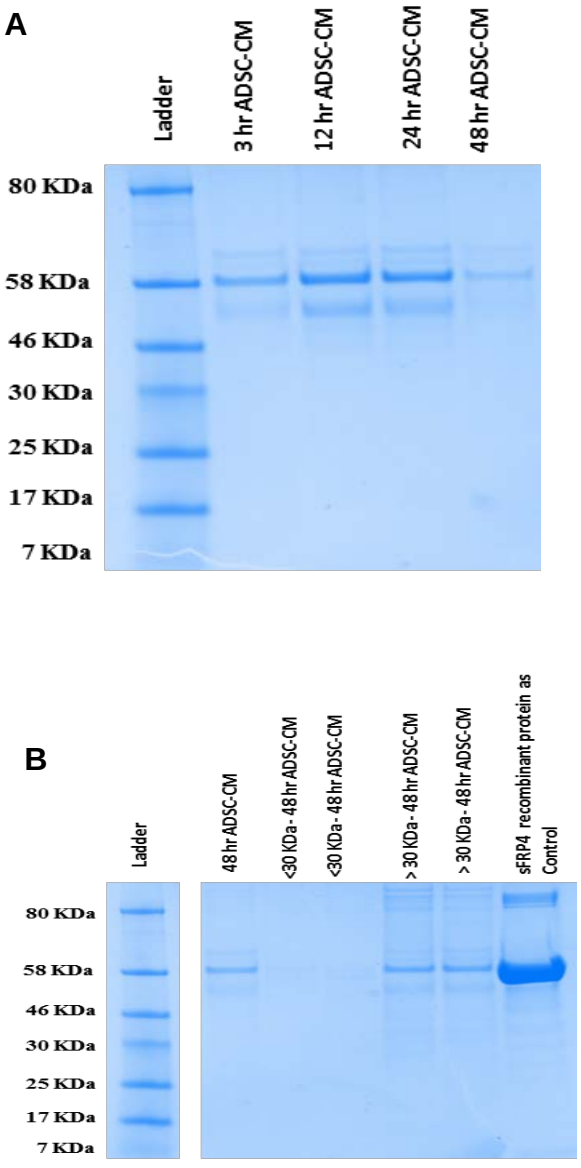


**Figure S1 Molecular size determination of ADSC-CM proteins**

(A) ADSC-CM harvested at various time-points of conditioning run on SDS-PAGE gel. (B) Whole ADSC-CM (harvested at 48 hour time-point of conditioning), <30 KDa filtrate, and >30KDa retentate of the ADSC-CM obtained through 30KDa MWCO run on SDS-PAGE gel.

**Effect of ADSC-CM and sFRP4 on viability of tumour cell lines**

**Sensitisation using sFRP4**

Apart from the co-treatment strategy, a pre-treatment strategy was also performed was performed to examine the sensitisation property of sFRP4. Briefly, an overnight pre-treatment was performed on the tumour cells using 250pg/mL sFRP4, following which the medium was removed and fresh non-conditioned medium/ADSC-CM was added. The cells were then incubated to measure cell viability (section 3.2.3) across 3 time-points – 24, 48, and 72hr. ADSC-CM inhibited the cell viability of both tumour cell lines throughout the 3 time-points (Figure S2A, S2B, S2C). Secondly, it was determined whether an overnight pre-treatment with sFRP4 was sufficient to induce changes in the tumour cell viability. sFRP4 pre-treatment resulted in a significant lowering of the cell viability in both MCF7 and MDA MB 231 cell lines at all 3 time-points. This indicates that a short-term sensitisation with sFRP4 was sufficient to produce sustained changes in cell viability, even at later time-points (72hr) in the tumour cell lines (Figure S2A, S2B, S2C).

Thirdly, when compared to the ADSC-CM treatment alone, it was found that in groups pre-treated with sFRP4 followed by ADSC-CM treatment, there was a further

significant reduction in cell viability of MCF7 cells at the 72 hour time-point. However, this was not observed in MDA MB 231 cells (Figure S2A, S2B, S2C).

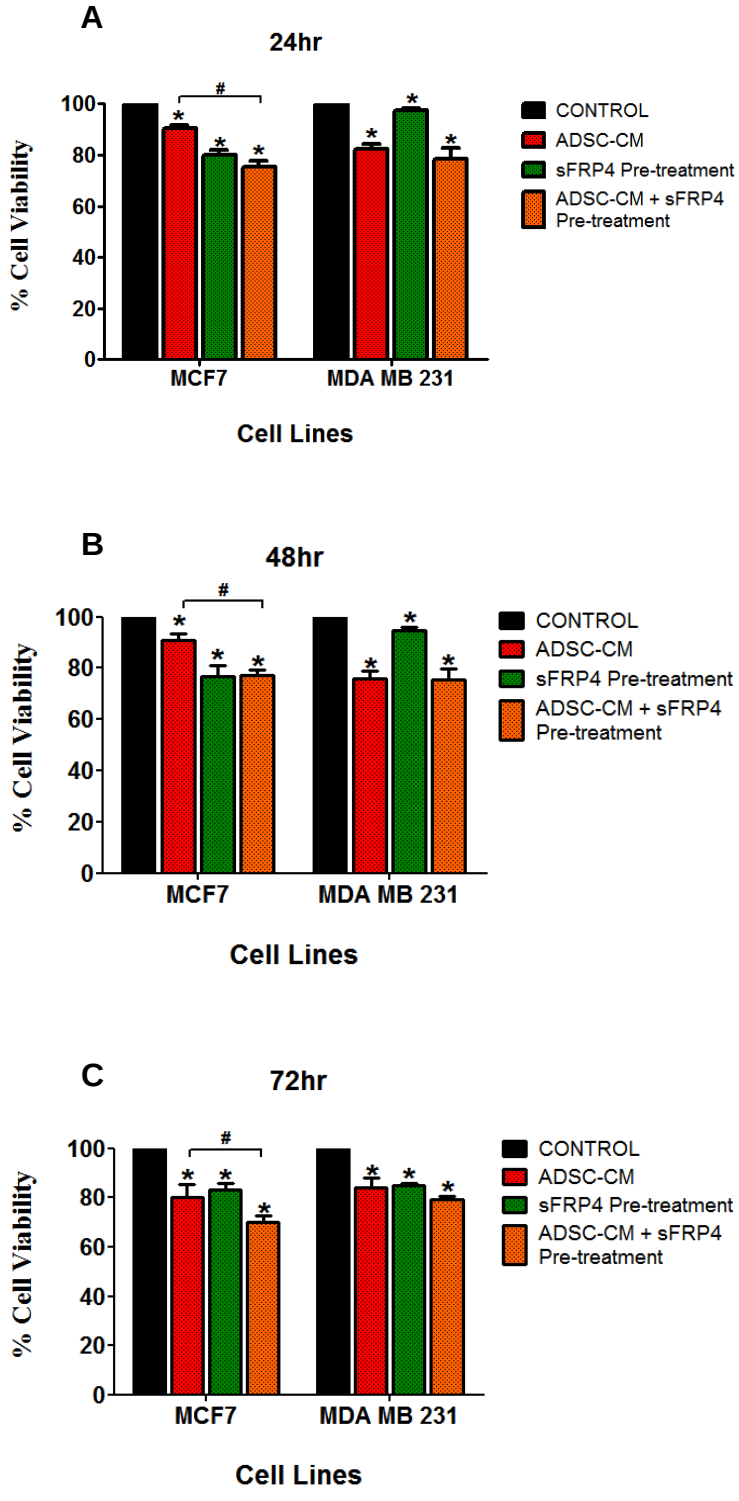

**Figure S2 Effect of ADSC-ECM and pre-treatment of sFRP4 on the cell viability of tumour cell lines**

Effect of ADSC-ECM and pre-treatment of 250pg/mL sFRP4 on the viability of tumour cell lines at (A) 24 hour time-point. (B) 48 hour time-point. (C) 72 hour time-point. *p<0.05 versus untreated control, #p<0.05 between treatment groups.

## Protein expression of total β-catenin

In addition to active β-catenin, the expression of total β-catenin was also determined following the treatment of ADSC-CM in combination with sFRP4 and sFRP4-associated peptides (SC301+SC401). There was no change in expression of total β-catenin in response to the treatments in both tumour cell lines (Figure S3, S4).

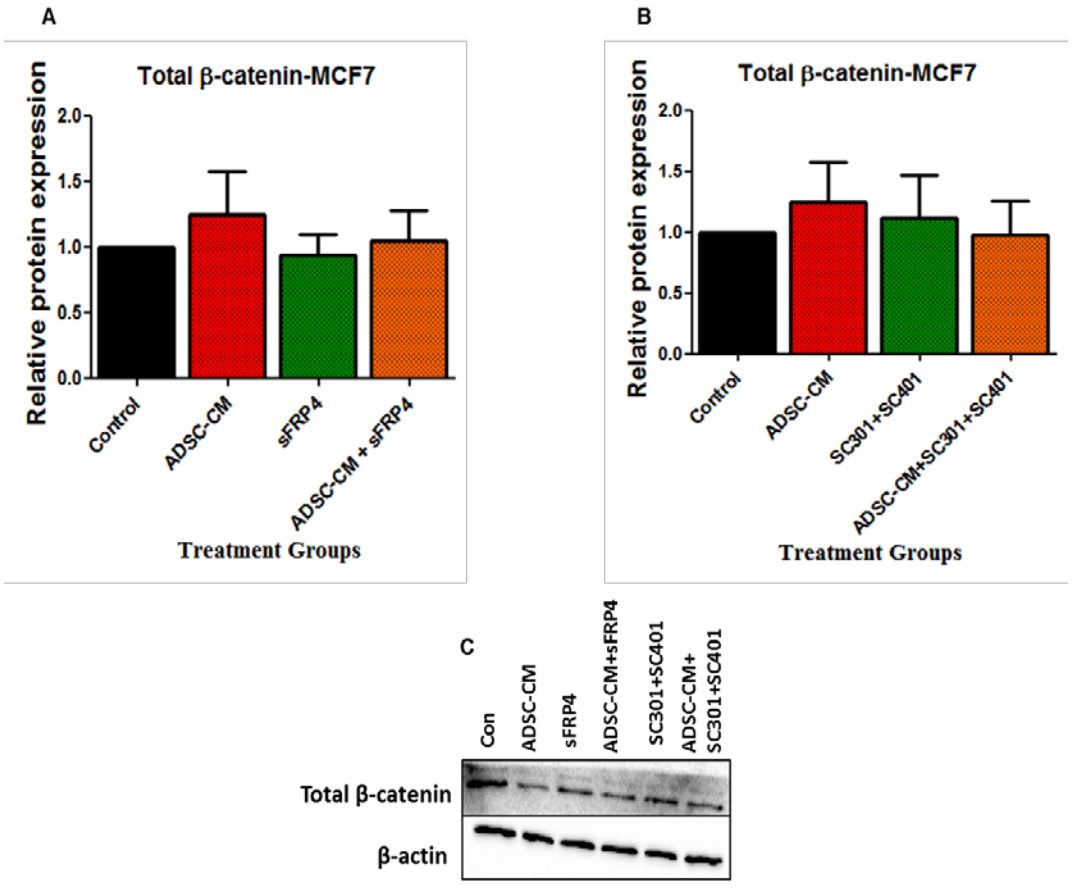

**Figure S3 Effect of ADSC-CM and sFRP4/sFRP4-associated peptides on the expression of total β-catenin protein**

Total β-catenin expression of MCF7 cell line in response to ADSC-CM in the presence of (A) sFRP4, and (B) sFRP4-associated peptides SC301+SC401. (C) Representative blot images for total β-catenin.

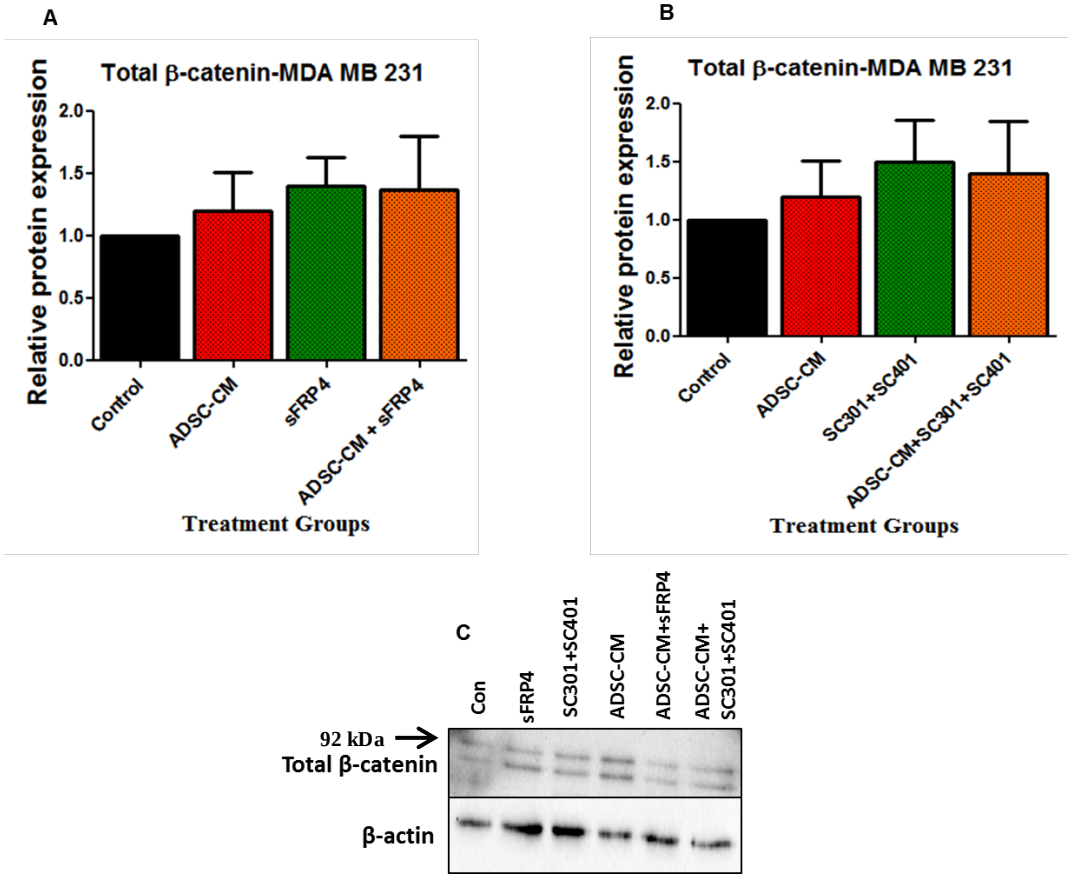


**Figure S4 Effect of ADSC-CM and sFRP4/sFRP4-associated peptides on the expression of total β-catenin protein**

Total β-catenin expression of MDA MB 231 cell line in response to ADSC-CM in the presence of (A) sFRP4, and (B) sFRP4-associated peptides SC301+SC401. (C) Representative blot images for total β-catenin.

**sFRP4 Transfection**

Transfection of ADSCs using sFRP4 plasmid was performed. This was performed to examine the effect of ADSC-CM harvested from sFRP4-overexpressing ADSCs on the two tumour cell lines. Lipofectamine-based transfection method was used. Unfortunately, transfection could not be successfully achieved in ADSCs after several trials and optimisations. Lipofectamine-2000 and lipofectamine-3000 (superior transfection efficiency than lipofectamine-2000) were used. As a positive control for the technique, transfection was performed on tumour cells as well. Transfection was successful in tumour cells, with MCF7 cells showing higher degree of transfection as compared to MDA MB 231 cells (Figure S5).

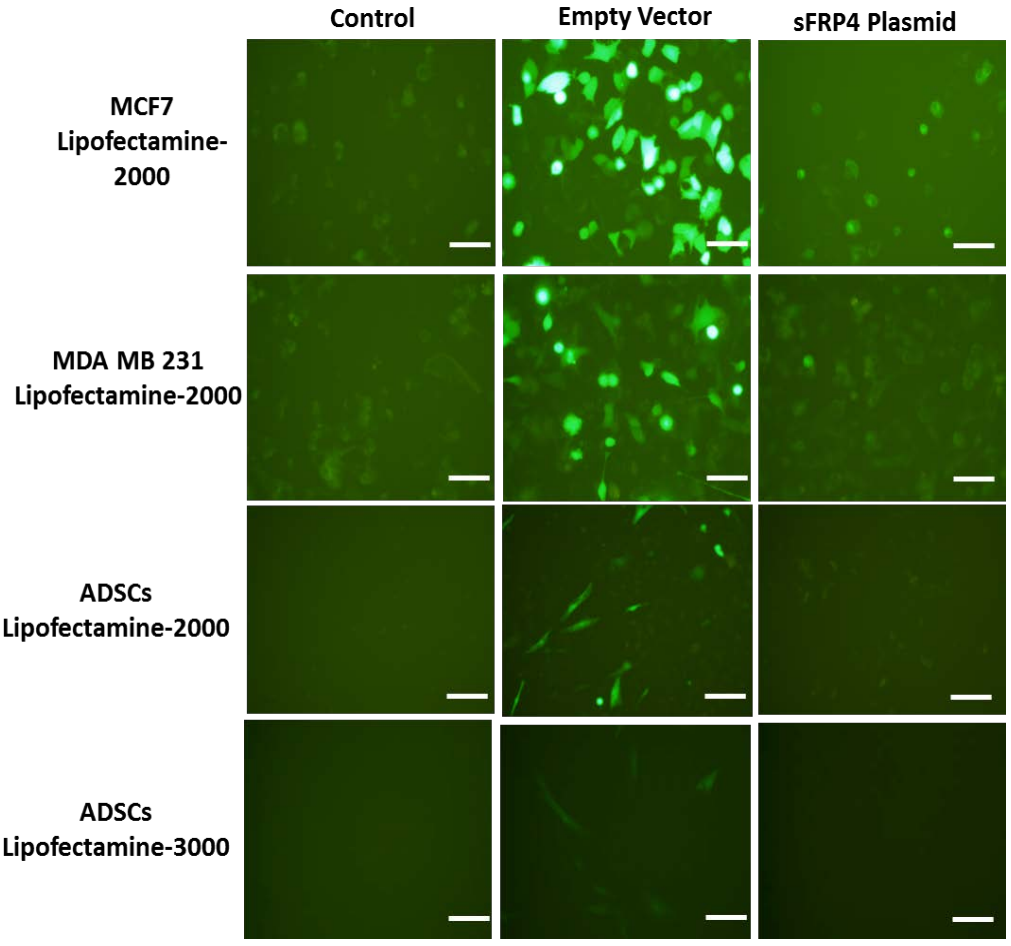

**Figure S5 Transfection of tumour cells and ADSCs using sFRP4 plasmid**

Lipofectamine-based transfection was used to transfect tumour cells and ADSCs with sFRP4 plasmid. First Row: MCF7 tumour cells were transfected with empty vector/sFRP4 plasmid using lipofectamine-2000. Second Row: MDA MB 231 tumour cells were transfected with empty vector/sFRP4 plasmid using lipofectamine-2000. Third Row: ADSCs were transfected with empty vector/sFRP4 plasmid using lipofectamine-2000. Fourth Row: ADSCs were transfected with empty vector/sFRP4 plasmid using lipofectamine-3000. Scale bar = 100µM.

**Exosome Isolation and Characterisation**

ADSCs were cultured to 80-90% confluence in T75 flasks, following which the medium was harversted, followed by addition of ExoQuick-TC exosome isolation reagent to selectively isolate the exosomes from the medium. ADSCs were grown in their normal growth medium containing 10% bovine exosome-free FBS, which was specifically used so as to prevent the isolation of bovine exosomes present in the normal FBS. The protocol was performed as below (Figure S6A). After isolation of exosomes, it was characterised using immunoblotting for HSP 70 marker protein. HSP70 was expressed in the exosomal lysate, however, the signal obtained was very faint (Figure S5B). This indicated that the exosome yield was very less, despite after harvesting from 80-90% confluent ADSCs grown in a T75 flask. As a positive control, ADSCs (cells) were used for the HSP-70 expression and it showed high expression of HSP 70 (Figure S6B). To improve exosome yield, the scaling up of the exosome isolation by growing ADSCs to 80-90% confluence in a larger tissue culture flask, such as T175 flask had to be performed. This demanded more time, as ADSCs were very slow-growing. Also, considering the requirement to procure exosomes each time by this upscaled isolation protocol was thought to be practically infeasible and hence these experiments were not further carried out.

A

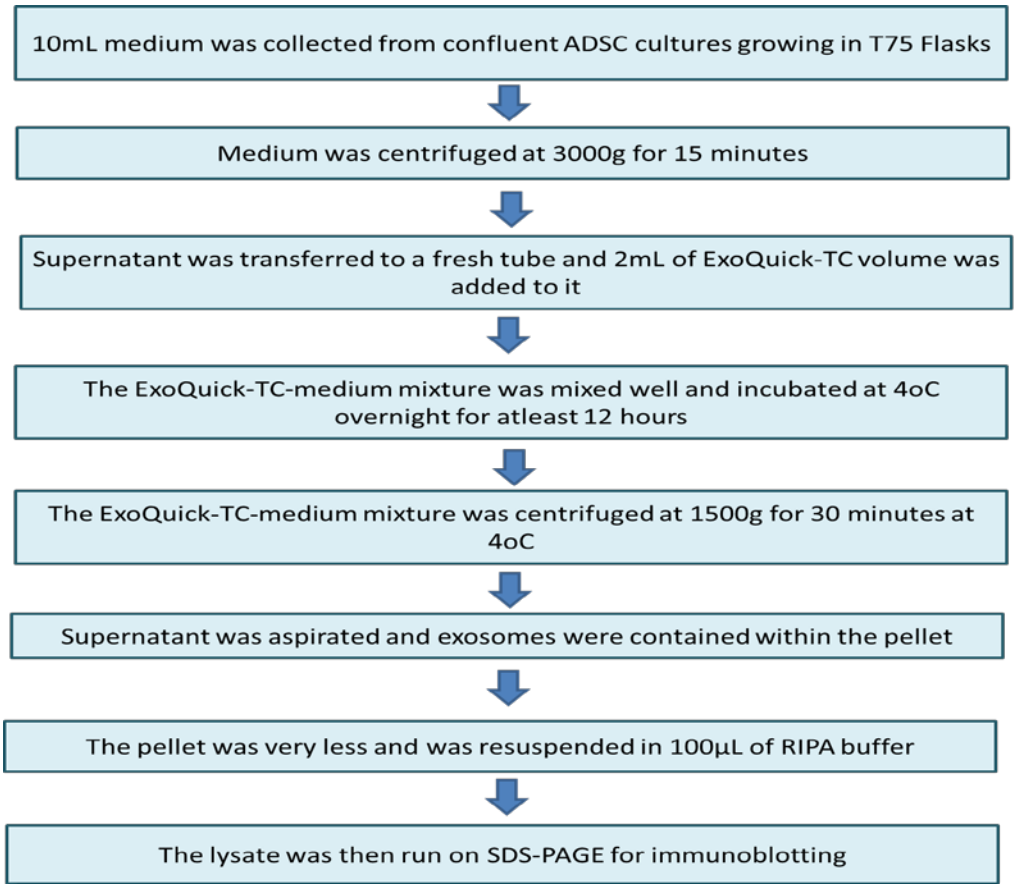


B

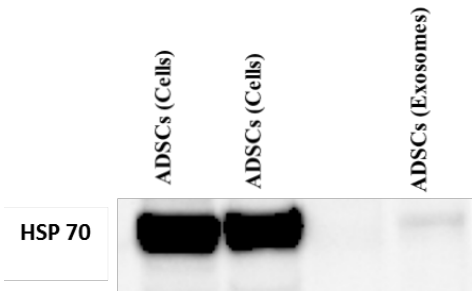


**Figure S6 Exosome isolation and characterisation**

(A) Exosome isolation protocol using ExoQuick-TC kit (B) Characterisation of exosomes by immunoblotting for HSP 70.

**Mitochondrial respiration during transformation of ADSCs into TAFs**

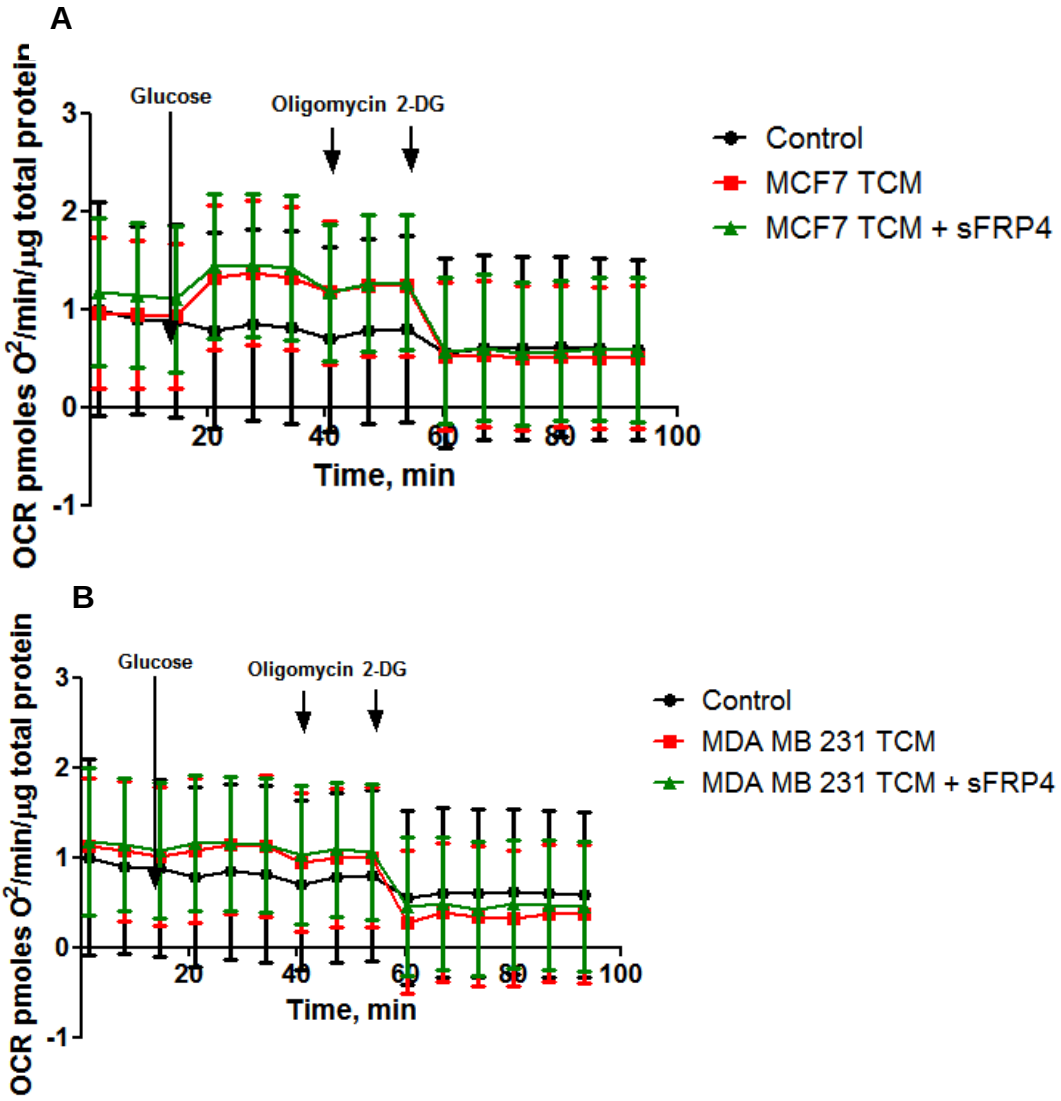


**Figure S7 OCR of ADSCs during transformation into TAFs**

Metabolic profile of ADSCs following treatment with (A) MCF7 TCM, (B) MDA MB 231 TCM in the presence of sFRP4, measuring the OCR using a glycolysis stress test.

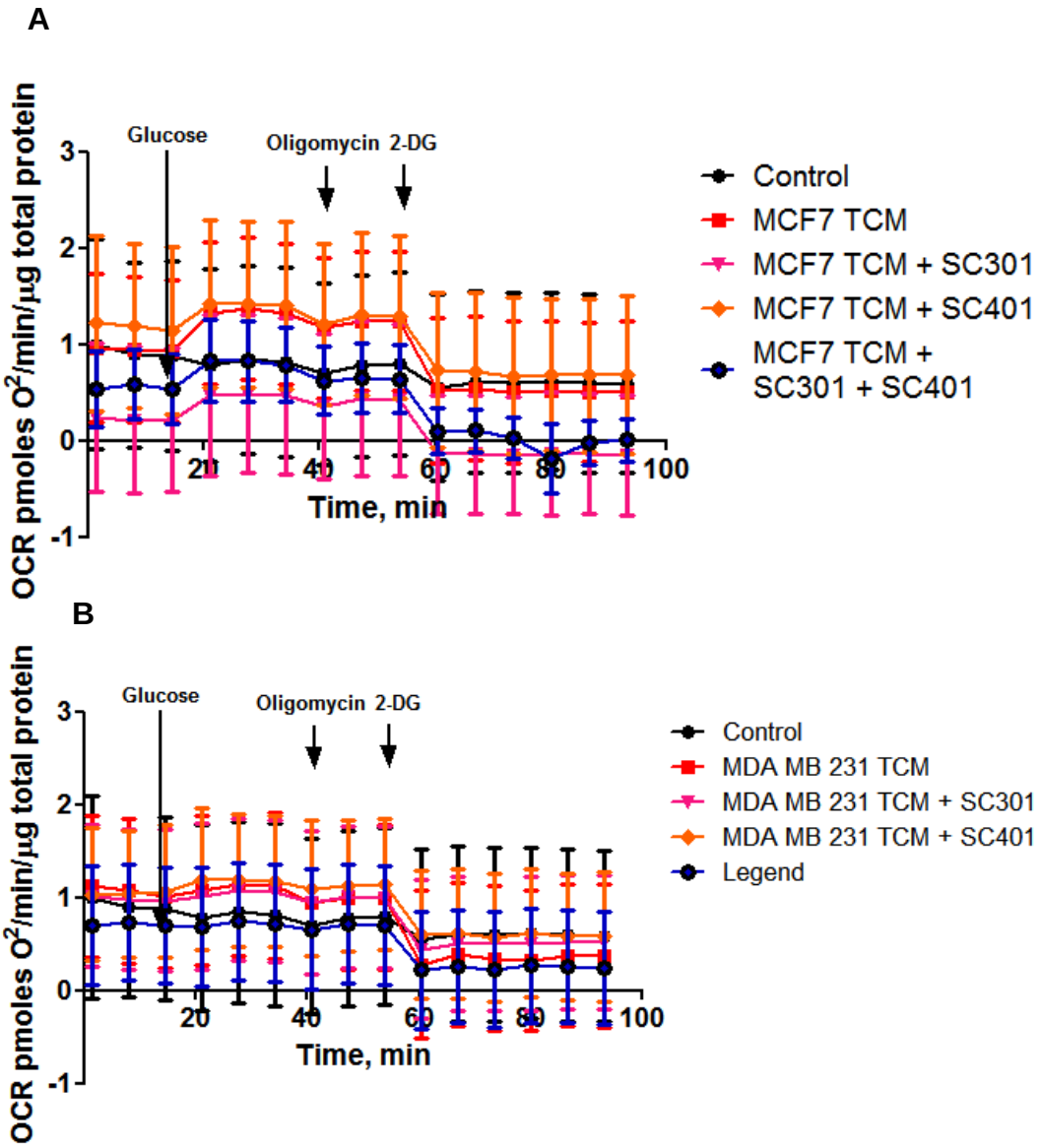


**Figure S8 OCR of ADSCs during transformation into TAFs**

Metabolic profile of ADSCs following treatment with (A) MCF7 TCM, (B) MDA MB 231 TCM in the presence of sFRP4-associated peptides, measuring the OCR using glycolysis stress test

**Seahorse-Day 4**

In addition to assessing the metabolic profile of ADSCs after 10 days of treatment, it was also performed after 4 days of treatment. However, the changes in ADSCs following treatment with TCM were not significant as compared to control ADSCs, irrespective of the presence of Wnt antagonists (Figure S9-12).

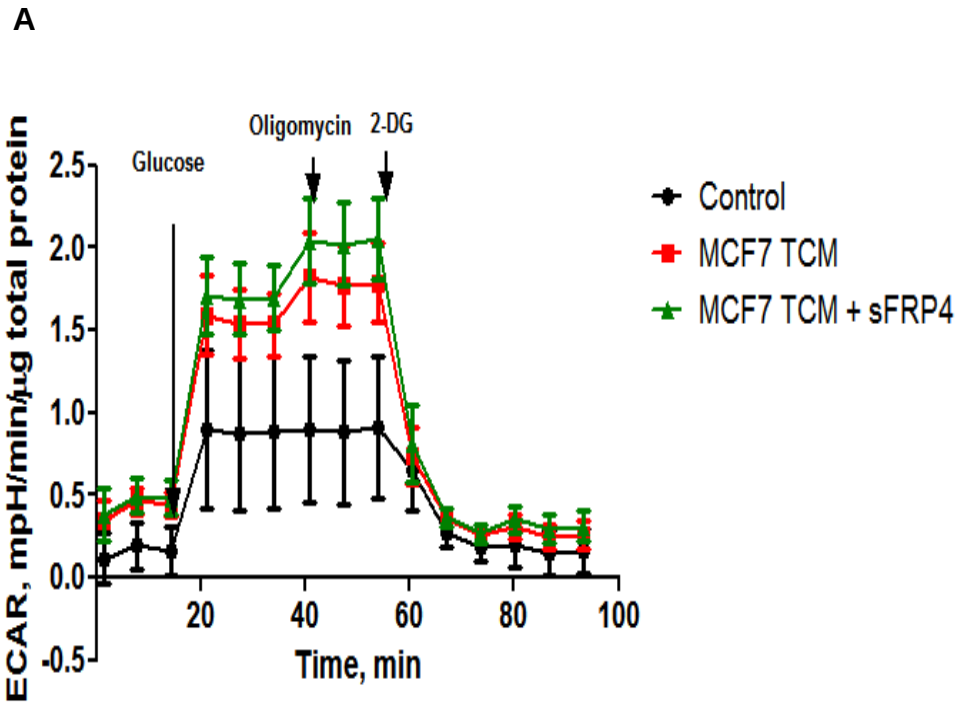

B

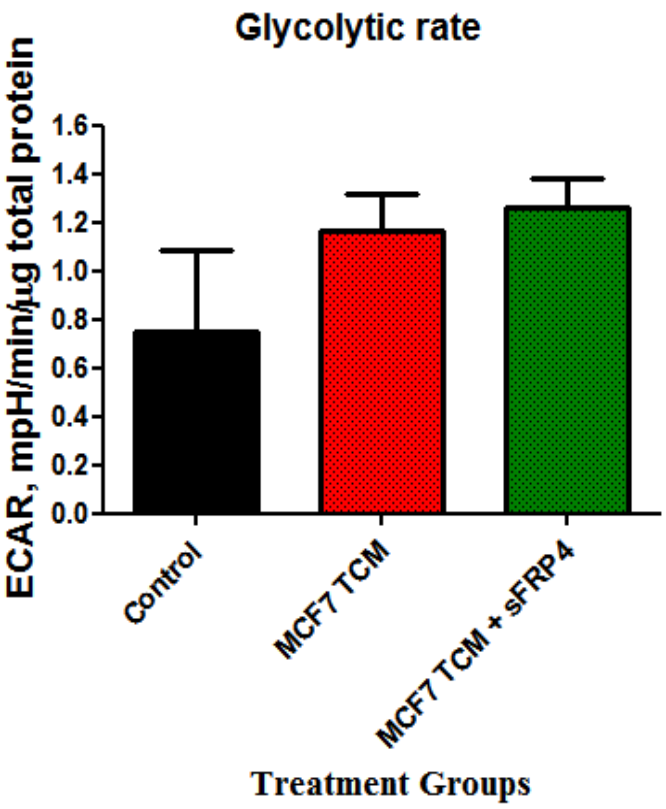
Glycolytic rate
ECAR, mpH/min/µg total protein
1.6
1.4
1.2
1.0
0.8
0.6
0.4
0.2
0.0
Control
MCF7 TCM
MCF7 TCM + sFRP4
Treatment Groups

C

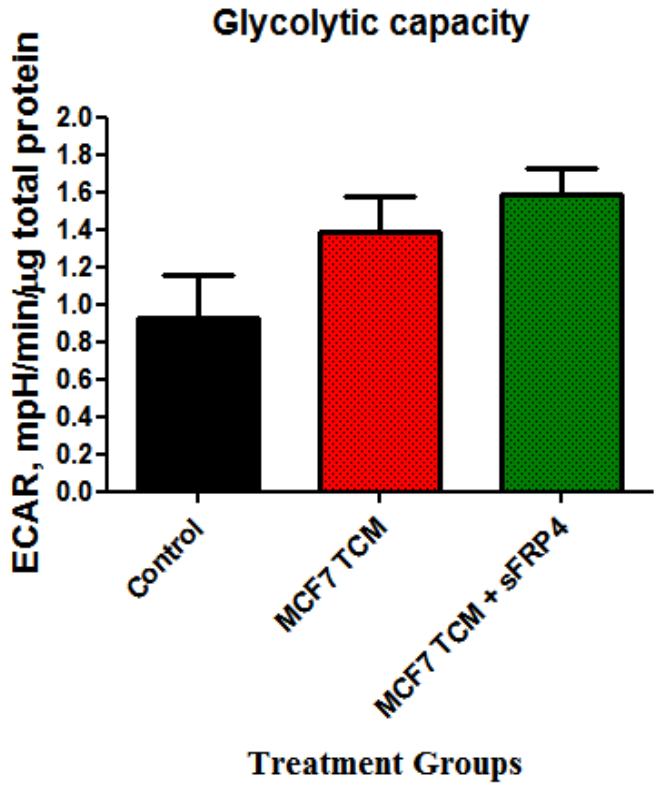
Glycolytic capacity
ECAR, mpH/min/µg total protein
2.0
1.8
1.6
1.4
1.2
1.0
0.8
0.6
0.4
0.2
0.0
Control
MCF7 TCM
MCF7 TCM + sFRP4
Treatment Groups

D

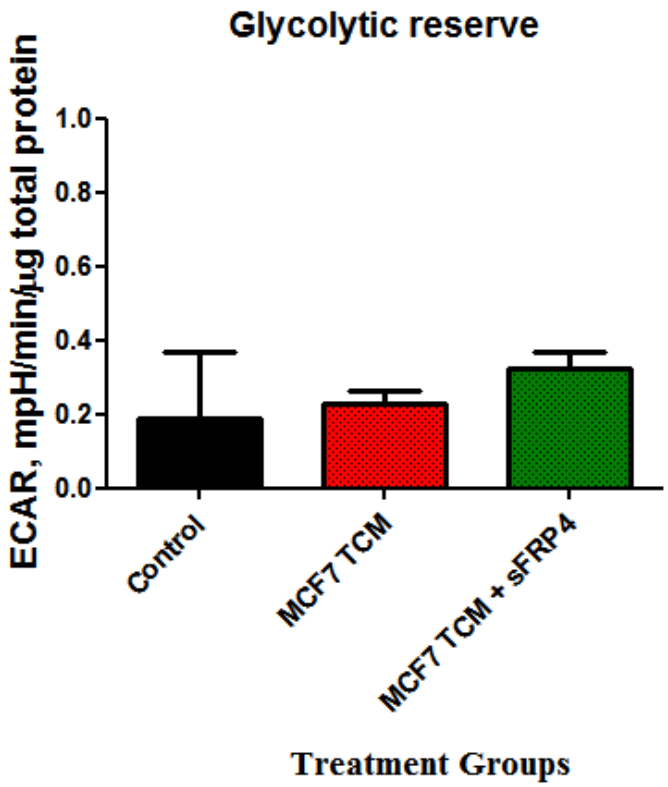
Glycolytic reserve
ECAR, mpH/min/µg total protein
1.0
0.8
0.6
0.4
0.2
0.0
Control
MCF7 TCM
MCF7 TCM + sFRP4
Treatment Groups

E

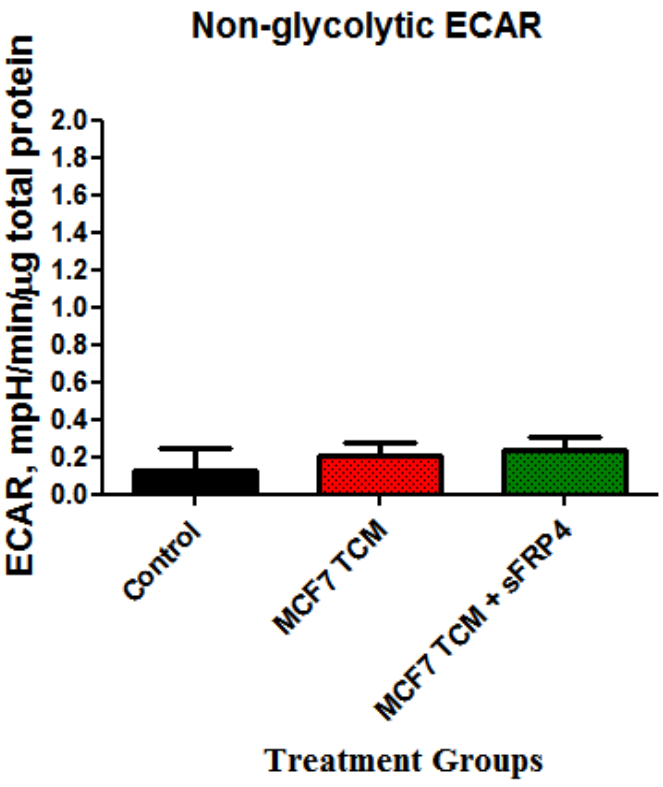
Non-glycolytic ECAR
ECAR, mpH/min/µg total protein
2.0
1.8
1.6
1.4
1.2
1.0
0.8
0.6
0.4
0.2
0.0
Control
MCF7 TCM
MCF7 TCM + sFRP4
Treatment Groups

**Figure S9 Metabolic profile of ADSCs during transformation into TAFs**

ADSCs were treated with MCF7 TCM ± sFRP4 for 4 days. (A) Metabolic profile of ADSCs during glycolysis stress test by measuring the ECAR using the Seahorse Flux Bioanalyser, (B) Glycolytic rate, (C) Glycolytic capacity, (D) Glycolytic reserve, and (E) Non-glycolytic ECAR.

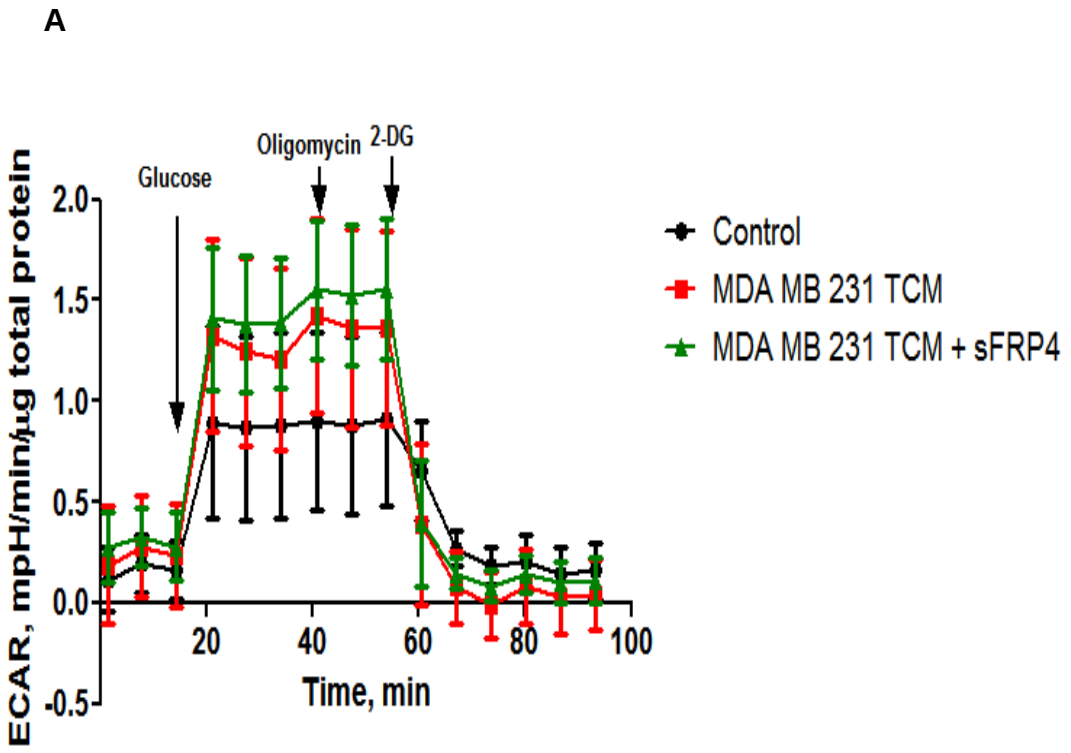

B

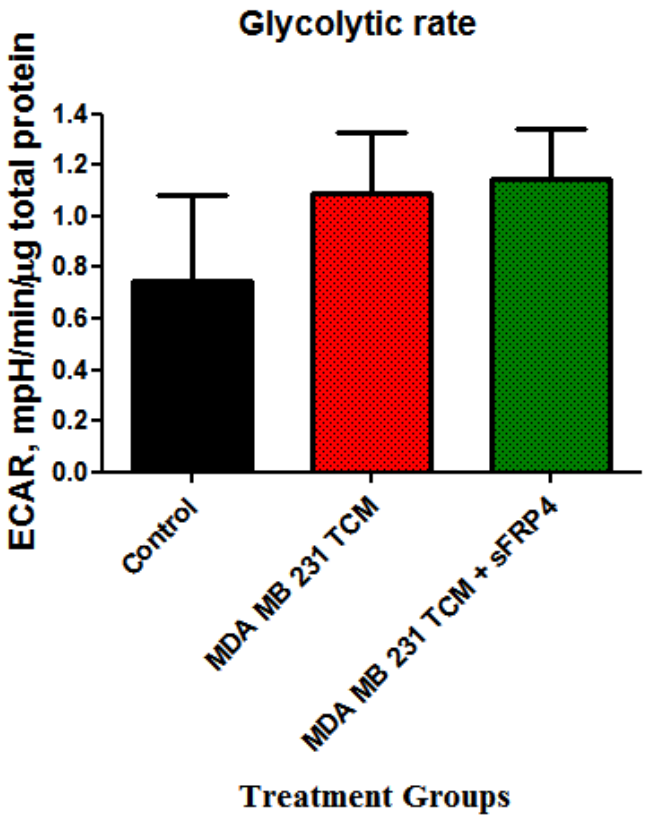
Glycolytic rate
ECAR, mpH/min/µg total protein
1.4
1.2
1.0
0.8
0.6
0.4
0.2
0.0
Control
MDA MB 231 TCM
MDA MB 231 TCM + sFRP4
Treatment Groups

C

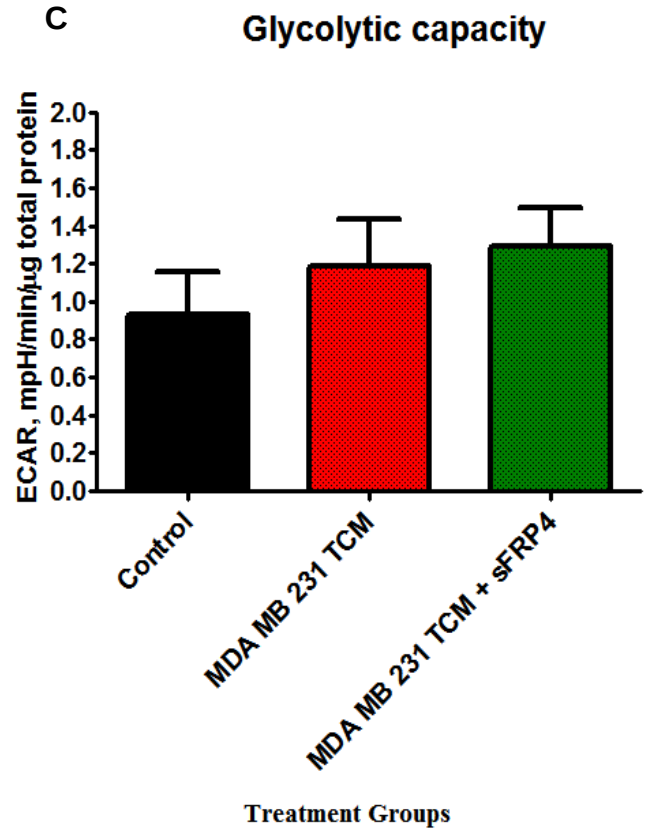
Glycolytic capacity
ECAR, mpH/min/µg total protein
2.0
1.8
1.6
1.4
1.2
1.0
0.8
0.6
0.4
0.2
0.0
Control
MDA MB 231 TCM
MDA MB 231 TCM + sFRP4
Treatment Groups

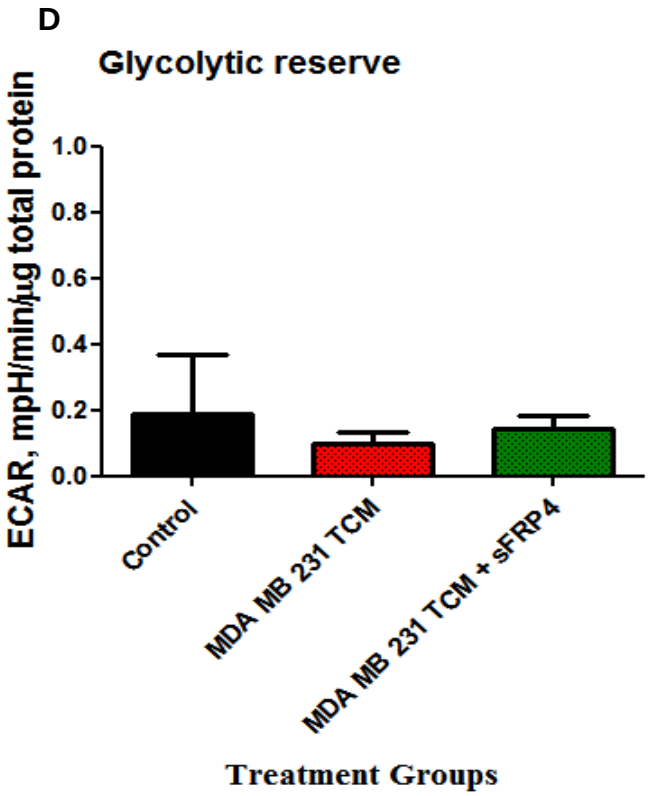
D
Glycolytic reserve
ECAR, mpH/min/µg total protein
1.0
0.8
0.6
0.4
0.2
0.0
Control
MDA MB 231 TCM
MDA MB 231 TCM + sFRP4
Treatment Groups

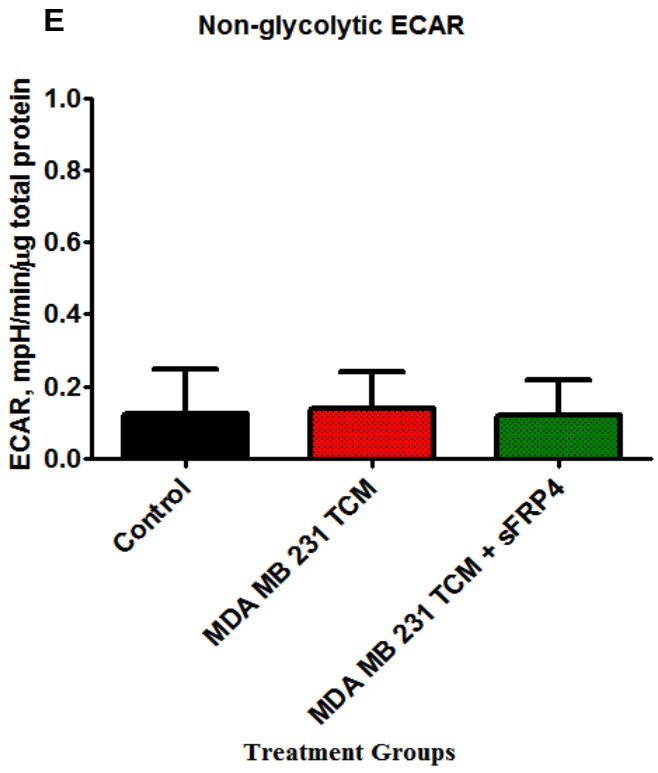
E
Non-glycolytic ECAR
ECAR, mpH/min/µg total protein
1.0
0.8
0.6
0.4
0.2
0.0
Control
MDA MB 231 TCM
MDA MB 231 TCM + sFRP4
Treatment Groups

**Figure S10 Metabolic profile of ADSCs during transformation into TAFs**

ADSCs were treated with MDA MB 231- TCM ± sFRP4 for 4 days. (A) Metabolic profile of ADSCs during glycolysis stress test by measuring the ECAR using the Seahorse Flux Bioanalyser, (B) Glycolytic rate, (C) Glycolytic capacity, (D) Glycolytic reserve, and (E) Non-glycolytic ECAR.

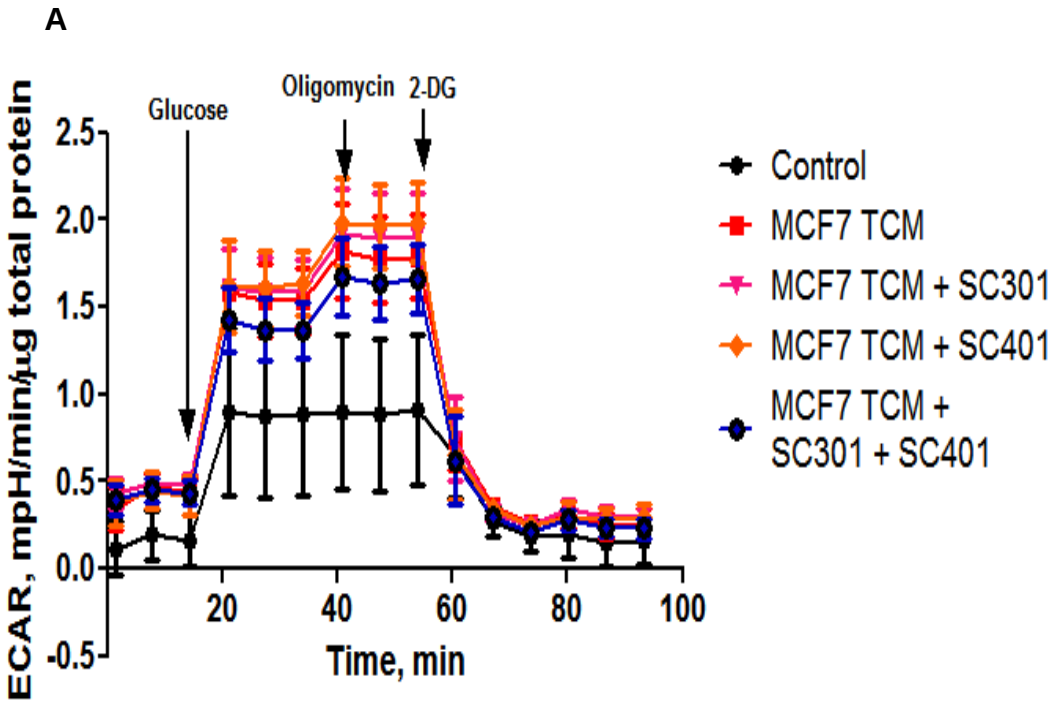

B

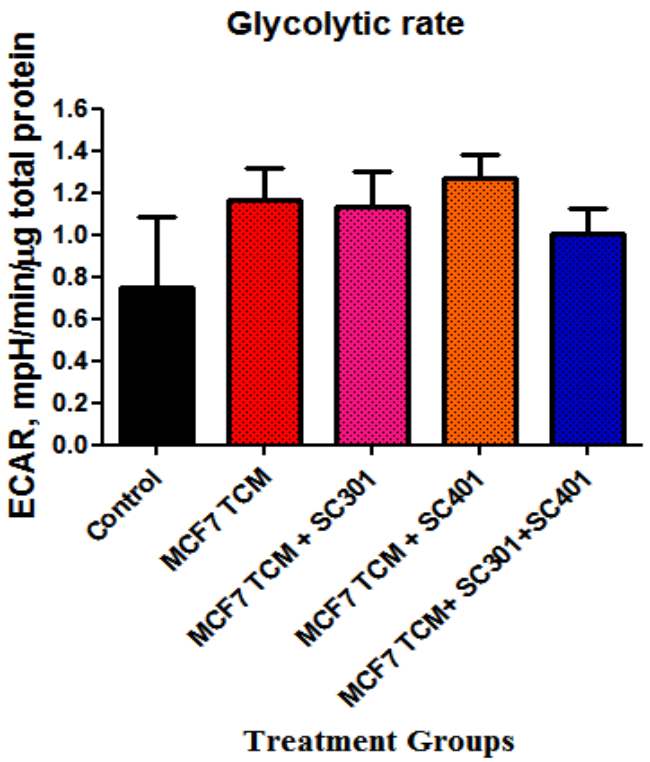
Glycolytic rate
ECAR, mpH/min/µg total protein
1.6
1.4
1.2
1.0
0.8
0.6
0.4
0.2
0.0
Control
MCF7 TCM
MCF7 TCM + SC301
MCF7 TCM + SC401
MCF7 TCM+ SC301+SC401
Treatment Groups

C

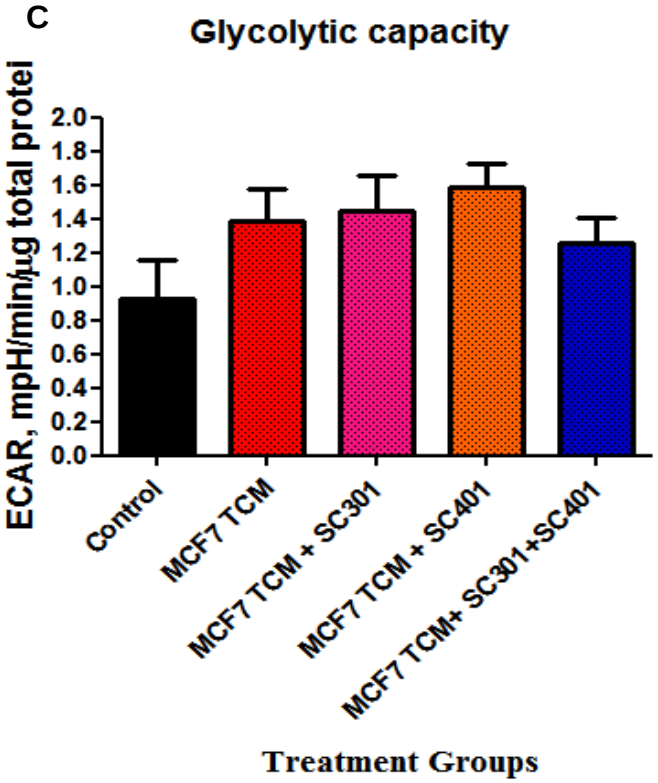
Glycolytic capacity
ECAR, mpH/min/µg total protei
2.0
1.8
1.6
1.4
1.2
1.0
0.8
0.6
0.4
0.2
0.0
Control
MCF7 TCM
MCF7 TCM + SC301
MCF7 TCM + SC401
MCF7 TCM+ SC301+SC401
Treatment Groups

D

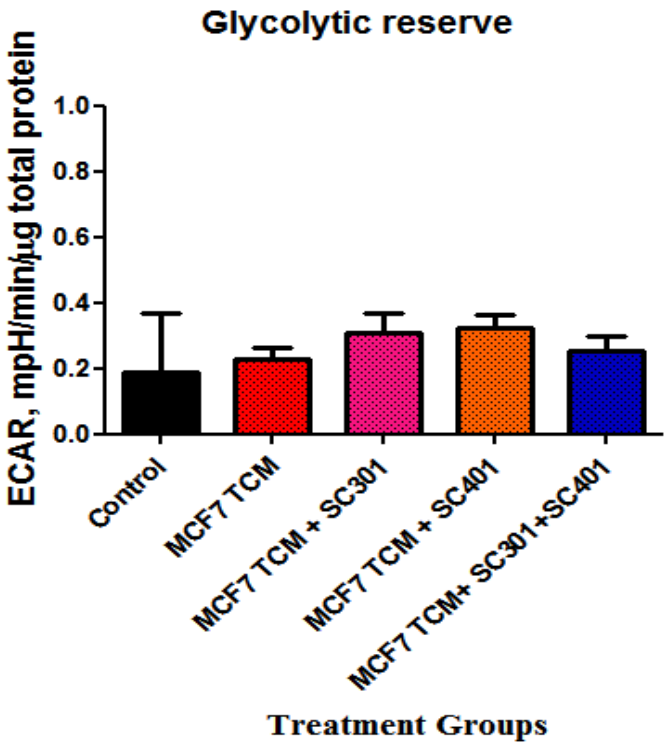
Glycolytic reserve
ECAR, mpH/min/µg total protein
1.0
0.8
0.6
0.4
0.2
0.0
Control
MCF7 TCM
MCF7 TCM + SC301
MCF7 TCM + SC401
MCF7 TCM+ SC301+SC401
Treatment Groups

E

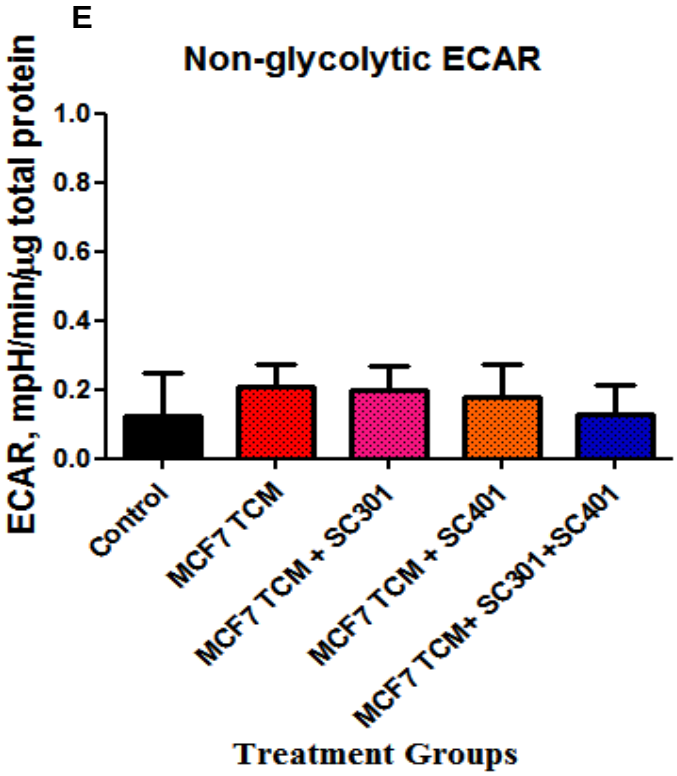
Non-glycolytic ECAR
ECAR, mpH/min/µg total protein
1.0
0.8
0.6
0.4
0.2
0.0
Control
MCF7 TCM
MCF7 TCM + SC301
MCF7 TCM + SC401
MCF7 TCM+ SC301+SC401
Treatment Groups

**Figure S11 Metabolic profile of ADSCs during transformation into TAFs**

ADSCs were treated with MCF7 TCM ± SC301 and/or SC401 for 4 days. (A) Metabolic profile of ADSCs during glycolysis stress test by measuring the ECAR using Seahorse Flux Bioanalyser (B) Glycolytic rate (C) Glycolytic capacity (D) Glycolytic reserve (E) Non-glycolytic ECAR.

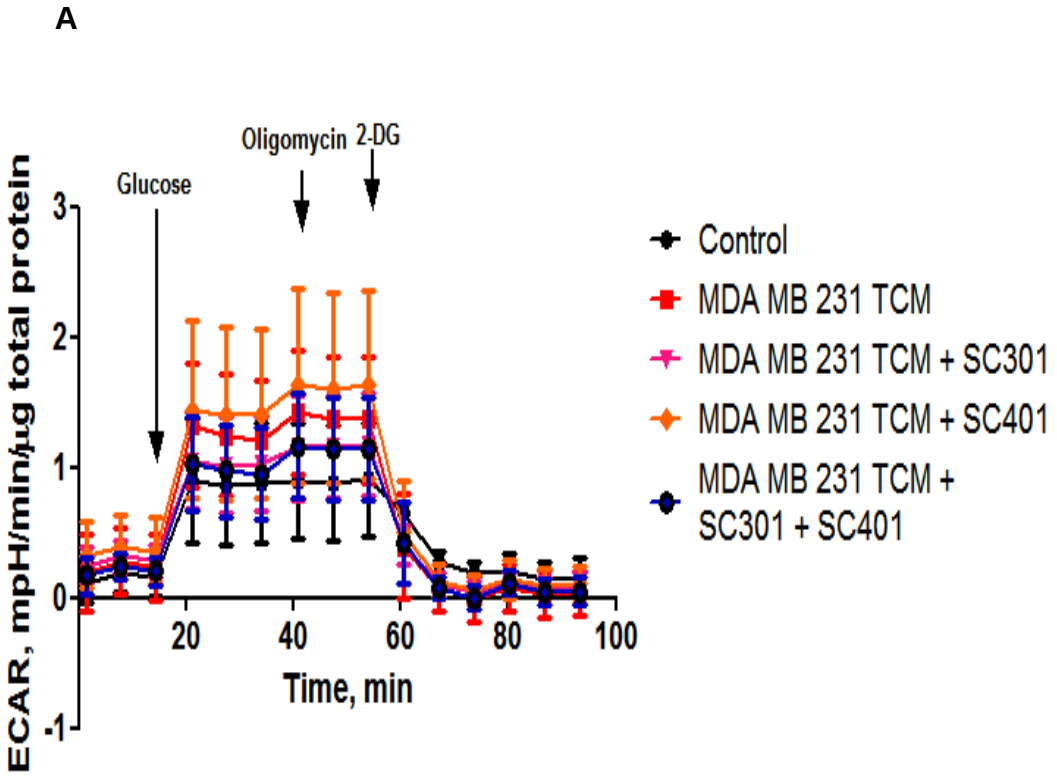

B

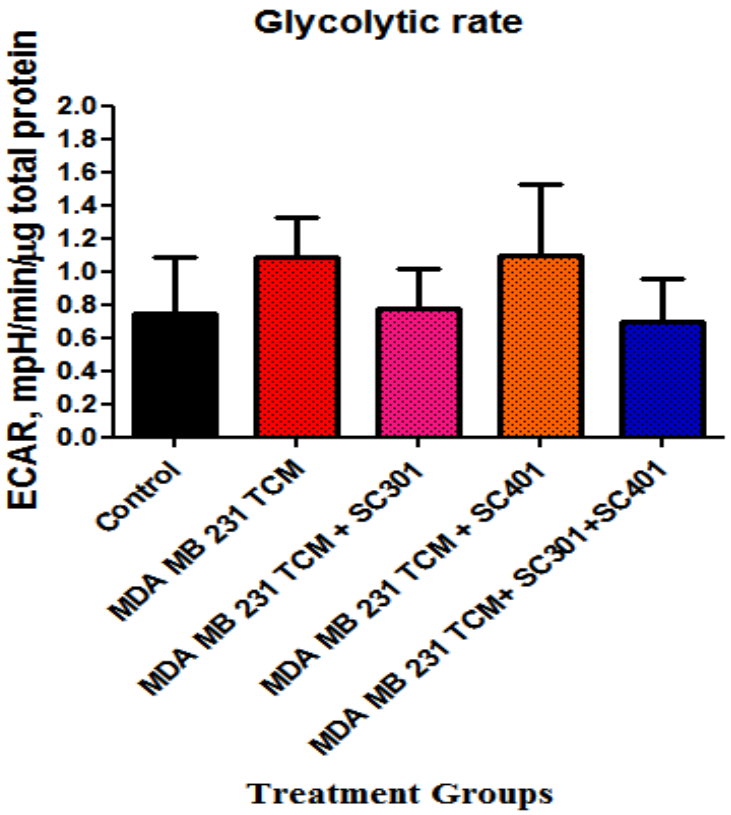
Glycolytic rate
ECAR, mpH/min/µg total protein
2.0
1.8
1.6
1.4
1.2
1.0
0.8
0.6
0.4
0.2
0.0
Control
MDA MB 231 TCM
MDA MB 231 TCM + SC301
MDA MB 231 TCM + SC401
MDA MB 231 TCM+ SC301+SC401
Treatment Groups

C

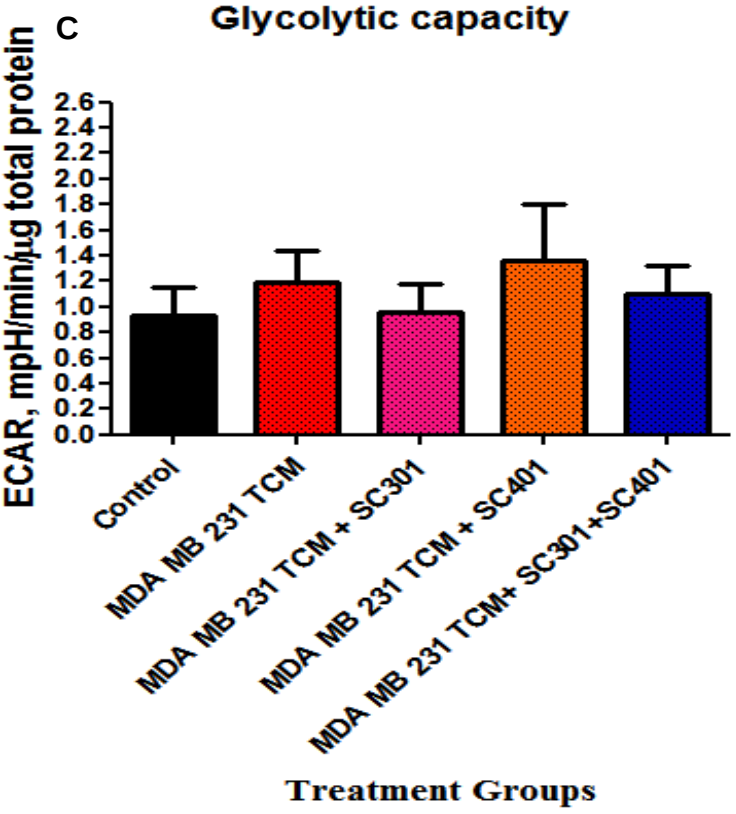
Glycolytic capacity
ECAR, mpH/min/µg total protein
2.6
2.4
2.2
2.0
1.8
1.6
1.4
1.2
1.0
0.8
0.6
0.4
0.2
0.0
Control
MDA MB 231 TCM
MDA MB 231 TCM + SC301
MDA MB 231 TCM + SC401
MDA MB 231 TCM+ SC301+SC401
Treatment Groups

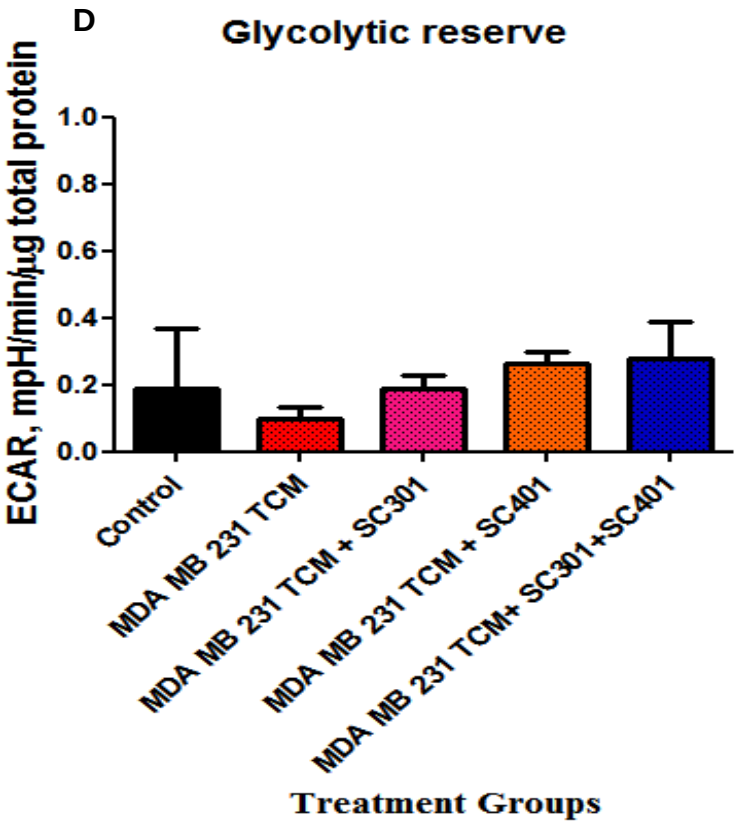
D
Glycolytic reserve
ECAR, mpH/min/µg total protein
1.0
0.8
0.6
0.4
0.2
0.0
Control
MDA MB 231 TCM
MDA MB 231 TCM + SC301
MDA MB 231 TCM + SC401
MDA MB 231 TCM+ SC301+SC401
Treatment Groups

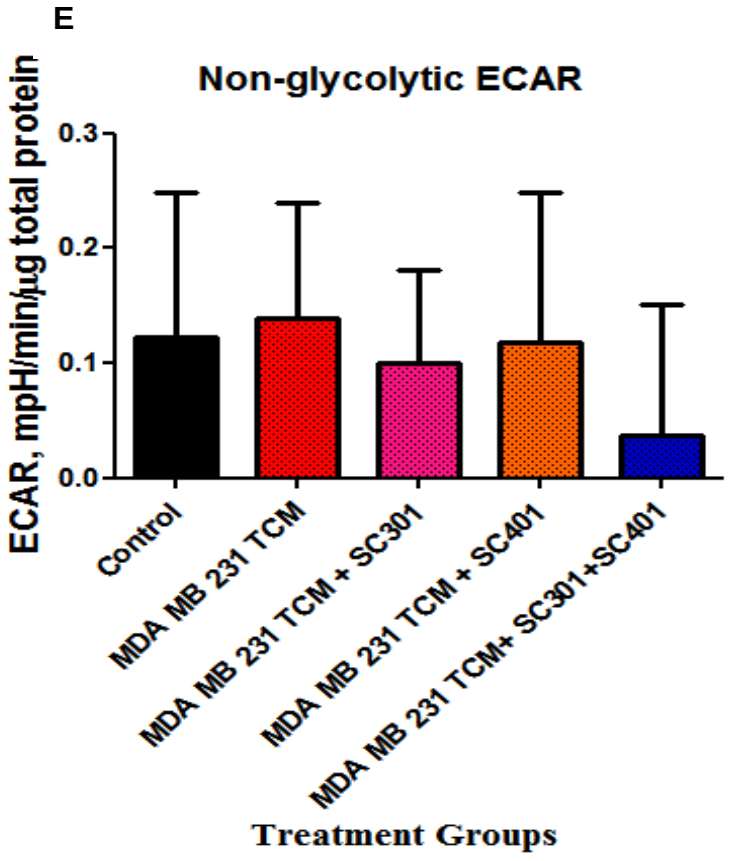
E
Non-glycolytic ECAR
ECAR, mpH/min/µg total protein
0.3
0.2
0.1
0.0
Control
MDA MB 231 TCM
MDA MB 231 TCM + SC301
MDA MB 231 TCM + SC401
MDA MB 231 TCM+ SC301+SC401
Treatment Groups

## Figure S12 Metabolic profile of ADSCs during transformation into TAFs

ADSCs were treated with MDA MB 231- TCM ± SC301 and/or SC401 for 4 days. (A) Metabolic profile of ADSCs during glycolysis stress test by measuring the ECAR using Seahorse Flux Bioanalyser (B) Glycolytic rate (B) Glycolytic capacity (C) Glycolytic reserve (D) Non-glycolytic ECAR.

**Separate channels for the Immunofluoroscence Images**

Following are the images of individual channels (FITC, DAPI, and Merged) captured while performing immunofluorescence of ADSCs after undergoing transformation into TAFs supplemented with Wnt antagonists – sFRP4/SC301/SC401/SC301 + SC401 (Figure S13-S20).

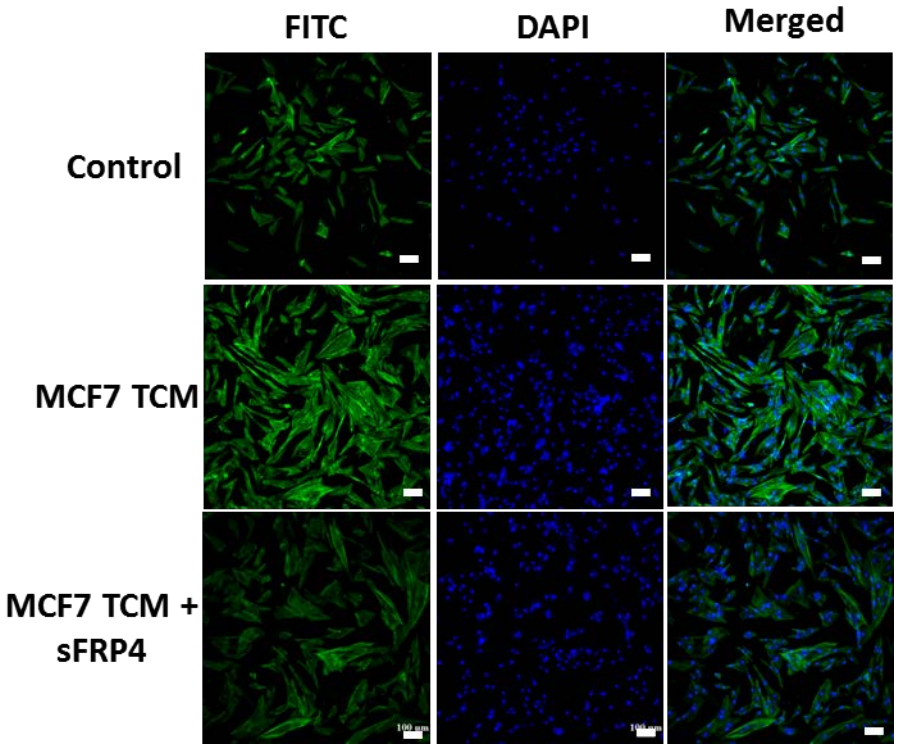


**Figure S13 Individual channels of confocal immunofluorescent imaging for α-SMA expression after treatment with MCF7 TCM**

First column: FITC Only, Second column: DAPI, Third column: Merged channel Scale bar = 100µM.

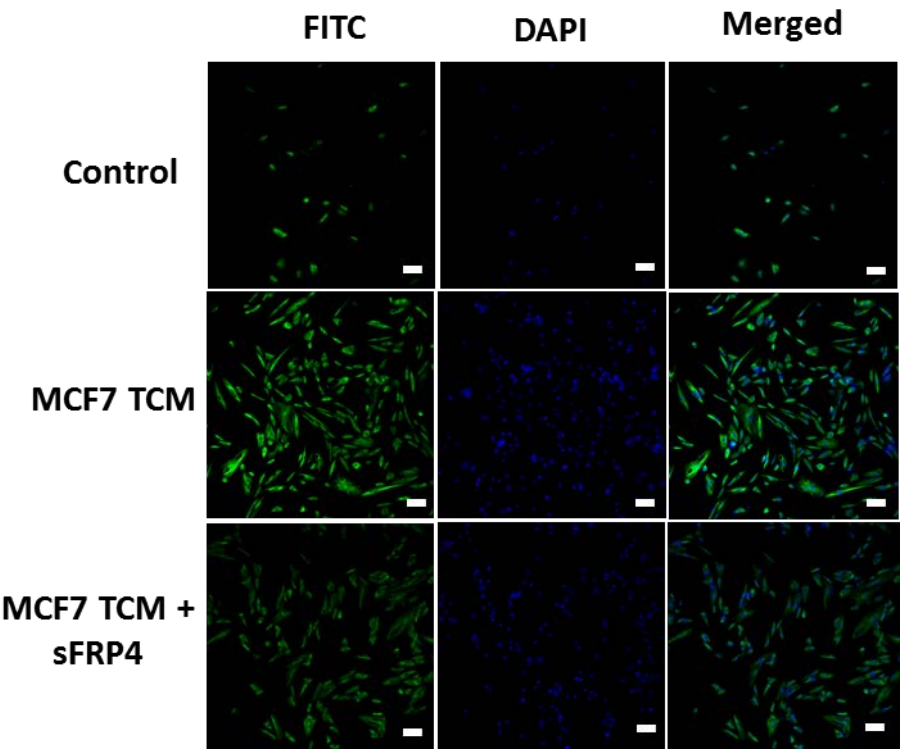


**Figure S14 Individual channels of confocal immunofluorescent imaging for vimentin expression after treatment with MCF7 TCM**

First column: FITC Only, Second column: DAPI, Third column: Merged channel Scale bar = 100µM.

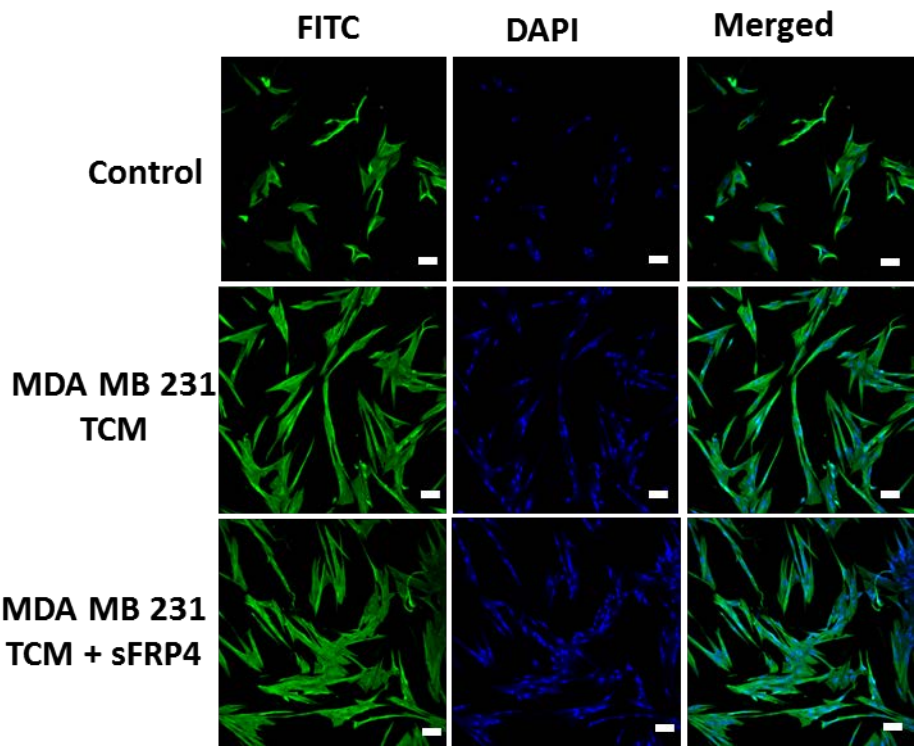


**Figure S15 Individual channels of confocal immunofluorescent imaging for α-SMA expression after treatment with MDA MB 231 TCM**

First column: FITC Only, Second column: DAPI, Third column: Merged channel Scale bar = 100μM.

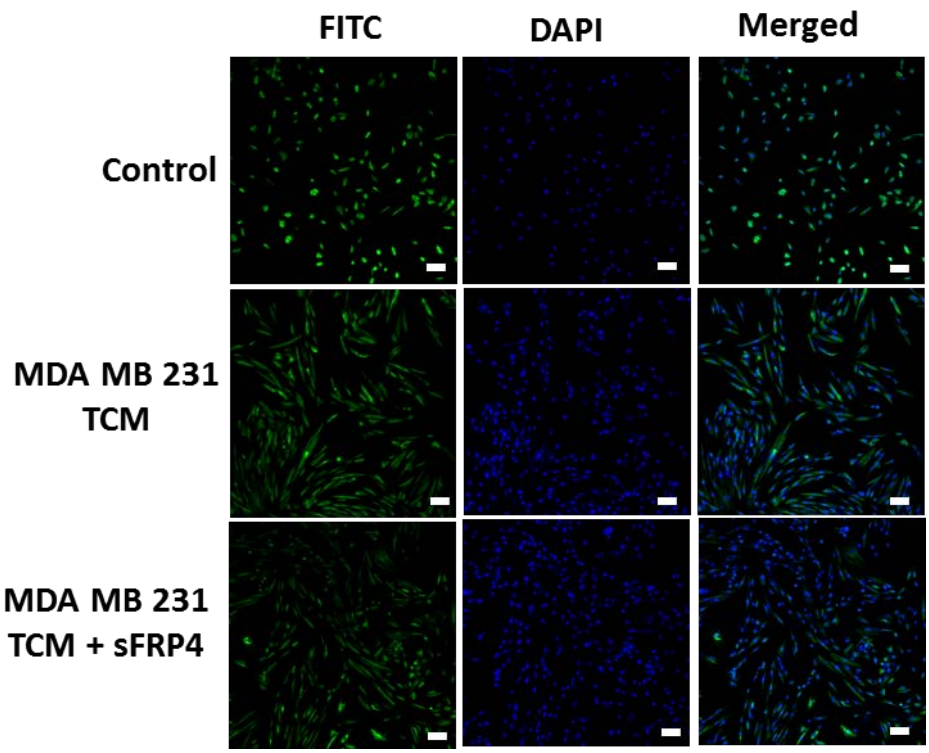


**Figure S16 Individual channels of confocal immunofluorescent imaging for vimentin expression after treatment with MDA MB 231 TCM**

First column: FITC Only, Second column: DAPI, Third column: Merged channel Scale bar = 100µM.

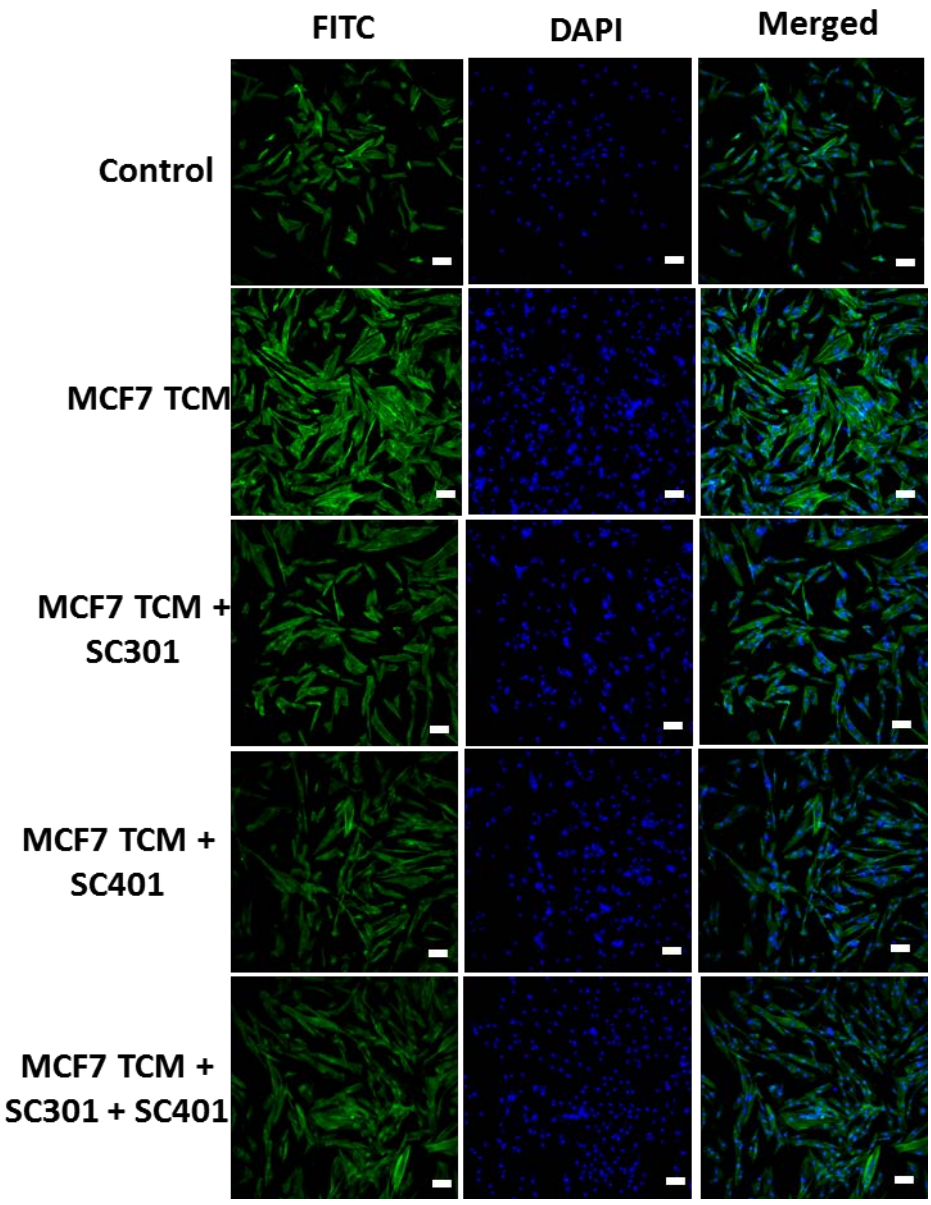


**Figure S17 Individual channels of confocal immunofluorescent imaging for α-SMA expression after treatment with MCF7 TCM**

First column: FITC Only, Second column: DAPI, Third column: Merged channel Scale bar = 100μM.

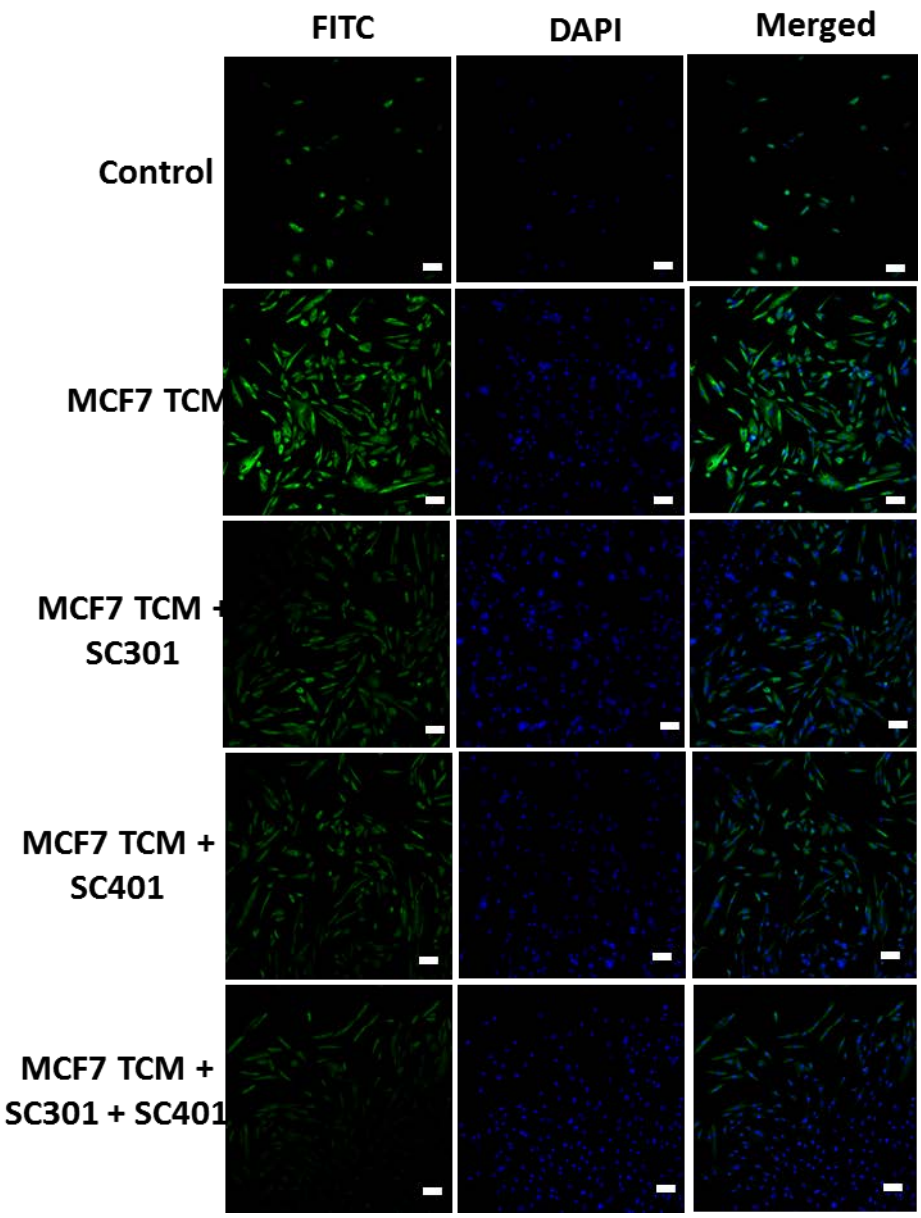


**Figure S18 Individual channels of confocal immunofluorescent imaging for vimentin expression after treatment with MCF7 TCM**

First column: FITC Only, Second column: DAPI, Third column: Merged channel Scale bar = 100μM.

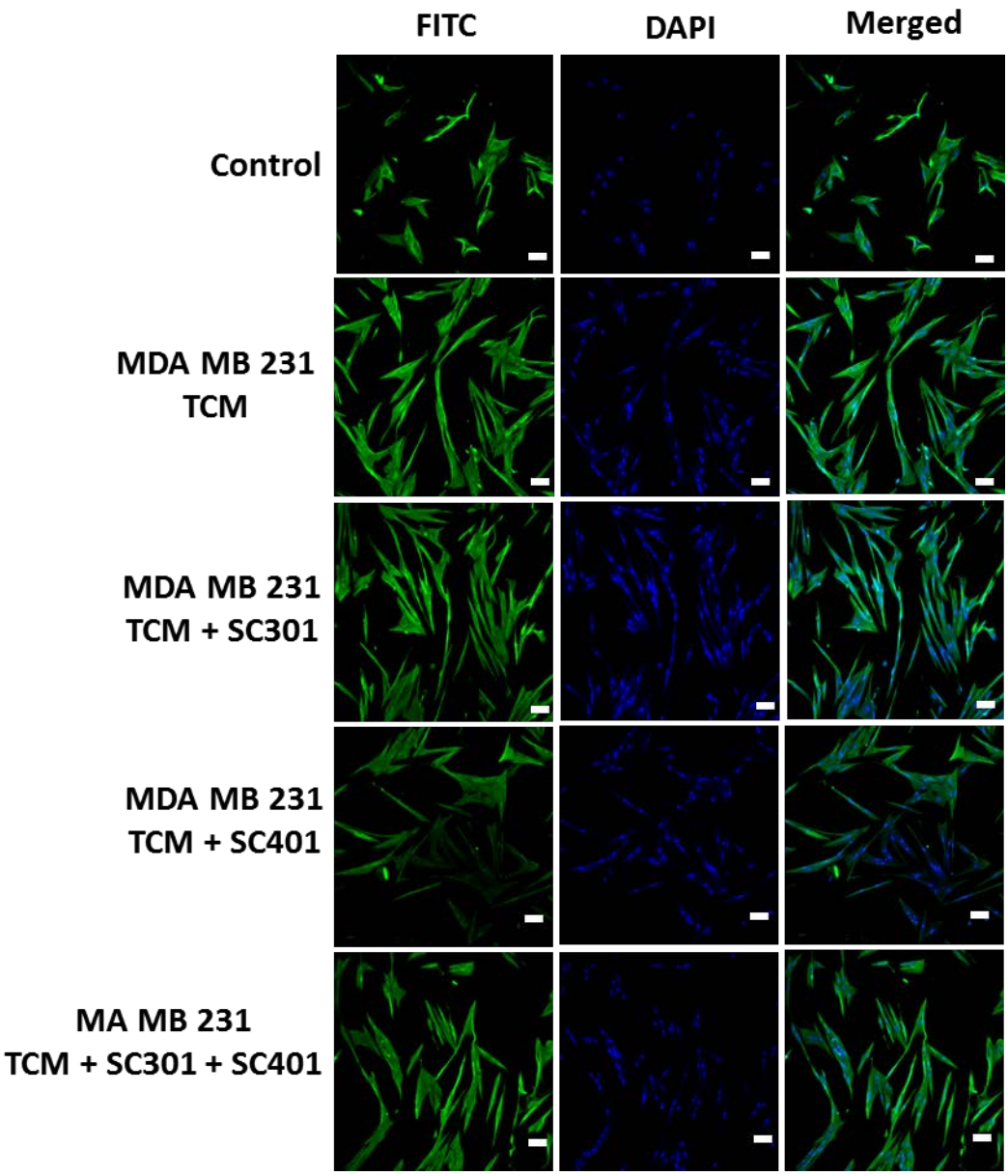


**Figure S19 Individual channels of confocal immunofluorescent imaging for α-SMA expression after treatment with MDA MB 231 TCM**

First column: FITC Only, Second column: DAPI, Third column: Merged channel Scale bar = 100μM.

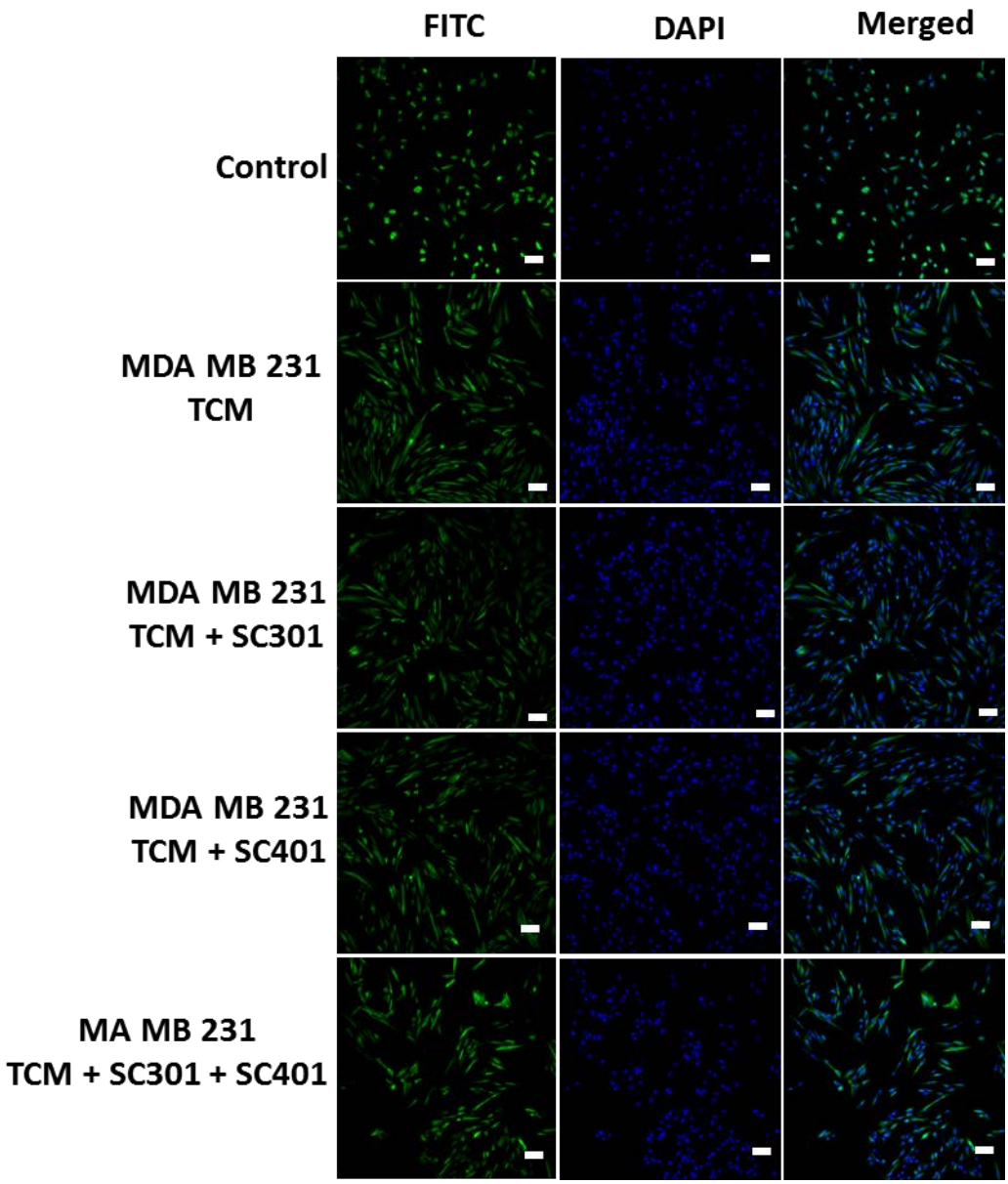


**Figure S20 Individual channels of confocal immunofluorescent imaging for α-SMA expression after treatment with MDA MB 231 TCM**

First column: FITC Only, Second column: DAPI, Third column: Merged channel

Scale bar = 100µM.

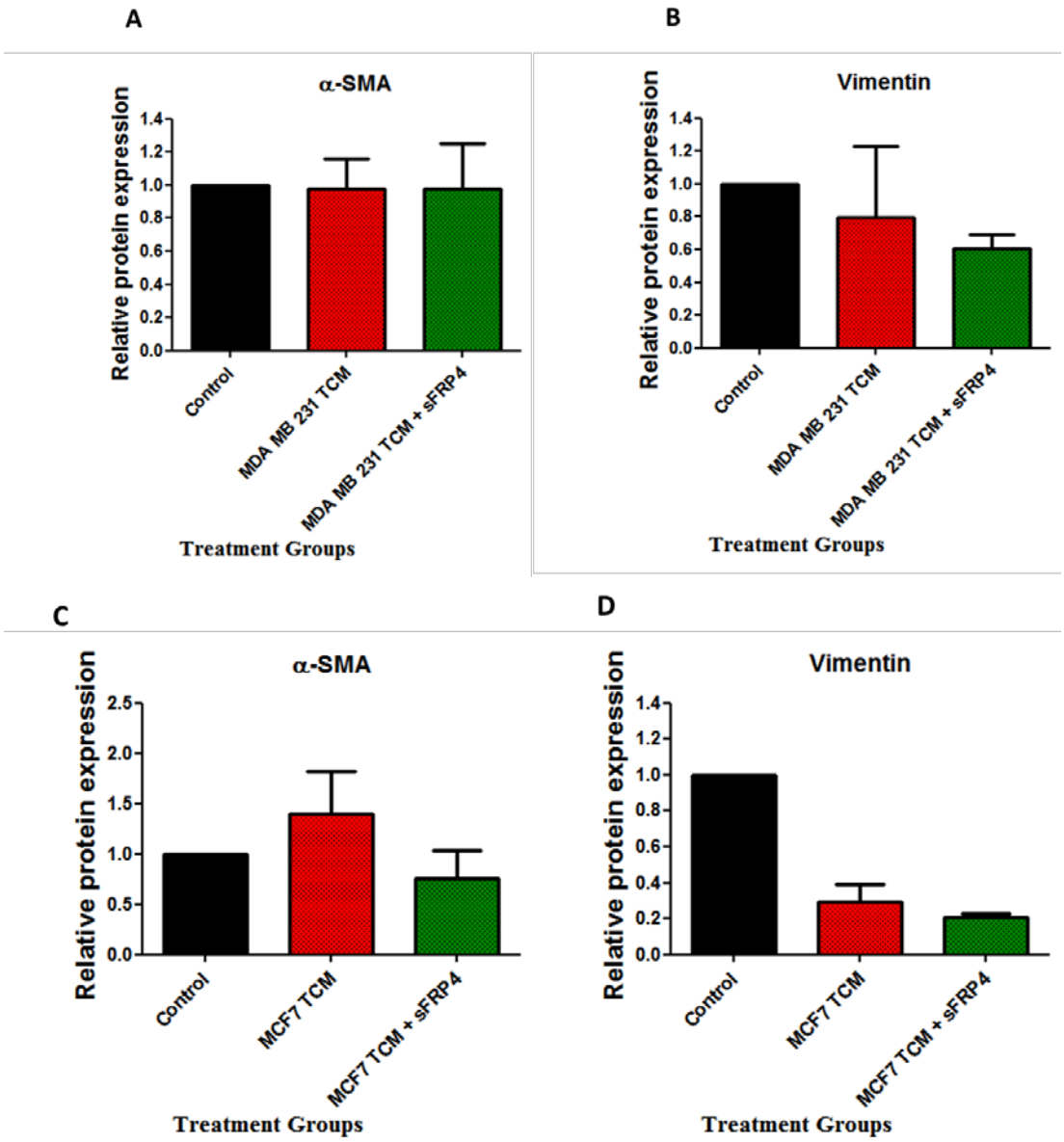


**Figure S21 Protein expression of ADSCs after treatment with TCM in the presence of sFRP4 for 10 days**

Relative protein expression of (A) α-SMA, and (B) vimentin in ADSCs after treatment with MCF7 TCM in the presence of sFRP4 for 10 days. Relative protein expression of (C) α-SMA, and (D) vimentin in ADSCs after treatment with MDA MB 231 TCM in the presence of sFRP4 for 10 days.

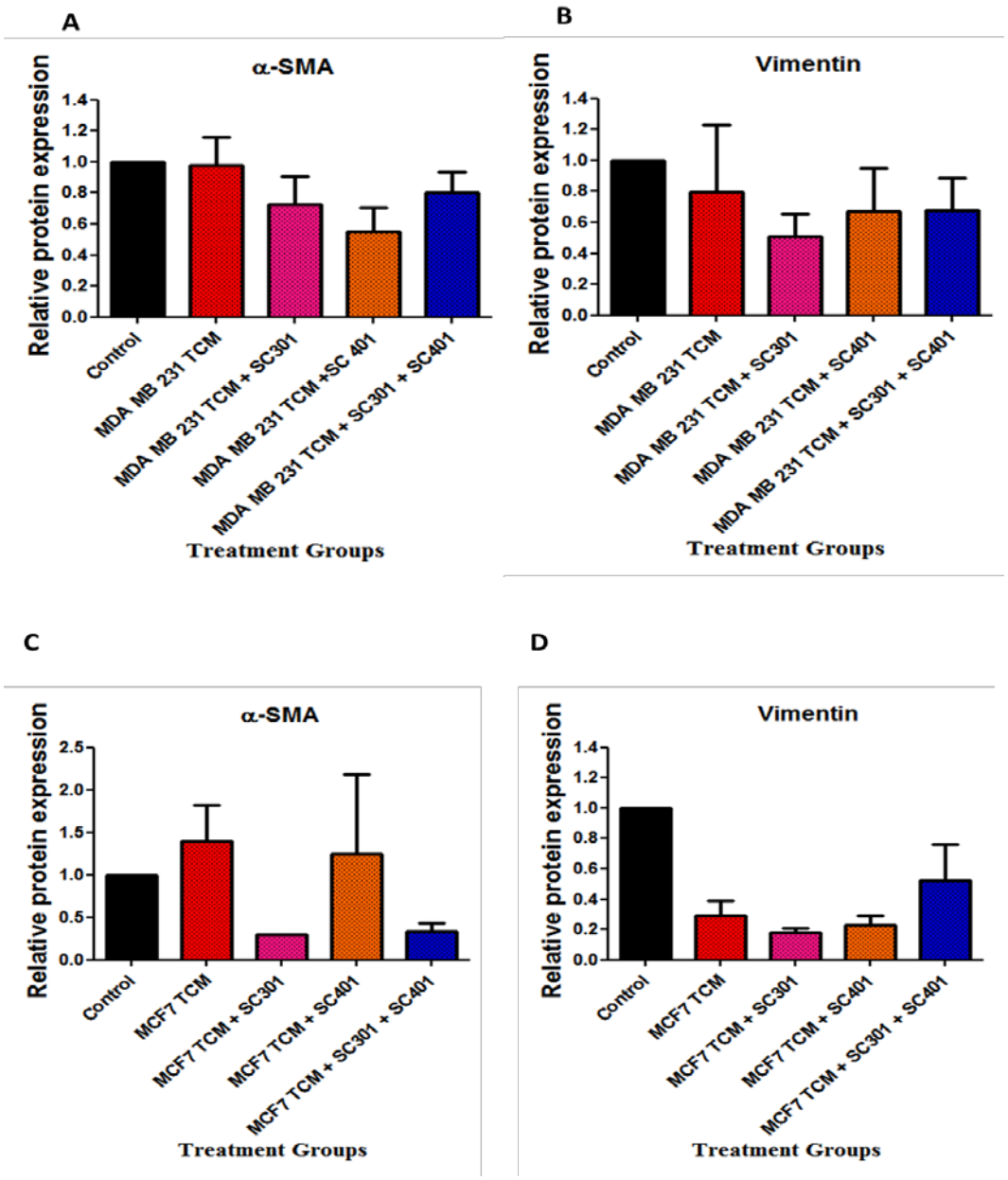


**Figure S22 Protein expression of ADSCs after treatment with TCM in the presence of sFRP4-associated peptides for 10 days**

Relative protein expression of (A) α-SMA, and (B) vimentin in ADSCs after treatment with MCF7 TCM in the presence of SC301/SC401/SC301+SC401 for 10 days. Relative protein expression of (C) α-SMA, and (D) vimentin in ADSCs after treatment with MDA MB 231 TCM in the presence of C301/SC401/SC301+SC401 for 10 days.

# APPENDIX – II

# (List of Chemicals/Reagents)

**Table S1: List of laboratory consumables used in the study**

| Item | Cat No: | Company |
|---|---|---|
| 0.2µM bottle-top sterile filter unit | Z358223 | Nalgene, Thermo Scientific, Australia |
| 10X Bolt Sample Reducing agent | B0009 | Thermo Fisher Scientific, Australia |
| 1X RIPA Buffer | R0278 | Sigma, Australia |
| 2-(N-morpholino)ethanesulfonic acid (MES) running buffer | NP0002 | Thermo Fisher Scientific, Australia |
| 20X Bolt MES SDS Running buffer | B0002 | Thermo Fischer Scientific, Australia |
| 2-deoxyglucose (2-DG) | D6134 | Sigma, Australia |
| 30% acrylamide/bisacrylamide | 161-0158 | BioRad |
| 4-12% Bis Tris Plus Gel, 10 well | BG04120 BOX | Thermo Fischer Scientific, Australia |
| 4X Bolt Lithium dodecyl sulphate (LDS) sample buffer | B0007 | Thermo Fisher Scientific, Australia |
| Adipose-derived mesenchymal stem cells (ADSCs) | PT-5006 | Lonza, Australia |
| Alanyl-glutamine (200mM) | G8541 | Sigma, Australia |
| Alcian blue solution | B8438 | Sigma, Australia |
| Amersham ECL Western Blotting Detection Reagent | RPN2209 | GE Healthcare |
| Ammonium hydroxide | 380539 | Sigma, Australia |
| Ammonium persulphate (APS) | 161-0700 | BioRad |
| B27 Supplement (50X) | 17504044 | Thermo Fischer Scientific, Australia |
| Bicinchoninic acid (BCA) assay | 23227 | Pierce |
| Bis-Tris SDS-PAGE gels | BG04120 | Thermo Fisher Scientific, Australia |
| Bovine serum albumin (BSA) | BSAS 0.1 | Bovogen |
| CCK-8 Kit | 96992-500TESTS-F | Sigma, Australia |

| | | |
|---|---|---|
| DAPI nuclear stain | D1306 | Thermo Fisher Scientific, Australia |
| DCFDA | D6883 | Sigma, Australia |
| DMSO (molecular biology-grade) | D8418 | Sigma, Australia |
| DMSO (Reagentplus®) | 5879 | Sigma, Australia |
| Enzcheck® Caspase-3 assay kit #2, DEVD-R110 substrate | E13184 | Thermo Fisher Scientific, Australia |
| Epidermal growth factor (EGF), Human | CYT-217 | Prospec Protein Specialists |
| ExoQuick TC exosome precipitation solution | EXOTC10A-1 | Intergrated Sciences, Australia |
| Exosome-depleted FBS Media supplement | EXO-FBS-50A-1 | Intergrated Sciences, Australia |
| Fibroblast growth factor (FGF2), Human, HEK | CYT-085-10µg | Prospec Protein Specialists |
| Foetal bovine serum (FBS) | SFBSF6 | Interpath |
| Glucose | G8769 | Sigma, Australia |
| Glucose uptake assay kit | J1342 | Promega, Australia |
| Glucose-free DMEM powder | D5030 | Sigma, Australia |
| Glycine | G7126 | Sigma, Australia |
| Ibidi culture insert in µ-dish 35mm, high | 81176 | DKSH, Australia |
| iBlot transfer stacks, nitrocellulose regular size | IB3010-01 | Thermo Fisher Scientific, Australia |
| JC1 Assay kit | 10009172 | Cayman Chemical |
| Lipofectamine-2000 | 11668030 | Thermo Fischer Scientific, Australia |
| Lipofectamine-3000 | L3000001 | Thermo Fischer Scientific, Australia |
| Low glucose-DMEM | 10567020 | Thermo Fischer Scientific, Australia |
| Lysophosphatidic acid | L7260 | Sigma, Australia |
| Methylthiazolyldiphenyl-tetrazolium | M5655 | Sigma, Australia |

| | | |
|---|---|---|
| bromide (MTT) | | |
| Mr. Frosty | 525000 | Interpath, Australia |
| Nitrocellulose membrane | 10600017 | Amersham Protran, GE Healthcare |
| Normal goat serum | 16210-072 | Thermo Fischer Scientific, Australia |
| Oil Red O stain | O1391 | Sigma, Australia |
| Oligomycin | O4876 | Sigma, Australia |
| Paraformaldehyde (PFA) | 158127 | Sigma, Australia |
| Penicillin-Streptomycin (PS) | 15140-122 | Thermo Fischer Scientific, Australia |
| Phenol red | P0290 | Sigma, Australia |
| Pre-stained ladder | 161-0375 | BioRad |
| Protease-phosphatase inhibitor cocktail | 5872S | Cell Signaling |
| Recombinant sFRP4 protein | 1875-SF-025 | R&D Systems, Inc., Minneapolis, MN, USA |
| Recombinant TGF-β protein | RDS240B002 | R&D Systems, Inc., Minneapolis, MN, USA |
| RPMI-1640 | R8758 | Sigma, Australia |
| RPMI-1640 – Phenol red-free | 7509 | Sigma, Australia |
| Saponin | S-219 | Sigma, Australia |
| Seahorse Flux Kit | SEA102416100 | Agilent Technolgies |
| Silver nitrate | S6506 | Sigma, Australia |
| Sodium dodecyl sulphate (SDS) | L4390 | Sigma, Australia |
| Sodium hydroxide (NaOH) | 221465 | Sigma, Australia |
| Sodium pyruvate (100mM) | S8636 | Sigma, Australia |
| Sodium thiosulphate | 217263 | Sigma, Australia |
| Stempro Adipogenic differentiation medium | A10070-01 | Thermo Fischer Scientific, Australia |
| Stempro Chondrogenic differentiation medium | A10071-01 | Thermo Fischer Scientific, Australia |
| Stempro Osteogenic differentiation medium | A10072-01 | Thermo Fischer Scientific, Australia |

| | | |
|---|---|---|
| Tetramethylethylenediamine (TEMED) | 161-0801 | BioRad, Australia |
| Tris Base | T1503 | Sigma, Australia |
| Triton-X 100 | X100 | Sigma, Australia |
| Trypan Blue dye | T8154 | Sigma, Australia |
| TrypLE Express | 12604-013 | Thermo Fischer Scientific, Australia |
| Ultrafree-15 Centrifugal filter device | UFV2BTK10 | Millipore |
| β-mercaptoethanol | 161-0710 | BioRad, Australia |

**Table S2: List of tissue-culture consumables used for the study**

| Item | Cat No: | Company |
|---|---|---|
| 10mL serological pipette | 607180 | Thermo-Fischer Scientific, Australia |
| 125cm vented | NUN159910 | Thermo-Fischer Scientific, Australia |
| 15ml graduated sterile | 188271S | Greiner |
| 24 well | NUN142475 | Thermo-Fischer Scientific, Australia |
| 25cm vented flask | NUN156367 | Thermo-Fischer Scientific, Australia |
| 25mL serological pipette | 760180 | Thermo-Fischer Scientific, Australia |
| 50ml graduated sterile tubes | 227261S | Greiner |
| 5mL serological pipette | 606180 | Thermo-Fischer Scientific, Australia |
| 6 well plate | NUN140675 | Thermo-Fischer Scientific, Australia |
| 75cm vented flask | NUN156499 | Thermo-Fischer Scientific, Australia |
| 96 well plate | NUN167008 | Thermo-Fischer Scientific, Australia |
| Black 96 well plate | 655086 | Interpath, Australia |
| Black 96 well plate (non-cell culture treated, non-sterile) | 655076 | Interpath, Australia |
| White 96-well plate | 6005680 | Perkin Elmer, Australia |
| Cell Scrapers 23cm$^2$ | NUN179693 | Thermo-Fischer Scientific, Australia |
| Cryopreservation Vials | 122263 | Thermo-Fischer Scientific, Australia |

| | | |
|---|---|---|
| Millex 0.22µm syringe filter | SLGP033RS | Millipore |
| PBS w/o calcium magnesium and phenol red | HYCSH30256.02 | Hyclone |
| SSI 0.5ml box of 1000 | 1110-00 | SSI |
| SSI 1.5ml box of 500 | 1210-00 | SSI |
| Terumo luer slip tip 10ml syringe | SS10S | Terumo |
| Terumo luer slip tip 5ml syringe | SS05S | Terumo |
| Ultra-low adherence 96 well plate | 7007 | Corning |
| Ultra-low adherence 6-well plate | 3471 | Corning |

**Table S3: List of antibodies used for the study**

| **Item** | **Cat No:** | **Company** |
|---|---|---|
| β-actin | 4970S | Cell Signaling |
| Active β-catenin | 8814S | Cell Signaling |
| Total β-catenin | 9562S | Cell Signaling |
| α-smooth muscle actin | ab124964 | Abcam |
| Vimentin | 5741P | Cell Signaling |
| Bax | 5023S | Cell Signaling |
| Bcl-xL | 2764S | Cell Signaling |
| Cyclin D1 | ab134175 | Cell Signaling |
| Anti-rabbit IgG, HRP-linked secondary antibody | 7074S | Cell Signaling |
| Goat anti-rabbit IgG H&L (Alexa Fluor-488) secondary antibody | ab150077 | Abcam |